

1994

# The development of novel chromatographic systems utilizing charge-controllable stationary phases for optimization of separations in liquid chromatography

Randall Scott Deinhammer  
*Iowa State University*

Follow this and additional works at: <https://lib.dr.iastate.edu/rtd>

 Part of the [Analytical Chemistry Commons](#)

## Recommended Citation

Deinhammer, Randall Scott, "The development of novel chromatographic systems utilizing charge-controllable stationary phases for optimization of separations in liquid chromatography" (1994). *Retrospective Theses and Dissertations*. 10690.  
<https://lib.dr.iastate.edu/rtd/10690>

This Dissertation is brought to you for free and open access by the Iowa State University Capstones, Theses and Dissertations at Iowa State University Digital Repository. It has been accepted for inclusion in Retrospective Theses and Dissertations by an authorized administrator of Iowa State University Digital Repository. For more information, please contact [digirep@iastate.edu](mailto:digirep@iastate.edu).

95

03543

U·M·I  
MICROFILMED 1994

## INFORMATION TO USERS

This manuscript has been reproduced from the microfilm master. UMI films the text directly from the original or copy submitted. Thus, some thesis and dissertation copies are in typewriter face, while others may be from any type of computer printer.

**The quality of this reproduction is dependent upon the quality of the copy submitted.** Broken or indistinct print, colored or poor quality illustrations and photographs, print bleedthrough, substandard margins, and improper alignment can adversely affect reproduction.

In the unlikely event that the author did not send UMI a complete manuscript and there are missing pages, these will be noted. Also, if unauthorized copyright material had to be removed, a note will indicate the deletion.

Oversize materials (e.g., maps, drawings, charts) are reproduced by sectioning the original, beginning at the upper left-hand corner and continuing from left to right in equal sections with small overlaps. Each original is also photographed in one exposure and is included in reduced form at the back of the book.

Photographs included in the original manuscript have been reproduced xerographically in this copy. Higher quality 6" x 9" black and white photographic prints are available for any photographs or illustrations appearing in this copy for an additional charge. Contact UMI directly to order.

# U·M·I

University Microfilms International  
A Bell & Howell Information Company  
300 North Zeeb Road, Ann Arbor, MI 48106-1346 USA  
313/761-4700 800/521-0600



**Order Number 9503543**

**The development of novel chromatographic systems utilizing  
charge-controllable stationary phases for optimization of  
separations in liquid chromatography**

**Deinhammer, Randall Scott, Ph.D.**

*Iowa State University, 1994*

**U·M·I**

300 N. Zeeb Rd.  
Ann Arbor, MI 48106



**The development of novel chromatographic systems utilizing charge-controllable  
stationary phases for optimization of separations in liquid chromatography**

by

**Randall Scott Deinhammer**

**A Dissertation Submitted to the  
Graduate Faculty in Partial Fulfillment of the  
Requirements for the Degree of  
DOCTOR OF PHILOSOPHY**

**Department: Chemistry  
Major: Analytical Chemistry**

**Approved:**

Signature was redacted for privacy.

**In Charge of Major Work**

Signature was redacted for privacy.

**For the Major Department**

Signature was redacted for privacy.

**For the Graduate College**

**Iowa State University  
Ames, Iowa**

**1994**

**TABLE OF CONTENTS**

<b>ACKNOWLEDGMENTS</b>	<b>x</b>
<b>GENERAL INTRODUCTION</b>	<b>1</b>
Dissertation Organization	1
Literature Review	2
Range and Scope of the Dissertation	9
Historical Perspective	9
Column Hardware Configuration	11
Charge-Controllable Stationary Phase Materials	15
<b>CHAPTER 1. ION CHROMATOGRAPHIC SEPARATIONS USING STEP AND LINEAR VOLTAGE WAVEFORMS AT A CHARGE- CONTROLLABLE POLYMERIC STATIONARY PHASE</b>	<b>18</b>
ABSTRACT	18
INTRODUCTION	19
EXPERIMENTAL	20
Chromatographic Column Design	20
Polypyrrole Film Formation	23
Instrumentation	24
Reagents and Chemicals	26
RESULTS AND DISCUSSION	26



<b>Basis for Separations using a Conductive Polymer as a Charge-Controllable Stationary Phase</b>	<b>26</b>
<b>Dependence of the Retention of AMP and ATP on the Voltage Applied to the Polypyrrole Stationary Phase</b>	<b>29</b>
<b>Separation of AMP and ATP by a Voltage Step Waveform</b>	<b>31</b>
<b>Separations of AMP and ATP with Linear Voltage Ramps</b>	<b>32</b>
<b>CONCLUSIONS</b>	<b>38</b>
<b>ACKNOWLEDGMENTS</b>	<b>39</b>
<b>REFERENCES</b>	<b>39</b>
<b>CHAPTER 2. EVALUATION OF THE RETENTION CHARACTERISTICS OF POLYPYRROLE AS A STATIONARY PHASE FOR THE ELECTROCHEMICAL ION CHROMATOGRAPHIC (ECIC) SEPARATION OF DANSYL AMINO ACIDS</b>	<b>42</b>
<b>ABSTRACT</b>	<b>42</b>
<b>INTRODUCTION</b>	<b>43</b>
<b>EXPERIMENTAL</b>	<b>45</b>
<b>Construction of the Electrochemical Chromatographic Column</b>	<b>45</b>
<b>Characterization of the Glassy Carbon Support</b>	<b>46</b>
<b>Polypyrrole Film Formation</b>	<b>46</b>
<b>General Mode of Operation</b>	<b>49</b>
<b>Instrumentation</b>	<b>50</b>
<b>Chemicals</b>	<b>51</b>

<b>RESULTS AND DISCUSSION</b>	<b>51</b>
<b>Relationship Between the Applied Voltage and the Exchange Capacity of Polypyrrole</b>	<b>51</b>
<b>Alteration of the Capacity Factors for the Dansyl Amino Acids as a Function of Applied Voltage</b>	<b>59</b>
<b>Dansyl Amino Acid Separations</b>	<b>65</b>
<b>Concentration of Dilute Solutions using ECIC</b>	<b>70</b>
<b>CONCLUSIONS</b>	<b>74</b>
<b>ACKNOWLEDGMENTS</b>	<b>75</b>
<b>LITERATURE CITED</b>	<b>75</b>
<b>CHAPTER 3. ELECTROCHEMICALLY-MODULATED LIQUID CHROMATOGRAPHY (EMLC): A NEW APPROACH TO GRADIENT ELUTION SEPARATIONS</b>	<b>79</b>
<b>ABSTRACT</b>	<b>79</b>
<b>INTRODUCTION</b>	<b>80</b>
<b>EXPERIMENTAL</b>	<b>81</b>
<b>Construction of the Chromatographic System</b>	<b>81</b>
<b>Mode of Operation</b>	<b>83</b>
<b>Instrumentation</b>	<b>83</b>
<b>Reagents and Chemicals</b>	<b>84</b>
<b>RESULTS AND DISCUSSION</b>	<b>84</b>

Basis for the Relationship Between the Applied Voltage and Analyte Retention at the GC Stationary Phase	84
Alteration of the Separation of a Mixture of Aromatic Sulfonates as a Function of a Fixed Applied Voltage	86
Electrochemical Gradient Elution of the ASF Mixture at the GC Stationary Phase	92
CONCLUSIONS	93
ACKNOWLEDGMENTS	94
REFERENCES	94
<b>CHAPTER 4. DYNAMIC MODIFICATION OF SEPARATIONS USING ELECTROCHEMICALLY-MODULATED LIQUID CHROMATOGRAPHY (EMLC)</b>	<b>97</b>
ABSTRACT	97
INTRODUCTION	99
EXPERIMENTAL	100
Glassy Carbon Stationary Phase Characterization	100
Mode of Operation	105
Instrumentation	106
Reagents and Chemicals	107
RESULTS AND DISCUSSION	108
Separation of a Mixture of Aromatic Sulfonates at Open Circuit	110
Alteration of the Separation of the Aromatic Sulfonates Through Application of Various Fixed Applied Voltages	117

Discussion of the Electrochemical Retention Mechanism	121
Electrochemical Gradient Elution at the GC Stationary Phase	133
Response Time of the EMLC Column	138
Characterization of the GC Surface	140
Effect of oxygen functional groups	140
Stability of the GC surface	149
Effect of surface area	150
CONCLUSIONS	156
ACKNOWLEDGMENTS	157
LITERATURE CITED	158
<b>CHAPTER 5. THE SIMULTANEOUS SEPARATION OF ORGANIC ANIONS AND CATIONS USING ELECTROCHEMICALLY-MODULATED LIQUID CHROMATOGRAPHY</b>	<b>162</b>
ABSTRACT	162
INTRODUCTION	163
EXPERIMENTAL	165
Chromatographic Column Construction	165
Mode of Operation	166
Reagents and Chemicals	167
RESULTS AND DISCUSSION	167
Separation of the Mixture of Anions and Cations at Open Circuit	167

Separation of the Mixture of Anions and Cations at Various Constant Applied Voltages	174
Overview of the electrochemical retention mechanism	174
Variation in retention with applied voltage	178
Discussion of the electrochemical retention mechanism for anions and cations	184
Improvement of the Separation Through Application of Fixed and Variable Voltages	190
CONCLUSIONS	194
ACKNOWLEDGMENTS	195
REFERENCES	196
<b>CHAPTER 6. THE FINE-TUNING OF PHENOL SEPARATIONS USING ELECTROCHEMICALLY-MODULATED LIQUID CHROMATOGRAPHY (EMLC)</b>	<b>200</b>
ABSTRACT	200
INTRODUCTION	201
EXPERIMENTAL	203
Chromatographic Column Construction	203
Mode of Operation	204
Molecular Orbital Calculations	204
Reagents and Chemicals	204
RESULTS AND DISCUSSION	205

Separation of the Mixture of Phenols at Open Circuit	207
Modification of the Separation Through Alteration in Applied Voltage Prior to Elution	212
Modification of the Separation Through Dynamic Changes in Applied Voltage and Mobile Phase Composition	224
Separation of Phenolates	231
CONCLUSIONS	238
ACKNOWLEDGMENTS	239
REFERENCES	239
<b>CHAPTER 7. ELECTROCHEMICAL OXIDATION OF AMINE-CONTAINING COMPOUNDS: A ROUTE TO THE SURFACE MODIFICATION OF GLASSY CARBON ELECTRODES</b>	<b>243</b>
ABSTRACT	243
INTRODUCTION	244
EXPERIMENTAL	246
Reagents and Chemicals	246
Carbon Substrate Preparation	248
Electrochemistry	248
X-ray Photoelectron Spectroscopy	249
RESULTS AND DISCUSSION	250
Feasibility of Immobilizing Amine-Containing Molecules at GCEs via Scheme I	250

<b>Immobilization of Various N-Substituted Alkylamines at the GCE Surface</b>	<b>256</b>
<b>Immobilization of Dopamine at the GCE Surface</b>	<b>261</b>
<b>Proposed Mechanism of Bonding</b>	<b>266</b>
<b>CONCLUSIONS</b>	<b>269</b>
<b>ACKNOWLEDGMENTS</b>	<b>270</b>
<b>REFERENCES AND NOTES</b>	<b>270</b>
<b>SUMMARY AND DISCUSSION</b>	<b>274</b>
<b>REFERENCES</b>	<b>278</b>

## ACKNOWLEDGMENTS

Noted here are several persons who have contributed to my growth both personally and professionally, and who deserve much of the credit for this work. Their contribution has often been so continuous that I failed to realize its impact on my life until many years later.

To Professor Marc Porter, I give my heartfelt appreciation for supporting and encouraging me throughout these past five years. His enthusiasm and eternally optimistic attitude have taught me valuable lessons about what comprises a great scientist. Thanks for never giving up on me and for always believing in my abilities, even when I doubted them. The experience was worth a hundred bottles of wine.

I am also indebted to each of the Porter research group members both past and present. In particular, I would like to thank Mankit Ho for his friendship, for sharing his many scientific talents and insights with me, and for making the arduous task of fixing the evaporator on a weekly (daily?) basis a little less so. Thanks is also extended to Brian Lamp and Carla Alves, who each voluntarily took on many group managerial tasks in addition to their research duties, and who were the glue that held the Porter research group together. Further, the help of my co-worker En-Yi Ting and the many helpful discussions concerning polypyrrole chemistry, carbon microstructure, and electrochemistry with Dr. Chuanjian Zhong, Drs Mark and Christie McDermott, and Dr. Jerzy Zak are appreciated. Other group members who deserve special thanks include Mohammed Omer for keeping me culturally aware, Neal Simmons for always having a joke to brighten the day, and the group secretary Marilyn Forsling for handling all those last minute jobs with a smile.



Appreciation is also extended to Jim Anderegg of the Ames Laboratory, who ran countless XPS samples, often on a moments notice, and who provided friendship over the past several years. The loan of equipment by Professors Dennis Johnson, James Fritz, and Glen Schrader of the Ames Laboratory is also greatly appreciated.

To Dr. Katsuaki Shimazu from Hokkaido University in Sapporo, Japan, I also extend my thanks for his companionship and for sharing his electrochemical expertise with me during the initial three months of this work.

To Drs. Heino Nitsche at Lawrence Berkeley National Laboratory and Marcin Majda at the University of California at Berkeley, I extend my appreciation for taking a chance on a young fledgling scientist and for instilling in me a sturdy foundation of research skills.

For her unconditional love, understanding, and patience, I would like to give my deepest appreciation to my wife, Kimberly. She has brought great happiness and perspective to my life, and has held me together during the past five years. Without her this work would not have been possible.

And last but certainly not least, I am eternally indebted to my parents, Larry and Phyllis, whose unique way of nurturing and supporting my sister and me over the years has yet to find an equal. Thanks for the many happy memories. You're both the greatest.

This work was supported by the National Science Foundation (Grant CHE-9003308) and by an American Chemical Society Analytical Division Summer Fellowship sponsored by Dow Chemical, USA.

## **GENERAL INTRODUCTION**

### **Dissertation Organization**

This dissertation explores a new approach to analytical separations that is based on the electrochemical manipulation of the composition of various charge-controllable stationary phases. The literature review, which precedes seven papers, provides a general background and overview of the efforts that have been put forth by others toward the development of this novel separation strategy. This section is followed by a brief discussion which defines the range and scope of this dissertation in terms of the new approaches to electrochemically-based separations described herein that have led to dramatic improvements in their efficiency and applicability. The seven papers which follow investigate the theoretical basis for and the applications of this new technique, termed electrochemically-modulated liquid chromatography (EMLC), by examining the separations of various organic anions, organic cations, and neutral species.

The papers included in Chapters 1 and 2 examine the electrochemical modulation of the separations of adenosine nucleotides and dansyl amino acids, respectively, at polypyrrole-coated glassy carbon particles. Chapters 3 and 4 describe some improvements in the design of the EMLC column that led to large increases in its chromatographic efficiency and allowed for the baseline resolution of more complex mixtures of analytes to be obtained. Insights into the mechanism by which analyte retention can be controlled electrochemically are gained through examination of the separations of several aromatic sulfonate derivatives at both porous and nonporous carbon spheres. A series of guidelines for using this new separation methodology

are also provided. The fifth chapter extends further these studies by investigating the utility of EMLC for manipulating and improving the separations of mixtures containing both organic anions and cations. The application of EMLC to the separation of uncharged species is demonstrated in Chapter 6, in which the electrochemical manipulation of the separation of fifteen phenolic compounds is probed. Improvements in the separation obtained by alteration in the applied voltage during elution are compared to those obtained using conventional solvent gradient elution methods to illustrate the advantages and features of the electrochemically-controlled elution method. The final chapter describes a new route to the surface functionalization of glassy carbon electrodes that can be potentially used as a tool for tailoring the specificity of the charge-controllable stationary phase for various analytes. This route is also shown to be a viable approach for the construction of modified glassy carbon electrodes that can be used for electrocatalytic and biosensor purposes. Together, these papers provide the first convincing evidence of the unique ability of EMLC to manipulate and fine-tune separations electrochemically while maintaining high chromatographic efficiency. Following these papers is a general summary and discussion which highlights the results of this work, provides an overview of the future directions of EMLC, and which gives a list of references cited in the introduction.

### **Literature Review**

The diverse application of modern liquid chromatographic-based separation techniques arises from their ability to separate and determine quantitatively the amounts of constituents in

a variety of complex mixtures. With an appropriate choice of a stationary phase material and a mobile phase composition, virtually any mixture can be separated and its components quantitated. Examples of the diversity of these applications include the analysis of foodstuffs [1-4], the determination of trace contaminants in wastewaters and soils [5-8], the diagnosis of metabolic disorders [9,10], the profiling of biological fluids [11-14], the purification of biological molecules [15-17], drug testing [18-20], and the chiral separation of enantiomers [21-23]. A limitation of these techniques, however, lies in the fixed properties of the stationary phases, which requires that a large number of different phases and elution methods be available to accomplish the diversity of separations required in the analytical laboratory.

As a starting point for overcoming this limitation, Fujinaga et al in 1963 [24] as well as Strohl [25] and Roe [26] in 1964 proposed a new method by which the composition of the stationary phase could be controlled electrochemically. The new concept involved the marriage of well established thin-layer electrochemical techniques [27-31] with liquid chromatographic technology. In their approach, the liquid chromatographic column was converted into a three-electrode electrochemical cell. The working electrode, which became the stationary phase, consisted of either glassy carbon [25], amalgamated nickel [26], or amalgamated platinum [32] particles that were packed into a porous vycor tube. The vycor tube served as a separator of the working electrode and a high surface area counter electrode and reference electrode. The conductive nature of the stationary phase allowed for alterations in the applied voltage to be used as a convenient means for changing its surface charge. These compositional changes were facilitated by the use of a mobile phase containing a high

concentration ( $\sim 0.1$  M) of an inert electrolyte, which increased the rate at which such changes could be produced.

Initial applications of such columns involved their use in an anodic stripping mode, in which metal ions were reductively deposited onto the stationary phase and then stripped in a stepwise manner to effect simple separations of a few metals. Using an alternate design, Fujinaga further demonstrated that a voltage gradient could be applied between the ends of the column to enhance these separations [33,34]. Other applications that were investigated included the preparation of unstable redox species and the elucidation of reaction mechanisms.

This adsorption and stepwise method of separation was extended to organic species in 1969 when Strohl demonstrated that changes in the voltage applied to a bed of carbonaceous particles could also be used to modify the adsorption of organic species [35,36]. Termed 'electrosorption', this new method was shown to be effective for separating simple mixtures of quinones based on differences in their voltage-dependent adsorption at the carbon surface. Once adsorbed, the quinones could be eluted from the column sequentially through modification in the applied voltage. These studies illustrated clearly the ability of this new technology to separate species without changing their chemical form.

In 1978, Strohl further demonstrated that, in addition to changing the redox state of the analyte or the properties of the stationary phase, modifications in the applied voltage could also be used to produce compositional changes in the mobile phase to manipulate analyte separations [37]. The method was based on the irreversible adsorption of organic chelating agents having a pH-dependent binding chemistry with various metal ions onto the surface of

graphite particles [36,38,39]. Electrochemically-induced decreases in the pH of the mobile phase produced through oxidation of the aqueous mobile phase to generate hydrogen ions were used as a means for dissociating the metal ion-chelate complexes. Differences in the stability constants for the binding of various metals with the chelants were then used to separate binary mixtures of metal ions.

A significant advance in the area of electrochemically-controlled separations occurred in 1984 when Yacynych et al proposed 'electrochromatography', in which differences in the continuous partitioning of analytes between the mobile and stationary phases, as opposed to differences in their adsorption strengths, was employed as the primary separation mechanism [40,41]. These differences in the partitioning of analytes, as given by their capacity factors [42], could be modulated through application of various constant voltages to the carbonaceous column. The ability to alter the capacity factors of three test analytes (i.e., phenol, pyridine, and toluene) electrochemically was attributed to changes in the electrical double layer at the carbon surface induced by the imposition of a surface charge [43,44]. This conclusion was supported by later studies which found that the magnitude of the capacity factor changes was highly dependent on the electrolyte used in the mobile phase [45]. A further advance made by Yacynych et al was the development of a column able to withstand high pressures (~3000 psi). This development, together with the advances noted above, launched a new era in electrochemically-controlled separations, in which separations obtained using conventional chromatographic packing materials and partition methods could potentially be accomplished.

As a means for tailoring the selectivity of the carbon surface for various analytes, several groups then focused on functionalization of the carbon surface with electroactive ionomers [46-49] and electroactive polymers [50-57]. The basis for the use of these materials as stationary phases stems from the ability to convert them electrochemically between their oxidized and reduced forms, with the concomitant uptake or expulsion of electrolyte (or analyte) ions [58-62]. For example, Martin et al demonstrated in 1986 that the retention of the organic dication methylviologen could be modulated by altering electrochemically the oxidation state of ferrocenyl groups bound within a styrene, styrenesulfonate, and vinylferrocene terpolymer [47]. Further, Wallace et al have performed detailed studies designed to probe the effects alterations in the applied voltage on the retention of various species expected to display predominately hydrophobic, proton donor, anion-exchange, electron donor, and dipole interactions with a polypyrrole stationary phase that was coated onto reticulated vitreous carbon [51,52]. These studies revealed that, in addition to modifying its ion-exchange capacity, alterations in the applied voltage can modify significantly the hydrophobicity of polypyrrole as well as its ability to participate in dipole and electron donor-acceptor interactions. Simple separations of binary mixtures of acidic and basic compounds obtained both in the presence and in the absence of an applied voltage were used to illustrate the improvements in resolution that can be obtained electrochemically. The use of polypyrrole-coated silica spheres as a stationary phase in conventional liquid chromatography [63-65] as well as 'affinity electrochromatography' [53] were also proposed by Wallace.

More recently, Nagaoka et al have investigated the separation of a variety of organic and inorganic ions at an electrochemically-controlled column packed with either microporous glassy carbon [66] or glassy carbon spheres coated with crown ethers [53], polyaniline [56,57], or polypyrrole [57]. Changes in the applied voltage were used to modify the retention of these species on the column and to effect separations of simple 2-3 component mixtures. For the polypyrrole stationary phases, studies of the effects of analyte size on its retention revealed that small inorganic ions could easily be taken up and released from the film, whereas larger organic ions (i.e., benzenesulfonate) were often irreversibly trapped within the oxidized films and could only be released by reduction of the film. The effects of the column length and the pH of the mobile phase were also studied as a means for optimizing the method.

As a whole, the work described above points to the potential use of electrochemically-controlled chromatography as a versatile and exciting new method for manipulating analyte retention and elution. The interest in this new method has stemmed largely from the potential to take advantage of the features of two powerful analytical techniques, thin-layer electrochemistry and liquid chromatography, to manipulate and control analytical separations. In each of the works detailed above, however, the difficulties encountered when coupling these two techniques has resulted in an electrochemically-controlled column that *lacks* many of the desirable qualities commonly attributed to each individual technique.

For example, the relatively fast electrolysis times observed with conventional thin-layer electrochemical cells [67] are generally compromised to some extent by the high surface area



of the stationary phase and the electrical resistance (i.e., contact resistance between the stationary phase particles and the solution resistance) present within the column. More importantly, the high chromatographic efficiency routinely obtained with conventional liquid chromatographic columns (~5,000 to 100,000 theoretical plates/meter) has, *without exception*, been unacceptably compromised through the conversion of the liquid chromatographic column into a three-electrode electrochemical cell. Poor choices for charge-controllable stationary phase materials have also contributed to this low efficiency, which has been generally reported as ~10-200 theoretical plates/meter [45]. It further appears that prior work in this area has focused more on obtaining a fast electrolysis time than on obtaining a high chromatographic efficiency. Although a fast electrolysis time is clearly important to facilitate equilibration of the column upon changes in the applied voltage, a low chromatographic efficiency *hinders severely* the practical application of this technique to the separation and quantitation of the complex analyte mixtures routinely encountered in the analytical laboratory. Further, each of these columns would appear to be somewhat complex and difficult to assemble. As a result of these factors, the benefits of using such columns to obtain separations as opposed to the use of more conventional column formats are questionable. In our opinion, a *compromise* between a column displaying a fast electrolysis time and one displaying a high chromatographic efficiency must be reached to increase the viability of this new separation scheme.

Although the effects of various static applied voltages on the separations of simple binary mixtures were outlined in these works, the potentially more useful and exciting

possibility of manipulating analyte separations dynamically *during the elution process* was not investigated. In such an experiment, changes in the applied voltage could be made during elution as a means for sharpening elution bands, for improving resolution, and for decreasing the total analysis time of a particular separation. In this way, improvements in separations analogous to those obtained with conventional solvent gradient elution techniques could be realized without compositional modifications in the mobile phase. Although not investigated by others, a galvanostatic approach could also be used, in which the charge on the column could be altered during the separation. The potential for further fine-tuning a particular separation by combining these electrochemically-induced changes in retention with those produced through modification in the mobile phase composition would appear to be a valuable method that also deserves investigation. We feel that each of these issues, in addition to the development of a mechanism that explains the electrochemical manipulation of analyte retention, needs to be addressed before placement of this new separation technique in the broad and advanced world of chemical separations can be justified and successfully accomplished.

### **Range and Scope of the Dissertation**

#### **Historical Perspective.**

Our interests in the area of electrochemically-controlled separations developed from ongoing studies in our group that have focused on molecular recognition at interfaces [68]. These studies have largely entailed an in-depth examination of the molecular recognition

properties of thiol-derivatized cyclodextrins that are immobilized as a monomolecular layer at gold surfaces. The strong binding of organothiol compounds at gold surfaces was utilized as a means for creating a well-organized and compact monolayer of cyclodextrin moieties [69-71]. The unique feature of these monolayers is their ability to restrict access to the gold surface to those molecules whose size, shape, and polarity allow them to enter the cyclodextrin cavity [72-74].

As a means for probing the interaction of various analytes with these immobilized cyclodextrins, we envisioned utilizing cyclodextrins as a liquid chromatographic stationary phase and employing differences in the retention of various analytes on the column to quantitate their interaction. The liquid chromatographic column was to be constructed by packing monodisperse gold spheres of  $\sim 3 \mu\text{m}$  in diameter into a stainless steel column and derivatizing the gold surface with the cyclodextrin moieties. During the course of these studies, it occurred to us that the conductive nature of the gold particles might allow, with an appropriate redesign of the column, for a voltage to be applied to the gold surface to manipulate the interaction of various analytes with the cyclodextrins through modification in the electrical double layer [44,45].

Although difficulties in packing the column uniformly with these dense gold spheres as well as their excessive cost hindered the detailed exploration of this idea, we opted to investigate a more general application of this concept in terms of its use for manipulating analytical separations in liquid chromatography. In this context, alterations in the voltage applied to the conductive stationary phase (i.e., glassy carbon particles) could be used to alter

the interaction of analytes with the stationary phase and therefore their retention on the column. Differences in the strength of the interactions of analytes with the stationary phase as a function of the applied voltage would then serve as a basis for separating mixtures of analytes. This goal proved to be quite challenging, since our background was primarily in both electrochemistry and spectroscopy, with little practical experience in liquid chromatography. Therefore, we initially approached this problem from the viewpoint of electrochemists, and, in the process of launching successfully this new area of chemical separations, became separation scientists.

The following two sections outline briefly our approaches to the configuration of the column hardware and the charge-controllable stationary phase material that are discussed in more detail in Chapters 1-6. Use of these new approaches has led, for the first time, to the development of an electrochemically-controlled column that has a reasonable electrolysis time as well as a chromatographic efficiency comparable to commercially available columns. These large improvements have allowed our columns to be used for the separation of complex mixtures of analytes in a variety of applications, as discussed in Chapters 1-6.

#### **Column Hardware Configuration.**

The most challenging obstacle faced when designing an electrochemically-controlled column concerns the incorporation of electrical control over the stationary phase composition into a liquid chromatographic column without compromising its chromatographic efficiency. This task is a formidable one, since the column must contain all of the components of a conventional high efficiency liquid chromatographic column in addition to electrical contacts

to working, counter, and reference electrodes, and an ion-permeable membrane to separate these electrodes from each other. As noted above, routes for the successful completion of this task have not been put forth in the literature. As a starting point, our earlier designs [75,76] utilized a Nafion tube both as a container for the conductive stationary phase and as an ion-exchange membrane to separate the working electrode from the counter and reference electrodes. Effective electrical contact to the particulate phase was made by insertion of a gold wire spot-welded to a strip of gold mesh into the Nafion tube prior to packing with the conductive stationary phase. This mode of electrical contact was found to provide a reasonably fast electrolysis time, such that the column could be re-equilibrated in 1-2 min after changes in the applied voltage had been made. A high surface area platinized platinum mesh counter electrode, which was wrapped around the outside of the Nafion tube, provided a uniform electric field between the working and counter electrodes [44]. This electrode, as well as an Ag/AgCl reference electrode, were placed into a glass column containing an electrolyte solution that surrounded the Nafion tube. This column design was used in Chapters 1 and 2.

Although this column functioned reasonably well (maximum number of theoretical plates ~300) when compared to the columns described in the literature [51,52,57], the lack of support given to the Nafion tube resulted in three major deficiencies: (1) the column could only withstand very low pressures (<10 psi), which limited the diameter of the packing material to ~25  $\mu\text{m}$ , (2) the low pressure limit prevented the use of high pressure methods for column packing, and (3) the column could not be used with mobile phases containing organic

solvents due to swelling of the Nafion tube. Since the efficiency of a chromatographic column increases dramatically with decreasing diameter of the packing material [42], the limitation on the particle diameter prevented these potentially large increases in efficiency from being obtained. The inability to use high pressure methods for column packing likely resulted in additional decreases in column efficiency due to ineffective packing and column voids. Further, the inability to use organic solvents as mobile phase additives did not allow for the enhancement in the shapes of elution bands often provided by these additives [77,78] to be utilized. Together, these deficiencies limited severely the obtainable chromatographic efficiency.

As an approach to address these deficiencies, a new column design was constructed [79,80] in which the Nafion tube was placed inside of a porous stainless steel column. This porous stainless steel column served to support the Nafion tube, allowing it to withstand very high pressures (up to ~6000 psi), and prevented its deformation or swelling in the presence of organic solvents. This improvement allowed for the use of conductive stationary phase packing materials of less than 10  $\mu\text{m}$  in diameter, for column packing to be performed at high pressures, and for organic solvents to be used as mobile phase additives. Each of these features improved dramatically the chromatographic efficiency obtainable with these columns (up to ~20,000 plates/meter). Such a column configuration is described in more detail in Chapter 3.

An additional improvement that was made concerns the mode of electrical contact to the conductive particulate phase. Although the wire/mesh approach employed previously by

us [75,76] and others [47,51,52,56] does provide good electrical contact to the particulate phase and a rapid electrolysis time, it creates unnecessary elution band broadening at the head of the column, since the wire must extrude from the column to allow for electrical contact. This requirement introduces a considerable extra-column void volume to the system and causes the analyte injection plug to be broadened significantly prior to its entering the particulate phase. Further, the presence of a high surface area wire/mesh within the particulate phase may result in both secondary retention effects [81] and small voids in the particulate phase due to poor packing around the wire/mesh. Both of these effects will result in elution band broadening and a decrease in the efficiency of the column.

The unique feature of the porous stainless steel-supported Nafion column is that electrical contact to the particulate phase can be made through the stainless steel itself, without the need for wires or mesh. This strategy is effective since the particulate phase is in electrical contact with the stainless steel endfittings and frits placed at both ends of the column. Electrical contact to the particulate phase can thus be made by simply contacting either of these endfittings. Effective contact throughout the column is facilitated by packing the column at a high pressure (5000-6000 psi), which results in a minimal electrical resistance down the length of the column (20-40  $\Omega$ ). Although the effectiveness of this contact is reduced somewhat when compared to the wire/mesh approach, this mode of contact minimizes extra-column dead volumes and results in improvements in the widths and shapes of the chromatographic elution bands. As pointed out earlier, we found this small compromise in the electrolysis time to be necessary to obtain acceptable chromatographic efficiencies with

these columns. Furthermore, in this configuration, the column is virtually identical to a conventional liquid chromatographic column, except that the stainless steel column is lined with a Nafion tube. This design modification greatly facilitates column assembly when compared to the designs proposed by others [47,51,52,56]. These features will undoubtedly make the use of this new technique much more attractive to the analytical community.

### **Charge-Controllable Stationary Phase Materials.**

The requirements imposed on the stationary phases used to obtain electrochemically-controlled separations are equally as demanding as those imposed on the column hardware. The stationary phase must possess all of the requirements of a good liquid chromatographic stationary phase such as particle rigidity, small particle size, high surface area, chemical inertness, and surface homogeneity as well as additional requirements such as high electrical conductivity and stability over a range of voltages. Although no stationary phase can fulfill all of these requirements, we have found that carbonaceous materials meet many of these requirements. Such materials are mechanically strong [82], are available in a range of particle sizes and porosities, and are highly inert both to chemical attack and to voltage-induced transformations [83-86]. Further, they display good conductivity [87] and have a largely homogeneous surface [88,89].

Our initial studies, as described in Chapters 1 and 2, involved the surface functionalization of nonporous carbon particles and spheres with the conductive polymer polypyrrole. This polymer is an attractive candidate as a charge-controllable stationary phase since its positive charge density, and therefore its anion-exchange capacity, can be



manipulated selectively through its oxidation or reduction [58-62]. This results in a capacity of the column for anions that is readily tunable. Despite this advantage, a limitation of this approach lies in the difficulty of coating the carbonaceous particles uniformly with the polymer, which leads to significant elution band broadening and tailing as a result of a nonuniform interaction energy [81]. Further, the stability of these polymers is often relatively low (1-2 weeks) due to their facile oxidative degradation [90,91]. These problems somewhat limit the use of the columns described in Chapters 1 and 2 as well as those constructed by others using similar approaches [51,52,56].

An alternate approach which we investigated involved the use of uncoated carbonaceous materials as charge-controllable stationary phases. This approach is attractive from several viewpoints: (1) the uniformity of the stationary phase is improved dramatically, (2) the construction of the column is greatly simplified, (3) the stability of the stationary phase is increased (several months), and (4) the use of carbonaceous materials as conventional liquid chromatographic stationary phases has been established in the literature [92-106]. Importantly, the latter feature facilitates a comparison of the separations obtained at commercially available columns to those obtained at electrochemically-controlled columns. This comparison can be used to provide a clear illustration of the features of the electrochemical elution method. Each of these features increase significantly the attractiveness of this new separation technique.

A further improvement made in the charge-controllable stationary phase material that increased dramatically its chromatographic efficiency was the use of macroporous

carbonaceous spheres [107,108]. To our knowledge, macroporous materials have not been used previously to obtain electrochemically-controlled separations. These materials are attractive since their high surface area ( $\sim 200 \text{ m}^2/\text{g}$ ) increases significantly the capacity of the column, thereby allowing for more complex mixtures of analytes to be separated. This capacity increase also requires organic solvents to be used as mobile phase additives to obtain reasonable run times, which improves the mass transfer of organic analytes in the mobile phase and therefore also improves their bandshapes [109]. Together, these improvements in the column hardware and the charge-controllable stationary phase material have allowed separations based on the electrochemical control of analyte retention to be respected as viable alternatives to the myriad of separation techniques currently used in the analytical laboratory.

**CHAPTER 1. ION CHROMATOGRAPHIC SEPARATIONS USING STEP AND  
LINEAR VOLTAGE WAVEFORMS AT A CHARGE-  
CONTROLLABLE POLYMERIC STATIONARY PHASE**

A paper published in *Analytical Chemistry*<sup>1</sup>

Randall S. Deinhammer, Katsuaki Shimazu, and Marc D. Porter<sup>2</sup>

**ABSTRACT**

A novel ion chromatographic system for separations using a conductive-polymer stationary phase has been developed. The stationary phase consists of polypyrrole-coated glassy carbon particles and is connected as the working electrode in a three-electrode cell arrangement. Electrochemically-induced changes between the neutral (reduced) and cationic (oxidized) forms of polypyrrole lead to the transformation from an uncharged stationary phase to one with a high positive charge density. The compositional changes result in a "charge-controllable" stationary phase, which can potentially be coupled with a variety of voltage waveforms to develop separation approaches analogous to temperature-programmed gas chromatography and gradient-elution liquid chromatography. Preliminary results using this system to manipulate during elution the separation of AMP and ATP are presented through the application of step and linear voltage waveforms.

---

<sup>1</sup>Reprinted with permission from *Anal. Chem.* 1991, 63, 1889-94. Copyright © 1991 the American Chemical Society.

<sup>2</sup>Author to whom correspondence should be addressed.

## INTRODUCTION

Separations using ion chromatography generally rely on a stationary phase with a fixed composition, i.e., a fixed number of exchange sites [1,2]. With such phases, changes in separation characteristics are accomplished by altering the composition and flow rate of the mobile phase. Recently, the possibility of manipulating separations via electrochemically-induced changes of stationary phases constructed from conductive materials has been explored [4-10]. These studies, which tested uncoated [4,5], surface functionalized [6,7], and conductive polymer coated [8-10] carbon particles as stationary phases, demonstrated that the retention of analytes could be controlled by the voltage applied to the stationary phase prior to analyte injection. The approaches based on conductive polymers are particularly appealing because such coatings can be electrochemically transformed between their oxidized and reduced forms, resulting in a "charge-controllable" stationary phase. Surprisingly, however, the possibility of inducing changes in these stationary phases through the application of voltage waveforms during elution has yet to be explored. Such a development would open a new dimension for separations based on ion chromatography, where, for example, changes in the charge density of a stationary phase using a linear voltage sweep would be analogous to temperature programming in gas chromatography and gradient elution in liquid chromatography.

In this paper, we describe the development and preliminary testing of a novel chromatographic system for separations that are based on manipulating a charge-controllable stationary phase via step and linear sweep voltage waveforms during analyte elution. The

stationary phase was formed by electropolymerizing a thin ( $\sim 0.03 \mu\text{m}$ ) conductive coating of polypyrrole onto glassy carbon particles. Polypyrrole was selected as a coating primarily because switching between its neutral (reduced) and cationic (oxidized) forms through alterations in an applied voltage results in the transformation of an uncharged stationary phase to one with a high positive charge density. The chromatographic system was constructed to ensure both effective electrical contact throughout the carbon particulate stationary phase and a reasonably uniform current density across the stationary phase. Using this system, we have found that a variety of voltage waveforms can be applied to alter the composition of the conductive stationary phase during elution, which leads to changes in the separation of anionic analytes. Results demonstrating this capability are presented for the adenosine nucleotides AMP and ATP. Possible extensions of this new separation technique are also briefly discussed.

## EXPERIMENTAL

### Chromatographic Column Design.

The design of the chromatographic column is shown schematically in Figure 1. A Nafion #110 cation exchange tube (25 cm in length and 0.21 cm i.d.; Perma Pure Products, Inc.) was heated at both ends and flanged for mating to standard liquid chromatographic screw fittings (Alltech Associates). The tube was then plugged at one end with Teflon wool and packed with a slurry of 0.90 g of glassy carbon (GC) particles in a 0.1 M solution of the sodium salt of *p*-toluenesulfonic acid (NaOTs). The GC particles were made by crushing GC

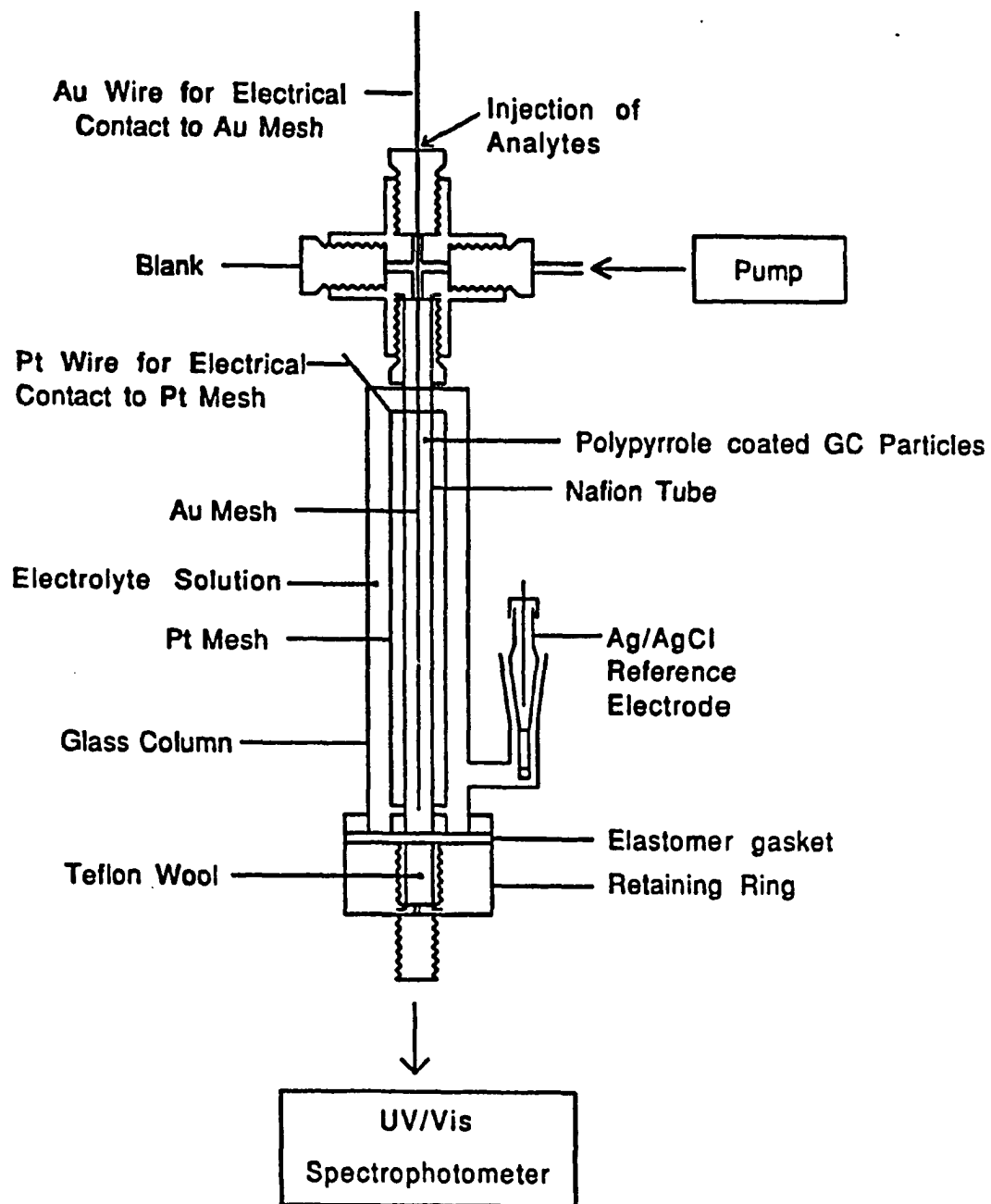


Figure 1. Diagram of the electrochemical chromatographic column (see text for details).

plates (Tokai Carbon) in a diamond mortar and sizing the resulting particles using 200 and 300 mesh sieves (Fisher Scientific). This procedure resulted in a size distribution of irregularly shaped particles between ~70 and ~230  $\mu\text{m}$  in size, based on characterizations using scanning electron microscopy. Though the size and shape distributions are less than ideal for high efficiency separations, these particles have proven suitable for our proof of concept experiments. After sieving, the GC particles were activated in an  $\text{O}_2$  plasma (Harrick Scientific, Inc.) for 5 min at a base pressure of  $2 \times 10^{-2}$  torr. Gold wire (Johnson Matthey) was spot welded to a strip of gold mesh (1.3 cm x 24 cm x 0.2 cm, Nilaco Corp) and was inserted into the Nafion tube prior to packing. It was only after using a large surface area gold mesh to insure effective electrical contact throughout the particulate phase that separations using voltage waveforms could be obtained. In this arrangement, the Nafion tube served both as a "container" for the GC particles and as a cation-permeable membrane for electrical contact to reference and counter electrodes. The Nafion tube was encircled with a cylinder of platinized platinum mesh (Thomas Scientific), which functioned as a high surface area counter electrode. The mesh-encased tubing was placed inside a glass column and connected to both a Kel-F retaining plate and a four-way Tefzel cross using chromatographic screw fittings. The retaining plate was then sealed to the flanged bottom of the glass column with an inert elastomer gasket and a screw clamp. After assembly, the supporting electrolyte of the mobile phase was added to the solution contact channel. This channel is defined by the interior of the glass column and the exterior of the Nafion tubing. Analyte was injected onto the stationary phase through a small port next to the Au wire that connected the Au mesh to the electrical

leads of a potentiostat. An Ag/AgCl (sat'd KCl) electrode was placed in an adjoining glass tube; all voltages are given with respect to this electrode.

### **Polypyrrole Film Formation.**

Thin ( $\sim 0.03 \mu\text{m}$ ) polypyrrole films were electropolymerized onto GC particles immediately after packing into the Nafion tubing. Fifty milliliters of a deaerated aqueous solution consisting of 0.1 M pyrrole and 0.1 M NaOTs were pumped through the column at a flow rate of 1 mL/min, after which the pump was disengaged. The pyrrole was electropolymerized by applying a voltage of +1.00 V for 2 sec for film nucleation, immediately followed by a step to +0.60 V for film growth. Growth proceeded until a charge that corresponded to an estimated average film thickness of  $\sim 0.03 \mu\text{m}$  was passed. Although other voltage and temporal limits were tested, the noted conditions were optimal for the long term stability and reproducible functioning of the polypyrrole stationary phase. The stationary phase generally exhibited useful lifetimes of 2-4 days, which are typical of polypyrrole films [11]. During this period, retention times varied by  $\sim 10\%$  for replicate separations. The average film thickness was estimated from the quantity of film deposited (based on the charge passed during electropolymerization), the density of pyrrole, and the average geometric surface area of the uncoated GC particles. For this calculation, the particles were assumed to be spherical with an average diameter of  $63 \mu\text{m}$ , a value representative of the average size of the meshes used for sieving the particles. Detailed characterizations of the size and shape distributions of the particles as well as film uniformity, however, have yet to be completed.



After film formation, the column was flushed for ~30 min with a deaerated aqueous solution of 10 mM LiClO<sub>4</sub>, which also served as the mobile phase. The electrochemical properties of our polypyrrole-coated stationary phase in 10 mM LiClO<sub>4</sub> are shown in the steady-state cyclic voltammetric current-potential (i-E) curve in Figure 2. In comparison to those reported in the literature at planar electrodes [12], the broad shape of the i-E curve reflects a larger uncompensated electrolyte resistance and a slower rate of charge transfer, both of which arise primarily from the low electrolyte concentration of the mobile phase. This electrolyte concentration represents a compromise between minimizing charge-transfer resistance and incorporating AMP and ATP into the polypyrrole film, the latter of which is in competition with the ClO<sub>4</sub><sup>-</sup> of the mobile phase [13]. Further discussion of the characteristics of the i-E curve is deferred until later.

#### **Instrumentation.**

The voltage applied to the chromatographic column was controlled by a Princeton Applied Research Model 173 potentiostat/galvanostat and Model 175 universal programmer. A mobile phase flow rate of 1 mL/min was maintained with a DuPont Model 870 pump and Model 8800 pump controller. Analytes were detected by passing the eluent through an 8  $\mu$ L flow cell (Hellma Cells, Inc.) that was positioned in a Varian DMS 200 UV-Vis Spectrophotometer. The detection wavelength of 254 nm was found to be optimal for providing large analyte absorptivities and minimal mobile phase absorbance. Chromatograms

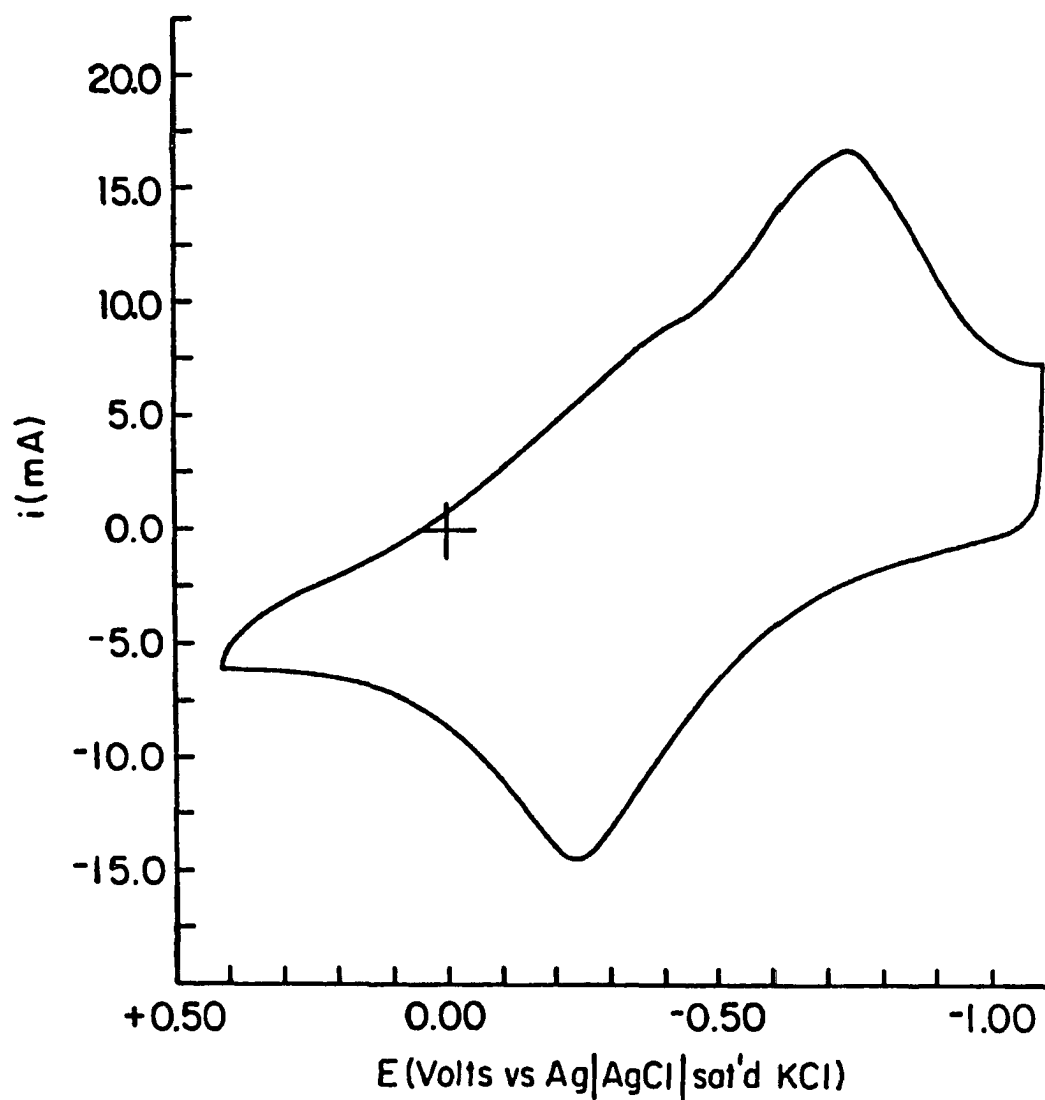


Figure 2. Steady-state cyclic voltammogram obtained using the electrochemical column for a 0.036  $\mu\text{m}$  polypyrrole coating that was electropolymerized onto GC particles. The supporting electrolyte was a 10 mM aqueous solution of  $\text{LiClO}_4$ . The scan rate was 10 mV/s.

were recorded as plots of absorbance vs. time with a Houston Instruments Omnigraphic 2000 XY recorder.

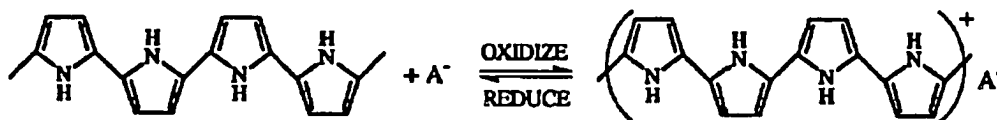
### **Reagents and Chemicals.**

All reagents were analytical grade. Adenosine triphosphate, as its disodium salt (ATP), and adenosine monophosphate monohydrate (AMP) were stored at 10°C and were used as received (both >99 % purity, Aldrich). Stock solutions of ATP and AMP were prepared daily as a consequence of slow phosphate hydrolysis [14]. Pyrrole (Aldrich) was vacuum distilled, and the colorless distillate was stored under nitrogen at 10°C. Lithium perchlorate (G. Frederick Smith Co.) and NaOTs (Aldrich) were used as received. Water was distilled and further purified using a Millipore Milli-Q water filtration system. The pH of the mobile phase was ~5.0. Based on their pK<sub>a</sub> values [15], equilibrium calculations indicated that at pH 5.0, AMP exists as a monovalent anion, whereas ATP exists as a trivalent anion.

## **RESULTS AND DISCUSSION**

### **Basis for Separations using a Conductive Polymer as a Charge-Controllable Stationary Phase.**

The functional basis for the use of a conductive polymer as a charge-controllable stationary phase for ion chromatography stems principally from the ability to transform the polymer between its oxidized and reduced forms by changes in applied voltage [8,10].

**Scheme I**

Polypyrrole is an attractive candidate for such purposes since, as shown in Scheme I, switching between its neutral (reduced) and cationic (oxidized) forms will lead to a change from an uncharged stationary phase to one with a high positive charge density. Upon oxidation, anions ( $A^-$ ) from the supporting electrolyte are incorporated into the film to maintain electroneutrality. In contrast, the reduction of polypyrrole leads to the expulsion of anions from the film [12,16]. As is apparent from the *i*-*E* curve in Figure 2, applied voltages greater than  $\sim 0.0$  V result in the extensive oxidation of the film, whereas those less than  $\sim -1.0$  V lead to the extensive reduction of the film. Though difficult to quantitate, it follows from the *i*-*E* curve that the fractional amounts of the oxidized and reduced forms of polypyrrole and, hence, the anion-exchange capacity of the stationary phase, can be controlled by the alteration of the applied voltage between these two limits. If a negatively charged analyte is then injected into the mobile phase, one can envision an approach to change the retention of  $A^-$  by altering electrochemically the fractional amounts of the oxidized and reduced forms of polypyrrole. By extension, two or more analytes could then be separated based on their differing affinities for the stationary phase.

In addition to the capability of altering the number of charged sites, polypyrrole as a stationary phase offers several other options for manipulating separations. For example, the porosity of a polypyrrole film exhibits a marked dependence on the size of the dopant anion used in the electropolymerization process. Once the film is formed, the rates of incorporation and expulsion of anions, i.e., the rates of the forward and reverse reactions in Scheme I, are strongly dependent on the size of the anionic counterion [17,18]. Therefore, small pore sizes would preferentially incorporate small anions, as well as restrict the interactions of large anions to the outermost layers of the film. This preparative dependence could be utilized for tailoring the porosity of the film, thus adding size discrimination as a variable for enhancing a separation. Similar strategies have recently been devised using conductive polymers as coatings on electrochemical detectors in liquid chromatography [19,20] and as electrochemically controlled membranes [21,22]. Furthermore, it is possible to modify the separation characteristics of polypyrrole films by incorporating functional groups as substituents on the pyrrole monomer [23-28]. Through such processing, the ionic characteristics of polypyrrole could be systematically designed by the incorporation of electroactive groups such as ferrocene [23] or viologen [24], whereas hydrophobic/hydrophilic groups could be added to tune interactions based on dispersion forces [25-28].

It is also important to note from an experimental viewpoint that the use of a coating material of high conductivity is desirable to facilitate charge propagation throughout the stationary phase. Ineffective propagation can result in longer film charging times and slower response characteristics, and will inevitably lead to temporal limitations in the waveforms

which can be applied to the stationary phase to effect a separation. In this regard, polypyrrole is an attractive stationary phase coating because it has a higher conductivity in its oxidized form than many of the other presently known conductive polymers [29].

### **Dependence of the Retention of AMP and ATP on the Voltage Applied to the Polypyrrole Stationary Phase.**

With conventional ion chromatography, the binding of an analyte reflects a mixture of chemical and physical interactions with the stationary phase. In general, the more highly charged analytes are more strongly retained by the stationary phase, eluting after analytes with a lower charge [30,31]. Other properties of the analyte (e.g., polarizability and hydrophobicity/hydrophilicity) typically play a secondary role in determining the strength of interaction. Since, as noted earlier for our experimental conditions, AMP exists mainly as a singly-charged anion and ATP as a triply-charged anion, it follows that the more highly charged ATP will compete more effectively for binding sites on the oxidized polypyrrole film. Both AMP and ATP will also compete for binding sites with  $\text{ClO}_4^-$ , the mobile phase anion. Figure 3 shows the percentage of a 1  $\mu\text{L}$  injection of a 10 mM AMP or ATP solution that is strongly retained on the stationary phase as a function of applied voltage. The solid and dashed curves give the data for AMP and ATP, respectively. 'Strongly retained' is defined here to mean that the injected species does not elute from the column in less than ten minutes. As shown in Figure 3, both AMP and ATP are totally retained on the column at applied voltages more positive than  $\sim -0.30$  V, where the anion-exchange capacity of polypyrrole is

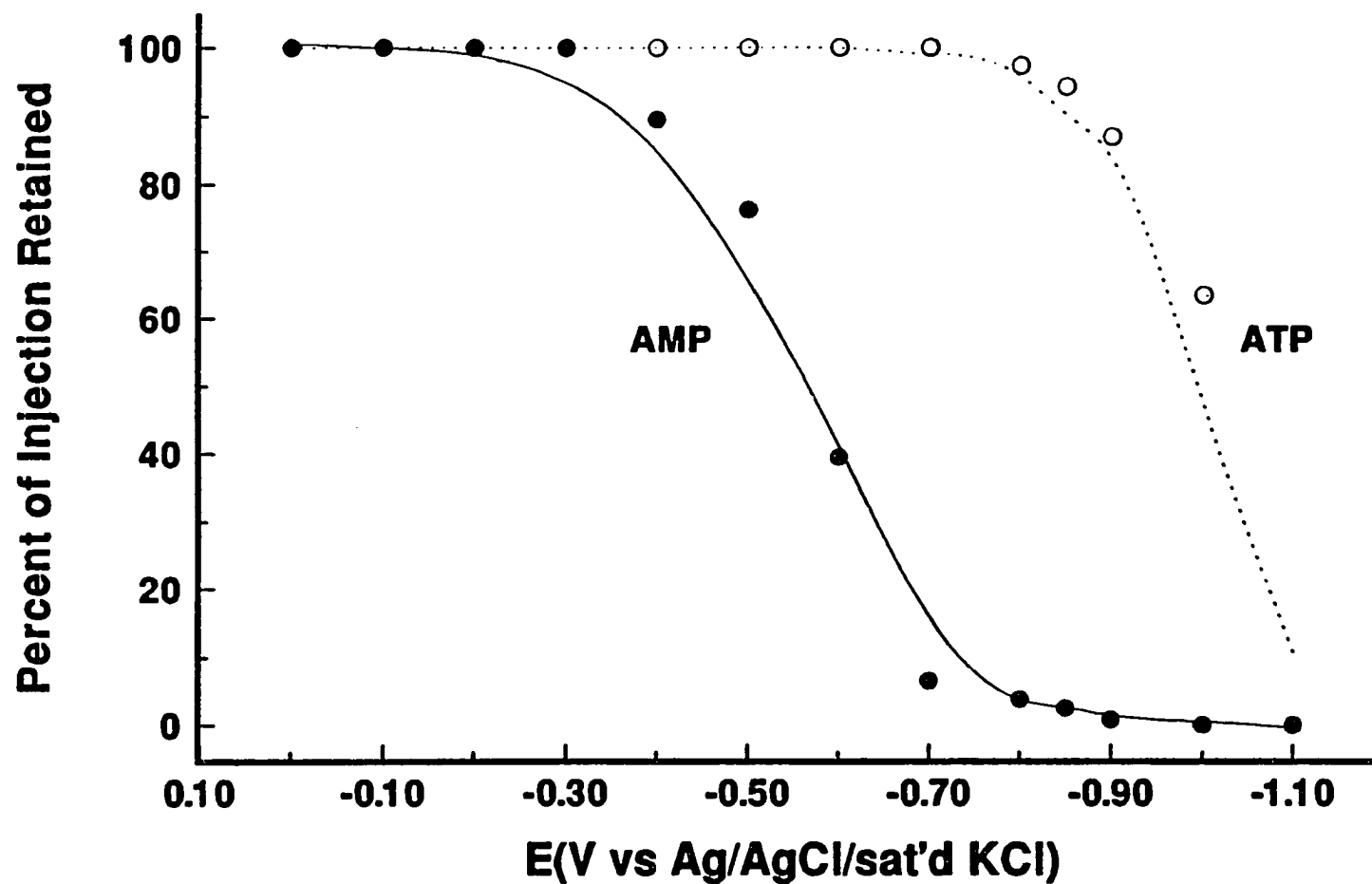


Figure 3. Plot of the percent of a 1  $\mu$ L injection of a 10 mM solution of either AMP (—) or ATP (.....) that is strongly retained at the polypyrrole stationary phase as a function of the applied voltage. The percent retention was calculated by integrating the chromatographic bands obtained at each applied voltage and normalizing to that at -1.10 V. The elution of AMP and ATP was monitored for ten min.

large due to its extensive oxidation. As the applied voltage becomes more negative, however, the retention of both AMP and ATP decrease with the elution of ATP occurring at  $\sim 0.4$  V more negative than that for AMP. This decrease in the retention of AMP and ATP occurs as a result of the decrease in the anion-exchange capacity of polypyrrole due to its reduction. At  $-1.10$  V, both AMP and ATP are completely unretained at polypyrrole due to its extensive reduction. These data illustrate clearly the ability of changes in the applied voltage to alter selectively the capacity of the polypyrrole stationary phase for these analytes. Further, the difference in the voltage-dependent behavior of AMP and ATP is consistent with the general principles for separating analytes of differing negative charges via ion chromatography [30,31], which confirm the feasibility of using polypyrrole as a charge-controllable stationary phase for ion chromatographic separations of AMP and ATP.

#### **Separation of AMP and ATP by a Voltage Step Waveform.**

The curves in Figure 3 also serve as a guide for selecting conditions for separating a mixture of AMP and ATP at a polypyrrole-coated stationary phase using an aqueous solution of  $10$  mM  $\text{LiClO}_4$  as the mobile phase. As discussed, the retention of AMP and ATP exhibit markedly different dependencies on the applied voltage. This difference is most notable between  $\sim -0.7$  V and  $\sim -0.9$  V. Throughout this voltage range, ATP is retained on the column to a much higher degree than AMP. One can then envision a method for separating the two species using, for example, a voltage waveform with an initial voltage that corresponds to the preferential retention of ATP and final voltage that results in the exhaustive expulsion of ATP from the stationary phase. The results of such a separation as well as comparative data for



each analyte are summarized in Figure 4. Figures 4a and 4b are chromatograms obtained after separate 0.5  $\mu\text{L}$  injections of 10 mM AMP and ATP solutions, respectively, at an applied voltage of -0.85 V. The applied voltage was stepped to -1.10 V 220 sec after injection. Figure 4a shows that AMP exhaustively elutes from the column while the applied voltage is held at -0.85 V. In contrast, Figure 4b shows that essentially all of the ATP is retained on the stationary phase until the voltage is stepped to -1.10 V. The portion of ATP (~6 %) that eluted prior to the voltage step, as evidenced by the broad, weakly absorbing peak in the chromatogram, is attributed to the limited capacity of the column at -0.85 V. Both chromatograms reflect the behavior expected from the curves in Figure 3, and, more importantly, suggest the possible separation of a mixture of AMP and ATP with the noted voltage waveform.

Figure 4c shows a separation of a mixture of AMP and ATP using the described voltage waveform. For this separation, a 1  $\mu\text{L}$  aliquot of an aqueous solution 5 mM in both AMP and ATP was injected onto the column. Consistent with the data for the injection of each individual component, the chromatogram in Figure 4c is essentially a superposition of those in Figures 4a and 4b. Together, these results demonstrate the ability to achieve separations at an electrochemically manipulated charge-controllable stationary phase.

#### **Separations of AMP and ATP with Linear Voltage Ramps.**

Because the stationary phase charge density and capacity can be altered electrochemically, a wide variety of voltage waveforms can be utilized to "fine-tune" a separation. Simple linear and triangular ramps as well as the more complex sine and square

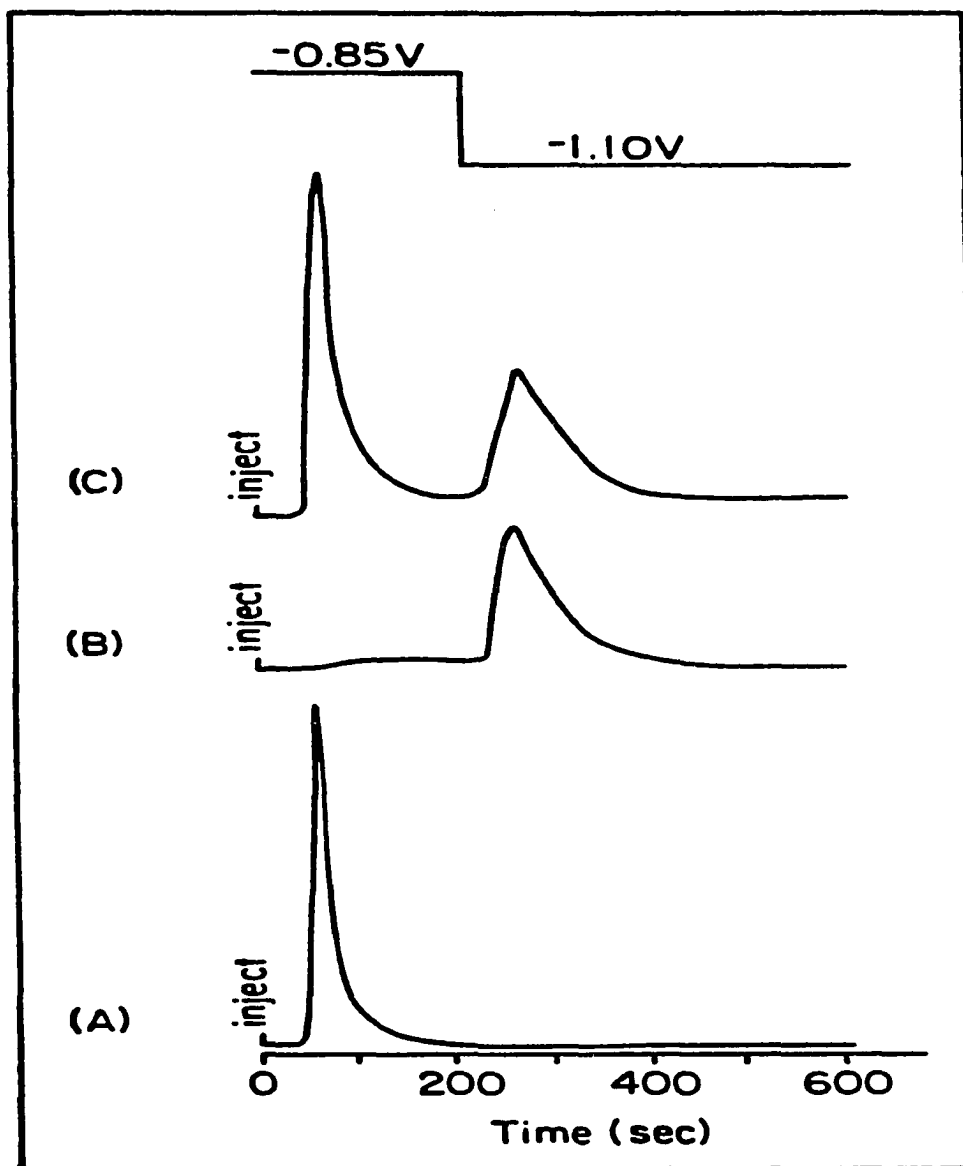


Figure 4. Chromatograms for AMP and ATP obtained by applying a voltage step to the polypyrrole coated stationary phase at an initial applied voltage of  $-0.85\text{ V}$ : (A) AMP; (B) ATP; (C) AMP + ATP. The voltage was stepped to  $-1.10\text{ V}$  220 sec after injection. Injection volumes equalled  $0.5\ \mu\text{L}$  of a  $10\text{ mM}$  solution for each chromatogram. The mobile phase electrolyte was  $10\text{ mM LiClO}_4$ .

functions could all conceivably be applied as voltage waveforms. Together with the selection of temporal variables (e.g., sweep rate) and the initial and final applied voltages, the possible voltage waveforms present a myriad of variables to employ in optimizing a separation. The chromatograms in Figures 5 and 6 demonstrate the manipulation of the separation of AMP and ATP at the polypyrrole-coated stationary phase through the application of a linear voltage ramp. The chromatograms in Figures 5a-g were obtained using respective initial voltages of -0.40 V, -0.50 V, -0.60 V, -0.70 V, -0.80 V, -0.90 V, and -1.00 V, with a 5 mV/s cathodic linear voltage ramp applied 10 sec after analyte injection. Injections were 2  $\mu$ L aliquots of the AMP/ATP mixture used for Figure 4c. As shown in Figure 3, the different initial voltages correspond to values where there are marked differences in the retention of the two species. Figure 5a shows a chromatogram for the injection of the AMP and ATP mixture at an initial applied voltage where both species are fully retained on the column (-0.40 V). With this set of conditions, the separation is ineffective, as the elution of both species strongly overlap. As the initial voltage becomes more negative, the retention of AMP on the stationary phase decreases with respect to that of ATP. As a consequence, AMP elutes prior to ATP. Coupled with the imposed linear voltage ramp, separations under such conditions are more effective, as illustrated in Figures 5b-e.

It is also important to note that the retention times of both AMP and ATP are dramatically altered by the changes in the initial applied voltage, as shown in Figure 5. For example, changes in the initial voltage from -0.50 V to -0.80 V leads to changes in the retention time of AMP from 110 sec to 60 sec. For the same set of conditions, the retention

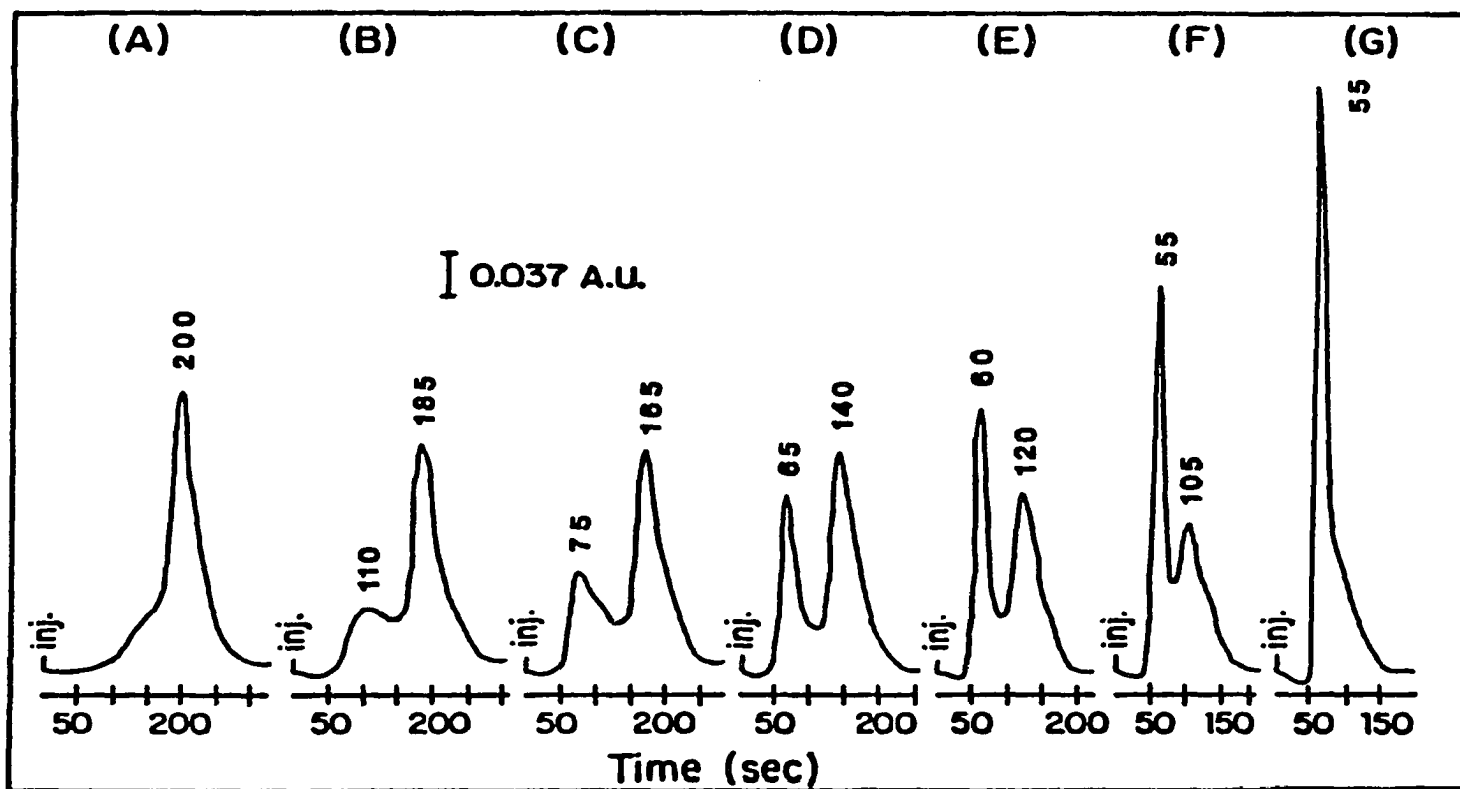


Figure 5. Chromatograms for AMP and ATP obtained by applying a 5 mV/s cathodic voltage ramp to the polypyrrole coated stationary phase at varying initial voltages: (A) -0.40 V; (B) -0.50 V; (C) -0.60 V; (D) -0.70 V; (E) -0.80 V; (F) -0.90 V; (G) -1.00 V. The final voltages were all -1.10 V. Injection volumes were 2  $\mu$ L of a 5mM solution of AMP and ATP. The voltage sweep was initiated 10 seconds after injection. The retention times for each elution band are given above each peak.

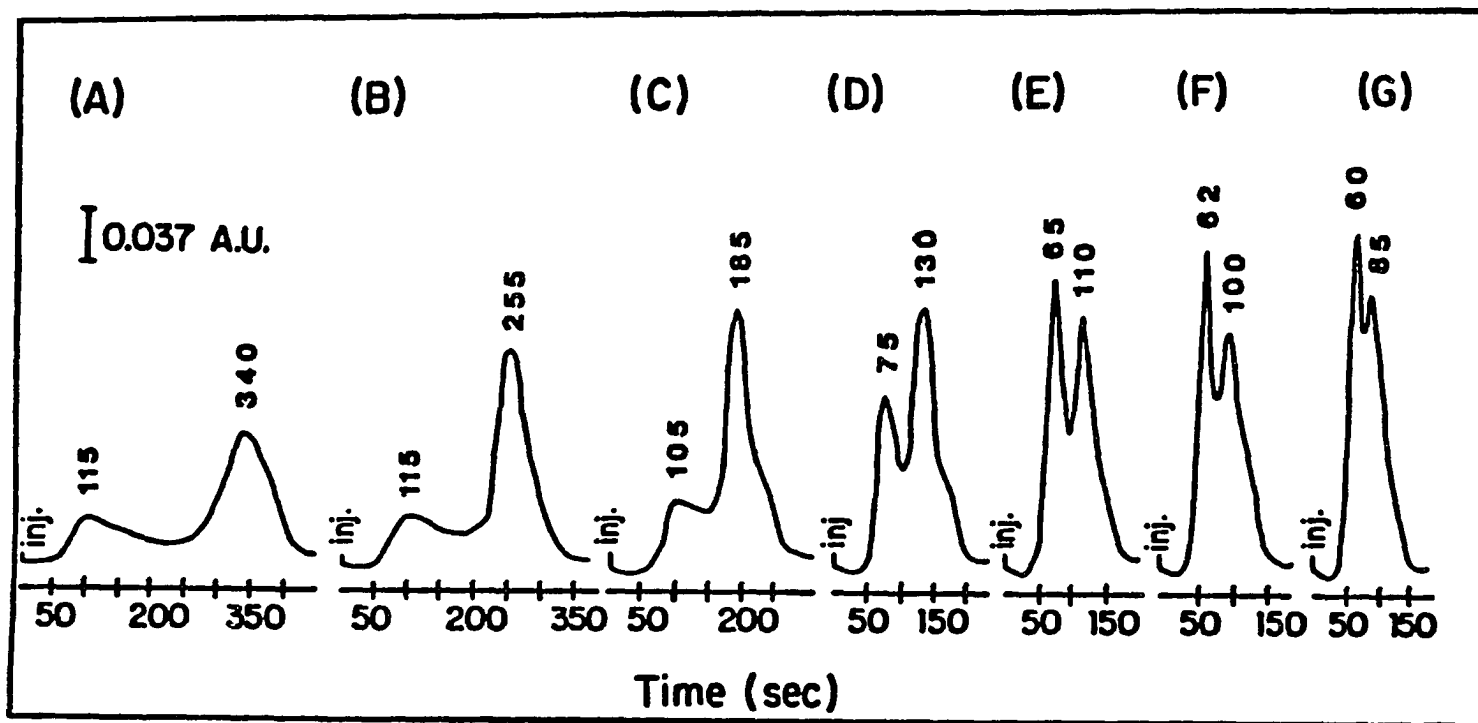


Figure 6. Chromatograms for AMP and ATP obtained by applying a cathodic linear voltage ramp to the polypyrrole-coated stationary phase at varying sweep rates: (A) 2 mV/s; (B) 3 mV/s; (C) 5 mV/s; (D) 10 mV/s; (E) 15 mV/s; (F) 20 mV/s; (G) 30 mV/s. The initial and final voltages were all -0.50 V and -1.10 V, respectively. Injection volumes were 2  $\mu$ L of a 5 mM solution of AMP and ATP. The voltage sweep was initiated 10 sec after injection. The retention times for each elution band are given above each peak.

times for ATP decrease from 185 sec to 120 sec. In contrast, if the initial voltage is such that the polypyrrole-coated stationary phase exists largely in its reduced (neutral) form, neither AMP or ATP are strongly retained on the column. This results in a decrease in separation ability, as shown by the chromatograms in Figures 5f and 5g. Thus, by adjusting the voltage applied to the stationary phase prior to the linear voltage sweep, the retention times of both AMP and ATP can be altered, which leads to the differences in separation efficiency.

In addition to changes in the initial applied voltage on the stationary phase, alterations of the slope of the linear voltage ramp presents another possible approach for manipulating the separation of AMP and ATP. The chromatograms shown in Figure 6 were obtained by ramping the voltage linearly from -0.50 V to -1.10 V at different sweep rates. Figures 6a-g display the chromatograms resulting from sweep rates of 2, 3, 5, 10, 15, 20, and 30 mV/s, respectively. The retention times for both AMP and ATP in each of the chromatograms are also listed in Figure 6. Injections consisted of 2  $\mu$ L of the aforementioned 5 mM AMP/ATP mixture. The voltage was ramped 10 sec after injection. In these experiments, the fractional amount of oxidized polypyrrole and therefore the retention of AMP and ATP is held at a constant initial level with variations in sweep rate used to alter the separation. This is in contrast to the conditions used for the separations in Figure 5, where differences in the initial applied voltage and therefore the fractional amount of oxidized polypyrrole were used primarily as the means to change retention. As is apparent, increases in sweep rate markedly decrease the retention times of the two species. The changes essentially reflect the rate at which the column is changed from its oxidized to its reduced form during elution. At slow

sweep rates (e.g., 2 mV/s), the elution of AMP proceeds to a significant level before that of ATP begins. However, as the sweep rate increases, the elution of both species begins to overlap. The chromatograms in Figures 6b-f demonstrate the decreases in resolution and retention time of the AMP and ATP elution bands with increases in sweep rate. At larger sweep rates (e.g. 30 mV/s), the retention of ATP is insufficient to allow the prior elution of AMP, which yields chromatograms such as that in Figure 6g. These changes are also reflected in the decrease in the retention times and peak widths of the bands with increasing sweep rate. Though not shown, as the sweep rate is increased further, the retention times of both species decrease and eventually converge. Consequently, only one elution peak is evident at sweep rates greater than 40 mV/s. These results further demonstrate the feasibility of manipulating separations through electrochemically-induced changes in a charge-controllable stationary phase.

## CONCLUSIONS

The feasibility of using a conductive polymer coating as a charge-controllable stationary phase for ion chromatographic separations has been demonstrated. Through electrochemically-induced changes in the positive charge density and therefore the anion-exchange capacity of a stationary phase consisting of polypyrrole coated glassy carbon particles, the retention and hence the separation efficiency of AMP and ATP could be manipulated. Separations could be manipulated using both voltage steps and linear voltage sweeps, which suggest a myriad of new avenues for optimizing a separation. In addition to

assessing the range and scope of this new technique, experiments to address fundamental questions concerning the retention mechanism (e.g., the competitive binding of analytes and electrolyte) are in progress. Approaches to fabricate GC particles with a more uniform size and shape are also being tested.

### ACKNOWLEDGMENTS

Discussions with W. LaCourse are appreciated, as well as the loan of the PAR 175 universal programmer by D.C. Johnson. M.D.P. gratefully acknowledges the support of a Dow Corning Assistant Professorship. K.S. expresses appreciation for the travel expenses provided by the Yoshida Foundation for Science and Technology. This work was supported by the National Science Foundation (Grant CHE-9003308). Ames Laboratory is operated for the U.S. Department of Energy by Iowa State University under Contract No. W-7405-Eng-82.

### REFERENCES

1. Poole, C.F.; Schuette, S.A. *Contemporary Practice of Chromatography*, Elsevier: Amsterdam, 1984.
2. Fritz, J.S.; Gjerde, D.T. *Ion Chromatography*, 2nd ed., Heidelberg: Huthig, 1986.
3. Blaedel, W.J.; Strohl, J.H. *Anal. Chem.* **1964**, *36*, 1245.
4. Strohl, J.H.; Dunlap, K.L. *Anal. Chem.* **1972**, *44*, 2166.
5. Fujinaga, T.; Kihara, S. *CRC Crit. Rev. Anal. Chem.* **1977**, *7*, 223.
6. Hern, J.L.; Strohl, J.H. *Anal. Chem.*, **1978**, *50*, 1955.



7. Antrim, R.F.; Scherrer, R.A. Yacynych, A.M. *Anal. Chim. Acta.* **1984**, *164*, 283.
8. Ghatak-Roy, A.R.; Martin, C.R. *Anal. Chem.* **1986**, *58*, 1574.
9. Ge, H.; Wallace, G.G. *Anal. Chem.* **1989**, *61*, 198.
10. Ge, H.; Wallace, G.G. *Anal. Chem.* **1989**, *61*, 2391.
11. Skotheim, T.; Rosenthal, M.V.; Linkous, C.A. *J. Chem. Soc. Chem. Comm.* **1985**, 612.
12. Bull, R.A.; Fan, F.F.; Bard, A.J. *J. Electrochem. Soc.* **1982**, *129*, 1009.
13. Miller, L.L.; Zinger, B.; Zhou, Q. *J. Am. Chem. Soc.* **1987**, *109*, 2267.
14. Stryer, L. *Biochemistry*, 3rd ed., W.H. Freeman & Co.: New York, 1988, pp. 317-18.
15. Hata, L. *Handbook of Chemistry*, Vol. 2, Chemical Society of Japan, Maruzen, Tokyo, 1984.
16. Diaz, A.F.; Castillo, J.I.; Logan, J.A.; Lee, W.Y. *J. Electroanal. Chem.* **1981**, *129*, 115.
17. Shimidzu, T.; Ohtani, A.; Iyoda, T.; Honda, K. *J. Electroanal. Chem.* **1987**, *224*, 123.
18. Orata, D.; Buttry, D.A. *J. Am. Chem. Soc.* **1987**, *109*, 3574.
19. Ikariyama, Y.; Heineman, W.R. *Anal. Chem.* **1986**, *58*, 1803.
20. Ye, J.; Baldwin, R.P. *Anal. Chem.* **1988**, *60*, 1982.
21. Burgmayer, P.; Murray, R.W. *J. Am. Chem. Soc.* **1982**, *104*, 6139.
22. Factor, A.; Rouse, T.O. *J. Electrochem. Soc.* **1980**, *127*, 1313.
23. Inagaki, T.; Skotheim, T.A.; Lee, H.S.; Okamoto, Y.; Samuelson, L.; Tripathy, S. *Synth. Met.* **1989**, *28*, C245.
24. Ofer, D.; Crooks, R.M.; Wrighton, M.S. *J. Am. Chem. Soc.* **1990**, *112*, 7869.
25. Andereux, C.P.; Audebert, P. *J. Electroanal. Chem.* **1990**, *285*, 163.

26. Rahman, A.K.M.; Samuelson, L.; Minehan, D.; Clough, S.; Tripathy, S.; Inagaki, T.; Yang, X.Q.; Skotheim, T.A.; Okamoto, Y. *Synth. Met.* **1989**, *28*, C237.
27. Diaz, A.F.; Martinez, A.; Kanazawa, K.K.; Salmon, M. *J. Electroanal. Chem.* **1981**, *130*, 181.
28. Anderson, H.J.; Loader, C.E. *Synthesis* **1985**, 353.
29. Kanatzidis, M.G. *C & E News* **1990**, *68*, 36.
30. Haddad, P.R.; Jackson, P.E. *Ion Chromatography*, Elsevier: Amsterdam, 1990.
31. Small, H. *Ion Chromatography*, Plenum Press: New York, 1989.

**CHAPTER 2. EVALUATION OF THE RETENTION CHARACTERISTICS OF  
POLYPYRROLE AS A STATIONARY PHASE FOR THE  
ELECTROCHEMICAL ION CHROMATOGRAPHIC (ECIC)  
SEPARATION OF DANSYL AMINO ACIDS**

*A paper to be submitted to the Journal of Electroanalytical Chemistry*

Randall S. Deinhammer, Katsuaki Shimazu, and Marc D. Porter<sup>1</sup>

**ABSTRACT**

An approach for the dynamic modification of the separations of dansyl amino acids (DAAs) prior to and during elution using a novel electrochemical ion chromatographic (ECIC) system is described. The ECIC system consists of polypyrrole (PPy)-coated glassy carbon spheres which are connected as the working electrode in a three-electrode electrochemical cell arrangement. Electrochemical switching of PPy between its oxidized (cationic) and reduced (neutral) forms allowed for alteration of the anion-exchange capacity of the stationary phase over a wide range. Modification of the voltage applied to the PPy prior to injection was used to alter the capacity factors of the DAAs by at least an order of magnitude. Voltage steps applied to the column during elution were used to optimize the separation of a mixture of three DAAs. In a manner directly analogous to gradient elution in conventional anion-exchange chromatography, both peak half-widths and retention times

---

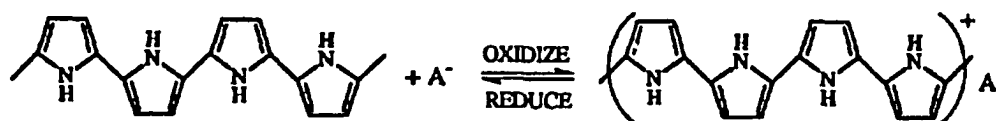
<sup>1</sup>Author to whom correspondence should be addressed.

could be significantly decreased using this technique. These studies also provided evidence for the preferential interaction of PPy in its fully oxidized, partially oxidized, and reduced forms with hydrophobic,  $\pi$ -electron containing anions. Such interactions were investigated through analysis of the PPy films using both energy-dispersive x-ray analysis and quartz crystal microbalance techniques. The application of the ECIC system to the concentration of dilute (~1 ppm) solutions of the DAAs is also briefly discussed.

## INTRODUCTION

The use of high performance ion-exchange chromatography has grown explosively during the past several years [1-13]. Applications include the separation of inorganic [1-4] and macromolecular [5-7] ions, the profiling of biological fluids [8-12], and the diagnosis of metabolic disorders [13]. Such separations, however, generally utilize a stationary phase with a fixed composition, i.e. materials with a fixed number of exchange sites. As a consequence, the optimization of a separation relies on alteration of the composition (e.g., concentration of organic modifier, ionic strength, and pH) [14-16] and/or flow rate of the mobile phase.

Recent reports have described the testing of conductive polymers as stationary phases for a new form of chemical separations [17-23]. The interest in this new method stems from the potential to alter the capacity of the column through electrochemically-induced changes in the composition of the stationary phase. As shown in Scheme I, a material such as polypyrrole (PPy) can be switched electrochemically between its oxidized and reduced forms with the concomitant uptake or expulsion of anions ( $A^-$ ) [24,25]. Thus, changes in the applied

**Scheme I**

voltage transform the stationary phase between one devoid of exchange sites to one with a large number of exchange sites. This approach has led to the development of stationary phases with a capacity that can be altered *prior to analyte elution* [18-20].

As part of our interests in this area, we have recently extended the above concept through the construction and preliminary testing of what we have dubbed an electrochemical ion chromatographic (ECIC) system [19]. Therein, we demonstrated that a variety of voltage waveforms could be applied *during analyte elution* to a stationary phase fabricated from PPy-coated glassy carbon (GC) particles for manipulating the separation of the nucleotides adenosine monophosphate (AMP) and adenosine triphosphate (ATP). However, both the strong retention of AMP and ATP at the PPy stationary phase and the nonuniformity of the GC particles precluded an in-depth assessment of the general utility of this new separation methodology. These complications also hindered the development of insights into the retention mechanism. This paper, and others to follow, presents the findings of efforts that address these issues.

In the subsequent sections, the retention and separation of a variety of dansyl amino acids (DAAs) are examined as a function of the voltage applied to a PPy stationary phase *both*

*prior to and during analyte elution.* The DAAs (see Table I) were chosen to probe the effects of both the charge and the hydrophobicity of the analyte on retention. This range of analyte properties reflects the potential capability of PPy to function not only in an anion exchange (anex) mode, but also in a reverse phase mode; the latter arises largely as a consequence of donor-acceptor (i.e.,  $\pi$ - $\pi$  and  $n$ - $\pi$ ) and hydrophobic interactions between the aromatic backbone of PPy and analyte anions [20,26]. The stationary phase was prepared by the electropolymerization of PPy at GC with tosylate (OTs) as the dopant anion (PPy/OTs). The resulting ion-transport properties of these films, the characterization of which constitutes a significant portion of the effort herein, were investigated using energy dispersive x-ray analysis (EDX) and quartz crystal microbalance techniques (QCM). Sodium benzoate (NaBz) was used as the mobile phase electrolyte because of its strength as an eluent, which facilitated determinations of capacity factors ( $k'$  values). Changes in applied voltage prior to elution probed the retention of DAAs as a function of the extent of PPy/OTs oxidation. Alterations in applied voltage during elution were tested as a starting point for developing separations using ECIC under conditions similar to those in gradient elution anex chromatography.

## EXPERIMENTAL

### Construction of the Electrochemical Chromatographic Column.

The general construction of the ECIC column is described elsewhere [19].

### **Characterization of the Glassy Carbon Support.**

A scanning electron micrograph of the GC support (custom preparation by Tokai Carbon) is shown in Figure 1. Both large spherically shaped particles as well as agglomerated clusters of smaller particles are evident. The diameters of the individual particles range from 15 to 30  $\mu\text{m}$ ; with an estimated average of  $\sim 25 \mu\text{m}$  (neglecting the clusters). The clusters comprise  $\sim 30\%$  of the sample, and could not be removed by repeated sieving. Both the size and shape of the custom-made support represent large improvements over those in our earlier study, which were nonspherical in shape and had diameters between 70 and 230  $\mu\text{m}$ . However, further decreases in the diameter and improvements in uniformity are needed to minimize their deleterious effects on the widths of the elution bands [27].

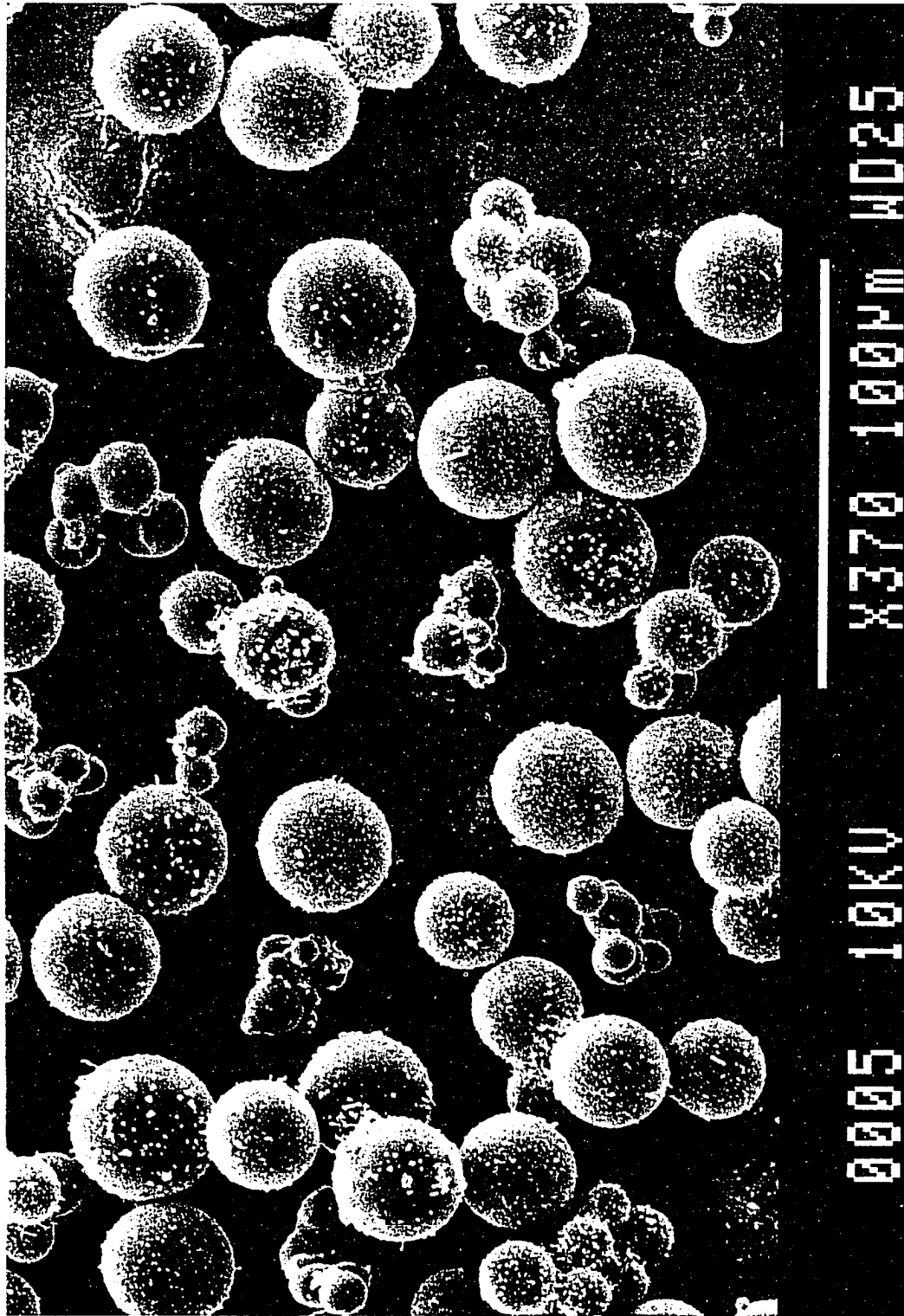
Prior to deposition of PPy, the spheres were activated [28-30] in an oxygen plasma (Harrick Scientific, Model PD-32G) for about seven minutes. The plasma pressure was  $3 \times 10^{-2}$  torr. The surface area of the plasma oxidized GC spheres was determined using a BET surface area analyzer (Micromeritics Accusorb 2100E). With Kr as the adsorption gas, an eight point linear plot ( $r=1.00$ ) yielded a surface area of  $0.42 \text{ m}^2/\text{g}$ .

### **Polypyrrole Film Formation.**

Thin PPy/OTs films were electropolymerized onto the GC spheres in a step-wise manner prior to packing into the Nafion tubing. First, 1.1 g of the GC spheres were split into three equal portions, each dispersed separately in a solution of 0.15 M pyrrole and 0.15 M NaOTs. Each portion was then slurry packed into a 12 cm long Nafion tube, which was

**Figure 1. Scanning electron micrograph of the uncoated 25  $\mu\text{m}$  GC spheres. The accelerating voltage was 10 kV.**





mounted in a smaller version of the described chromatographic column. The PPy/OTs was electropolymerized onto the GC spheres by applying a double voltage step: 0.00 V to +1.00 V for 2 sec and then to +0.60 V [19]. The applied voltage was held at +0.60 V until a charge corresponding to a film thickness of ~5 nm had passed (assuming a GC density of 1.5 g/cm<sup>3</sup> and a BET surface area of 0.42 m<sup>2</sup>/g). The PPy/OTs-coated spheres were then removed from the Nafion tube, rinsed with 0.15 M NaOTs, and repacked into the tube. The above procedure was then repeated to polymerize a second PPy/OTs layer. Finally, the three portions of the twice-coated spheres were combined and slurry packed into the 24 cm long Nafion tube in 0.15 M NaOTs. These films provided reproducible chromatograms, i.e., retention times varied by  $\pm 10\%$  (RSD), for ~ one week of continued use.

We believe the above coating procedure leads to a more uniform deposition of PPy onto the GC spheres than our previous single-coating method [19]. The multiple coating procedure exposes regions of the packing ineffectively coated during the first polymerization step to additional polymerization, thereby increasing the capacity and uniformity of the column. The ineffectiveness of a single coating process arises from the relatively large electrical resistance (i.e. contact resistance between GC spheres, ion transport resistance of Nafion, and solution resistance) in our ECIC column. Similar complications have been found for the in situ coating of PPy onto graphite particles in a pulsed-bed reactor [31].

#### **General Mode of Operation.**

Prior to use, the chromatographic column was equilibrated with the degassed mobile phase (0.10 M NaBz, pH 7.0) at 0.90 mL/min for ~30 min. The dead volume of the column

(0.60 mL) was estimated by injection of water. A minimum of three dead volumes of mobile phase were passed through the column for re-equilibration between experiments. Capacity factors were calculated as described previously [27].

### **Instrumentation.**

The voltage applied to the stationary phase was controlled by a Princeton Applied Research Model 173 galvanostat/potentiostat and Model 175 universal programmer. The chromatographic system consisted of a DuPont Model 870 liquid chromatographic pump and Model 8800 pump controller. A Varian DMS 200 UV-Vis spectrophotometer with an 8  $\mu$ L flow-through cell (Hellma) served as the detector. The detection wavelength was 325 nm. Chromatograms were recorded using a Houston Instruments Omnigraphic 2000 X-Y-t recorder.

Scanning electron micrographs and EDX spectra were obtained using a JEOL Model SM12 electron microscope equipped with a Kevex Delta 4 Quantum thin window x-ray detector. The accelerating voltages were 10 and 5 kV, respectively. Acquisition times for the EDX spectra were 100 sec, and the incident angle was 70° from the surface normal.

Quartz crystal microbalance studies were performed using gold-coated AT-cut crystals (5 MHz). The crystals were mounted in a MAXTEK Model TPS500 EQCM sensor, and connected to a Philips Model PM6654C frequency counter.

**Chemicals.**

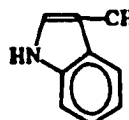
All DAAs (>98% purity) were from Sigma and were used as received. The solid compounds were stored at 0°C to prevent hydrolysis [32]. Analyte solutions were stored at 10°C, with fresh solutions prepared every two days. The chemical structures of the DAAs are listed in Table I, together with their hydrophobicity parameters (log P) [33,34]. The log P values in Table I are for the deprotonated forms of the DAAs [35], and have been normalized such that glycine has a log P value of zero. As such, molecules with positive values of log P are more hydrophobic than glycine, and molecules with negative values of log P are more hydrophilic than glycine.

Sodium tosylate (NaOTs), sodium benzoate (NaBz), and benzoic acid (all from Aldrich) were reagent grade and used as received. Pyrrole (Aldrich) was vacuum distilled, with the colorless distillate stored under nitrogen at 10°C. Solutions were prepared with water purified using a Millipore Milli-Q system.

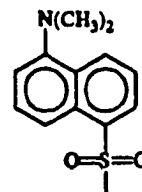
**RESULTS AND DISCUSSION****Relationship Between the Applied Voltage and the Exchange Capacity of Polypyrrole.**

The fundamental basis for the use of PPy as a charge-controllable stationary phase derives from the ability to switch the polymer between its oxidized and reduced forms by changes in applied voltage. In order to describe adequately the interaction of analytes with PPy in each of its redox states, a relationship between its exchange capacity and the applied voltage is needed. Such a relationship will be largely dependent on the ion-transport

Table I. Structures and normalized hydrophobicity constants of selected DAAs.

DANSYL AMINO ACID STRUCTURE <sup>a</sup>	ACRONYM	log P
$\begin{array}{c} \text{DAN} \\   \\ \text{NH} \\   \\ \text{OOC}-\text{CH}_2-\text{CH} \\   \\ \text{COO}^- \end{array}$	DASP	-4.83
$\begin{array}{c} \text{DAN} \\   \\ \text{NH} \\   \\ \text{H}_2\text{N}-\text{C}(=\text{O})-\text{CH}_2-\text{CH} \\   \\ \text{COO}^- \end{array}$	DASN	-0.60
$\begin{array}{c} \text{DAN} \\   \\ \text{NH} \\   \\ \text{HO}-\text{CH}_2-\text{CH} \\   \\ \text{COO}^- \end{array}$	DSER	-0.04
$\begin{array}{c} \text{DAN} \\   \\ \text{NH} \\   \\ \text{CH}_2 \\   \\ \text{COO}^- \end{array}$	DGLY	0.00
$\begin{array}{c} \text{DAN} \\   \\ \text{NH} \\   \\ \text{CH}_2-\text{CH} \\ / \quad   \quad \backslash \\ \text{CH}_3 \quad \text{COO}^- \quad \text{CH}_3 \end{array}$	DLEU	1.70
$\begin{array}{c} \text{DAN} \\   \\ \text{NH} \\   \\ \text{C}_6\text{H}_5-\text{CH}_2-\text{CH} \\   \\ \text{COO}^- \end{array}$	DPHE	1.79
$\begin{array}{c} \text{DAN} \\   \\ \text{NH} \\   \\ \text{CH}_2-\text{CH} \\   \\ \text{COO}^- \end{array}$ 	DTRP	2.25

<sup>a</sup>DAN represents the 1-dimethylaminonaphthalene-5-sulfonyl group



characteristics of PPy, which will determine the types of ions (i.e. cations or anions) that can interact with both the oxidized and reduced forms of PPy.

Figure 2 presents a steady-state cyclic voltammogram (CV) at the PPy/OTs ECIC column. The CV was recorded at 5 mV/s in stagnant 0.10 M NaBz, and is only slightly different from that in 0.10 M NaOTs. The positions of both the anodic and cathodic waves (near -0.5 V) suggest that cation transport [36-45], as opposed to anion transport [46], is the predominate mode of charge compensation. Cation-dominated transport would arise from the entrapment of large dopant anions (e.g., OTs [36,37], dodecylsulfonate [38-41], and polymeric anions [42-45]) within the polymeric matrix during electrodeposition. Thus, PPy would require the respective incorporation or expulsion of cations upon reduction or oxidation to maintain electroneutrality. Conversely, the electrodeposition of PPy in electrolytes composed of small inorganic anions (e.g.,  $\text{Cl}^-$  and  $\text{ClO}_4^-$ ) would result in a film effectively devoid of entrapped dopant anions in its fully reduced state [46]. Charge compensation in these latter cases would require the respective expulsion or incorporation of anions upon reduction or oxidation. Importantly, the electrochemical transformation of PPy in the anion transport case should occur at applied voltages more positive than in the cation transport case. Such a voltage shift arises from an increase in the hydrophilicity of PPy as a result of anion entrapment [47]. The enhanced hydrophilicity decreases the thermodynamic barrier for movement of ions within the film upon electrolysis. In contrast, the electrochemical transformation of PPy dominated by anion transport requires the movement of ions in a more hydrophobic material, a process which is thermodynamically less favorable.

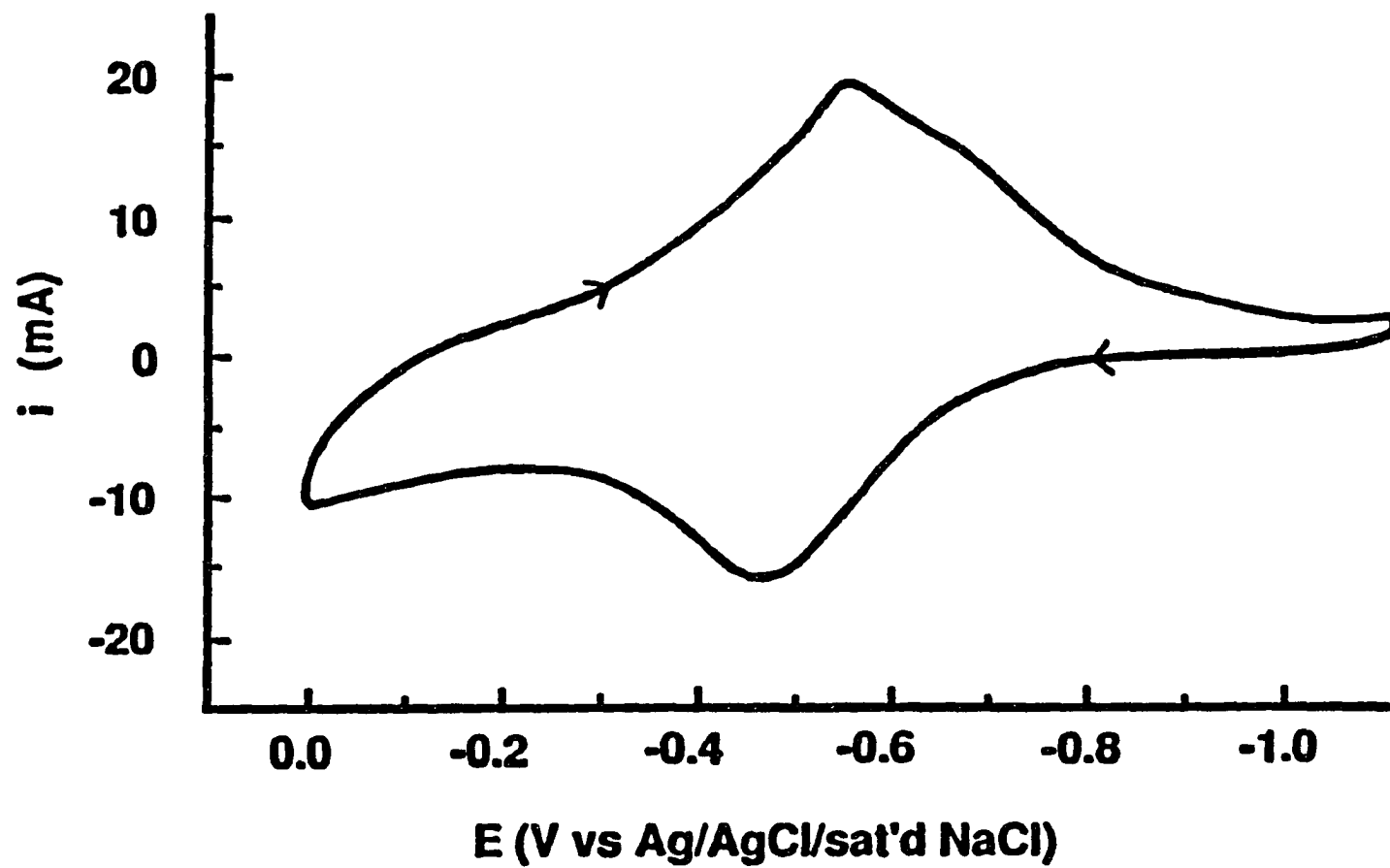


Figure 2. Cyclic voltammetric curve for PPy/OTs in aqueous 0.10 M NaBz. An Ag wire electrode was used as a quasi reference electrode. The sweep rate was 5 mV/s.

Although the CV in Figure 2 points to a strongly cation-dominated ion transport mechanism for our PPy/OTs, several recent reports have suggested a mixed mode mechanism for PPy/OTs, in which both electrolyte anions and cations participate in charge compensation [36,37,46]. To compare our PPy/OTs films with those prepared by others, we attempted to simulate the growth conditions of PPy on the column at GC plate electrodes (area  $\sim 0.5 \text{ cm}^2$ ). Use of the GC plate electrodes for these studies facilitated characterization of the resulting PPy/OTs films using EDX and QCM techniques. For these studies, growth of PPy was accomplished from a 50 mM pyrrole, 50 mM NaOTs solution by applying a constant voltage of +0.60 V until a film thickness of  $\sim 30 \text{ nm}$  was obtained. Such preparation conditions were found to produce voltammetry most similar to that in Figure 2. A constant voltage, rather than a two voltage step waveform, was used for polymerization to mimic the large electrical resistance likely present in the column.

Figures 3a-d show EDX spectra in the sulfur region for PPy/OTs films electrochemically cycled to steady-state in either 0.1 M NaOTs (Figures 3a,b) or 0.1 M NaBz (Figures 3c,d). The spectrum in Figure 3f serves as a blank and was obtained for an uncoated GC electrode cycled in 0.1 M NaOTs only. In all cases, the electrodes were withdrawn from solution under voltage control at either 0.00 V (Figures 3a,c) or -1.00 V (Figures 3b,d) to prevent alteration of the ion content of the films. The sulfur signal in each spectrum arises from the sulfur-containing OTs anions present in the PPy film. Figures 3a,b indicate that the sulfur content  $[(\text{count rate of sulfur}/\text{count rate of carbon}) \times 100, \text{ S/C}]$  of the PPy film decreases by  $\sim 40\%$  upon its reduction ( $\text{S/C}=2.33$  vs 1.35), consistent with the expulsion of OTs anions. However, the significant portion ( $\sim 60\%$ ) of the OTs anions not expelled at -1.00 V suggests



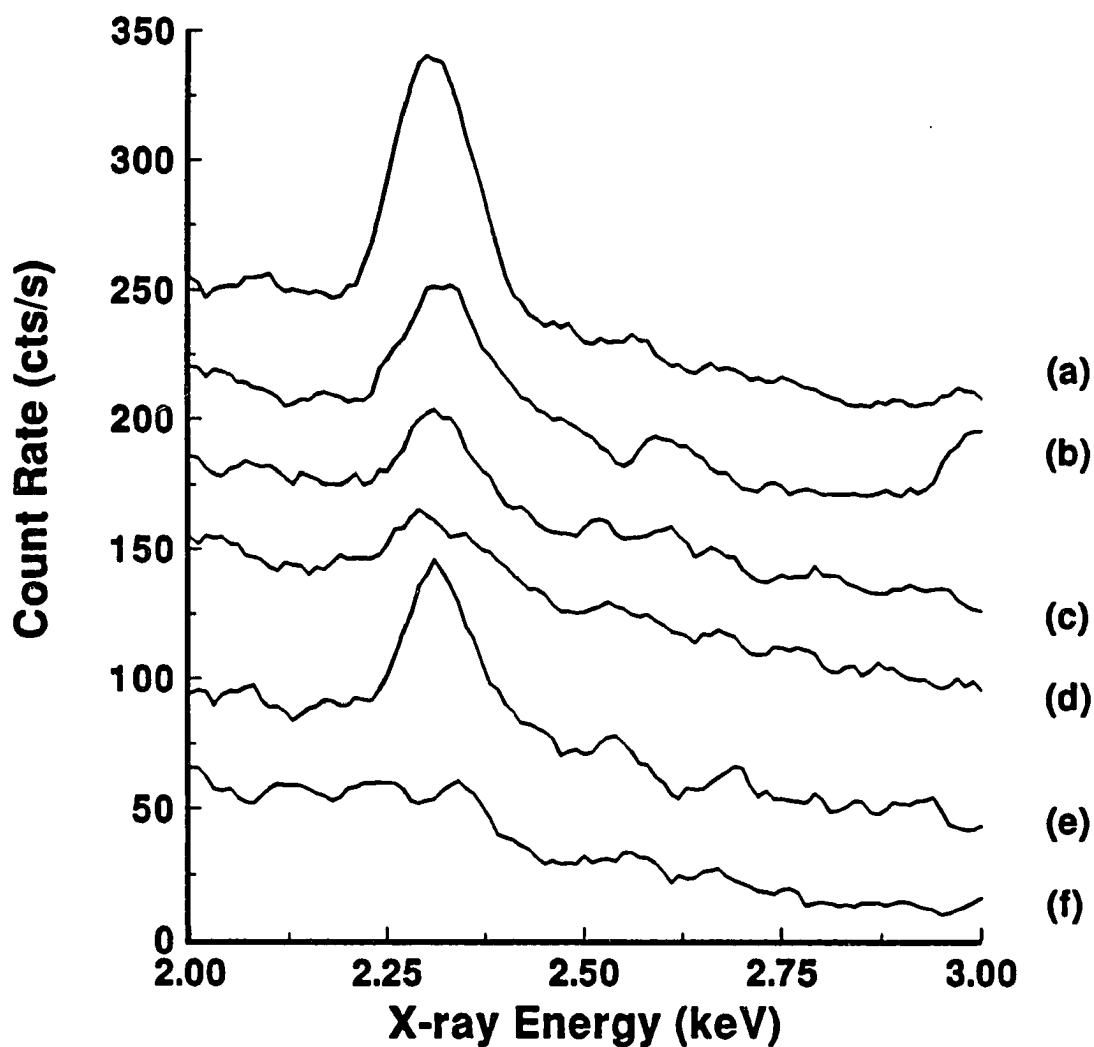


Figure 3. Energy-dispersive x-ray spectra in the sulfur region of 30 nm PPy/OTs films cycled to steady-state in 0.10 M NaOTs (a, b), 0.10 M NaBz (c,d), or 5 mM DGLY (pH 7.0 ,e). The spectra in (a), (c), and (e) were obtained at GC electrodes withdrawn from solution at 0.00 V, whereas those in (b) and (d) were obtained at GC electrodes withdrawn from solution at -1.00 V. The spectrum in (f) was obtained for an uncoated GC electrode cycled in 0.10 M NaOTs. The incident angle was  $70^\circ$  from the surface normal.

the dominance of cation transport in the overall ion transport mechanism. This decrease in sulfur content also results in a corresponding increase in sodium content upon reduction (data not shown), consistent with the cation transport mechanism. The dominance of cation transport in these films was also confirmed through preliminary QCM measurements, which showed an increase in resonant frequency upon PPy oxidation (i.e., cation expulsion). Upon cycling the PPy/OTs film in 0.1 M NaBz, a significant decrease in the sulfur content of the PPy film at 0.00 V is observed (S/C=1.03 vs 2.33). This decrease in S/C is consistent with the exchange of OTs anions for Bz anions, since the Bz anions contain no sulfur in their chemical structures. Such a decrease further points to the extensive exchange of OTs anions with Bz anions upon voltage cycling. However, a portion of the OTs anions appear to be strongly entrapped within the PPy film, and cannot be easily exchanged. This conclusion is supported by the essentially unchanged sulfur content of the PPy film observed upon its reduction (S/C=0.85, Figure 3d). These conclusions are in accord with those described previously for PPy films containing entrapped long alkyl chain anionic surfactants [39,41]. In addition, the sodium content of these Bz exchanged films continues to follow the changes seen for the PPy films cycled in OTs only, suggesting the continued contribution of cation transport in these films.

The above discussion indicates that ion transport in our PPy films likely consists of both an anion (~40%) and a cation (~60%) component. Although a significant portion of PPy should therefore be available for charge interaction with the DAAs, their large size relative to the OTs anions used for film polymerization (~1100 Å<sup>3</sup> vs 300 Å<sup>3</sup>) likely limit interactions

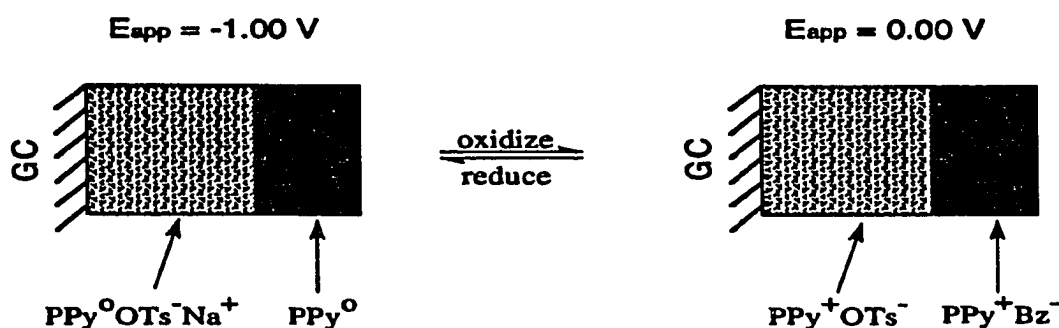
relevant to retention to the outermost portion of PPy/OTs. Estimates of the anion capacity of our PPy/OTs stationary phase using DTRP as the test analyte yield a value of  $\sim 0.038$  meq/g PPy. This is compared to a total *cationic uptake* of 0.83 meq/g PPy, as calculated by integrating the charge under the oxidative wave in Figure 2 and by assuming a dopant ion to PPy ratio of 0.25 [48,49]. Therefore, only about 5% of the capacity of the column is accessed by the DAAs, which argues favorably for our surface-confined retention mechanism.

Such a surface-confined retention mechanism is also substantiated by the data given in Figure 3e, which shows an EDX spectrum in the sulfur region for a PPy/OTs film cycled in 0.1 M NaOTs and then in 5 mM DGLY (pH 7.0) until a steady-state CV was obtained. The GC electrode was removed from solution under voltage control at 0.00 V. Comparison of the S/C ratio for the PPy/OTs oxidized in DGLY to that for reduced PPy/OTs should provide a qualitative indication of the extent of incorporation of DGLY into oxidized PPy/OTs. As is evident from Figure 3e, oxidation of PPy/OTs in the DGLY solution results in only a small increase in sulfur (S/C=1.47) over that obtained at -1.00 V in the NaOTs solution (S/C=1.35). This small increase suggests that DGLY is not significantly incorporated into oxidized PPy/OTs.

From the above discussion, a model for the surface-confined retention mechanism then emerges, with the capacity of the column defined by the competition between analyte and mobile phase anions for sites near the exterior of the film. Such a model is illustrated in Scheme II. At an applied voltage of -1.00 V, the bulk of the reduced PPy contains both entrapped OTs anions and incorporated sodium cations, whereas the outer surface of the PPy

exists in its neutral, nonionic state. At an applied voltage of 0.00 V, the bulk of the oxidized PPy contains entrapped OTs anions, whereas the outer surface contains Bz anions from the mobile phase electrolyte. Anion-exchange of these Bz mobile phase anions with the DAAs results in retention of the DAAs at PPy/OTs. The electrochemical characteristics of each region, however, is determined by its ion transport characteristics, with the electrochemical transformation for the anion-exchange region occurring at somewhat more positive voltages

### Scheme II



than that for the cation-exchange region. In accord with this model, all of our subsequent references to "anex capacity" will refer only to those sites at the outer surface of PPy/OTs.

### **Alteration of the Capacity Factors for the Dansyl Amino Acids as a Function of Applied Voltage.**

As discussed, the outer surface of PPy/OTs should be available for anex type interaction with the DAAs. A series of experiments were designed to probe the strength of

these interactions as a function of the extent of PPy/OTs oxidation. The  $k'$  values of the DAAs served as a measure of the strength of their interaction with PPy/OTs, while PPy/OTs oxidation was controlled by altering the applied voltage. Figure 4 summarizes the results of such a study. The solid curve in Figure 4 is a plot of the extent of PPy/OTs oxidation as a function of the applied voltage, and is included for the development of a rough correlation with the  $k'$  values for the DAAs. This curve was calculated, after compensating for charging current, by integrating incrementally the area under the CV in Figure 2 from a lower limit of -1.00 V to an increasing upper voltage limit. The dashed plot for each of the DAAs was obtained for 1  $\mu$ L injections of 4 mM solutions of the analyte. Error bars for each curve are roughly equivalent to the size of the data points. Importantly, the DAAs exist as either singly-charged (i.e. DASN, DSER, DGLY, DLEU, DPHE, DTRP) or doubly-charged (i.e. DASP) anions at the pH of the mobile phase (pH 7.0).

Figure 4 reveals that the relative changes in the  $k'$  values for all seven DAAs generally follow that roughly predicted from the voltammetric data for PPy/OTs. At applied voltages where PPy/OTs should exist entirely in its reduced form (i.e., -1.00 V), the  $k'$  values are small ( $k' < 0.5$ ). In contrast, at applied voltages where PPy/OTs should exist in its fully oxidized, cationic form (i.e., 0.00 V), the  $k'$  values are much larger ( $0.5 < k' < 16$ ). The  $k'$  values at intermediate applied voltages generally show a sigmoidal-type change between these two voltage limits, in qualitative agreement with the change in anion capacity predicted from the solid curve in Figure 4. Therefore, the DAAs appear to interact with PPy/OTs, in part, through anion-type interactions. In qualitative agreement with this conclusion, the doubly charged DASP ( $\log P = -4.83$ ) shows a more rapid increase in  $k'$  with increasing applied

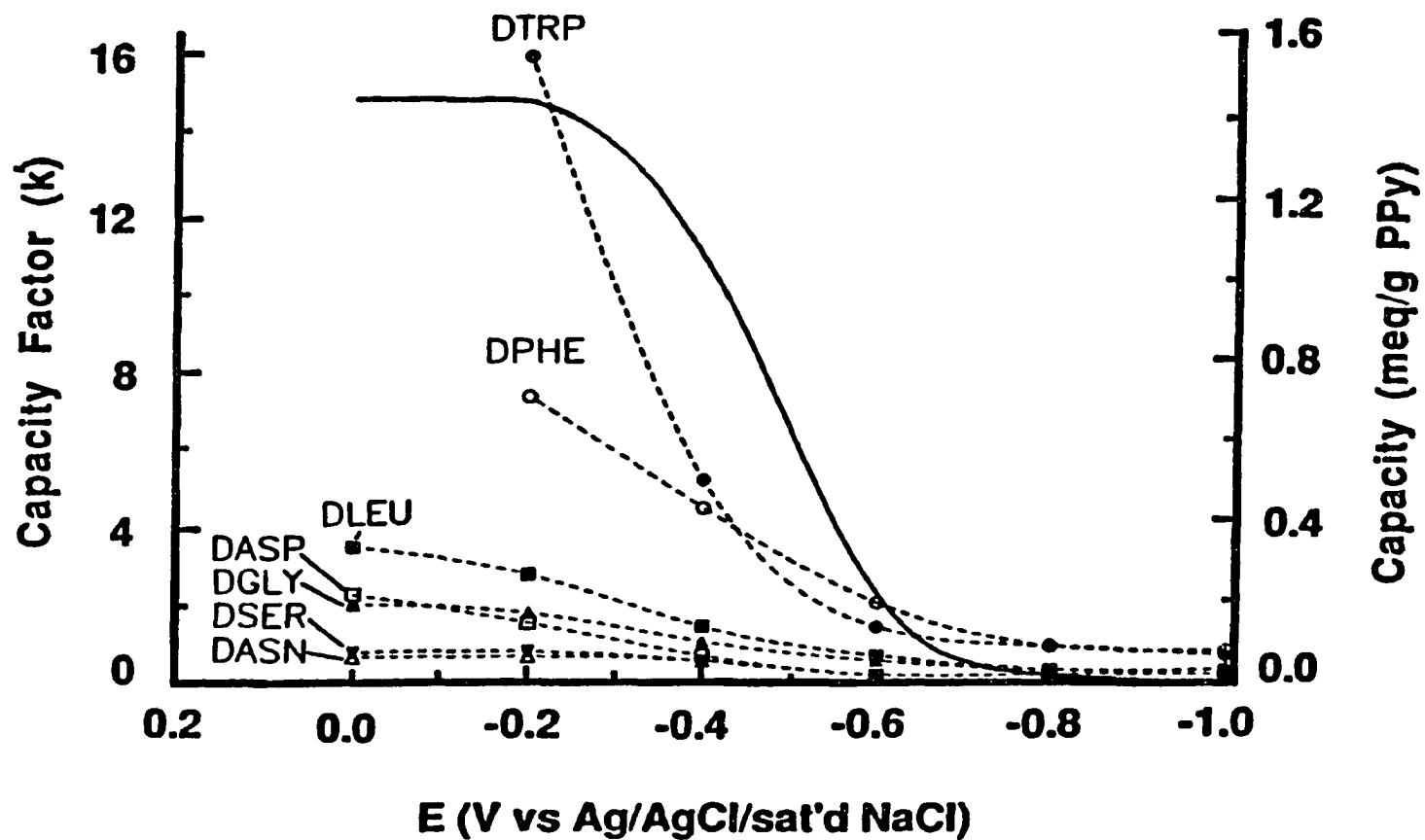


Figure 4. Capacity factors for the seven DAAs as a function of the applied voltage. The solid curve gives an estimate of the anex capacity of PPy/OTs as a function of applied voltage, and was calculated by integration of the oxidative peak in the CV shown in Figure 2, after compensating for the charging current.

voltage than several of the singly-charged DAAs (i.e., DASN, DSER, DGLY) due to a stronger ionic interaction at cationic PPy/OTs.

Although the retention of the DAAs at PPy/OTs generally correlates with its anion capacity, some important differences are evident. In particular, Figure 4 indicates that the more strongly retained DAAs such as DGLY, DASP, and DLEU show significant changes in their  $k'$  values at applied voltages more positive than -0.20 V. This is in contrast to the solid curve in Figure 4, which predicts the complete oxidation of PPy/OTs at -0.20 V. Similarly, DPHE and DTRP also show large increases in their retention throughout this voltage range, resulting in effectively unmeasurable  $k'$  values because of significant elution band broadening. Although DASN and DSER should also display analogous changes, their very weak retention results in no observable changes in their  $k'$  values above the experimental uncertainty. These observations likely result from the different voltages required for oxidation of the inner cation-exchange region and the outer anion-exchange region of PPy/OTs, as discussed above. Preliminary QCM measurements on PPy/OTs films corroborate this conclusion, and show a resonant frequency crossover at  $\sim -0.20$  V from increasing frequency (i.e. cation expulsion) to decreasing frequency (i.e. anion incorporation). Such a crossover indicates that, in contrast to the predictions made from the CV in Figure 2, PPy oxidation is not complete at -0.20 V. As mentioned above, the CV data in Figure 2 mainly describes the electrolysis of the dominant inner cation-exchange region of PPy/OTs, and predicts complete oxidation at -0.20 V. However, the electrolysis of the outer anion-exchange region of PPy/OTs, which is not adequately described by Figure 2, appears to be shifted more positively such that oxidation

still occurs at applied voltages more positive than -0.20 V. Since the DAAs likely interact exclusively with this outer anion-exchange region, their retention *should increase* as this anion-transport dominated PPy is further oxidized between -0.20 V and 0.00 V.

However, Figure 4 also reveals that the retention of the DAAs at PPy/OTs cannot be completely attributed to a charge interaction, since the singly-charged DTRP, DPHE, and DLEU anions have larger  $k'$  values at oxidized PPy/OTs than the doubly-charged DASP anion. This argues that the retention of the DAAs at PPy/OTs is also highly dependent on their hydrophobicities. Figure 4 indicates that the  $k'$  values for anions with the more hydrophilic, monovalent amino acid side chains such as DASN ( $\log P = -0.60$ ) and DSER ( $\log P = -0.04$ ) increase comparatively little with increases in applied voltage. In contrast, the  $k'$  values for anions with the most hydrophobic, aromatic amino acid side chains such as DTRP ( $\log P = 2.25$ ) and DPHE ( $\log P = 1.79$ ) increase rapidly. Anions with nonaromatic amino acid side chains of intermediate hydrophobicity such as DGLY ( $\log P = 0.00$ ) and DLEU ( $\log P = 1.70$ ) display increases in their  $k'$  values that fall between these two groupings. Further, although the  $\log P$  values for DLEU and DPHE are effectively the same, DPHE appears to interact more strongly with PPy/OTs at applied voltages more positive than -0.60 V because of its more extensive donor-acceptor (i.e.,  $\pi$ - $\pi$ ) interactions with the PPy/OTs aromatic backbone.

In addition, the magnitude of these hydrophobic and donor-acceptor interactions appear to follow the increasing oxidation of PPy/OTs, with stronger interactions occurring at the more highly oxidized polymer surface. Although not yet fully clear, we attribute this effect



to an increase in the porosity of the outer anion-exchange region of PPy/OTs upon oxidation, which allows for increased hydrophobic and donor-acceptor interaction between the newly exposed PPy aromatic backbone and the DAAs. Increases in the porosity of anion transport dominated PPy films by factors of  $\sim 1000$  upon oxidation have been previously estimated [50]. This increasing affinity of PPy for hydrophobic anions upon oxidation is also evident in the crossover of the curves for DPHE ( $\log P=1.79$ ) and DTRP ( $\log P=2.25$ ) at  $-0.45$  V in Figure 4. Reduced PPy, in contrast, should be much less porous due to its nonionic nature, and therefore should show weaker reverse phase interactions with the DAAs. This latter conclusion is consistent with the data in Figure 4, which shows only a weak retention of all DAAs at reduced PPy/OTs. The differences in the  $k'$  values for the DAAs at reduced PPy/OTs are, however, sufficient to obtain separations of a binary mixture of a single hydrophilic DAA (i.e. DASP, DASN, DSER) and a single hydrophobic DAA (i.e. DPHE, DTRP). Since such separations rely largely on hydrophobic and donor-acceptor interactions, PPy/OTs can be changed from a stationary phase that operates on effectively a reverse phase mechanism to one that includes an ion exchange component.

It is important to note that although the relative increase in the  $k'$  values for the singly-charged DAAs at a given applied voltage generally follows the order of increasing  $\log P$ , some inconsistencies are apparent. Such inconsistencies are evidenced, for example, in the nonlinear change in the  $k'$  values at  $0.00$  V for DASN ( $k'=0.63$ ,  $\log P=-0.60$ ), DSER ( $k'=0.75$ ,  $\log P=-0.04$ ), and DGLY ( $k'=2.00$ ,  $\log P=0.00$ ). These inconsistencies suggest that the retention of the DAAs at PPy/OTs is dependent on other factors such as steric size of the

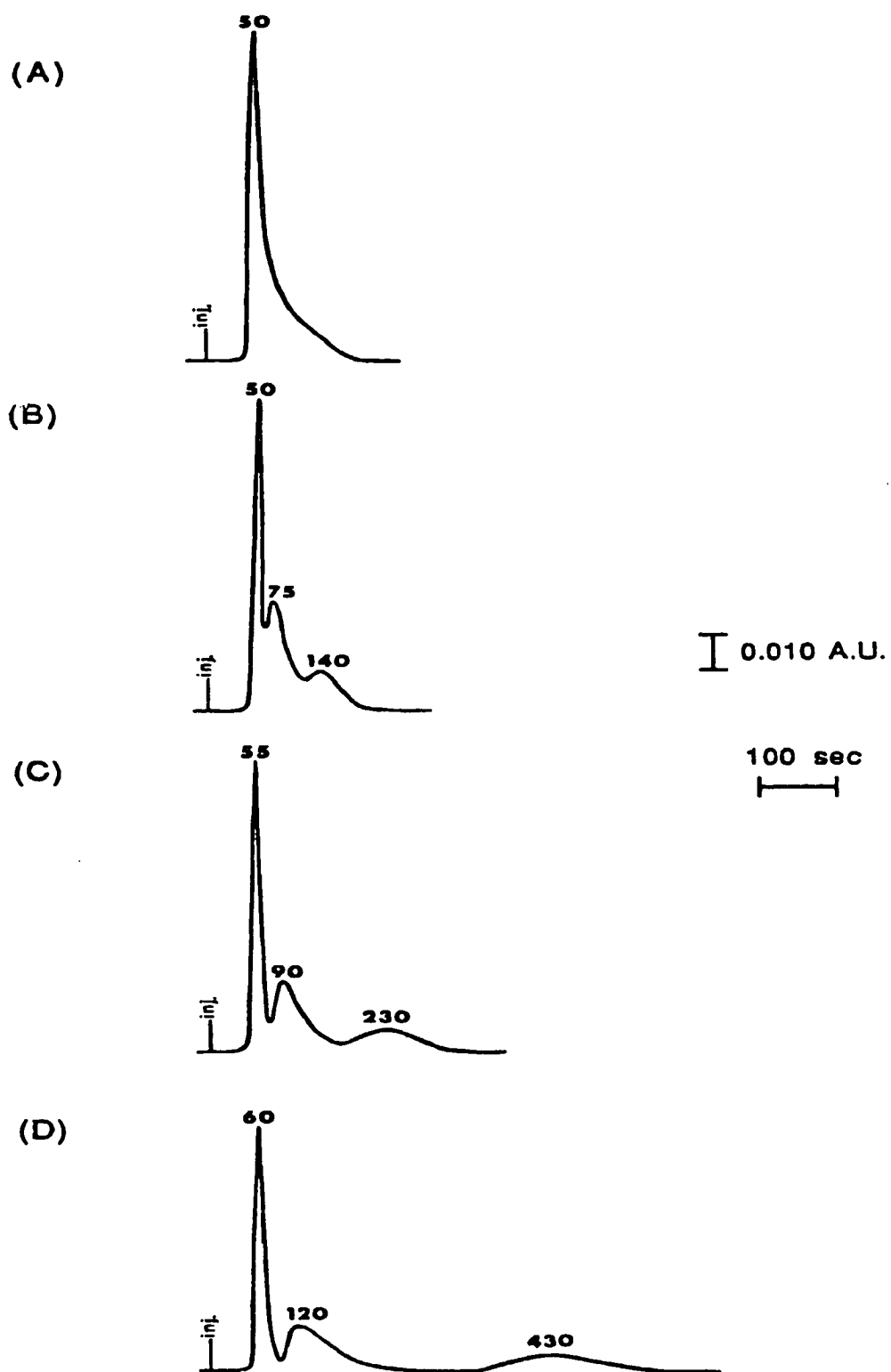
amino acid side chain which are not accounted for in the calculation of the log P values [51,52].

Together, these results demonstrate that (1) the  $k'$  values for anions at PPy/OTs can be altered by changing the applied voltage; (2) the relative changes in these  $k'$  values *qualitatively* follow the changes in column capacity predicted from the CV data; and (3) the strength of interaction of anions with PPy/OTs at a given applied voltage is determined not only by ionic charge but also by the extent of hydrophobic and donor-acceptor interactions.

#### **Dansyl Amino Acid Separations.**

The  $k'$  values in Figure 4 provide a guide for identifying the optimal applied voltage for separation of the DAAs at PPy/OTs. Figures 5a-d demonstrate how the separation of a mixture of DASN, DLEU, and DTRP is affected by the application of a *constant voltage during elution*. The applied voltages (-0.60 V to -0.30 V) were chosen to span a large range of capacity. The separations are for 1  $\mu$ L injections of a mixture of 4 mM DASN, DLEU, and DTRP. At applied voltages more negative than -0.60 V (Figure 5a), the separation of the mixture was ineffective due to the small differences in the  $k'$  values for the DAAs in this voltage region. As the applied voltage is made more positive (Figures 5b-d), the  $k'$  values for the three DAAs begin to diverge, and three eluate bands emerge. The first band is DASN (i.e., low  $k'$ ), the second is DLEU (i.e., intermediate  $k'$ ), and the third is DTRP (i.e., large  $k'$ ). At -0.30 V (Figure 5d), a separation at nearly baseline resolution is achieved. These results illustrate clearly the large changes in the separations that can be produced through modification in the applied voltage *prior to elution*.

**Figure 5. Separations of a mixture of DASN, DLEU, and DTRP obtained at PPy/OTs at applied voltages of (a) -0.60 V, (b) -0.50 V, (c) -0.40 V, (d) -0.30 V. A 1  $\mu$ L injection of a solution 4 mM in DASN, DLEU, and DTRP was used to obtain each chromatogram.**



Since the anion capacity of PPy/OTs can be controlled electrochemically, a variety of voltage waveforms (e.g., linear ramps and steps) can be applied *during elution* to affect retention. For example, a linear voltage ramp initiated at a large anion capacity and scanned toward a decrease in anion capacity could be used both to decrease the total analysis time and to sharpen the bands of the more strongly retained anions. More rapid changes in the stationary phase composition could also be induced through voltage steps. In this case, the extent of the change would be dependent on the size of the voltage step. The application of a constant current could be used to manipulate separations as well. This galvanostatic approach would have the added advantage of affecting a change in capacity that would be linear with time, with the rate and the direction of the change altered by the magnitude and polarity of the applied current. The application of electrochemical waveforms is therefore directly analogous to the effects achieved using gradient elution in conventional liquid chromatography [53,54]. In our case, however, separations are manipulated by changes in the composition of the stationary phase rather than the mobile phase. Such an approach represents a simple, effective pathway for implementing the advantages of our novel ECIC system.

The chromatograms in Figure 6 illustrate how the separations obtained at -0.40 V (Figure 5c) and -0.30 V (Figure 5d) can be improved through application of voltage steps at PPy/OTs. Figure 6a starts with the mixture injected onto the column at an applied voltage of -0.40 V, with the voltage stepped to -1.00 V immediately after elution of DASN and DLEU. Consistent with the electrochemically-induced change in the capacity of the column, the retention time for DTRP is decreased from 230 sec (see Figure 5c) to 170 sec. This change

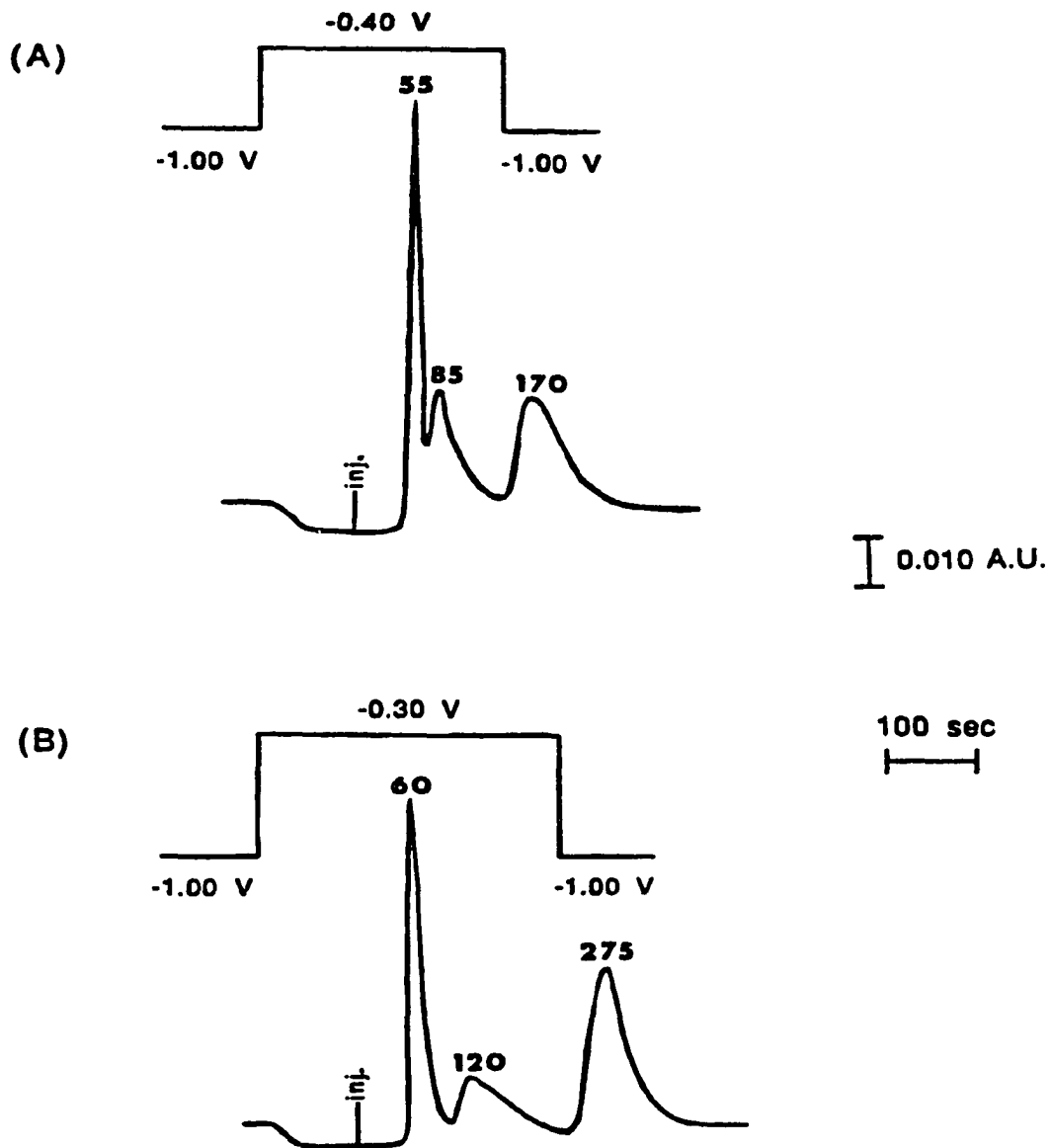


Figure 6. Separations of a mixture of DASN, DLEU, and DTRP obtained at PPy/OTs through application of voltage steps from (a) -0.40 V to -1.00 V, and (b) -0.30 V to -1.00 V after the complete elution of DASN and DLEU. A 1  $\mu$ L injection of a solution 4 mM in DASN, DLEU, and DTRP was used to obtain each chromatogram.

translates to a decrease in  $k'$  from 5.0 to 3.3. Additionally, the elution band for DTRP is sharpened, with a decrease in the half-width of ~50%. The change in the baseline observed in Figure 6a results from the release of the benzoate mobile phase anion from the PPy upon application of the voltage step.

The separation in Figure 6b further illustrates the advantages of using electrochemically-induced changes in the composition of PPy/OTs. In contrast to Figure 6a, the mixture is injected onto the column at -0.30 V, i.e., where all three components are more strongly retained on the column. The voltage step after elution of DASN and DLEU again leads to an improvement in the overall separation. Comparatively, the retention time for DTRP decreases from 430 sec (see Figure 5d) to 275 sec, representing a decrease in  $k'$  from 9.8 to 5.9. This decrease in retention time is also accompanied by a decrease in the half-width of the band by ~77%. Together, these two chromatograms demonstrate the effectiveness of voltage steps in decreasing the retention time and in improving the shapes of the bands of strongly retained anions.

#### **Concentration of Dilute Solutions Using ECIC.**

The ability to modulate the capacity of PPy/OTs for the DAAs over a wide range also suggests its potential use in preconcentrating dilute solutions of these compounds. In such an experiment, the ECIC column would function analogously to a solid phase extraction column, except that changes in the applied voltage rather than changes in solvent would be used to concentrate and then strip the analyte from the column [27]. To investigate the usefulness of the ECIC column for such applications, we attempted to concentrate a dilute solution of

DTRP at PPy/OTs. A solution consisting of 1.6 ppm DTRP in 10 mM pH 6 acetate buffer was used as the mobile phase; the competitively strong interaction of DTRP with PPy/OTs ensured that it was not displaced by the acetate ion, thereby allowing for its concentration on the column.

Figure 7 outlines the experiment, and shows a breakthrough curve obtained for the concentration process [55]. The DTRP-containing mobile phase was passed through the column continuously at 0.90 mL/min while the applied voltage was held initially at -1.00 V. The applied voltage was then stepped to and held at 0.00 V to oxidize PPy/OTs. Upon application of the voltage step, the absorbance of the eluent rapidly decreased to the value of the acetate mobile phase, reflecting the exhaustive uptake of DTRP by PPy/OTs. After 66.7 min, the absorbance slowly increased to the value at -1.00 V, signaling the saturation of PPy/OTs with DTRP. Saturation appeared to be complete at 72.5 min. The applied voltage was then stepped to -1.00 V to reduce PPy/OTs and to strip the DTRP from the column in a narrow elution band. The sharpness of this band is clearly evident from the ten-fold difference in the absorbance scales observed for the concentration and stripping steps (Figure 7). A comparison of the base-width of this stripping band (2.2 min) to the time required to reach the breakthrough point (66.7 min) yielded a concentration factor of  $\sim 33$  under these conditions. The area of the stripping band was compared to that for an injection of a known amount of DTRP under the same operational conditions but at -1.00 V to calculate the number of moles of DTRP ( $2.4 \times 10^{-7}$  mol) retained by PPy/OTs at 0.00 V. This value, together with an estimation of the number of moles of DTRP passed through the column prior to the voltage



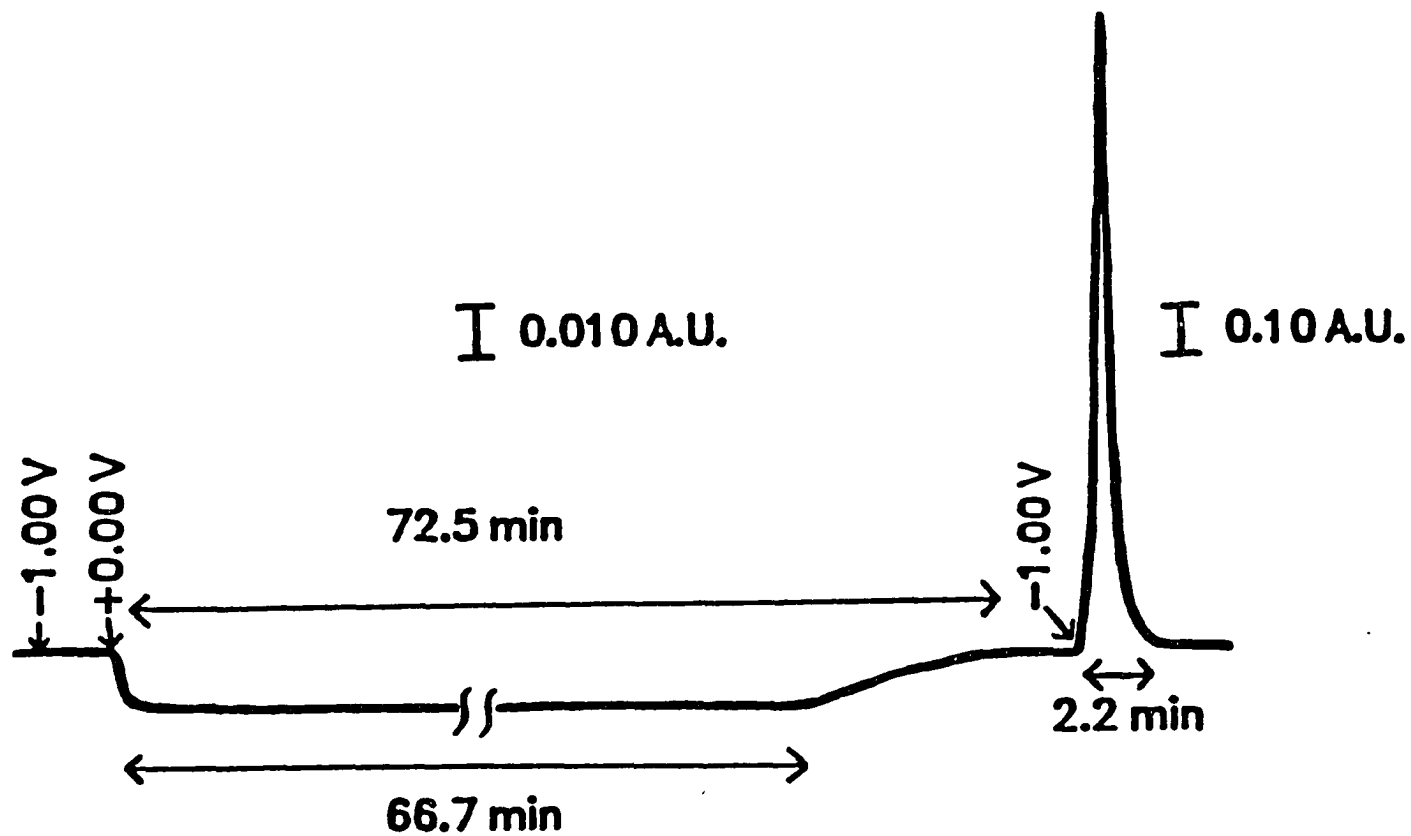


Figure 7. Breakthrough curve showing the concentration of a 1.6 ppm solution of DTRP at PPy/OTs. The applied voltage, which was initially held at -1.00 V, was stepped to and held at 0.00 V for 72.5 min and then stepped back to -1.00 V. The mobile phase consisted of 1.6 ppm DTRP in 10 mM pH 6 acetate buffer. The flow rate was 0.90 mL/min.

step from 0.00 V to -1.00 V, yielded a percent recovery of ~98 %. Similar experiments performed with the other DAAs also proved successful, but at somewhat lower concentration factors because of their weaker interactions with PPy/OTs at 0.00 V (see Figure 4). The significant concentration and high recovery of DTRP that could be obtained highlights the potential use of the ECIC column for the concentration of dilute analyte solutions. Further studies are planned to investigate this effect in more detail.

An additional parameter that can be obtained from such measurements is an estimate of the absolute capacity of the ECIC column for the DAAs. Based on the data in Figure 7 and on the average number of grams of PPy/OTs ( $6 \times 10^{-3}$  g), the density of PPy/OTs ( $1.5 \text{ g/cm}^3$  [56]), and its average volume ( $10^{-6}$  cm thickness  $\times$   $4600 \text{ cm}^2$  surface area =  $4.6 \times 10^{-3} \text{ cm}^3$ ), we estimate a capacity of PPy/OTs for DTRP of ~0.038 meq/g PPy/OTs. This value is compared to that obtained from the CV data in Figure 2 (~0.83 meq/g PPy/OTs). Therefore, as discussed above, interaction of the DAAs with PPy/OTs appears to be strictly a surface phenomenon. Such an observation has direct ramifications to the concentration studies, since it reveals that only a small fraction of the total PPy/OTs film capacity is being accessed for concentration. Therefore, we expect that much larger concentration factors could be obtained for smaller analytes which can more effectively penetrate into the PPy/OTs film. Experiments are planned to examine this possibility.

## CONCLUSIONS

The ability to modify selectively the  $k'$  values and separations of a variety of DAAs prior to and during elution has been demonstrated. Such changes were accomplished by altering the voltage applied to a conductive PPy-coated GC stationary phase to effect changes in its anion capacity, hydrophobicity, and porosity. Examination of the magnitude of these  $k'$  value changes as a function of applied voltage indicated that the retention mechanism for the DAAs at PPy/OTs consisted of both an anion and a reverse phase component. Cyclic voltammetry was used to correlate the electrochemical transformation of PPy/OTs with the observed  $k'$  value changes. Although qualitative agreement between the extent of PPy/OTs oxidation (as measured by its CV response) and the  $k'$  value changes was found, some significant differences were apparent. These differences were attributed to the composite structure of PPy/OTs, which contains both anion and cation exchange domains. The ability to modulate electrochemically the anion capacity of PPy/OTs was also utilized to illustrate the potential use of ECIC for concentrating dilute solutions of the DAAs.

Future studies will be primarily aimed at improving the efficiency of the chromatographic system to allow for further demonstration of its usefulness for modifying and optimizing analytical separations. These studies will address such issues as the particle diameter, the stationary phase composition, and the column configuration which likely limit the efficiency of our present chromatographic system. In addition, future studies will examine other types of "gradient elution" waveforms such as linear voltage and charge ramps for their use in optimizing analyte separations. Such studies are currently underway.

**ACKNOWLEDGMENTS**

R.S.D. acknowledges the support of an ACS Analytical Division Summer Fellowship sponsored by Dow Chemical, USA. Several helpful discussions with Duane Weisshaar, Jerzy Zak, and Chuanjian Zhong are appreciated. Discussions with Sue Lunte of the Center for Bioanalytical Research at the University of Kansas are also appreciated. This work was supported by the National Science Foundation (M.D.P., Grant CHE-9003308) and by the Kurata Foundation (K.S.).

**LITERATURE CITED**

1. R.C. Ludwig, *J. Chromatogr.* 592 (1992) 101.
2. K. Ito, Y. Ariyoshi, and H. Sunahara, *J. Chromatogr.* 598 (1992) 237.
3. P.R. Haddad and A.L. Heckenberg, *J. Chromatogr.* 300 (1984) 357.
4. C.F. Buck, P.A. Mayewski, M.J. Spencer, S. Whitlow, M.S. Twickler, and D.J. Barrett, *J. Chromatogr.* 594 (1992) 225.
5. R.M. Mhatre and I.S. Krull, *J. Chromatogr.* 591 (1992) 139.
6. D. Wu and R.R. Walters, *J. Chromatogr.* 598 (1992) 7.
7. D.N. Vacik and E.C. Toren, *J. Chromatogr.* 228 (1982) 1.
8. K. Stulik, V. Pacakova, and H. Wang, *J. Chromatogr.* 552 (1991) 439.
9. J.A. Grunau and J.M. Swiader, *J. Chromatogr.* 594 (1992) 165.
10. R.H. Nieman and R.C. Clark, *J. Chromatogr.* 317 (1984) 271.
11. J.F. Davey and R.S. Ersser, *J. Chromatogr.* 528 (1990) 9.

12. A.S. Feste, *J. Chromatogr.* 574 (1992) 23.
13. H. Miyagi, J. Miura, Y. Takata, S. Kamitake, S. Ganno, and Y. Yamagata, *J. Chromatogr.* 239 (1982) 733.
14. G. Vanecek and F.E. Regnier, *Anal. Biochem.* 109 (1980) 345.
15. J.J. Johnston, W.M. Draper, and R.D. Stephens, *J. Chrom. Sci.* 29 (1991) 511.
16. H.K. Lee and N.E. Hoffman, *J. Chrom. Sci.* 30 (1992) 98.
17. T. Nagaoka, M. Fijimoto, H. Nakao, K. Kakuno, J. Yano, and K. Ogura *J. Electroanal. Chem.* 364 (1994) 179.
18. T. Nagaoka, M. Fijimoto, H. Nakao, K. Kakuno, J. Yano, and K. Ogura *J. Electroanal. Chem.* 350 (1993) 337.
19. R.S. Deinhammer, K. Shimazu, and M.D. Porter, *Anal. Chem.* 63 (1991) 1889.
20. H. Ge and G.G. Wallace, *J. Liq. Chromatogr.* 13 (1990) 3245.
21. H. Ge and G.G. Wallace, *Anal. Chem.* 61 (1989) 2391.
22. A.R. Ghatak-Roy and C.R. Martin, *Anal. Chem.* 58 (1986) 1574.
23. Y. Ikariyama, C. Gallatsatos, and W.R. Heineman, *Sensors and Actuators* 12 (1987) 455.
24. A.F. Diaz, J.I. Castillo, J.A. Logan, and W.Y. Lee, *J. Electroanal. Chem.* 129 (1981) 115.
25. T. Shimidzu, A. Ohtani, T. Iyoda, and K. Honda, *J. Electroanal. Chem.* 224 (1987) 123.
26. A.K. Bakhshi, J. Ladik, J., and M. Seel, *Phys. Rev. B* 35 (1987) 704.
27. C.F. Poole and S.A. Schuette, *Comtemporary Practice of Chromatography*, Elsevier, New York, 1984.
28. J.F. Evans and T. Kuwana, *Anal. Chem.* 51 (1979) 358.

29. J.F. Evans, T. Kuwana, M.T. Henne, and G.P. Royer, *J. Electroanal. Chem.* 80 (1977) 409.
30. L.J. Kepley and A.J. Bard, *Anal. Chem.* 60 (1988) 1459.
31. S. Pouzet, A. Ricard, and A. Boudet, *Electrochim. Acta* 36 (1991) 1953.
32. V.T. Wiedmeier, S.P. Porterfield, and C.E. Hendrich, *J. Chromatogr.* 231 (1992) 410.
33. J. Fauchere and V. Pliska, *Eur. J. Med. Chem.* 18 (1983) 369.
34. J.L. Cornette, K.B. Cease, H. Margalit, J.L. Spouge, J.A. Berzofsky, and C.J. DeLisi, *J. Mol. Biol.* 195 (1987) 659.
35. A. Leo, C. Hansch, and D. Elkins, *Chem. Rev.* 71 (1971) 525.
36. K. Naoi, M. M. Lien, and W.H. Smyrl, *Proceedings of the Symposium on Rechargeable Lithium Batteries, Electrochemical Society Meeting, 1989, p. 90.*
37. V. M. Schmidt and J. Heitraum, *Electrochim. Acta* 38 (1993) 349.
38. J.M. Pernaut, R.C.D. Peres, V.F. Juliano, and M.A. DePaoli, *J. Electroanal. Chem.* 274 (1989) 225.
39. C. Zhong and K. Doblhofer, *Electrochim. Acta* 35 (1990) 1971.
40. W. Wernet and G. Wegner, *Makromol. Chem.* 188 (1987) 1465.
41. M.A. DePaoli, R.C.D. Peres, S. Panero, and B. Scrosati, *Electrochim. Acta* 37 (1992) 1173.
42. F. Li and W.J. Albery, *J. Chem. Soc. Faraday Trans.* 87 (1991) 2949.
43. C. Zhong, K. Doblhofer, and G. Weinberg, *Faraday Discuss. Chem. Soc.* 88 (1989) 307.
44. H. Yoneyama, T. Hirai, S. Kuwabata, and O. Ikeda, *Chem. Lett.* (1986) 1243.

45. J. Wang, Z. Sun, and Z. Lu, *J. Electroanal. Chem.* 310 (1991) 269.
46. K. Naoi, M.M. Lien, and W.H. Smyrl, *J. Electroanal. Chem.* 272 (1989) 273.
47. V.M. Schmidt and J. Heitbaum, *Synth. Met.* 41 (1991) 425.
48. M. Salmon, A.F. Diaz, A.J. Logan, M. Krounbi, and J. Bargon, *Mol. Cryst. Liq. Cryst.* 83 (1982) 265.
49. J.L. Bredas, J.C. Scott, K. Yakushi, and G.B. Street, *Phys. Rev. B* 30 (1984) 1023.
50. H. Mao and P.G. Pickup, *J. Phys. Chem.* 93 (1989) 6480.
51. M.S. Mirrlees, S.J. Moulton, C.T. Murphy, and P.J. Taylor, *J. Med. Chem.* 19 (1976) 615.
52. C. Hansch, *Structure-Activity Relationships*, C.J. Cavallito, Ed., Pergamon Press, Oxford, 1973.
53. L.R. Snyder, J.W. Dolan, and J.R. Gant, *J. Chromatogr.* 165 (1979) 3.
54. C. Liteanu and S. Gocan, *Gradient Elution Chromatography*, Wiley, New York, 1974.
55. C.E. Werkhoven-Goewie, U.A.Th. Brinkman, and R.W. Frei, *Anal. Chem.* 53 (1981) 2072.
56. A. Diaz, In *Electrochemical Preparation and Characterization of Conducting Polymers, Proceedings of the International Conference on Low Dimensional Synthetic Metals; Chemica Scripta*, 1981.

### **CHAPTER 3. ELECTROCHEMICALLY-MODULATED LIQUID CHROMATOGRAPHY (EMLC): A NEW APPROACH TO GRADIENT ELUTION SEPARATIONS**

A paper published in the *Journal of Electroanalytical Chemistry*<sup>1</sup>

Randall S. Deinhammer, EnYi Ting, and Marc D. Porter<sup>2</sup>

#### **ABSTRACT**

A new approach to gradient elution separations that is based on the electrochemical manipulation of the capacity factors of analytes during the elution process is discussed. Changes in the capacity factors of six aromatic sulfonate derivatives are produced by altering electrochemically the excess charge at a glassy carbon stationary phase which is packed into a modified version of our earlier column design. The redesign of our earlier column led to dramatic improvements in chromatographic efficiency, which facilitated the separation of more complex mixtures of analytes. Using this technique, alterations in the separation of the six aromatic sulfonates obtained by modification of the applied voltage both prior to and during their elution could be readily performed. The latter approach was used to improve the resolution between the analytes, to sharpen considerably their elution bands, and to decrease the total analysis time when compared to the separation obtained at open circuit. These

---

<sup>1</sup>Reprinted with permission from *J. Electroanal. Chem.* **1993**, *362*, 295-99. Copyright © 1993 Elsevier Sequoia S.A.

<sup>2</sup>Author to whom correspondence should be addressed.



improvements are analogous to those obtained with conventional solvent gradient elution methods, but were accomplished without modification in the composition of the mobile phase.

## INTRODUCTION

Several reports have described the testing of electrochemically-modulated liquid chromatography (EMLC) as a novel separation strategy [1-9]. The focus of these studies was the development of the ability to induce electrochemically changes in the composition of the stationary phase and to exploit the subsequent changes in separation efficiency. Changes in column composition have been accomplished through alterations in the applied voltage ( $E_{app}$ ) both prior to [1-5,7,8] and, as we have shown [6,9], during analyte elution. Although the earlier efforts clearly demonstrated the principles and possible applications of EMLC, the low efficiency of the columns severely limited their analytical utility. In this paper, we describe preliminary results of studies that have overcome this problem.

The following sections present the findings of a study aimed at redesigning the earlier version of our EMLC column. Through the described design changes, large increases in chromatographic efficiency have resulted. Both the widths and tailing of the elution bands have been dramatically decreased as compared to the earlier efforts [1-9]. The improvements are demonstrated by separations of a mixture of six structurally similar aromatic sulfonates (ASFs) using uncoated glassy carbon (GC) spheres as the stationary phase. The ASFs were selected as test analytes based on both their structural similarities and on their presence as components in several types of hazardous wastes [10,11]. Changes in  $E_{app}$  prior to analyte

elution were used to probe the effect on the separation of the excess charge at the GC surface. We also show that the manipulation of  $E_{app}$  via a linear voltage ramp during analyte elution leads to a gradient elution-type separation without changing the mobile phase composition.

## EXPERIMENTAL

### Construction of the Chromatographic System.

Figure 1 presents a schematic diagram of the EMLC column. The column consists of a Nafion cation-exchange tube (2.1 mm i.d., 14 cm length) placed inside of a porous (0.5  $\mu\text{m}$  pore size, 3.1 mm i.d., 14 cm length) stainless steel cylinder. The cylinder prevents deformation of the Nafion tube under the high pressure of chromatographic flow ( $\sim 240$  bar at 0.75 mL/min). After insertion into the cylinder, the ends of the Nafion tube were flanged to secure it within the cylinder. One end was mated to a 1/4 in stainless steel endfitting that contained a 0.5  $\mu\text{m}$  stainless steel frit, and the other to a high pressure slurry packer. The GC spheres ( $\sim 0.7$  g, 2-6  $\mu\text{m}$  dia., 2.39  $\text{m}^2/\text{g}$  surface area) were then dispersed in aqueous 0.1 M  $\text{LiClO}_4$  and slurry packed at 310 bar. After packing, the Nafion tube was mated to a second endfitting and frit. Electrical contact to the GC spheres, which served as the working electrode in a three-electrode cell, was made through the endfitting at the solution outlet. A platinized platinum mesh counter electrode and a  $\text{Ag}/\text{AgCl}/\text{sat'd NaCl}$  reference electrode were placed inside of a mobile phase-filled glass reservoir that was sealed around the bottom of the steel cylinder. Finally, the EMLC column was connected to the chromatographic

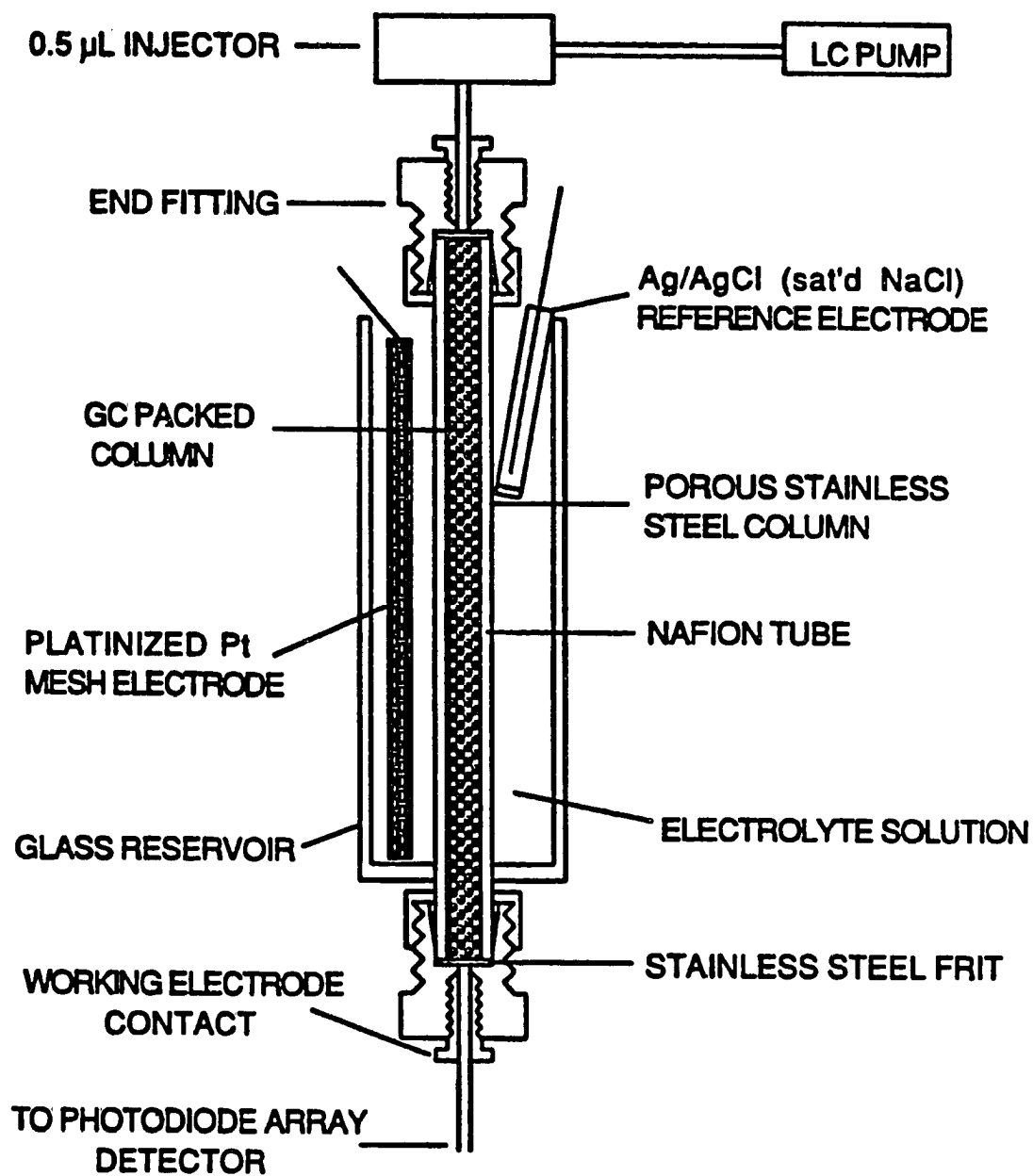


Figure 1. Schematic diagram of the EMLC column. The spheres are shown for illustration purposes, and do not represent a closest packed density.

system (see below). The results of a physical and chemical characterization of the EMLC column will appear elsewhere [12].

#### **Mode of Operation.**

Prior to initial use, the column was equilibrated with deaerated mobile phase (aqueous 0.1 M LiClO<sub>4</sub> containing 1.5 % CH<sub>3</sub>CN) at 0.75 mL/min until a stable detector baseline was obtained (~8-10 hr). Equilibration between experiments required ~5-10 min. The dead volume of the column (260 μL) was determined by injection of water. The components in the elution bands were identified from their absorbance spectrum. Analyte concentrations were ~200 ppm.

#### **Instrumentation.**

The chromatographic system consisted of a Waters Model 610 pump, Model 600E pump controller, and valve station. A Waters Model 996 photodiode array detector was used for identifying the components in the elution bands and was operated between 200-300 nm at 0.2 sec collection intervals. Chromatograms were extracted from the absorbance data at 220 nm. A Waters Millennium 2010 Data Manager was used to collect and process the data. Solutions were injected using a 0.5 μL injector loop (Rheodyne Model 7413). The voltage applied to the stationary phase was controlled by a Princeton Applied Research Model 173 galvanostat/potentiostat and a Model 175 programmer. The surface area of the GC spheres was determined using a Micromeritics Accusorb 2100E BET surface area analyzer.

**Reagents and Chemicals.**

Disodium 1,2-benzenedisulfonate (BDS), sodium benzenesulfonate (BS), 4-ethylbenzenesulfonic acid (EBS), sodium 4-hydroxybenzenesulfonate (HBS), lithium perchlorate, and acetonitrile (HPLC grade) were obtained from Aldrich. Disodium 1,5-naphthalenedisulfonate (NDS) was from Eastman, and sodium 4-chlorobenzenesulfonate (CBS) was from TCI America. At the pH of the mobile phase (pH~6), all analytes existed as either singly- (BS, HBS, EBS, CBS) or doubly-charged (BDS, NDS) anions. Aqueous solutions were prepared with water purified using a Millipore Milli-Q system.

**RESULTS AND DISCUSSION****Basis for the Relationship Between the Applied Voltage and Analyte Retention at the GC Stationary Phase.**

Separations at carbonaceous stationary phases have typically been founded on charge-transfer (i.e.,  $\pi$ -donor-acceptor and proton donor-acceptor) and dispersion interactions between the analytes and the carbon surface [13-15]. These interactions are dominated by the extensive aromaticity of the carbon surface; however, the small relative amount of acidic functional groups at the surface (e.g., carboxylic acid, quinone, phenol) also contribute to retention through dipole and hydrogen bonding interactions [13,16,17]. Hydrophobic interactions add a further dimension for retention, although their relative importance is small upon comparison to, for example, octadecylsilane stationary phases [15,18]. Based on these interactions, carbonaceous materials exhibit a unique specificity toward hydrophobic, aromatic

molecules with functional groups capable of charge-transfer interactions. Although retention of the ASFs at our GC stationary phase will be determined in part through such interactions, the ability to modulate dynamically the voltage applied to the stationary phase adds a new dimension for manipulating and fine-tuning separations.

The relationship between the excess charge at the GC surface and  $E_{app}$  relative to the potential of zero charge (pzc) serves as a starting point for predicting the effects of our proposed separation scheme. At values of  $E_{app}$  positive of the pzc, the excess charge is positive, leading to an electrostatic attraction of anions to the surface. In contrast, at values negative of the pzc, the excess charge is negative, and anions are electrostatically repelled from the surface [19-21]. At the pzc ( $\sim 0.0$  V vs Ag/AgCl/sat'd KCl [22]), the excess charge is zero and anions are neither electrostatically attracted to or repelled from the surface. Importantly, the extent of the interaction is dependent on the magnitude of  $E_{app}$ , with larger effects occurring with more extensive departures from the pzc.

The above discussion suggests the feasibility of altering the retention of anions at the GC stationary phase through the selective manipulation of  $E_{app}$ . Voltages positive of the pzc should increase the retention and resolution of a separation of anions by increasing the effective capacity of the stationary phase. Voltages negative of the pzc should, in contrast, decrease the retention of anions by decreasing the effective capacity of the GC stationary phase. Importantly, a combination of the improved resolution at  $E_{app}$ 's positive of the pzc with the shorter elution times at  $E_{app}$ 's negative of the pzc could then serve as a basis for a new type of separation scheme. Such an approach would be directly analogous to gradient elution in

conventional liquid chromatography, except that changes in the stationary phase composition rather than the mobile phase composition would be used to alter retention. We envision the use of voltage steps and linear ramps as routes to take advantage of this possibility. The following two sections present results that demonstrate the realization of this possibility.

### **Alteration of the Separation of a Mixture of Aromatic Sulfonates as a Function of a Fixed Applied Voltage.**

Figures 2a-d present separations of the mixture of the six ASFs at four different fixed conditions: open circuit (Figure 2a); +0.30 V (Figure 2b); +0.50 V (Figure 2c); and -1.00 V (Figure 2d). Table I lists the capacity factors ( $k'$ ) for each analyte under each condition.

Figure 2a demonstrates that a separation of the mixture at near baseline resolution is possible at open circuit ( $\sim +0.15$  V vs Ag/AgCl/sat'd NaCl [12]) in less than 3 min. Importantly, the shapes of the elution bands with the new version of our EMLC column represent a dramatic and much needed improvement over those previously obtained by us [6,9] and by others [3,4,7,8]. Earlier results were plagued by large band widths and by band tailing, which led to ineffective separations. We attribute the enhanced performance to both the smaller (2-6  $\mu\text{m}$ ), more uniformly shaped spheres used as a stationary phase and the more effective packing of these spheres into the column, both of which are enhancements over our earlier design [6].

The relative elution order of the ASFs at open circuit qualitatively follows that expected using carbonaceous stationary phases in a conventional chromatographic mode [14,15]. These studies, which examined the retention of several monosubstituted benzenes,

**Figure 2. Separations of the mixture of ASFs at the EMLC column: (a) open circuit; (b) +0.30 V; (c) +0.50 V; and (d) -1.00 V. The mobile phase consisted of aqueous 0.1 M LiClO<sub>4</sub> containing 1.5 % CH<sub>3</sub>CN. The flow rate was 0.75 mL/min. Analyte concentrations were ~200 ppm.**



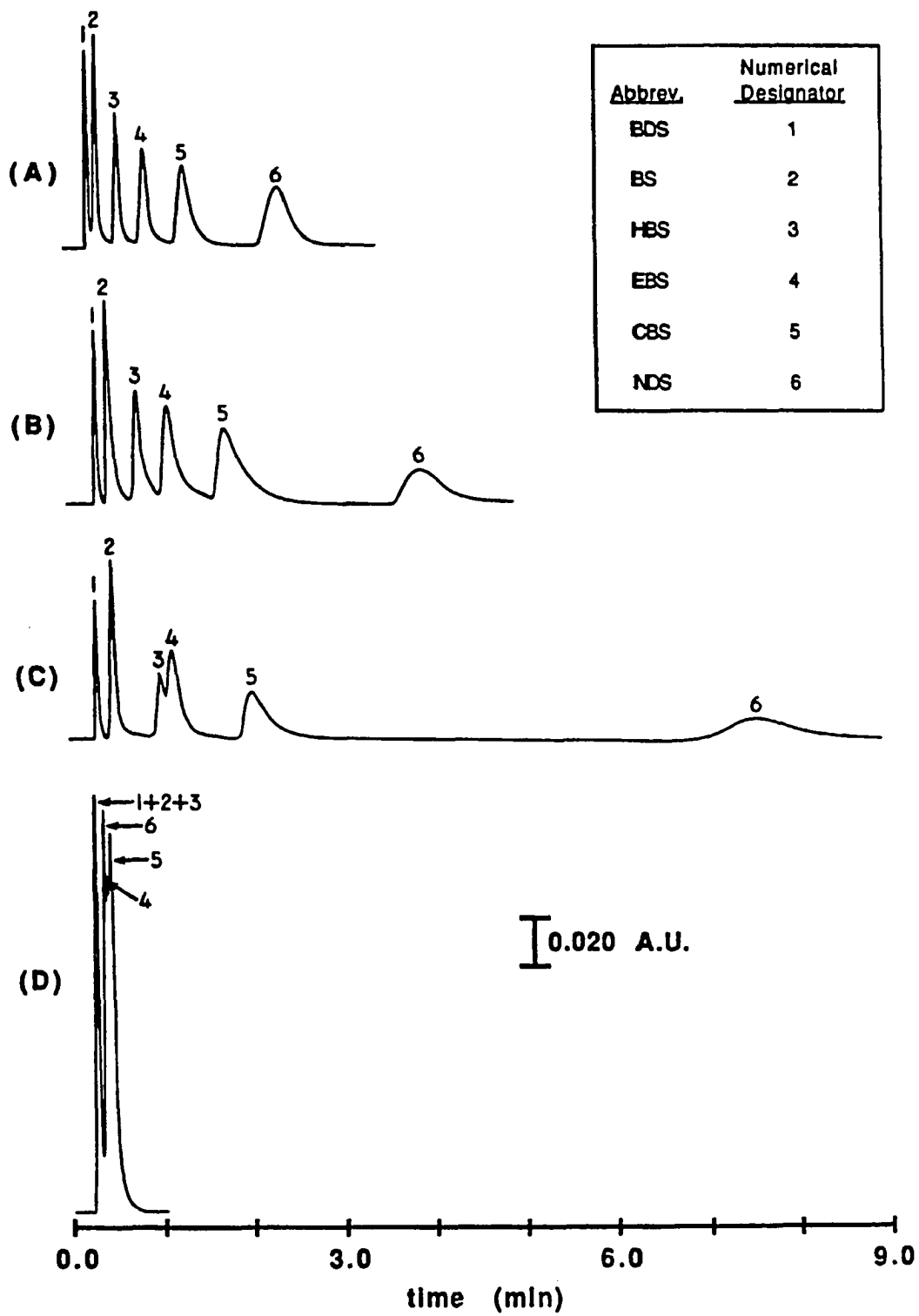


Table I. Capacity factors of six aromatic sulfonates at the GC stationary phase<sup>a,b</sup>.

<u>Analyte</u>	<u>Capacity Factor, k'</u>				
	<u>open circuit<sup>c</sup></u>	<u>+0.30 V</u>	<u>+0.50 V</u>	<u>-1.00 V</u>	<u>gradient<sup>d</sup></u>
BDS	~0	0.09	0.12	~0	0.09
BS	0.29	0.47	0.62	~0	0.38
HBS	0.97	1.38	2.15	~0	1.12
EBS	1.82	2.38	2.56	0.50	1.82
CBS	3.09	4.24	5.09	0.59	2.74
NDS	6.12	10.50	21.41	0.38	3.59

<sup>a</sup>The mobile phase was aqueous 0.1 M LiClO<sub>4</sub> containing 1.5 % CH<sub>3</sub>CN. The flow rate was 0.75 mL/min, and the detection wavelength was 220 nm.

<sup>b</sup>The injection volume was 0.5 μL.

<sup>c</sup>The open circuit voltage was ~+0.15 V vs Ag/AgCl/sat'd NaCl.

<sup>d</sup>The gradient was a linear voltage ramp from +0.30 V to -1.00 V applied immediately after sample injection at 10 mV/s.

predict an elution order based on the substituent of H<OH<Cl <Et<phenyl, in accordance with the aforementioned retention model. Our findings are qualitatively consistent with this prediction. For example, HBS (k'=0.97) and NDS (k'=6.12) are more strongly retained than BS (k'=0.29). The increased retention of HBS and NDS reflects their capability to interact at GC via proton donor-acceptor and π donor-acceptor interactions, respectively.

The effect of analyte charge on retention at our EMLC column can also be evaluated from Figure 2a through comparison of the elution order of BDS (k'~0) and BS (k'=0.29).

Clearly, the more highly charged analyte exhibits weaker retention. This finding is consistent with the affinity of GC for hydrophobic molecules, since the more ionic BDS has a greater hydrophilicity than BS. A comparison of the retention of BDS and NDS is also instructive. Both are doubly charged anions, but NDS is more strongly retained. This increase reflects the more extensive charge-transfer type interactions between NDS and GC. Together, these results suggest the dominance of charge transfer interactions on analyte retention, and provide a beginning of a basis for predicting the retention characteristics of our GC stationary phase.

Figures 2b,c illustrate the large increases in the retention for all six components of the ASF mixture observed upon application and maintenance of  $E_{app}$ 's positive of the pzc of GC: +0.30 V (Figure 2b) and +0.50 V (Figure 2c). As noted, these values result in a positive excess charge at the surface of GC that increases as  $E_{app}$  becomes more positive. At +0.30 V, the capacity factors for all ASFs increase by at least a factor of 1.3 over those at open circuit. Additionally, BDS and BS, which were not fully resolved at open circuit, are baseline resolved. Further increases in  $E_{app}$  (e.g., +0.50 V, Figure 2c) result in more extensive increases in retention. For example, the capacity factors for BS and HBS increase by more than a factor of two over those at open circuit. The capacity factor for the doubly charged NDS undergoes a larger increase (a factor of ~3.5) due to its more extensive ionic attraction to the positively charged GC surface. In contrast, the capacity factor for EBS increases by only a factor of 1.4, likely due to its more hydrophobic nature.

Figures 2a-c also point to several additional factors that play a role in the retention process, as seen by a comparison of the voltage-dependent retention of HBS and EBS. At

open circuit, HBS and EBS are effectively separated. However, the increase in the retention of HBS relative to EBS leads to an increased overlap of their elution bands at +0.30 V and an extensive overlap at +0.50 V. We presently attribute the differences in retention to the dipolar interaction of the hydroxyl group of HBS with the positively charged surface of GC. Since the strength of such an interaction would increase as the positive charge at the GC surface increases, the retention of HBS would increase more rapidly than that of EBS. A similar argument may also be valid in describing the differences in the retention of CBS relative to EBS. These findings also suggest several studies that could be directed toward unraveling the subtleties of GC surface chemistry, one of the long standing issues in electrochemical research.

In contrast to the above, the application of voltages negative of the pzc induces a very dramatic decrease in the retention of the ASFs. As shown in Figure 2d, an  $E_{app}$  of -1.00 V leads to the nearly complete overlap of the elution bands for all six ASFs. In particular, BDS, BS, and HBS are eluted with the void volume, and EBS, CBS, and NDS are only weakly retained. The weak retention for the latter three ASFs at -1.00 V corresponds to a respective decrease in their capacity factors by factors of 4, 5, and 15 with respect to open circuit. Interestingly, the strong electrostatic repulsion of the doubly-charged NDS at -1.00 V results in its elution before EBS and CBS. Taken together, the retention of all six ASFs can be altered over a very wide range through manipulation of  $E_{app}$ . This is perhaps best illustrated by NDS, whose capacity factor impressively changes by a factor of ~56 between -1.0 V and

+0.50 V. These results clearly demonstrate the unique ability of EMLC for modifying selectively and controlling separations without changes in mobile phase composition.

#### **Electrochemical Gradient Elution of the ASF Mixture at the GC Stationary Phase.**

Based on the findings in Figure 2, the enhanced resolution in the separation of the mixture of ASFs at the positive values of  $E_{app}$  (e.g., +0.30 V) can be coupled with the sharper elution bands and shorter retention times at -1.00 V for the development of a gradient-type elution process using EMLC. As a possibility, a linear ramp in voltage could be applied to the stationary phase from +0.30 V to -1.00 V. A myriad of other waveforms are also possible. Figure 3 demonstrates the effectiveness of such an approach. The above ramp was initiated immediately upon sample injection at 10 mV/s. As asserted, the separation is significantly improved. All six components of the mixture are separated at baseline resolution in ~1.7 min. By comparison, the separation at open circuit required 2.8 min with incomplete resolution of BDS and BS. The elution band widths of the ASFs are also significantly decreased using the voltage ramp. For example, the half-widths for EBS, CBS, and NDS are decreased from 6 sec to 4 sec, 9 sec to 5 sec, and 17 sec to 4 sec, respectively. The gradual increase in the baseline results from the release of the perchlorate mobile phase anion from the electrical double layer at GC. This is evident from the change in the background spectra collected upon application of the voltage ramp. Importantly, the improvements in the separation are analogous to those that would be obtained using solvent gradient elution, except that a change in the mobile phase composition is not required. In addition, the reduction in analysis time

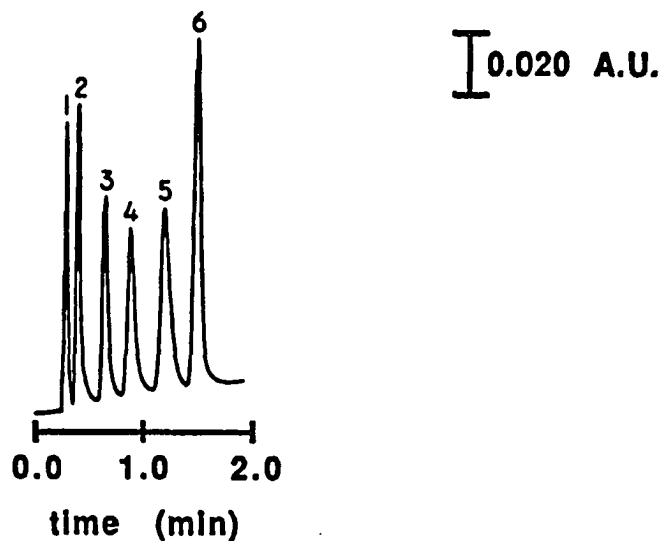


**Figure 3.** Separation of the mixture of ASFs at the EMLC column obtained by applying a linear voltage ramp from +0.30 V to -1.00 V. The voltage ramp was initiated immediately upon sample injection at 10 mV/s. The mobile phase consisted of aqueous 0.1 M LiClO<sub>4</sub> containing 1.5 % CH<sub>3</sub>CN. The flow rate was 0.75 mL/min. Analyte concentrations were ~200 ppm.

requisite for resolution of the mixture points to the potential utility of EMLC in performing quality, high speed separations.

### CONCLUSIONS

The results described herein have demonstrated the ability to modify separations selectively both prior to and during elution using a redesigned form of our earlier EMLC column. The redesign led to dramatic improvements in the chromatographic efficiency with

significant decreases in the half-width and tailing of elution bands as compared to those obtained earlier by us [6,9] and by others [3,4,7,8]. Changes in the separations were accomplished by altering electrochemically the excess charge at the GC surface both prior to and during analyte elution. Such an elution method represents a new form of gradient elution, and is accomplished without manipulation of mobile phase composition. These results provide the framework for future studies that will be aimed at evaluating the range and scope of this new separation method.

### ACKNOWLEDGMENTS

R.S.D. acknowledges the support of an ACS Analytical Division Summer Fellowship sponsored by Dow Chemical, USA. The authors also acknowledge the use of the slurry packer by J.S. Fritz, the air classification of the GC spheres by B.K. Lograsso and B. Patrick, and the use of the BET surface area analyzer by Professor G.M. Schrader. This work was supported by the National Science Foundation (Grant No. CHE-9003308).

### REFERENCES

1. J.L. Hern and J.H. Strohl, *Anal. Chem.*, 50 (1978) 1954.
2. R.F. Antrim, R.A. Scherrer, and A.M. Yacynych, *Anal. Chim. Acta.*, 164 (1984) 283.
3. A.R. Ghatak-Roy and C.R. Martin, *Anal. Chem.*, 58 (1986) 1574.
4. H. Ge and G.G. Wallace, *Anal. Chem.*, 61 (1989) 2391.
5. H. Ge and G.G. Wallace, *J. Liq. Chromatogr.*, 13 (1990) 3245.

6. R.S. Deinhammer, K. Shimazu, and M.D. Porter, *Anal. Chem.*, 63 (1991) 1889.
7. T. Nagaoka, M. Fujimoto, Y. Uchida, and K. Ogura, *J. Electroanal. Chem.*, 336 (1992) 45.
8. T. Nagaoka, M. Fujimoto, H. Nakao, K. Kakuno, J. Yano, and K. Ogura, *J. Electroanal. Chem.*, 350 (1993) 337.
9. R.S. Deinhammer, K. Shimazu, and M.D. Porter, in preparation.
10. I.S. Kim, F.I. Sasinis, R.D. Stephens, and M.A. Brown, *Environ. Sci. Technol.*, 24 (1990) 1832.
11. I.S. Kim, F.I. Sasinis, D.K. Rishi, R.D. Stephens, and M.A. Brown, *J. Chromatogr.*, 589 (1991) 177.
12. R.S. Deinhammer, E. Ting, and M.D. Porter, in preparation.
13. K.K. Unger, *Anal. Chem.*, 55 (1983) 361A.
14. J.H. Knox, B. Kaur, and G.R. Millward, *J. Chromatogr.*, 352 (1986) 3.
15. N. Tanaka, T. Tanigawa, K. Kimata, K. Hosoya, and T. Araki, *J. Chromatogr.*, 549 (1991) 29.
16. O. Chiantore, I. Novak, and D. Berek, *Anal. Chem.*, 60 (1988) 638.
17. N.L. Weinberg and T.B. Reddy, *J. Appl. Electrochem.*, 3 (1973) 73.
18. T.L. Hafkenschied and E. Tomlinson, *Adv. Chromatogr.*, 25 (1986) 1.
19. A. Soffer and M. Folman, *J. Electroanal. Chem.*, 38 (1972) 25.
20. J. Koresh and A. Soffer, *J. Electroanal. Chem.*, 147 (1983) 223.



21. T. Nagaoka, T. Fukunaga, T. Yoshino, I. Watanabe, T. Nakayama, and S. Okazaki, *Anal. Chem.*, 60 (1988) 2766.
22. R.K. Jaworski and R.L. McCreery, *J. Electrochem. Soc.*, 140 (1993) 1360.

## **CHAPTER 4. DYNAMIC MODIFICATION OF SEPARATIONS USING ELECTRO-CHEMICALLY-MODULATED LIQUID CHROMATOGRAPHY (EMLC)**

A paper to be submitted to Analytical Chemistry

Randall S. Deinhammer, En-Yi Ting, and Marc D. Porter<sup>1</sup>

### **ABSTRACT**

A new method for modifying and fine-tuning liquid chromatographic separations without manipulating the mobile phase composition is discussed. This method, termed electrochemically-modulated liquid chromatography (EMLC), is based on the electrochemical manipulation of the capacity factors ( $k'$  values) of analytes both prior to and during their elution from a liquid chromatographic column packed with nonporous glassy carbon (GC) spheres. The GC spheres are connected as the working electrode in the three-electrode electrochemical cell. Improvements in the separation of a mixture of eight aromatic sulfonates (ASFs) obtained at open circuit are demonstrated through the application of several fixed voltages as well as variable voltages and charges to the column. The latter approach, which was implemented through the use either a linear voltage or charge ramp, resulted in an improved resolution of the mixture, a dramatic decrease in the elution bandwidths of the analytes, and a large decrease in the total analysis time. A comparison of these separations to

---

<sup>1</sup>Author to whom correspondence should be addressed.

that obtained using conventional solvent gradient elution suggested that the overall improvements obtained with each method were similar, although the electrochemical elution method provided somewhat sharper elution bands for the early eluting analytes.

Investigation of the electrochemical retention mechanism revealed that changes in the applied voltage ( $E_{app}$ ) served to alter the ability of the carbon surface to participate in donor-acceptor and solvophobic interactions with the analytes, leading to changes in their  $k'$  values. In general, the  $k'$  values increased at positive  $E_{app}$ 's and decreased at negative  $E_{app}$ 's. Aromatic sulfonates having a higher charge as well as a strong electron-donating ability of their aromatic ring and its substituents were found to show the largest changes in  $k'$  values with changes in  $E_{app}$ .

This work also characterized both the EMLC system in terms of the effects of its re-equilibration time and response time to changes in  $E_{app}$  and the carbonaceous stationary phase in terms of the effects of surface oxides, its long term stability, and its surface area, on the separations. These characterizations highlight the usefulness of the EMLC technique for the facile and reproducible manipulation of analytical separations. The surface area studies further revealed that the use of porous carbon spheres as a stationary phase will potentially provide a convenient route for increasing the capacity of EMLC for separating more complex mixtures of analytes.

## INTRODUCTION

Several reports have described the use of electrochemically-modulated liquid chromatography (EMLC) as a possible pathway for fine-tuning analytical separations [1-11]. The basis of this alternative separation strategy derives from the ability to change electrochemically the composition of a stationary phase. Such changes can then be utilized to manipulate separations both prior to [1-5,7,8,10] and, as we have recently shown [6,9,11], during elution without changes in the composition of a mobile phase. The ability to control and fine-tune elution electrochemically using EMLC shows promise for environmental monitoring applications [12,13] as well as for reducing organic solvent consumption in HPLC analyses.

Past results using this new technique, although demonstrating feasibility, were plagued by low chromatographic efficiencies and minimal sample capacities. We have shown, however, in a recent preliminary report [9], that efficient electrochemically-controlled separations are possible using an improved version of our earlier EMLC system. The present paper has three specific goals. The first is to develop a qualitative picture of the mechanism by which the capacity factors ( $k'$  values) of analytes can be modulated electrochemically. This development also facilitated an assessment of the scope of the potential applications for this new separation technique. We chose eight aromatic sulfonates (ASFs) as probe molecules for these studies because their structural similarities aided in the development of this mechanism, and also because of their importance as hazardous waste materials [14-16].

The second goal is to present the results of a detailed characterization of our redesigned EMLC column. The redesign focused on the development of an electrochemically-controlled column that had a high chromatographic efficiency in addition to an effective electrochemical efficiency as in our previous design [6]. These studies were designed to probe the effects of several parameters, including the temporal response of the stationary phase composition to changes in the applied voltage ( $E_{app}$ ), and the stability and surface area of a carbonaceous stationary phase on the separations.

The third goal of this work focused on a more in depth investigation of the effects of alterations in the voltage applied to the GC stationary phase both prior to and during elution on the separations. We show that, in addition to performing electrochemical gradient elution through the use of voltage ramps and steps, linear ramps in charge can be used to effect similar types of improvements in the separations. A comparison of these separations to that obtained using solvent gradient elution is used to illustrate the features of the former methods over conventional elution techniques.

## EXPERIMENTAL

### Glassy Carbon Stationary Phase Characterization.

Scanning electron micrographs (SEM) of the GC stationary phase are shown in Figures 1a and 1b, with Figure 1b showing a higher magnification to emphasize the surface texture of the individual particles. The particles are nonporous, spherical in shape, and have diameters ranging from 2-6  $\mu\text{m}$ , with an average diameter of  $\sim 4 \mu\text{m}$ . The higher magnification micrograph in Figure 1b reveals that the surface of the spheres is relatively

**Figure 1a. Scanning electron micrograph of the GC spheres taken at a magnification of 1500x. The accelerating voltage was 15 kV.**

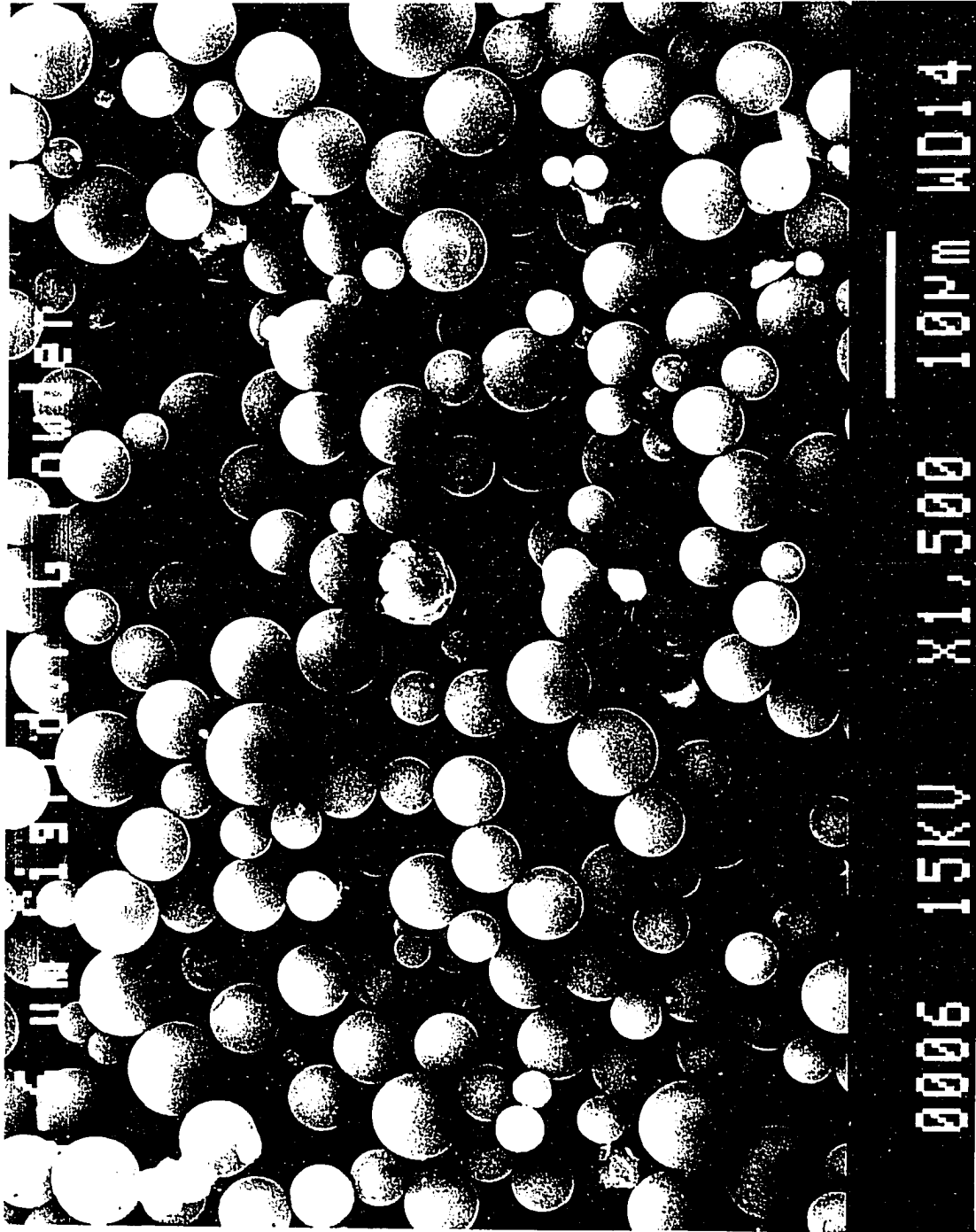
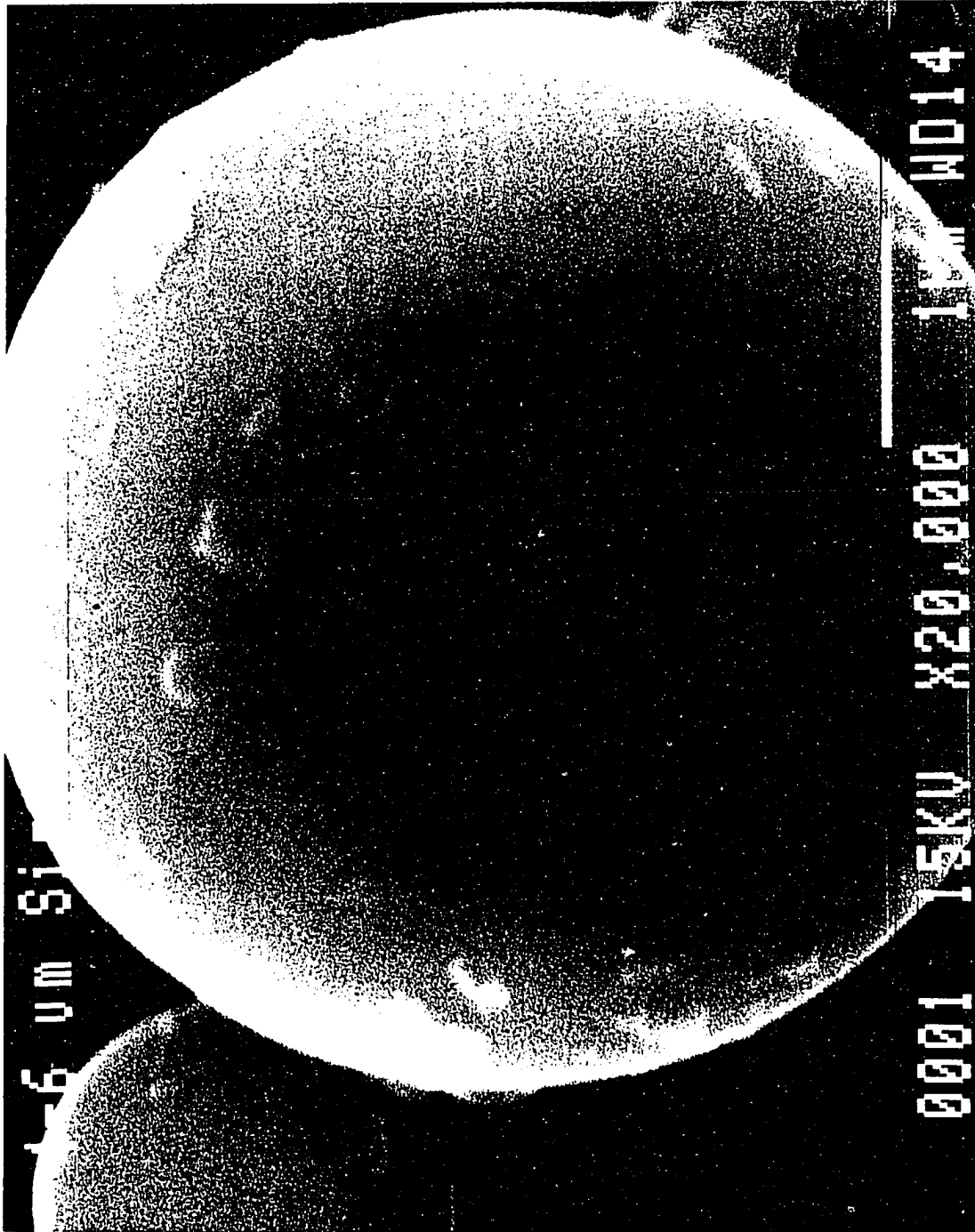


**Figure 1b. Scanning electron micrograph of the GC spheres taken at a magnification of 20,000x. The accelerating voltage was 15 kV.**





smooth, with few surface protrusions. These particles were obtained with a 0.4-12  $\mu\text{m}$  size range (Sigridur G from Sigri Corp.), and were subsequently sieved by air classification. The surface area of the sieved spheres was measured using a BET surface area analyzer. With Kr as the adsorption gas, a six point linear calibration curve (correlation coefficient,  $r=1.00$ ) at 77 K yielded a surface area of 2.39  $\text{m}^2/\text{g}$ .

The porous graphitic carbon (PGC) was obtained from Keystone Scientific and had a surface area of  $\sim 200 \text{ m}^2/\text{g}$  [17]. Scanning electron micrographs of the PGC showed that the particles were porous (pore diameter  $\sim 250 \text{ \AA}$ ), spherical in nature, and had an average diameter of  $\sim 7 \mu\text{m}$ .

#### **Mode of Operation.**

After packing, deaerated mobile phase (aqueous 0.1 M  $\text{LiClO}_4$  containing 1.5 %  $\text{CH}_3\text{CN}$ ) was passed through the column for 6-8 hr at 0.75 mL/min. Such a pretreatment appears to both clean the column and to improve the electrical contact between the GC spheres. Between experiments, the column was re-equilibrated with the mobile phase until a stable detector response was obtained (typically 5 min). The dead volume of the column (0.26 mL) was determined by injection of water. Operational back pressures were  $\sim 3600$  psi. The components in the elution bands were identified from their absorbance spectrum. Analyte concentrations were  $\sim 200$  ppm. Retention times for all of the analytes varied by less than 5% over a tested loading range of 20 to 1000 ppm. The open circuit voltages of the GC ( $\sim 0.15$  V vs  $\text{Ag}/\text{AgCl}/\text{sat'd NaCl}$ ) and the PGC ( $\sim 0.05$  V) stationary phases were estimated by comparison of the chromatograms at open circuit to those at several other  $E_{\text{app}}$ 's. The voltage

window accessible for the modification of separations in the mobile phase at the packed EMLC column was determined using cyclic voltammetry. The voltage limits of +0.80 V and -1.00 V are set primarily by the onset of the oxidation of the porous stainless steel tube and the reduction of the aqueous mobile phase, respectively.

### **Instrumentation.**

The construction of the EMLC column has been presented in detail elsewhere [9]. The chromatographic system consists of a Waters Model 610 pump and valve station, a Model 600E pump controller, and a Model 996 photodiode array absorbance detector. Absorbance spectra were collected at 0.2 sec intervals over a wavelength range of 200-300 nm. Chromatograms were extracted from the absorbance data at 220 nm. A Waters Millennium 2010 data manager was used to collect and process all data. Solutions were injected using a 0.5  $\mu\text{L}$  injector loop (Rheodyne Model 7410) equipped with a position sensing switch (Rheodyne Model 7161). The voltage applied to the stationary phase was controlled by a Princeton Applied Research Model 173 galvanostat-potentiostat and Model 175 universal programmer. Scanning electron micrographs were obtained with a JEOL Model SM 12 electron microscope using an accelerating voltage of 15 kV. The BET surface area measurements were performed at 77 K using a Micromeritics Accusorb 2100E surface area analyzer. Air classification of the GC spheres was accomplished with a Model A-12 Acucut air classifier (Donaldson Corp, Majak Division). The GC spheres were oxidized with a Harrick Model PGC-32G plasma cleaner in an oxygen atmosphere ( $\sim 500$  mtorr) for varying lengths of time.

The XPS spectra were acquired with a Physical Electronics Industries Model 5500 surface analysis system equipped with a hemispherical analyzer, a monochromator, and a multichannel detector. Monochromatic Al K $\alpha$ -radiation (1486.6 eV) at 300 W was used for excitation. The photoelectrons were collected at 45°. Binding energies were referenced to the C(1s) emission band at 284.3 eV. Acquisition times were typically 2 min for survey spectra and ~6 min for high resolution spectra. The base pressure of the ion-pumped UHV chamber was less than  $1 \times 10^{-9}$  torr during analysis. The elemental oxygen-to-carbon ratio (O/C) was calculated by dividing the total number of counts under the O(1s) band by that under the C(1s) band and multiplying the result by 100, after accounting for differences in sensitivity factors [18]. Curve fittings of the O(1s) bands were performed using mixed gaussian-lorentzian band shapes [19].

### Reagents and Chemicals.

Disodium 1,3-benzenedisulfonate (1,3 BDS), disodium 1,2-benzenedisulfonate (1,2 BDS), sodium benzenesulfonate (BS), sodium 4-hydroxybenzenesulfonate (HBS), sodium p-toluenesulfonate (MBS), trisodium naphthalenetrisulfonate (NTS-1 and NTS-2), 4-ethylbenzenesulfonic acid (EBS), potassium hydroquinonesulfonate (HQS), sodium 4-styrenesulfonate (VBS), disodium 2,6-naphthalenedisulfonate (2,6 NDS), lithium perchlorate, and acetonitrile (HPLC grade) were obtained from Aldrich. Disodium 1,5-naphthalenedisulfonate (1,5 NDS) was from Eastman, sodium 4-chlorobenzenesulfonate (CBS) was from TCI America, and mesitylenesulfonic acid (TMBS) was from K&K Laboratories. All chemicals were used as received. At the pH of the mobile phase (pH~6), the ASFs existed as

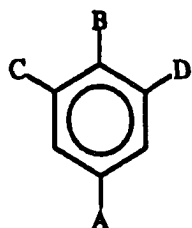
either singly-charged (BS, HBS, MBS, EBS, VBS, CBS, TMBS), doubly-charged (1,3 BDS, 1,2 BDS, 1,5 NDS, 2,6 NDS), or triply-charged (NTS-1 and NTS-2) anions. Table I lists the chemical structures for the deprotonated forms of each ASF. Aqueous solutions were prepared with water purified using a Millipore Milli-Q system.

## RESULTS AND DISCUSSION

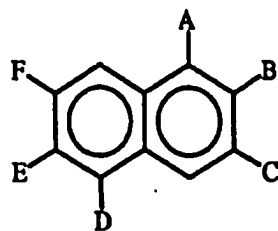
The following sections describe the results of a detailed characterization of our EMLC system and its use in modifying selectively the separations of a mixture containing several structurally similar ASFs. A primary goal is to probe the effectiveness of alterations in the voltage applied to the stationary phase as a means for modifying and optimizing analyte separations, and to develop a preliminary model of the retention mechanism. An additional goal is to investigate the effect of such factors as the temporal response of the stationary phase composition to changes in  $E_{app}$ , the stability and homogeneity of the GC surface, and the surface area of the stationary phase on the separations.

The characterization is divided into five parts. First, the fundamental interactions that influence the retention of the ASFs at the GC surface are identified and characterized through examination of the separation of an eight component mixture at open circuit. Second, separations of this mixture were obtained at several constant  $E_{app}$ 's and compared to that obtained at open circuit to assess the range over which analyte capacity factors ( $k'$  values) could be altered. A preliminary mechanism of the electrochemically-controlled retention of the ASFs is also proposed. Third, alterations in  $E_{app}$  and charge during analyte elution are used to improve the separation of the mixture over that obtained at open circuit. A

Table I. Chemical Structures of the Aromatic Sulfonate Derivatives.



A	B	C	D	Acronym
SO <sub>3</sub> <sup>-</sup>	H	SO <sub>3</sub> <sup>-</sup>	H	1,3 BDS
H	SO <sub>3</sub> <sup>-</sup>	SO <sub>3</sub> <sup>-</sup>	H	1,2 BDS
SO <sub>3</sub> <sup>-</sup>	H	H	H	BS
SO <sub>3</sub> <sup>-</sup>	OH	H	H	HBS
SO <sub>3</sub> <sup>-</sup>	CH <sub>3</sub>	H	H	MBS
SO <sub>3</sub> <sup>-</sup>	CH <sub>3</sub> CH <sub>2</sub>	H	H	EBS
SO <sub>3</sub> <sup>-</sup>	Cl	H	H	CBS
OH	OH	SO <sub>3</sub> <sup>-</sup>	H	DHBS
SO <sub>3</sub> <sup>-</sup>	CH <sub>2</sub> =CH	H	H	VBS
SO <sub>3</sub> <sup>-</sup>	CH <sub>3</sub>	CH <sub>3</sub>	CH <sub>3</sub>	TMBS



A	B	C	D	E	F	Acronym
SO <sub>3</sub> <sup>-</sup>	H	SO <sub>3</sub> <sup>-</sup>	H	SO <sub>3</sub> <sup>-</sup>	H	NTS-1
SO <sub>3</sub> <sup>-</sup>	H	SO <sub>3</sub> <sup>-</sup>	H	H	SO <sub>3</sub> <sup>-</sup>	NTS-2
SO <sub>3</sub> <sup>-</sup>	H	H	SO <sub>3</sub> <sup>-</sup>	H	H	1,5 NDS
H	SO <sub>3</sub> <sup>-</sup>	H	H	SO <sub>3</sub> <sup>-</sup>	H	2,6 NDS

comparison of these separations to a separation obtained at open circuit using solvent gradient elution is used to highlight the features of EMLC. Fourth, the EMLC column is characterized in terms of its temporal response to changes in  $E_{app}$ . Finally, the GC surface is characterized in terms of the effects of residual oxygen functional groups on the retention and band shapes of the analytes, its long term stability, and the effects of increases in surface area on the separation of a mixture of ASFs at open circuit and under conditions of applied voltage.

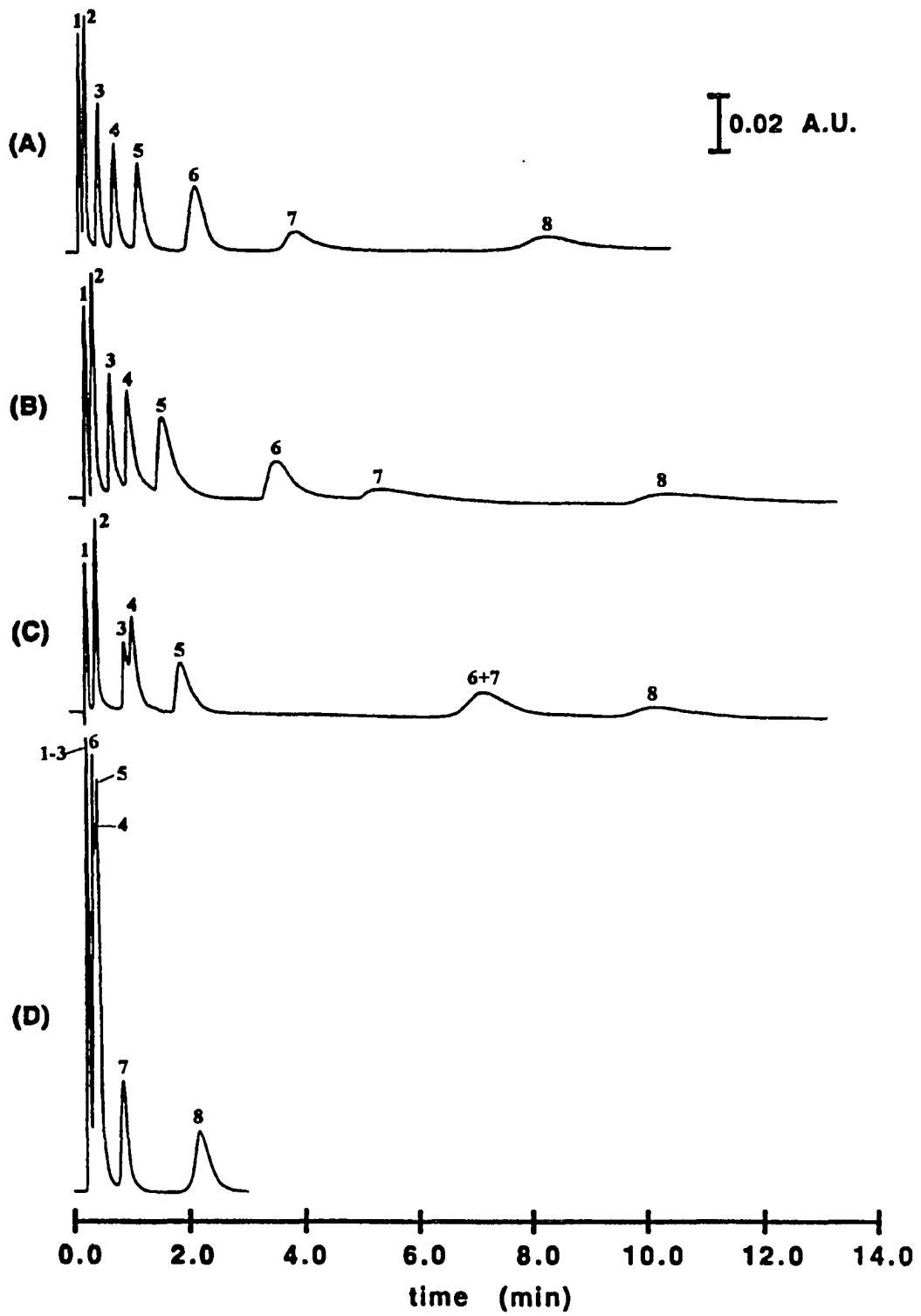
#### **Separation of a Mixture of Aromatic Sulfonates at Open Circuit.**

An important objective of this work is to begin to lay a foundation of the retention mechanism operative in EMLC at an uncoated GC stationary phase. In this section, we examine the separation of an eight component mixture of ASFs obtained at open circuit in terms of the fundamental interactions between these analytes and the GC surface that affect retention. The next section continues this investigation for separations obtained at several constant  $E_{app}$ 's.

Figure 2a shows a separation of the mixture obtained at open circuit ( $\sim 0.15$  V vs Ag/AgCl/sat'd NaCl). The test mixture contained 1,2 BDS, BS, HBS, EBS, CBS, 1,5 NDS, VBS, and TMBS, each at a concentration of  $\sim 200$  ppm. This chromatogram illustrates that the retention of these analytes at the GC surface leads to a near baseline resolution of the mixture in  $\sim 9$  min. Each elution band is symmetrically shaped and exhibits limited tailing. The elution order largely follows that predicted from studies of retention at carbonaceous materials [20-26]. Such separations reflect a complicated mixing of several interactions between the

**Figure 2. Separations of the eight component mixture of ASFs obtained at the EMLC column at open circuit (a); +0.30 V (b); +0.50 V (c); and -1.00 V (d). The mobile phase consisted of aqueous 0.10 M LiClO<sub>4</sub> containing 1.5% CH<sub>3</sub>CN. The flow rate was 0.75 mL/min.**





analytes and the carbon surface, with dispersion and donor-acceptor interactions generally dominant, and solvophobic interactions playing a secondary role. Briefly, dispersion interactions (i.e., nonspecific attractive interactions between two polarizable species) largely reflect the highly polarizable, delocalized electronic band structure of carbon. The strength of this type of interaction is related to the molecular weight of the analyte [27-29], and increases in general with increasing molecular weight.

Donor-acceptor interactions are electronic interactions between the n- and/or  $\pi$ -electrons of the analyte and the delocalized  $\pi$ -electrons at the carbon surface. These interactions have been examined using ab initio molecular orbital calculations [30]. According to these findings, the overall donor-acceptor interaction can be viewed as the sum of five components: the electrostatic interaction (ES), the polarization interaction (PL), the exchange repulsion (EX), the charge-transfer interaction (CT), and a coupling term (MIX). The ES component, which can be either attractive or repulsive, includes interactions between permanent charges and dipoles. The PL component includes attractive interactions between permanent dipoles and induced dipoles. The EX component is a short-range repulsive term caused by the interaction of the electron clouds of the donor and the acceptor. The CT component includes attractive interactions that involve the transfer of charge from the highest occupied molecular orbital (HOMO) of the donor to the lowest unoccupied molecular orbital (LUMO) of the acceptor (e.g., n- $\pi$ ,  $\pi$ - $\pi$ , proton donor- $\pi$  interactions). The MIX component is a coupling term that accounts for higher order interactions between the donor and the acceptor, and is generally weak.

The relative contribution of each of the above components of donor-acceptor interactions to the total interaction energy can be dissected using the polarity of the donor and acceptor. For polar-polar donor-acceptor complexes, the interaction energy is primarily determined by the ES component, with the CT component generally playing a secondary role. Polar-nonpolar complexes have an interaction energy that is determined by the ES, CT, and PL components, whose magnitudes are smaller than those for the polar-polar complex due to a larger intermolecular separation distance. In contrast, weak nonpolar-nonpolar complexes have a stabilization energy that is determined largely by the CT component. We can therefore expect that the donor-acceptor interactions between anionic analytes and the carbon surface will consist mainly of a strong ES component and weaker but significant CT and PL components.

In addition to dispersion and donor-acceptor interactions, analytes can interact with the carbon surface through solvophobic effects. The strength of these attractive but nonspecific interactions is governed by the relative extent of solvation of the stationary phase and the analyte by the mobile phase. These effects generally increase the retention of hydrophobic molecules when hydrophilic mobile phases are used as eluents, and are employed as a primary mechanism for retention and separation of molecules at bonded hydrocarbon stationary phases (e.g., octadecylsilane-coated silica) [31]. For our purposes, we have included the effects of the double layer structure at the carbon surface-mobile phase interface on the interaction of the analytes with the stationary phase as part of a solvophobic interaction. As will be detailed below, changes in the structure of the electrical double layer

induced by electrochemical alterations in the excess charge at the GC surface can modify the availability of the carbon surface to the analytes through increases or decreases in the interfacial concentration of ions [32]. In light of these discussions, we expect that the ASFs will interact with the carbonaceous stationary phase mainly through dispersion, donor-acceptor, and solvophobic type pathways. As will be elucidated later, the ability to alter  $E_{app}$  provides an effective route for manipulation of, to a large extent, the magnitude of the donor-acceptor and solvophobic interactions between the analyte and the carbon surface that can be exploited to fine-tune separations.

Comparison of the experimentally measured  $k'$  values of the substituted ASFs to that for BS yields insights into the role of each of these retention mechanisms at this mobile phase-stationary phase combination at open circuit. The general tendency for the  $k'$  values of the ASFs to increase as their hydrophobicity increases illustrates the effects of solvophobic interactions on retention. This tendency is clearly illustrated through the use of the hydrophobicity parameters ( $\log P$ ) of each ASF [33,34], as shown in Table II. For example, the relative elution order of 1,2 BDS ( $k'=0.00$ ,  $\log P=-7.39$ ), BS ( $k'=0.30$ ,  $\log P=-2.63$ ), EBS ( $k'=1.83$ ,  $\log P=-1.54$ ) and TMBS ( $k'=24.50$ ,  $\log P=-0.95$ ) follows their increase in hydrophobicity (i.e., more positive  $\log P$  value). As discussed, these interactions are nonspecific and are present in any reverse phase column. The unique feature of carbonaceous stationary phases is that their polarizable, delocalized electronic band structure provides an additional dimension (and selectivity) to the separations based on donor-acceptor and dispersion interactions.

Table II. Observed slopes positive and negative of the pzc, substituent electronic parameters ( $\sigma$ )<sup>a</sup>, substituent steric parameters ( $E_s$ )<sup>b</sup>, and hydrophobicity parameters ( $\log P$ )<sup>c</sup> for seven ASFs.

Analyte	slope (logk'/volt)		$\sigma$	$E_s$	$\log P$	Other <sup>d</sup>
	$E > \text{pzc}^e$	$E < \text{pzc}^f$				
BS	1.16	----	0.00	0.00	- 2.63	-----
HBS	1.32	----	- 0.37	0.32	- 3.30	proton donor
EBS	0.72	0.34	- 0.15	0.56	- 1.54	-----
CBS	1.10	0.45	0.23	0.55	- 1.92	dipole-dipole
1,5 NDS	1.78	0.54	----	----	- 6.07	dbl. chg, 2 rings
VBS	1.05	0.47	- 0.02	0.57	- 1.90	$\pi-\pi$
TMBS	0.71	0.43	- 0.17	0.52 <sup>g</sup>	- 0.95	-----

<sup>a</sup>Hammett electronic parameters for the non-sulfonate aromatic substituent [33].

<sup>b</sup>Charton steric parameters for the non-sulfonate aromatic substituent [33].

<sup>c</sup>Calculated using the method of Hansch [33].

<sup>d</sup>Miscellaneous donor-acceptor properties of the aromatic substituents.

<sup>e</sup>Includes k's between +0.30 V and -0.20 V.

<sup>f</sup>Includes k's between -0.40 V and -1.00 V.

<sup>g</sup>Value per methyl group.

The presence of these additional interactions results in an elution order of the ASFs that deviates greatly from the order predicted based solely on hydrophobicity considerations. These effects are most apparent in the increased retention of HBS ( $k'=0.96$ ,  $\log P=-3.30$ ) and 1,5 NDS ( $k'=6.12$ ,  $\log P=-6.07$ ) relative to BS ( $k'=0.30$ ,  $\log P=-2.63$ ), as well as the stronger retention of VBS ( $k'=11.26$ ,  $\log P=-1.90$ ) and CBS ( $k'=3.08$ ,  $\log P=-1.92$ ) relative to the

more hydrophobic EBS ( $k'=1.83$ ,  $\log P=-1.54$ ). Donor-acceptor interactions in these cases can occur through interaction of their aromatic substituents with the carbon surface largely by either ES or CT interactions. These interactions are facilitated by the extensive planar array of fused aromatic rings at the carbon surface, which favors  $\pi$ -stacking of the planar ASFs [35]. This mode of association allows for extensive donor-acceptor interaction between the  $\pi$ -electrons of the aromatic ring as well as the  $n$ - or  $\pi$ -electrons of its substituents with the delocalized  $\pi$ -electrons at the carbon surface. An important consequence of such interactions is that substituents on the aromatic ring, and in particular bulky substituents, can reduce the donor-acceptor interaction through steric effects [30,36,37]. As found below, this steric effect can have significant ramifications on the ability to modulate the  $k'$  values of the ASFs through changes in  $E_{app}$ . In addition, each of the ASFs can interact through dispersion forces which occur between their polarizable functionalities and the electronic band structure of carbon. Together, these discussions serve as the basis for a model of retention at the carbon surface that is founded on the combined strength of dispersion, donor-acceptor, and solvophobic effects between the analytes and the carbon surface.

#### **Alteration of the Separation of the Aromatic Sulfonates Through Application of Various Fixed Applied Voltages.**

As discussed, retention of the ASFs results from a combination of their dispersion, donor-acceptor, and solvophobic interactions with the GC surface. The basis for modification of separations through alterations in  $E_{app}$  stems from the ability to manipulate selectively the

strength of these interactions. To assess quantitatively this ability as well as the effectiveness of our electrochemically-controlled separation strategy, we examined the retention of the eight ASFs as a function of several fixed values of  $E_{app}$ . Figures 2b-f show separations of the mixture obtained at +0.30 V, +0.50 V, -1.00 V, -0.20 V, and -0.40 V, respectively. At +0.30 V, the  $k'$  values for all ASFs increase by at least a factor of 1.3 over those at open circuit. For example, the  $k'$  values for BS and 1,5 NDS increase from values of 0.30 and 6.12 at open circuit to values of 0.50 and 10.53 at +0.30 V, respectively. Further, the separation of 1,2 BDS and BS has improved somewhat over that at open circuit. The application of more positive values of  $E_{app}$  (e.g., +0.50 V) results in further increases in the  $k'$  values of the ASFs. These increases are clearly evident from the extensive overlap of the elution bands for HBS and EBS and for 1,5 NDS and VBS at +0.50 V. At this more positive  $E_{app}$ , the  $k'$  values for BS ( $k'=0.62$ ), HBS ( $k'=2.15$ ), VBS ( $k'=21.41$ ), and 1,5 NDS ( $k'=21.41$ ) show increases by more than a factor of two when compared to those at open circuit. The  $k'$  values of EBS ( $k'=2.56$ ), CBS ( $k'=5.09$ ), and TMBS ( $k'=30.50$ ), however, show somewhat smaller increases (factors of ~1.3-1.5).

In contrast, application of  $E_{app}$ 's more negative than the open circuit voltage (~+0.15 V) results in large decreases in the  $k'$  values for all eight ASFs. At -0.20 V, the  $k'$  values for HBS ( $k'=0.10$ ) and for 1,5 NDS ( $k'=1.44$ ) are smaller than those at open circuit by factors of 8.1 and 4.3, respectively. These large decreases are followed by the somewhat smaller but significant decreases for BS ( $k'=0.10$ ), EBS ( $k'=1.06$ ), CBS ( $k'=1.21$ ), VBS ( $k'=4.79$ ), and TMBS ( $k'=13.91$ ) by factors of 1.7-2.4. At -0.40 V, the  $k'$  values for all eight

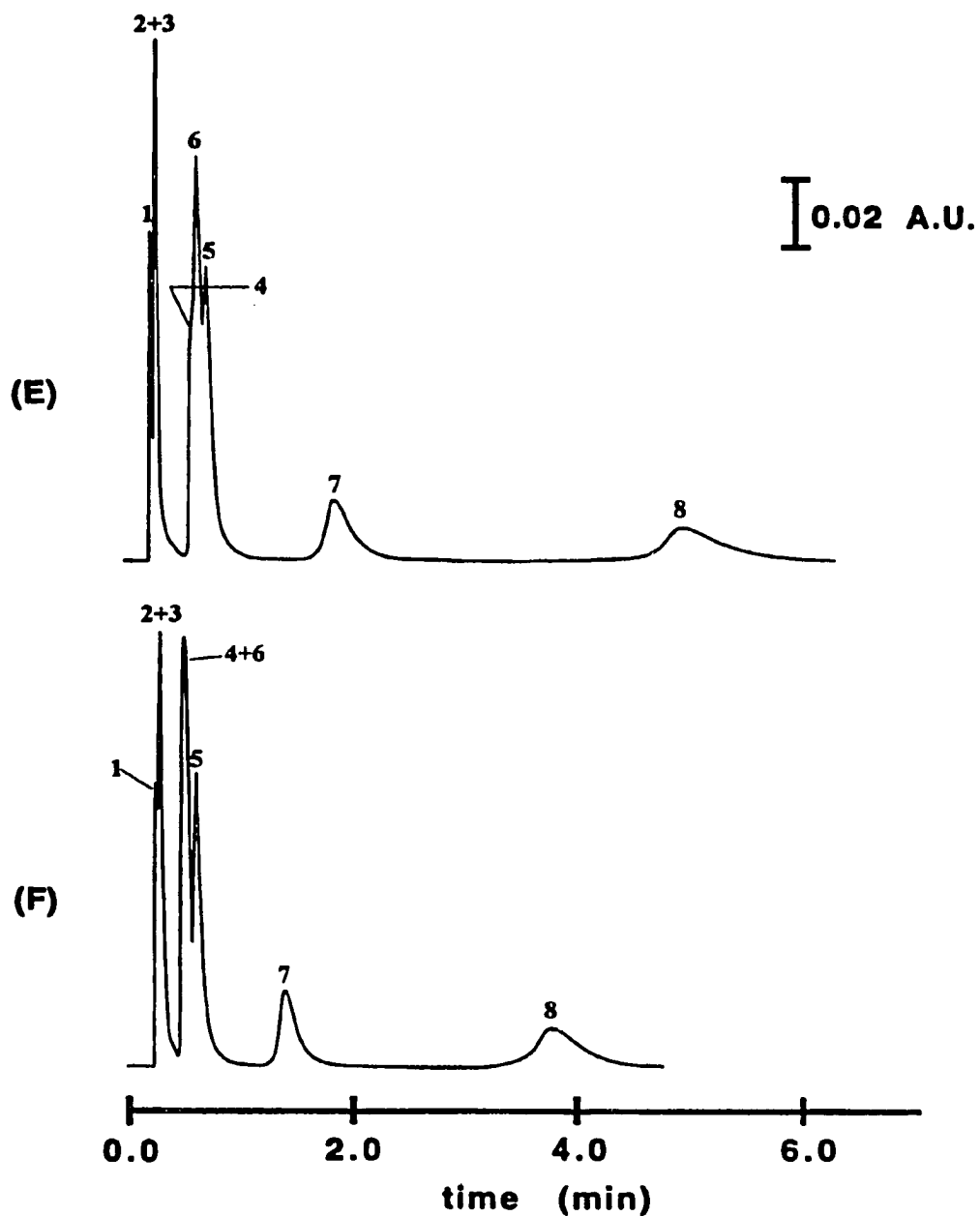


Figure 2 (cont'd). Separations of the eight component mixture of ASFs obtained at the EMLC column at -0.20 V (e); and -0.40 V (f). The mobile phase consisted of aqueous 0.10 M LiClO<sub>4</sub> containing 1.5 %CH<sub>3</sub>CN. The flow rate was 0.75 mL/min.



ASFs decrease further by factors of 1.2-1.7 as compared to those at -0.20 V. At extreme negative voltages such as -1.00 V, 1,2 BDS, BS, and HBS are unretained and elute with the void volume (i.e.,  $k'=0.00$ ). Further, the  $k'$  values for EBS ( $k'=0.50$ ), CBS ( $k'=0.57$ ), 1,5 NDS ( $k'=0.38$ ), VBS ( $k'=1.79$ ), and TMBS ( $k'=5.68$ ) decrease by factors of 3.6, 5.2, 16.1, 4.4, and 3.8, respectively, when compared to those at open circuit. Taken together, these data demonstrate the ability of EMLC to alter the  $k'$  values for the ASFs over a wide range. This ability is highlighted by 1,5 NDS, whose  $k'$  changes by a factor of ~56 between +0.50 V and -1.00 V.

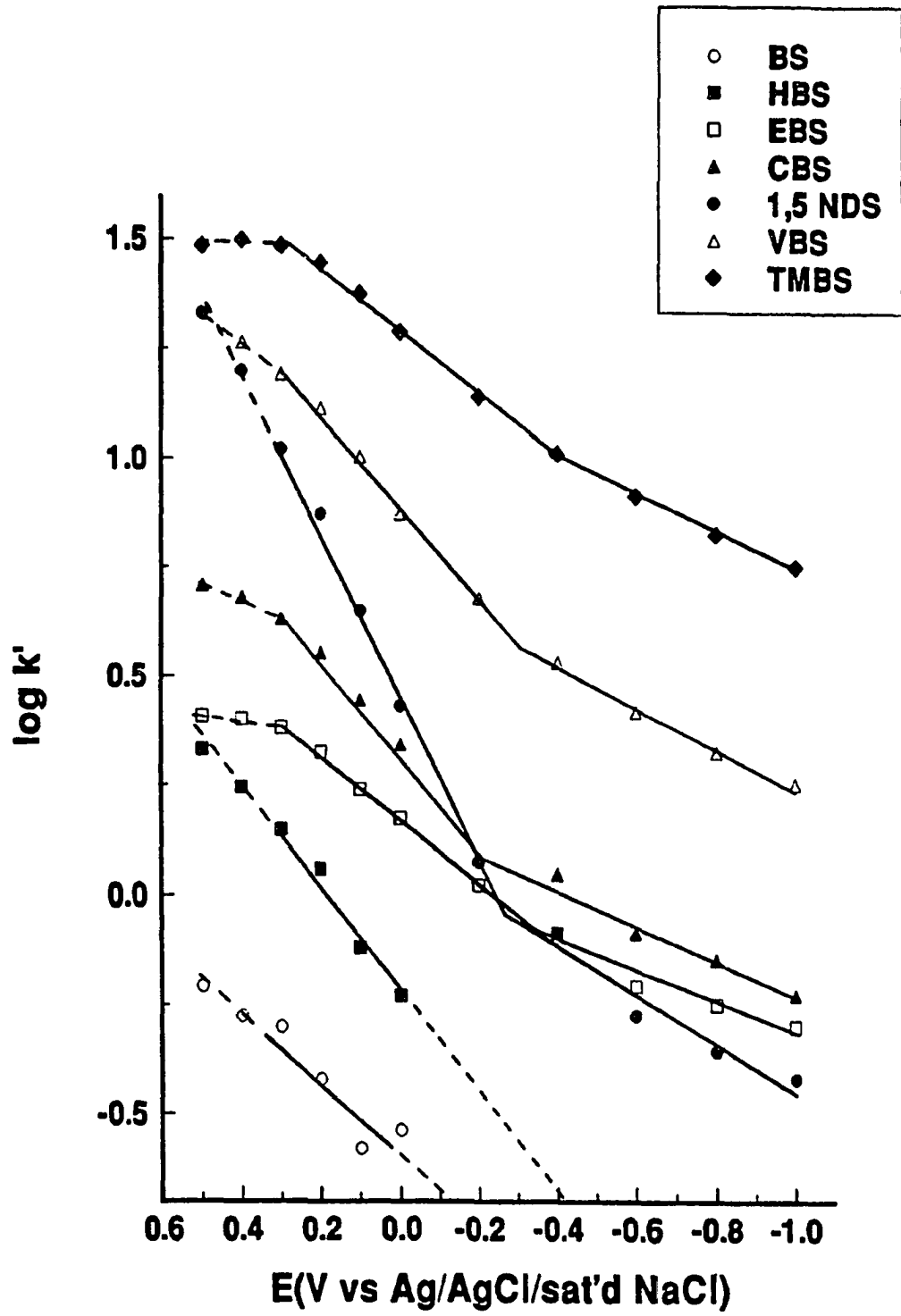
To compare these electrochemically-produced changes in the  $k'$  values to those produced through modification in the mobile phase composition, we systematically examined the separations of the eight component mixture at open circuit at various aqueous 0.10 M LiClO<sub>4</sub>/acetonitrile mobile phase combinations. The results revealed that a separation using a mobile phase composition of 99.5% aqueous 0.10 M LiClO<sub>4</sub> and 0.5% acetonitrile had a total analysis time (11.1 min) that was roughly equivalent to that obtained at +0.50 V (10.7 min), whereas a separation obtained at a composition of 96% aqueous 0.10 M LiClO<sub>4</sub> and 4% acetonitrile had an analysis time (2.7 min) similar to that obtained at -1.00 V (2.3 min). Therefore, alteration in  $E_{app}$  between +0.50 V and -1.00 V is roughly equivalent to modification of the acetonitrile concentration in the mobile phase from 0.5% to 4%. Although the change in analysis time produced electrochemically can therefore be easily mimicked through changes in the mobile phase composition, the electrochemical elution method, and in particular the electrochemical retention mechanism, appears to be more selective for particular

ASFs. For example, the differences in the elution order and the relative  $k'$  values of the ASFs observed at +0.50 V (Figure 2c) and -1.00 V (Figure 2d) were not observed in the separations obtained at the 0.5% and 4% acetonitrile concentrations. In the latter case, the  $k'$  values for each of the ASFs changed by roughly equivalent amounts when the mobile phase composition was altered, giving rise to a similar elution order at each composition tested. Therefore, it appears that changes in  $E_{app}$  can add some interesting and useful selectivity to the separations that is not easily gained through compositional alterations in the mobile phase.

#### **Discussion of the Electrochemical Retention Mechanism.**

Figure 3 shows a plot of the logarithm of  $k'$  vs  $E_{app}$  for each of the eight ASFs. The curve for 1,2 BDS as well as the curves for BS and HBS at  $E_{app} < 0.00$  V are omitted due to their lack of retention at the GC surface. The error bars for each ASF are about the size of the data points, and were determined by several replicate separations. As is apparent, some of the ASFs show at least three distinctly different regions of behavior between +0.50 V and -1.00 V, with each region exhibiting a dependence that appears linear with  $E_{app}$ . The relative slopes of these data serve as a starting point for a model of the electrochemically-modulated retention of analytes at the GC surface. The model is based on the changes in the ability of the GC surface to interact with the ASFs, to a large extent, via donor-acceptor and solvophobic pathways, as produced through alteration in  $E_{app}$  relative to the potential of zero charge ( $pzc$ ,  $\sim -0.15$  V vs Ag/AgCl/sat'd NaCl). Although the strength of the dispersion interaction between the ASFs and the GC surface may also be affected by changes in  $E_{app}$  [27], our experimental data suggests that this effect is insignificant when compared to the

**Figure 3. Plot of  $\log k'$  versus  $E_{app}$  for separations of an eight component mixture of ASFs obtained at the GC stationary phase. The mobile phase consisted of aqueous 0.10 M  $\text{LiClO}_4$  containing 1.5 %  $\text{CH}_3\text{CN}$ . The flow rate was 0.75 mL/min.**



electrochemically-produced changes in donor-acceptor and solvophobic interactions (see below). We will therefore treat this interaction as being independent of  $E_{app}$ , but important for the retention of the ASFs at the GC surface. In our model, the experimentally determined capacity factor,  $k'$ , reflects the sum of the  $k'$  values due to dispersion interactions,  $k'_{dis}$ , donor-acceptor interactions,  $k'_{da}$ , and solvophobic interactions,  $k'_{sol}$ . As discussed, the first term is treated as being independent of  $E_{app}$ , whereas the latter two terms have magnitudes that depend on  $E_{app}$ .

In light of our previous discussion, the donor-acceptor interaction term is assumed to consist largely of four interactions between the ASFs and the charged GC surface: (1) the electrostatic attraction or repulsion of the anionic sulfonate groups (ES term), (2) the dipole-dipole attraction or repulsion of the polar aromatic substituents of each ASF (ES term), (3) the HOMO-LUMO attraction of the aromatic ring  $\pi$ -electrons (CT term), and (4) the  $n$ - $\pi$ , proton donor- $\pi$ , or  $\pi$ - $\pi$  interaction of the aromatic substituents of each ASF (CT term). The magnitude of these interactions will be dependent on both the donor or acceptor ability of the GC surface as well as on the quantity and polarity of the excess charge at the carbon surface. In general, the positive excess surface charge at  $E_{app} > pzc$  will increase its electron-accepting ability, whereas the negative excess charge present at  $E_{app} < pzc$  will increase its electron-donating ability [38,39]. The magnitude of this electron-donating or accepting ability of GC should follow the changes in  $E_{app}$ , with larger excursions of  $E_{app}$  from the pzc producing an enhanced electron accepting or donating ability. At extreme departures of  $E_{app}$  from the pzc, the ability of the GC surface to attract or repel the ASFs via these pathways will level off,

however, because the effects of additional increases or decreases in surface charge or donor/acceptor strength will be small. Therefore, at  $E_{app} > pzc$ , we expect each of these donor-acceptor interactions to increase in magnitude. In contrast, at  $E_{app} < pzc$ , both the electrostatic and dipolar components should be repulsive, whereas the HOMO-LUMO and  $n-\pi$ , proton-donor- $\pi$ , or  $\pi-\pi$  interactions should decrease to zero as the carbon surface becomes an increasingly stronger electron donor.

The solvophobic term is considered only as an attractive term that has a maximum at the pzc and decreases with positive or negative excursions from the pzc. The decreases in  $k'_{sol}$  are attributed to the buildup of an excess surface charge and the resulting compaction of the electrical double layer [32,40,41], which sterically inhibits the ASFs from interacting with the GC surface. Solvophobic effects may also occur as a result of changes in the hydrophilicity of the GC surface induced by electrochemical alterations in the interfacial concentration of electrolyte ions. In total, our model then predicts that at  $E_{app} > pzc$ , donor-acceptor interactions are stronger than at the pzc, whereas solvophobic interactions are weaker. Conversely, at  $E_{app} < pzc$ , both solvophobic and donor-acceptor interactions decrease relative to those at the pzc. The observed  $k'$  thus largely represents the additive interplay of  $k'_{da}$  and  $k'_{sol}$ .

The additive effects of the above interactions can then be applied as a first working explanation of the  $k'$  data in Figure 3. We view our analysis only as a qualitative model at this time. At  $E_{app} > pzc$ ,  $k'_{da}$  appears to increase more rapidly with increasing  $E_{app}$  than the decreases in  $k'_{sol}$ , giving rise to a continual increase in the  $k'$  values for all ASFs. At

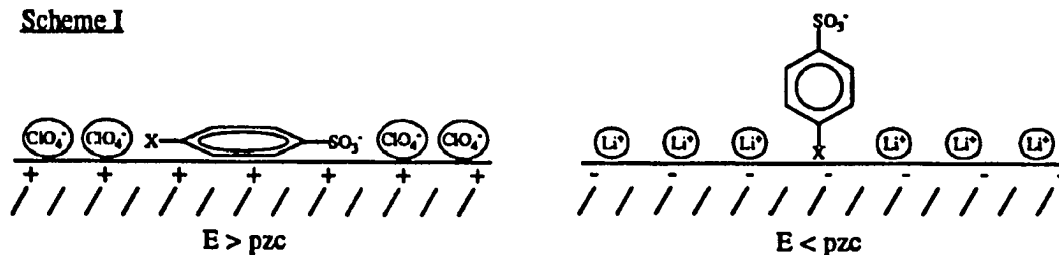
$E_{app} > +0.30$  V, however, the  $k'$  values for several of the ASFs (e.g., TMBS, VBS, CBS, EBS) show smaller increases than those between +0.30 V and -0.20 V (dashed curves).

Interestingly, TMBS shows no further increases in its  $k'$  as  $E_{app}$  is increased throughout this voltage range. Although this effect could potentially result from either a saturation of the GC surface with charge or from a compaction of the electrical double layer, we believe the former possibility to be most likely. This conclusion is supported by studies of the retention of CBS, for example, at  $E_{app} > +0.50$  V. These studies show that the magnitude of the change in its  $k'$  with  $E_{app}$  continues to decrease between +0.50 V and +0.80 V. At  $E_{app}$ 's between +0.80 V and +1.00 V, no further changes in its  $k'$  were found. These observations are *not* consistent with those expected from double layer compaction, since the  $k'$  values should show a *decrease* in such a case. Importantly, the magnitude of this effect on the  $k'$  values of the ASFs between +0.30 V and +0.50 V is related to the strength of their interaction with the carbon surface, with those ASFs that interact more strongly (i.e., 1,5 NDS and HBS) showing the weakest effects. Although not apparent in Figure 3, we expect the  $k'$  values for 1,5 NDS, HBS, and BS to also eventually show a decreased sensitivity to changes in  $E_{app}$ , but at more positive values of  $E_{app}$ . To allow for a more accurate comparison of the slopes among the ASFs, however, we have opted to neglect the data points at +0.40 V and +0.50 V for each ASF in the slope calculations. Although not shown, a similar compaction effect is seen at  $E_{app} < -1.00$  V, as expected due to the saturation of the GC surface with negative charge.

The slopes of the lines for the ASFs at  $E_{app} < pzc$  are smaller than those observed between +0.30 V and -0.20 V. At first glance, this result is surprising since the decrease in

$k'_{da}$  (i.e., repulsive ES term, decreased CT term) *coupled* with a decrease in  $k'_{mol}$  should result in a slope that is similar to or larger than that at  $E_{app} > pzc$ . We postulate that a change in the orientation of the ASFs at the GC surface accompanies a change in the polarity of the excess surface charge from positive ( $E_{app} > pzc$ ) to negative ( $E_{app} < pzc$ ). Such a situation, as roughly illustrated in Scheme I, is supported by the large body of literature available concerning the

**Scheme I**



voltage-dependent adsorption of charged aromatic species at electrode surfaces [38,39,41-44]. According to these studies, aromatic anions generally lie flat (i.e., ring parallel to the electrode surface) on electrode surfaces at  $E_{app} > pzc$  to maximize their electrostatic attraction and HOMO-LUMO interaction with the positively charged, electron-accepting surface. Although a competition for surface sites between these anions and those from the electrolyte exists, the strength of the electrostatic and HOMO-LUMO interactions of aromatic anions is sufficient to facilitate their preferential adsorption. In contrast, these interactions are much weaker at  $E_{app} < pzc$  since the electrode surface is an electron-donor and has a negative surface charge. The strong electrostatic repulsion of the anionic group from the electrode surface generally leads to a change in its orientation to minimize this repulsion, as illustrated in Scheme I. This orientational change is further aided through competition with electrolyte



cations for surface sites, a process that is facilitated by the weak interaction of the anions with the electrode surface in this voltage range. In addition, the electron-donating/accepting properties of the substituents on the aromatic ring, labeled as 'X' in Scheme I, can affect this reorientation significantly by increasing or decreasing the interaction of the analyte with the electrode surface.

Therefore, in light of these discussions, the decreased slopes at  $E_{app} < pzc$  observed in Figure 3 may result from a decreased interaction of the ASFs with the carbon surface due to the abovementioned orientational changes. In the parallel orientation, an ASF molecule can potentially interact with the GC surface through its aromatic ring and each of its substituents. This combined interaction renders the ASFs very sensitive to changes in  $E_{app}$ , and therefore leads to large slopes. In the perpendicular orientation, however, the ASFs largely interact with the GC surface through their substituents meta and para to the sulfonate group. This decreased voltage-dependent interaction results in a decreased sensitivity to changes in  $E_{app}$ , and thus to smaller slopes.

The variation in the slopes of the lines in Figure 3 for each ASF suggests that the ability to modify analyte  $k'$  values electrochemically provides a unique and interesting route for manipulating the selectivity of separations. Table II lists the observed slopes for each ASF both at  $E_{app}$ 's positive and negative of the pzc. The error bars on the slopes are  $\sim \pm 0.02$ . Notice that at  $E_{app} > pzc$ , the slopes vary from 1.78 for 1,5 NDS to 0.71 for TMBS, giving rise to an order of increasing slope of TMBS~EBS<VBS<CBS<BS<HBS<1,5NDS. At  $E_{app} < pzc$ , the slopes for all the ASFs are smaller, and vary from 0.54 for 1,5 NDS to 0.34 for EBS,

resulting in an order of  $EBS < TMBS \sim CBS \sim VBS < 1,5 \text{ NDS}$ . In addition, the range of slopes is significantly smaller at  $E_{app} < pzc$  than at  $E_{app} > pzc$ . The slopes for BS and HBS are unmeasurable at  $E_{app} < -0.00 \text{ V}$  due to their lack of retention at the GC stationary phase.

These differences in slope can be qualitatively understood largely through considerations of the specific types and extent of the donor-acceptor interactions that each ASF can participate in with the GC surface. Table II gives the electronic ( $\sigma$ ) and steric parameters ( $E_s$ ) for the aromatic substituents of each ASF. The  $\sigma$  parameters can be used as a relative measure of the electron-donating or electron-accepting ability of each substituent. As defined by Hammett [45], electron donation is expected for substituents with negative values, and electron withdrawal is expected for substituents with positive values. The  $E_s$  values have been used to predict the steric effects of substituents [33], and are used here to predict their steric inhibition of the HOMO-LUMO interaction of the aromatic ring with the carbon surface. As defined, more positive values indicate an increased steric effect.

According to our model, the ASFs having the largest slopes at  $E_{app} > pzc$  should be those with the highest charge (ES attraction), with substituents that can interact with the GC surface via CT or dipole-dipole pathways, and with minimal steric hindrance of the HOMO-LUMO interaction between their aromatic ring and the carbon surface. The actual order of increasing slopes can be qualitatively predicted using these guidelines. For example, 1,5 NDS has the highest charge, and a fused ring system capable of strong HOMO-LUMO interactions [44]; because of these two strong voltage-dependent interactions, the slope (1.78) for

1,5 NDS should therefore be the greatest. Of the singly-charged ASFs, HBS has the strongest electron-donating substituent, the hydroxyl group ( $\sigma=-0.37$ ), which also has the smallest steric effect on the aromatic ring ( $E_s=0.32$ ); its slope (1.32) should therefore be the largest of the singly-charged anions. Of the remaining ASFs, we can predict that although EBS and TMBS have electron-donating alkyl substituents, these substituents are bulky (i.e., large  $E_s$ ) and therefore decrease the HOMO-LUMO interaction of their aromatic rings with the GC surface. The importance of this steric effect is clearly seen in the large slope found for BS (1.16) relative to the other singly-charged ASFs. Only HBS has a larger slope than BS due to the strong interaction of its hydroxyl group with the carbon surface. The donor strength of the hydroxyl group has been noted previously at conventional carbonaceous stationary phases [24]. The increased slopes of CBS (1.10) and VBS (1.05) relative to EBS (0.72), for example, likely occur as a result of the dipole-dipole and  $\pi-\pi$  interactions of their substituents with the GC surface, respectively. Importantly, these large increases in slope for CBS and VBS occur despite the similar steric effects of their chloro and vinyl groups ( $E_s=0.55$  and 0.57, respectively) relative to the ethyl group of EBS ( $E_s=0.56$ ). These arguments can also be used to explain the relative extent of the decrease in slope at  $E_{app}>+0.30$  V, since the ASFs showing the most significant slope decrease are those which interact most weakly with the GC surface (i.e., TMBS and EBS), and have the smallest slopes between +0.30 V and -0.20 V.

In contrast, we expect a somewhat different behavior at  $E_{app}<pzc$ . In this voltage region, we expect that a higher charge will also contribute to a large slope due to electrostatic and dipolar repulsions, as evident from the increased slope of 1,5 NDS relative to the other

ASFs. However, the decrease in the magnitude of the HOMO-LUMO interactions will likely cause the slopes for the ASFs that interact strongly with the GC surface via these interactions at  $E_{app} > pzc$  (i.e., 1,5 NDS and VBS) to decrease relative to those ASFs whose retention is less dependent on HOMO-LUMO interactions (i.e., EBS and TMBS). In other words, the decrease in the voltage-dependent HOMO-LUMO interactions that caused the slopes for 1,5 NDS and VBS, for example, to be larger than those for EBS and TMBS at  $E_{app} > pzc$  results in a larger decrease in the slopes for the former species at  $E_{app} < pzc$ . It is important to note, however, that the slopes for *all* of the ASFs decrease at  $E_{app} < pzc$  relative to those at  $E_{app} > pzc$ , with those for the strongest electron-donors (i.e., 1,5 NDS and VBS) showing larger decreases. These trends are clearly evident from the data in Table II, which shows that the slopes for 1,5 NDS and VBS are decreased to a greater extent than those of EBS and TMBS. For example, the slope for 1,5 NDS decreases by a factor of 3.3, whereas that for TMBS decreases by only a factor of 1.7.

Interestingly, the order of increasing slope for EBS and TMBS is reversed, with TMBS having a significantly larger slope (0.43) than EBS (0.34). Although not yet clear, we attribute this reversal to either (1) a steric effect resulting from compaction of the electrical double layer, or (2) an increased hydrophilicity of the GC surface resulting from the electrochemical attraction of electrolyte ions to the GC surface. The compaction effect, which results from the increasing attraction of lithium mobile phase cations into the double layer as  $E_{app}$  becomes increasingly more negative than the pzc, can effectively “squeeze-out” the bulky TMBS anions from the double layer, resulting in a decreased retention and therefore a larger

slope. The increase in the hydrophilicity of the GC surface may further result in a decreased interaction of the more hydrophobic TMBS ( $\log P = -0.95$ ) with the GC surface relative to EBS ( $\log P = -1.54$ ), leading to an increased slope. Such effects, although present at  $E_{app} > pzc$ , are less significant as a result of the much stronger interaction of the ASFs with the GC surface.

As mentioned previously, alterations in  $E_{app}$  can also potentially modify the strength of the dispersion interactions of the ASFs with the GC surface, since the ability of the GC surface to participate in such interactions is related to its polarizability and therefore to  $E_{app}$  [27]. At  $E_{app} > pzc$ , the polarizability of the GC surface should decrease as electrons are removed from the surface, thereby decreasing dispersion interactions. At  $E_{app} < pzc$ , the polarizability of the GC surface should increase as electrons are added to the surface, thereby increasing dispersion interactions. Comparison of this prediction to our experimental data, however, does not support the presence of such an effect. For example, the increase in dispersion interactions at  $E_{app} < pzc$  should increase the retention of the large TMBS molecule relative to the smaller CBS molecule, resulting in a decrease in the slope for the former species [28,29]. In fact, the data in Table II show that the opposite effect is actually observed. Therefore, it appears that electrochemically-induced changes in  $k'_{di}$ , if present, do not significantly affect the retention of the ASFs at the carbon surface.

The predictions of our model also follow the results of preliminary studies of the electrochemically-modulated retention of various uncharged, neutral compounds. For example, comparison of the relative slopes of the lines at  $E_{app} > pzc$  in the  $\log k'$  versus  $E_{app}$  plot

for the ASFs (Figure 3) to those of substituted phenolic compounds showed that the former slopes were ~two times larger than the latter. This difference is likely due to the increased electrostatic attraction of the charged sulfonate group (i.e., ES interaction) [43,44]. This conclusion is further supported by the increase in the slope of the lines observed as the charge on the ASF increases. These studies also revealed that the ability to modulate analyte  $k'$  values decreased as the polarity of the neutral analyte decreased. For example, the  $k'$  values of polar neutral compounds such as substituted phenols can be modulated electrochemically much easier than those of nonpolar compounds such as alkyl-substituted benzene derivatives. Therefore, it appears that polar electron-donating functional groups, and in particular charged groups, are a necessary component of the analyte structure to allow for efficient manipulation of their  $k'$ s by EMLC. These discussions together serve as the beginnings of a model that can be used to predict qualitatively the effects of changes in  $E_{app}$  on the  $k'$  values of various analytes using EMLC. We are currently devising experiments to unravel further the mechanism and to evaluate the scope of our model. Work directed toward the development of a more quantitative model in terms of determining the relative importance of the various components of  $k'_{da}$  and  $k'_{so1}$  is also planned.

#### **Electrochemical Gradient Elution at the GC Stationary Phase.**

The results in the last section reveal that significant changes in the  $k'$  values of the ASFs can be produced through alterations in  $E_{app}$  prior to elution. These results, as we have briefly shown in a preliminary report [9], indicate that the dynamic alteration in  $E_{app}$  can be used as a route to improve separations. For example, a linear voltage ramp could be applied

to the GC stationary phase from an initial voltage of +0.30 V to a final voltage of -1.00 V. Use of this voltage ramp, as shown for a similar mixture [9], would combine the increased resolution of BS and 1,2 BDS at +0.30 V with the narrower elution bandwidths and shorter retention times for all ASFs at -1.00 V. Figure 4a clearly illustrates the effectiveness of this approach by demonstrating the complete baseline resolution of the mixture in ~4 min.

The voltage ramp was applied immediately upon sample injection at 10 mV/s. In contrast, the separation at open circuit required ~9 min for completion, but with an incomplete resolution of BS and 1,2 BDS. In addition, the elution bandwidths of all eight ASFs are significantly decreased in the voltage ramp. For example, the band widths of the three most strongly retained ASFs (i.e., 1,5 NDS, VBS, TMBS) are decreased from 16 sec to 4 sec, 32 sec to 8 sec, and 60 sec to 16 sec, respectively.

The gradual increase in the baseline absorbance during this separation results from a decrease in the interfacial concentration of the perchlorate mobile phase anion as  $E_{app}$  becomes increasingly negative. That is, as  $E_{app}$  becomes increasingly negative, the concentration of perchlorate anions in the mobile phase increases. This assertion is supported by spectra collected during a control experiment in the absence of analyte; these spectra reveal an increase in the perchlorate concentration in the mobile phase as the voltage is swept negatively. Although not shown, the background absorbance slowly decreases after completion of the voltage scan as the column equilibrates. Typical re-equilibration times are ~10 min.

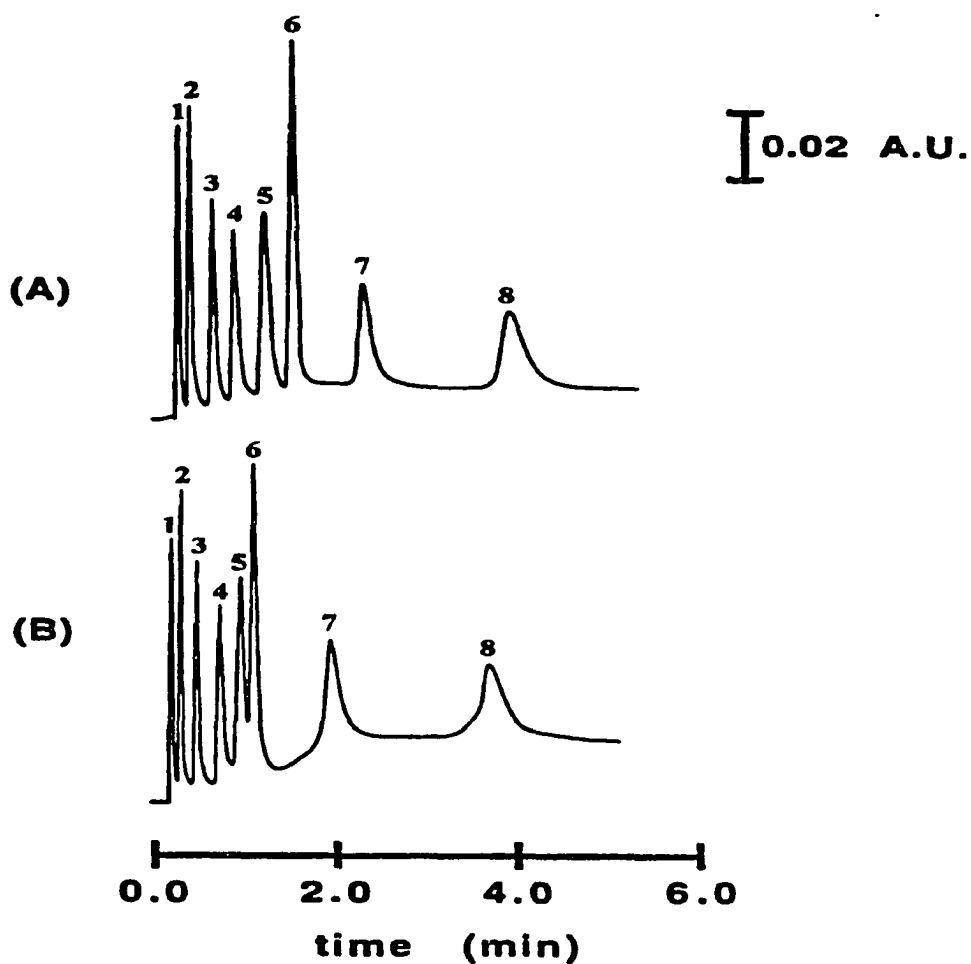


**Figure 4.** Separations of an eight component mixture of ASFs obtained by applying a linear voltage ramp (a) and a charge ramp (b) to the GC stationary phase. The voltage ramp was applied from +0.30 V to -1.00 V immediately upon sample injection at 10 mV/s. The charge ramp was generated by applying a constant current of +2 mA to the GC stationary phase immediately upon sample injection. The column was equilibrated at open circuit prior to application of the constant current. The mobile phase consisted of aqueous 0.10 M LiClO<sub>4</sub> containing 1.5 % CH<sub>3</sub>CN. The flow rate was 0.75 mL/min.



In addition to changing dynamically the voltage applied to the GC stationary phase to perform electrochemical gradient elution, we also envision controlling the charge at the GC surface through application of various constant currents. The advantage of this method is that the surface charge could be changed linearly during elution. Such a linear change in surface charge may, to a first approximation, be attractive for separations using GC stationary phases modified with a redox active species such as polypyrrole [4,6,9,10] and other conductive polymers [8]. A linear voltage ramp that transformed the redox species between its oxidized and reduced forms, for example, would result in a nonlinear change in the surface charge and therefore the capacity of the stationary phase, which may lead to an increased broadening of the elution bands in some cases [46].

Figure 4b shows the separation of the mixture of ASFs obtained by applying a constant current of +2 mA to the GC stationary phase immediately upon sample injection. Since the applied current was positive, the voltage moves negatively during the experiment. The column was equilibrated at +0.15 V (i.e., near open circuit conditions) before analyte injection. As expected, the decreases in the retention times and band widths for the elution of each component are similar to those obtained with the voltage ramp. The resolution of the first six eluting ASFs is decreased when compared to that obtained for the voltage ramp, however, because the initial voltage was  $\sim$ 0.15 V instead of +0.30 V for this separation. Nevertheless, this chromatogram illustrates the ability to perform electrochemical gradient elution through application of constant currents to the stationary phase. We expect this

elution method to compliment those based on voltage changes, and to be particularly useful in the situations outlined above.

To compare the above separations to that obtained under the conditions of conventional solvent gradient elution, we investigated the separation of the eight component mixture via a linear solvent ramp. For these experiments, the column was initially equilibrated at open circuit in a mobile phase consisting of 100% aqueous 0.10 M LiClO<sub>4</sub>. Use of such a mobile phase was required to completely resolve 1,2 BDS and BS. A linear solvent ramp was then applied to the column from 0-10% acetonitrile over a period of 6 min beginning upon injection. These conditions were found to give the optimal separation of the mixture, with near baseline resolution of all eight components. Comparison of this separation to that obtained using the voltage ramp showed that although both run times were similar (~4 min), the half-widths of the elution bands for the ASFs were generally sharper using the voltage ramp. This effect likely results from the necessity to use a 100% aqueous mobile phase for the initial starting point for the solvent ramp, which significantly broadens the elution bands of the ASFs during the initial stages of the ramp. The EMLC technique, however, allows for gradient elution to be accomplished beginning with a mobile phase that gives a narrow and symmetric band for each ASF, and therefore results in a narrower elution band during the voltage ramp. However, the ability of the solvent ramp to decrease the retention times of the more strongly retained ASFs (e.g., VBS and TMBS) is enhanced as compared to the voltage ramp. With the solvent ramp, the time observed between the elution of 1,5 NDS and VBS as well as between VBS and TMBS in Figure 4a is decreased significantly. Therefore, it appears

that changes in mobile phase composition are useful when the separation of a mixture containing analytes of widely different  $k'$  values is required, whereas changes in  $E_{app}$  are a more effective method for improving the separations of closely-eluting analytes.

### **Response Time of the EMLC Column.**

To assess the time required for the EMLC column to re-equilibrate fully upon alterations in  $E_{app}$ , we followed the changes in the retention for a six-component mixture of ASFs after a step in  $E_{app}$ . Such an assessment is important to ensure full re-equilibration of the column between experiments and to probe the usefulness of the EMLC technique for continuous on-line analyses. Although a qualitative assessment of the equilibration time can be made by monitoring the stability of the detector baseline, we have noticed that small changes in retention can occur after a stable detector baseline has been reached. This slow equilibration of the column may result from the electrical resistances (i.e., contact resistance between the GC spheres, solution resistance) present in our current column design. Therefore, we prefer to use changes in the retention times for the ASFs as a measure of the equilibration time. For this experiment, the GC stationary phase was initially equilibrated at +0.20 V. A mixture of 1,2 BDS, BS, HBS, EBS, CBS, and 1,5 NDS was then injected, and a chromatogram was collected. After the complete elution of all six components of the mixture,  $E_{app}$  was stepped to -1.00 V, and another injection of the mixture was immediately made. The latter step was repeated until no further changes in the retention times for the ASFs were observed. Under these conditions, the separation time between repetitive injections was ~one minute. Analysis of these data indicated that 95% of the change in the retention times for the

ASFs occurred within ~3.5 min after the voltage step. Similar experiments performed with voltage steps of smaller magnitude revealed that the equilibration time was directly proportional to the magnitude of the voltage step, with larger voltage steps requiring longer equilibration times. For example, a voltage step from +0.20 V to -0.50 V required about 2 min for 95% re-equilibration. This behavior is consistent with a response limited by uncompensated solution resistance, a complication often encountered in this type of electrochemical cell design [32].

An assessment of the response time of the column to changes in  $E_{app}$  is also an important parameter whose value is needed for the development of methods for optimization of analyte separations under electrochemical gradient elution conditions. This parameter is a measure of the delay between the application of a particular voltage and the time required for the GC surface to change to an extent that affects analyte retention. We estimated this delay time as follows. First, the EMLC column was equilibrated at +0.20 V. The six component ASF mixture used above was then injected. When 1,2 BDS began to elute from the column (0.34 min),  $E_{app}$  was stepped to and held at -1.00 V. The retention times for the remaining five ASFs were then monitored. The results indicated that the retention times for 1,2 BDS and BS were essentially identical to those obtained at a constant  $E_{app}$  of +0.20 V, whereas those for HBS, EBS, CBS, and 1,5 NDS became progressively shorter. In other words, although the voltage step was initiated prior to the elution of BS, its elution band was not affected by the voltage step. However, HBS, which elutes from the column about 22 sec after the dead time

(0.34 min) at +0.20 V, showed a slight decrease in its retention time by 1.2 sec. Further, EBS, which elutes about 40 sec after the dead time, showed a more significant decrease of 6 sec in its retention time, whereas CBS and 1,5 NDS showed 23 sec and 106 sec decreases, respectively. Therefore, we estimate that the column began to significantly respond to the change in  $E_{app}$  somewhere in-between the elution of HBS and EBS, or at about 30 sec after the voltage step. This delay time did not vary significantly for different magnitudes of the voltage step. Both the time required for re-equilibration of the column (~210 sec) and the delay observed between changes in  $E_{app}$  and changes in the column composition (~30 sec) suggest that factors such as the solution and Nafion membrane ionic transport resistances limit the rate of the electrochemical response. However, as observed, the column composition can be changed rapidly enough to allow for large alterations in the separations during elution to be readily accomplished. Improvements made through further redesign should only enhance the process.

#### **Characterization of the GC Surface.**

**Effect of oxygen functional groups.** Several studies aimed at characterizing carbonaceous materials have revealed that such surfaces often contain a distribution and varied amount of oxygen-containing functional groups [20,47-49]. Indeed, examination of the GC spheres by XPS indicates the presence of a small amount of oxygen (O/C~2.2) at their surfaces (Figure 5a). Deconvolution of the O(1s) region of a high resolution XPS spectrum taken of these spheres (Figure 6a) revealed the presence of three major bands, with maxima at

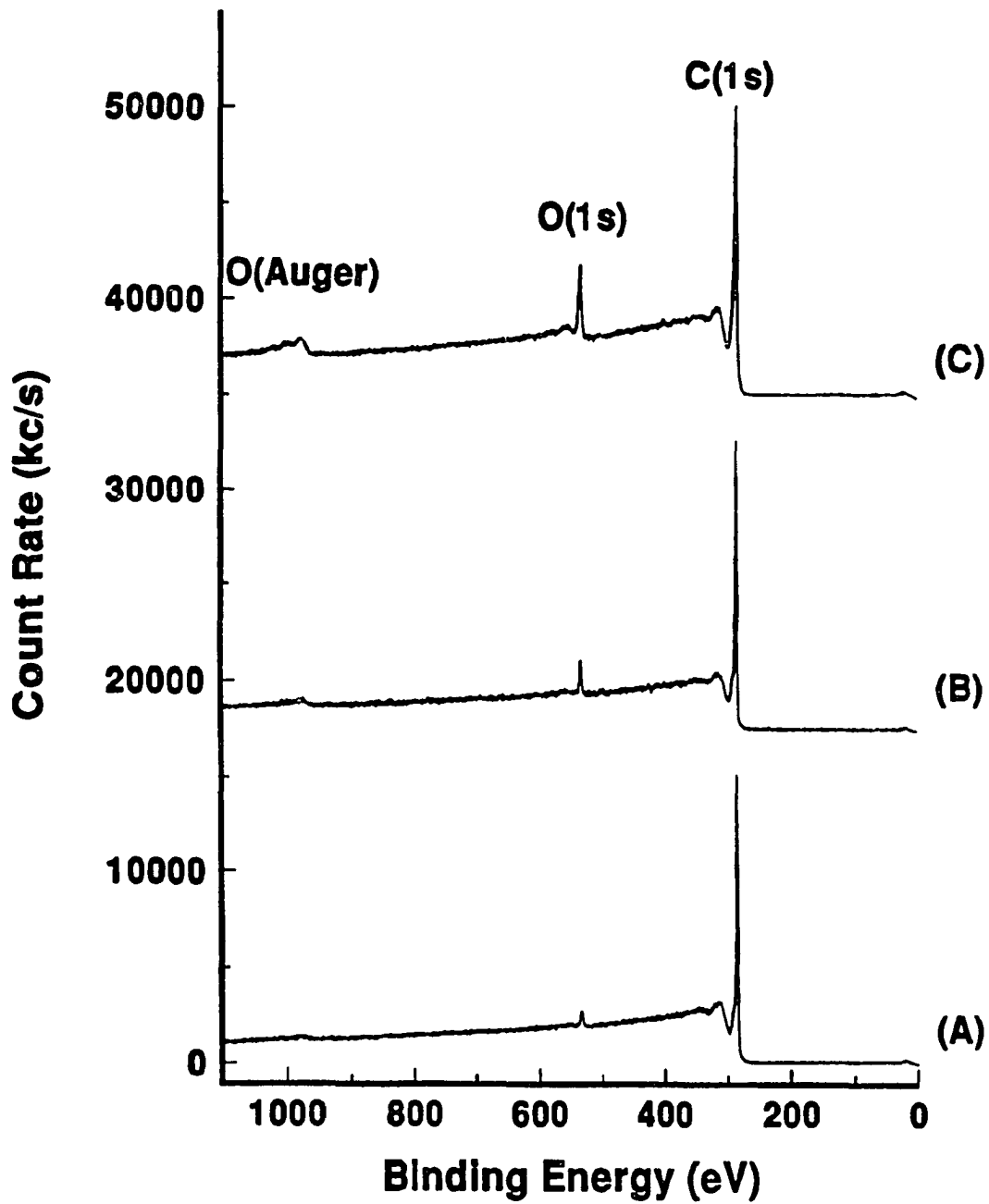


Figure 5. X-ray photoelectron survey spectra of untreated GC spheres (a) and GC spheres that were oxidized in a 500 mtorr oxygen plasma for 5 min (b); and for 10 min (c).

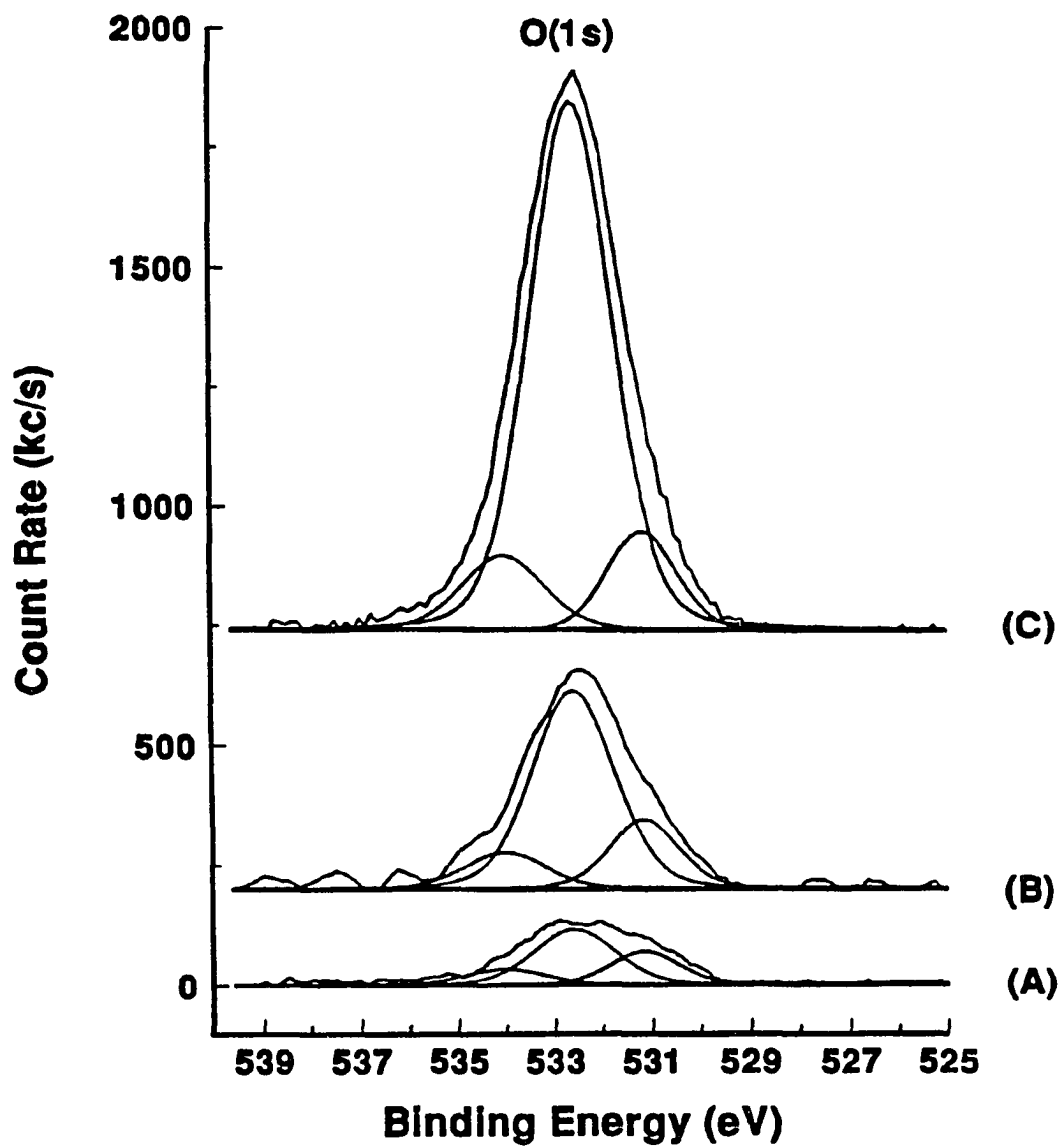


Figure 6. High resolution x-ray photoelectron spectra in the O(1s) region for untreated GC spheres (a) and for GC spheres that were oxidized in a 500 mtorr oxygen plasma for 5 min (b); and for 10 min (c). Each spectrum has been deconvoluted using mixed gaussian-lorentzian band shapes.

~531 eV, 532.6 eV, and 534 eV. These positions are close to those ascribed by others to quinone, phenol, and carboxylic acid groups, respectively, [19,50,51]. Integration of these three bands further revealed that most of the surface-bound oxygen existed as surface phenols (55%), with smaller amounts existing as surface quinones (29%) and carboxylic acids (16%). The data in Figure 6a also suggest the presence of a fourth band with a peak binding energy of ~537 eV, although its very weak intensity precludes an accurate assignment. This band has been attributed by others to carbonate, peroxyacid, or peroxyester groups [51].

To probe the effect of these oxides on the retention, band shapes, and separation of the ASF mixture, we compared the separation of the six component mixture of ASFs obtained at the untreated GC surface to those obtained at GC surfaces which were intentionally oxidized via an oxygen plasma. Figures 5b and 5c show XPS survey spectra of GC sphere samples obtained after oxidation in a oxygen plasma for 5 min (Figure 5b) and for 10 min (Figure 5c). Treatment of the GC spheres for 5 min results in an increase in surface oxygen by a factor of roughly 2.4, and treatment for 10 min gave rise to a ~ 4 fold increase. Deconvolution of high resolution spectra of these samples (Figures 6b and 6c) suggested that most of the additional oxygen formed at the GC surface as phenol groups. Integration of the deconvoluted bands showed that the amount of phenol groups at the carbon surface increased from 55% with no oxidation to 67% and 77% with 5 and 10 minute oxidations, respectively. In contrast, the amount of surface quinone on each sample decreased from 29% with no oxidation to 20% and 11% with 5 and 10 min oxidations, respectively. This decrease is clearly seen from the disappearance of the low energy shoulder on the O(1s) band in



Figure 6a. The amount of surface carboxylic acid groups appeared, however, to show only a slight decrease (16%, 13%, 11%, respectively).

To assess quantitatively the effects of plasma treatment on the surface roughness, the BET surface areas of the untreated and plasma treated samples were also determined. Table III summarizes the results. As expected, plasma treatment of the GC spheres also roughens the GC surfaces considerably [48,52], as is apparent from the increase in the surface area found for increasing oxidation times. This increase in surface roughness was confirmed by SEM examination of the treated spheres, which showed considerable surface pitting upon plasma oxidation. Figure 7 shows a close-up SEM image of a GC sphere that was oxidized for 10 min. As shown in Table III, plasma oxidation for 5 min and 10 min increased the surface area of the GC spheres by 20 and 30%, respectively.

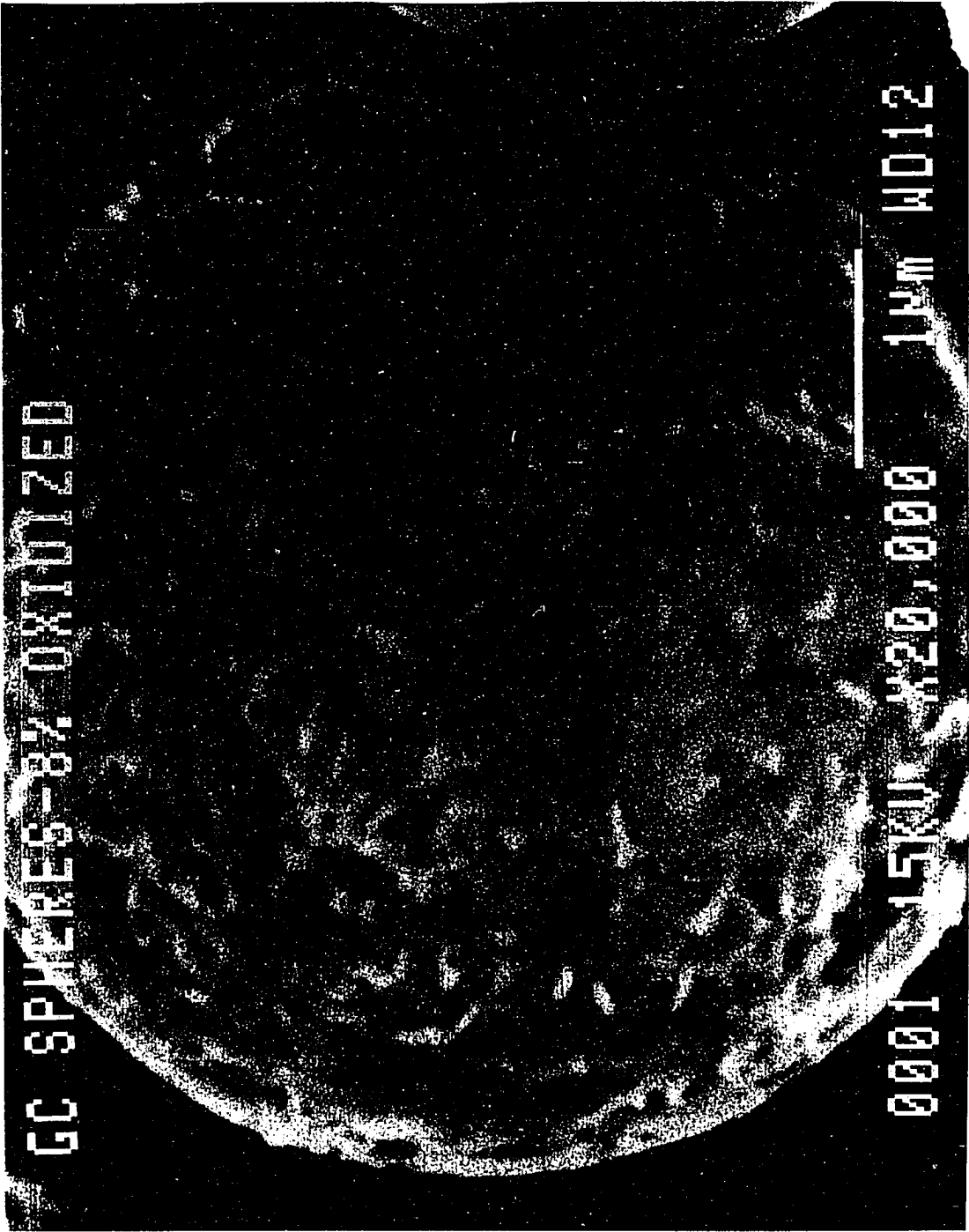
After characterization by XPS and BET surface area measurements, these samples were individually packed into separate EMLC columns and equilibrated with mobile phase. A six component mixture consisting of 1,2 BDS, BS, HBS, EBS, CBS, and 1,5 NDS was then injected onto each column at open circuit to determine the effects of surface oxidation on the separation. Interestingly, the retention of the mixture showed a strong dependence on the oxidation time. Oxidation of the GC spheres for 5 min resulted in a ~30 % *increase* in the  $k'$  values for BS, HBS, EBS, and CBS, and a ~15 % increase for 1,5 NDS. The unretained 1,2 BDS showed no increase. The band shape for each ASF was also qualitatively unchanged. Further oxidation of the GC spheres (e.g. 10 min) resulted in a significant *decrease* in the  $k'$  values for BS, HBS, EBS, CBS, and 1,5 NDS by 7 %, 19 %, 21 %, 17 %, and 56 %, respectively.

Table III. Capacity factors for six ASFs obtained at GC stationary phases with various XPS oxygen to carbon ratios and surface areas.<sup>a</sup>

<u>O<sub>2</sub> Treat. (min)</u>	<u>100 (O/C)</u>	<u>Surf. Area (m<sup>2</sup>/g)</u>	<u>Capacity Factor, k'</u>					
			<u>1,2 BDS</u>	<u>BS</u>	<u>HBS</u>	<u>EBS</u>	<u>CBS</u>	<u>1,5 NDS</u>
0	2.2	2.4	~0	0.30	0.96	1.83	3.08	6.12
5	5.3	2.9	~0	0.41	1.24	2.33	3.98	7.04
10	8.4	3.1	~0	0.28	0.81	1.51	2.63	3.92

<sup>a</sup>All chromatograms were obtained at open circuit in the aqueous 0.10 M LiClO<sub>4</sub> mobile phase containing 1.5 % CH<sub>3</sub>CN. The flow rate was 0.75 mL/min in each case.

**Figure 7. Scanning electron micrograph of a GC sphere taken at a magnification of 20,000x that was oxidized in an oxygen plasma for 10 min. The accelerating voltage was 15 kV.**



respectively, when compared to the untreated GC surface. The unretained 1,2 BDS again showed no change in its  $k'$ . In contrast to the 5 min oxidized GC sample, the chromatographic bands obtained at this surface appeared highly tailed and asymmetric. Further oxidation of the GC spheres (e.g., 15 min) yielded a GC surface that was essentially unretentive for the ASFs.

In light of the above data, it appears that extensive oxidation of the GC surface serves to both increase the roughness of the GC surface and to decrease the retention of the ASFs. This latter effect likely results from a decrease in the ability of the GC surface to interact with the ASFs through donor-acceptor, dispersion, and solvophobic interactions by destruction of its planar aromatic structure and by increasing its hydrophilicity. The increase in band tailing results from an increased heterogeneity of the surface, giving rise to multiple surface sites for interaction with the ASFs [53,54].

Surprisingly, however, less extensive oxidation of the GC spheres (e.g., 5 min oxidation time) resulted in a significant *increase* in the  $k'$  values for the ASFs. We suspect that the negative effect of an increase in the oxygen content at the GC surface is offset by an increase in surface area, which provides more surface for interaction with the ASFs. Since a large portion of the increase in surface roughness apparently occurs during the first 5 minutes of plasma oxidation (see Table III), further oxidation of the GC spheres may occur with smaller increases in roughness but larger increases in surface oxide content. This conclusion is supported by previous studies of the oxygen plasma oxidation of pyrolytic graphite and GC surfaces, which showed that the largest increase in surface roughness occurs within the first

2 min of exposure to the plasma [52]. Further, assuming a linear relationship between the surface area of the GC spheres and the O/C ratio, an O/C ratio of 8.4 as obtained for the 10 min oxidation time should give rise to a surface area of  $\sim 3.4 \text{ m}^2/\text{g}$ . Since the measured value was only  $3.1 \text{ m}^2/\text{g}$ , the above assertion seems reasonable.

In light of these findings, the oxygen content at the GC surface should be held at a minimum to prevent alterations in analyte retention times as well as increases in band tailing. Although an electrochemically-induced oxidation/reduction of the GC surface is also potentially possible through alterations in  $E_{app}$  during chromatographic experiments (e.g., surface quinone/hydroquinone couple [47]), we have found no evidence for such oxidation by XPS for values of  $E_{app}$  within the range of  $+0.60 \text{ V} > E_{app} > 1.00 \text{ V}$ . However, since the GC spheres are slowly oxidized at  $E_{app}$ 's more positive than  $\sim 1.0 \text{ V}$ , these extensive upper limits should be avoided.

**Stability of the GC surface.** The overall usefulness of the EMLC system for most practical applications is dependent on the reproducibility and stability of the column over extended periods of use or storage. This section outlines two experiments that were designed to qualitatively assess these parameters. The reproducibility of the GC surface was assessed by comparing the  $k'$  values of the 6 component mixture of ASFs obtained at  $+0.20 \text{ V}$  before and after 21 continuous injections made over a 1 hr period. These studies indicated that the GC stationary phase was very stable and reproducible, and gave less than a  $\pm 3\%$  change in the  $k'$  values of the ASFs over a 1 hr period. Additionally, comparison of a separation of the

ASFs obtained immediately after column packing and equilibration to that obtained after ~2 weeks of continuous use showed no significant changes in the  $k'$  values.

However, upon examination of an EMLC column that had been stored in the mobile phase solution for ~ 1.5 months, we noticed a significant decrease (~30-40%) in the  $k'$  values for the ASFs. Such a decrease was likely due to the adsorption of contaminants onto the GC surface during storage [17,55], thereby changing its retention characteristics. We found that the GC surface could be reactivated, however, by flushing the column for ~3 hr with 0.10 M LiClO<sub>4</sub> in CH<sub>3</sub>CN to remove the adsorbed contaminants. After such treatment, retention of the ASF mixture was found to vary by only 3-5% from that observed on the freshly packed column. Therefore, the EMLC column can be conveniently reactivated by flushing with a strongly eluting organic solvent such as acetonitrile if contamination occurs during column storage. These results confirm the excellent stability and reproducibility of the EMLC column over extended periods of time, and point to its usefulness for continuous analyses.

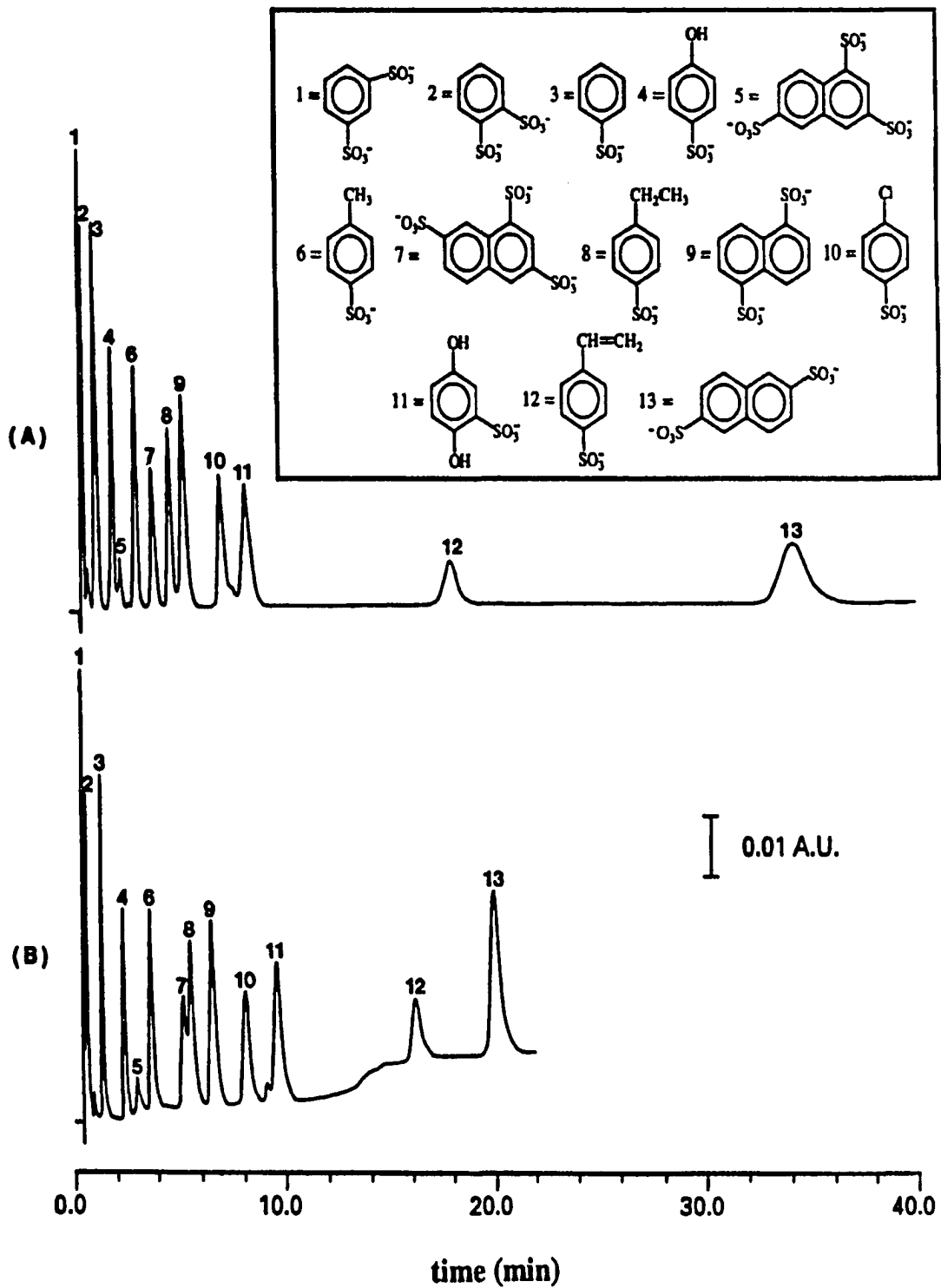
**Effect of surface area.** The surface area of the packing used in an HPLC column can have a pronounced effect on the quality of a particular separation. In general, nonporous packings with low surface area (~1-10 m<sup>2</sup>/g) exhibit decreased chromatographic efficiencies and sample capacities when compared to porous packing materials (100-400 m<sup>2</sup>/g) [54,56]. These factors lead to, in most cases, a decreased ability to obtain well resolved separations of complex mixtures. However, the low sample capacity of these materials has been widely exploited to obtain high speed separations of proteins, whose slow diffusional rates of mass transfer within the porous network of high surface area packings results in low recoveries and

poor band shapes [57-61]. A recent report discusses the application of these nonporous packing to the high speed separation of small molecules (e.g., alkylbenzenes, amino acids, vitamins) as well [56].

To investigate the effects of increasing the surface area of the carbonaceous support on the sample capacity, chromatographic efficiency, and electrochemical response of the EMLC column, we packed an EMLC column with a commercially available porous graphitic carbon (PGC). This PGC support is composed of  $\sim 7$   $\mu\text{m}$  spherical, porous particles with an average surface area of  $\sim 200$   $\text{m}^2/\text{g}$ . X-ray photoelectron spectra taken of these spheres contained the C(1s) band as the only detectable feature, pointing to a very pristine and hydrophobic surface with no oxygen functionalities. Initial experiments with this column provided separations that, as expected, had an enhanced sample capacity and efficiency (theoretical plate number,  $N^t \sim 14,000$  plates/meter vs 3500 plates/meter [54]) over those obtained at the nonporous GC column. Figure 8a shows a separation of a thirteen component mixture of ASFs obtained at open circuit. The mobile phase used consisted of 96 % aqueous 0.10 M  $\text{LiClO}_4$  and 4 % 0.10 M  $\text{LiClO}_4$  in  $\text{CH}_3\text{CN}$ . The flow rate was 1.0 mL/min. Table IV summarizes the chromatographic data. Interestingly, 1,2 BDS, BS, HBS, EBS, CBS, 1,5 NDS, and VBS (labeled as peaks 2, 3, 4, 8, 9, 10, and 12, respectively) are retained much more strongly at the PGC surface, leading to an increased resolution. Further, the higher capacity of PGC allows for the separation of a more complex mixture of ASFs, including the resolution of several pairs of isomeric compounds (i.e., 1,3 BDS and 1,2 BDS, NTS isomers, and 1,5 NDS and 2,6 NDS). The relative elution order of 1,2 BDS, BS, HBS, EBS, CBS,



**Figure 8. Separation of a thirteen component mixture of ASFs obtained at the PGC stationary phase at open circuit (a) and by applying a voltage step from 0.00 V to -1.00 V 7.2 min after sample injection (b). The mobile phase consisted of aqueous 0.10 M LiClO<sub>4</sub> containing 4.0 % CH<sub>3</sub>CN. The flow rate was 1.0 mL/min.**



1,5 NDS, and VBS is similar to that obtained at GC, except that the elution order of 1,5 NDS and CBS is reversed. We attribute this reversal to the increased hydrophobicity of PGC relative to GC (i.e., the lower oxygen content by XPS), which leads to an increased affinity of PGC for hydrophobic molecules via solvophobic interactions. The chromatographic efficiency observed at PGC is also dramatically improved due to an increase in the solubility of the ASFs

Table IV. Retention times for various ASFs at the PGC stationary phase at open circuit and under conditions of a voltage step<sup>a,b</sup>.

<u>ASF</u>	<u>retention time (min)</u>	
	<u>open circuit</u>	<u>voltage step</u>
1,3 BDS	0.55	0.56
1,2 BDS	0.66	0.69
BS	1.24	1.45
HBS	1.98	2.43
NTS-1	2.31	3.08
NTS-2	3.87	5.28
MBS	3.06	3.74
EBS	4.68	5.63
1,5 NDS	5.29	6.65
CBS	7.11	8.21
HQS	8.28	9.73
VBS	17.97	16.34
2,6 NDS	34.19	20.19

<sup>a</sup>For the voltage step gradient elution, the voltage, which was initially set at 0.00 V, was stepped to -1.00 V 7.2 min after injection.

<sup>b</sup>The mobile phase was 96 % aqueous 0.10 M LiClO<sub>4</sub> containing 4 % 0.10 M LiClO<sub>4</sub> in CH<sub>3</sub>CN. The flow rate was 1.0 mL/min.

in the mobile phase, which leads to an increase in the mass transport rate of the ASFs between the mobile and stationary phases [54,56].

As a test of the electrochemical response of the EMLC column, we attempted to improve the separation of this mixture through alteration of  $E_{app}$  prior to and during elution. First, a small positive voltage (e.g., 0.00 V) with respect to the open circuit voltage ( $\sim -0.05$  V) was applied to the PGC stationary phase to improve the resolution of the first 11 eluting ASFs. After the column had equilibrated, the 13 component mixture was injected. The voltage was then stepped to -1.00 V 7.2 min after injection to decrease the retention times of VBS and 2,6 NDS. Figure 8b shows the resulting separation. Application of the small positive voltage results in a significant improvement in the resolution of the first 11 eluting ASFs. For example, NTS-1 and HBS, EBS and 1,5 NDS, and CBS and HQS, which were not fully resolved at open circuit, are now baseline resolved. The resolution between 1,3 BDS and 1,2 BDS is also somewhat improved. However, the resolution of NTS-2 and EBS is reduced. Application of the voltage step also results in a significant decrease in the total analysis time ( $\sim 20$  min vs  $\sim 34$  min at open circuit), and a significant sharpening of the elution bands for VBS and 2,6 NDS (by factors of 1.7 and 3.4, respectively). Such effects are similar to those observed at the GC stationary phase. These separations clearly illustrate the large increases in chromatographic efficiency and sample capacity that can be gained by use of a porous carbon support, and also further demonstrate the unique ability of the EMLC technique for fine-tuning analyte separations.

Although the PGC stationary phase provides increased capacity and chromatographic efficiency when compared to the nonporous GC sphere stationary phase, it shows a slower response to changes in  $E_{app}$ . For example, a change in  $E_{app}$  between +0.20 V and -1.00 V requires ~20-30 min for 95% re-equilibration of the charge at the PGC surface. This effect is likely due to the ~100 fold larger surface area of the PGC support, which increases the voltage drop observed upon passage of a current within the EMLC column. We are currently investigating new column configurations which may help to overcome this problem.

## CONCLUSIONS

The studies described herein have demonstrated the utility of EMLC for modifying and fine-tuning analytical separations. Importantly, these manipulations can be performed both prior to and during analyte elution without the need for changes in mobile phase composition. Investigation of the mechanism of the electrochemically-controlled retention at the carbon surface revealed that changes in  $E_{app}$  serve as a means for altering systematically the strength of donor-acceptor and solvophobic interactions of the analytes with the carbon surface, which lead to changes in analyte retention and to the introduction of interesting selectivity to the separations. These mechanistic studies also suggest the potential use of this new technique for studying a variety of interfacial phenomena including double layer structure and the effects of functionalization of surfaces on their interaction with solution species.

Another primary goal of this work was to characterize the EMLC system in terms of the effects of re-equilibration time, response time, surface-bound oxides, long term stability,

and the surface area of the stationary phase on its performance. The results of these characterizations highlight the usefulness of the EMLC technique for the rapid and reproducible manipulation of analyte separations. These studies also provide the experimental guidelines necessary for successful use of this new technology. Future studies will be aimed toward investigating other potential applications of EMLC, including the separation of neutral compounds and a further investigation of the use of PGC as a stationary phase for EMLC. In addition, studies designed to unravel further the retention mechanism in terms of identifying the reasons for the small but significant differences in the voltages corresponding to the slope change in the  $\log k'$  versus  $E_{app}$  plots for the ASFs are currently being devised.

#### ACKNOWLEDGMENTS

R.S.D acknowledges the support of an ACS Analytical Division Summer Fellowship sponsored by Dow Chemical, USA. The authors also acknowledge the air classification of the GC spheres by B.K. Lograsso and B. Patrick, and the use of the BET surface area analyzer by Professor G.M. Schrader. Several helpful discussions with J. Zak are also greatly appreciated. This work was supported by the National Science Foundation (Grant CHE-9003308) and by Iowa State Universities' Microanalytical Instrumentation Center. The Ames Laboratory is operated for the U.S. Department of Energy by Iowa State University under contract No. W-7405-Eng-82.

## LITERATURE CITED

1. Antrim, R.F.; Scherrer, R.A.; Yacynych, A.M. *Anal. Chim. Acta* **1984**, *164*, 283-86.
2. Antrim, R.F.; Yacynych, A.M. *Anal. Lett.* **1988**, *21*, 1085-96.
3. Ghatak-Roy, A.R.; Martin, C.R. *Anal. Chem.* **1986**, *58*, 1574-75.
4. Ge, H.; Wallace, G.G. *J. Liq. Chromatogr.* **1990**, *13*, 3245-60.
5. Ge, H.; Teasdale, P.R.; Wallace, G.G. *J. Chromatogr.* **1991**, *544*, 305-16.
6. Deinhammer, R.S.; Shimazu, K.; Porter, M.D. *Anal. Chem.* **1991**, *63*, 1889-94.
7. Nagaoka, T.; Fujimoto, M.; Uchida, Y.; Ogura, K. *J. Electroanal. Chem.* **1992**, *336*, 45-55.
8. Nagaoka, T.; Fujimoto, M.; Nakao, H.; Kakuno, K.; Yano, J.; Ogura, K. *J. Electroanal. Chem.* **1993**, *350*, 337-44.
9. Deinhammer, R.S.; Ting, E.; Porter, M.D. *J. Electroanal. Chem.* **1993**, *362*, 295-99.
10. Nagaoka, T.; Fujimoto, M.; Nakao, H.; Kakuno, K.; Yano, J.; Ogura, K. *J. Electroanal. Chem.* **1994**, *364*, 179-88.
11. Deinhammer, R.S.; Shimazu, K.; Porter, M.D., to be submitted to *Journal of Electroanalytical Chemistry*.
12. Manthey, M.; Riley, P.J.; Wallace, G.G. *Amer. Lab.* **1988**, 21-29.
13. O'Toole, R.P.; Coldiron, S.J.; Deninger, W.D.; Deinhammer, R.S.; Burns, S.G.; Bastiaans, G.J.; Braymen, S.D.; Shanks, H.R.; Porter, M.D. *SAE Trans*, **1992**, #SAE921179.

14. Brown, M.A.; Kim, I.S.; Roehl, R.; Sasinos, F.I.; Stephens, R.D. *Chemosphere* **1989**, *19*, 1921-27.
15. Kim, I.S.; Sasinos, F.I.; Stephens, R.D. Brown, M.A. *Environ. Sci. Technol.* **1990**, *24*, 1832-36.
16. Kim, I.S.; Sasinos, F.I.; Rishi, D.K.; Stephens, R.D.; Brown, M.A. *J. Chromatogr.* **1991**, *589*, 177-83.
17. Knox, J.H.; Kaur, B.; Millward, G.R. *J. Chromatogr.* **1986**, *352*, 3-25.
18. Scofield, J.H. *J. Electron. Spectrosc. Relat. Phenom.* **1976**, *8*, 129-37.
19. Proctor, A.; Sherwood, P.M.A. *Carbon* **1983**, *21*, 53-59.
20. Knox, J.H.; Unger, K.K.; Mueller, H. *J. Liq. Chromatogr.* **1983**, *6*, 1-36.
21. Bassler, B.J.; Hartwick, R.A. *J. Chrom. Sci.* **1989**, *27*, 162-165.
22. Bassler, B.J.; Kaliszan, R.; Hartwick, R.A. *J. Chromatogr.* **1989**, *461*, 139-47.
23. Gu, G.; Lim, C.K. *J. Chromatogr.* **1990**, *515*, 183-92.
24. Tanaka, N.; Tanigawa, T.; Kimata, K.; Hosoya, K.; Araki, T. *J. Chromatogr.* **1991**, *549*, 29-41.
25. Forgacs, E.; Cserhati, T.; Valko, K. *J. Chromatogr.* **1992**, *592*, 75-83.
26. Lim, C.K. *Advan. Chromatogr.* **1992**, *32*, 1-19.
27. Moore, W.J. *Physical Chemistry; 4th ed.*, Prentice-Hall: Englewood Cliffs, NJ, 1972.
28. Engel, T.M.; Olesik, S.V. *Anal. Chem.* **1990**, *62*, 1554-60.
29. Engel, T.M.; Olesik, S.V.; Callstrom, M.R.; Diener, M. *Anal. Chem.* **1993**, *65*, 3691-700.
30. Morokuma, K. *Acc. Chem. Res.* **1977**, *10*, 294-300.



31. Horvath, C.; Melander, W.; Molnar, I. *J. Chromatogr.* 1976, 125, 29-56.
32. Bard, A.J.; Faulkner, L.R. *Electrochemical Methods, Fundamentals and Applications*; Wiley: New York, 1980.
33. Hansch, C.; Leo, A. *Substituent Constants for Correlation Analysis in Chemistry and Biology*; Wiley: New York, 1979.
34. Leo, A.; Hansch, C.; Elkins, D. *Chem. Rev.* 1971, 71, 525-55.
35. Kriz, J.; Adamcova, E.; Knox, J.H.; Hora, J. *J. Chromatogr. A* 1994, 663, 151-61.
36. Damaskin, B.B.; Dyatkina, S.L.; Gerovich, V.M. *Elektrokhimiya* 1985, 21, 716-18.
37. Kaganovich, R.I.; Gerovich, V.M.; Gusakova, O.Y. *Elektrokhimiya* 1967, 3, 946-52.
38. Nechaev, E.A. *Elektrokhimiya* 1984, 19, 972-74.
39. Rolle, D.; Schultze, J.W. *Electrochim. Acta* 1986, 31, 991-1000.
40. Sarangapani, S.; Venkatesan, V.K. *Proc. Indian Nat. Sci. Acad.* 1983, 49, 124-42.
41. Dutkiewicz, E.; Stuczynska, J. *Electrochim. Acta* 1988, 33, 19-23.
42. Parry, J.M.; Parsons, R. *J. Electrochem. Soc.* 1966, 113, 992-99.
43. Protskaya, E.N.; Gerovich, V.M.; Damaskin, B.B. *Elektrokhimiya* 1982, 17, 1391-96.
44. Dutkiewicz, E.; Stuczynska, J. *Electrochim. Acta* 1989, 34, 1513-17.
45. Hammett, L.P. *Chem. Rev.* 1935, 17, 126-36.
46. Jandera, P.; Churacek, J. *Gradient Elution in Column Liquid Chromatography*; Elsevier: Amsterdam, 1985.
47. Kinoshita, K. *Carbon: Electrochemical and Physicochemical Properties*; Wiley: New York, 1988.

48. Miller, C.W.; Karaweik, D.H.; Kuwana, T. *Anal. Chem.* **1981**, *53*, 2319-23.
49. Unger, K.K. *Anal. Chem.* **1983**, *55*, 361A-375A.
50. Clark, D.T.; Dilks, A. *J. Polym. Sci.* **1979**, *17*, 957-76.
51. Proctor, A.; Sherwood, P.M.A. *J. Electron. Spectrosc. Rel. Phenom.* **1982**, *27*, 39-56.
52. Evans, J.F.; Kuwana, T. *Anal. Chem.* **1979**, *51*, 358-65.
53. Giddings, J.C. *Dynamics of Chromatography, Part I*; Marcel Dekker: New York, 1965, pp. 255-57.
54. Poole, C.F.; Schuette, S.A. *Contemporary Practice of Chromatography*; Elsevier: Amsterdam, 1984.
55. Coughlin, R.W.; Ezra, F.S. *Environ. Sci. Technol.* **1968**, *2*, 291-97.
56. Itoh, H.; Kinoshita, T.; Nimura, N. *J. Liq. Chromatogr.* **1993**, *16*, 809-23.
57. Colwell, L.F.; Hartwick, R.A. *J. Liq. Chromatogr.* **1987**, *10*, 2721-44.
58. Kalghatgi, K.; Horvath, C. *J. Chromatogr.* **1987**, *398*, 335-39.
59. Rozing, G.P.; Goetz, H. *J. Chromatogr.* **1989**, *476*, 3-19.
60. Kalghatgi, K. *J. Chromatogr.* **1990**, *499*, 267-78.
61. Nimura, N.; Itoh, H.; Kinoshita, T.; Nagae, N.; Namura, M. *J. Chromatogr.* **1991**, *585*, 207-11.

## CHAPTER 5. THE SIMULTANEOUS SEPARATION OF ORGANIC ANIONS AND CATIONS USING ELECTROCHEMICALLY-MODULATED LIQUID CHROMATOGRAPHY

A paper to be submitted to the Journal of Chromatography

Randall S. Deinhammer, EnYi Ting, and Marc D. Porter<sup>1</sup>

### ABSTRACT

The simultaneous separation of a fifteen component mixture of organic anions and cations using electrochemically-modulated liquid chromatography (EMLC) is probed. The stationary phase consisted of porous graphitic carbon spheres that were packed into a novel liquid chromatographic column and connected as the working electrode in a three-electrode electrochemical cell. Tests of the retention of these species on the column at several constant applied voltages ( $E_{app}$ ) revealed that their capacity factors ( $k'$  values) could be altered by a factor of up to eighty through modification in  $E_{app}$  between +0.50 V and -1.00 V. Interestingly, the anions and cations displayed opposite responses to changes in  $E_{app}$ . The anions generally showed an increase in their  $k'$  values at positive  $E_{app}$ 's, for example, whereas the cations showed a decrease in their  $k'$  values. These differences, as well as the large variations observed in the sensitivity of each analyte to changes in  $E_{app}$ , were attributed largely to variations in their abilities to participate in donor-acceptor and solvophobic interactions

---

<sup>1</sup>Author to whom correspondence should be addressed.

with the carbon surface. Anions possessing the strongest electron-donating ability were found to have the greatest sensitivities to changes in  $E_{app}$ , whereas cations possessing the strongest electron-accepting ability showed the greatest sensitivities. The sensitivity of EMLC for improving and fine-tuning the separation of these compounds was illustrated through the application of a small voltage perturbation ( $\sim 0.025$  V) to the column relative to the open circuit voltage and also through the application of a voltage step during the elution of the mixture. In each of these examples, the separation is improved dramatically in terms of an increased resolution between the analytes and a decreased analysis time.

## INTRODUCTION

The separation and determination of organic anions and cations is of fundamental importance to several areas including clinical [1-7], food [8-13], and environmental chemistry [14-19]. In these areas, such separations are commonly used as tools for the diagnosis of metabolic disorders [1,2], for the profiling of physiological fluids [3-7], for the analysis of foodstuffs [8-13], and for the analysis of hazardous contaminants in environmental samples [14-19]. To date, several liquid chromatographic techniques have been used successfully to obtain separations of these compounds, including ion chromatography [4,9,11,15,18], reverse-phase chromatography [12,13,16], reverse-phase ion pair chromatography [19-22], ion exclusion chromatography [3,17,23,24], and zwitterion-pair chromatography [25]. Recently, several reports have appeared that describe the use of electrochemically-modulated liquid chromatography, dubbed EMLC, as an alternate method for modifying and optimizing the

separations of ionic species [26-35]. This new separation technique is founded on the ability to alter electrochemically the composition of a charge-controllable stationary phase to affect changes in the capacity of a column for various analytes. Importantly, these compositional changes can be produced both prior to and during analyte elution without alteration in the composition of a mobile phase, thereby enhancing the potential of EMLC for manipulating and fine-tuning analytical separations. As was shown previously by us [30,33,35], separations of anionic compounds obtained using EMLC compliment those obtained using conventional liquid chromatographic methodology.

The goals of the present work are threefold. First, we investigate the utility of EMLC for modifying the retention of organic cations at a porous graphitic carbon (PGC) stationary phase through the application of various fixed voltages to the column. An analyte mixture containing seven organic cations as well as several of the organic anions used in our previous studies [33,35], is used to facilitate a comparison between the electrochemically-modulated retention of both species. Several of these analytes have significance as environmental pollutants [15-18]. Second, a detailed analysis of the voltage-dependent retention of these species on the EMLC column is conducted to probe the mechanism by which the retention of both species, an in particular the cationic species, can be altered electrochemically. The results of this analysis both support our mechanism proposed earlier for anionic species [35] and provide additional insights into the unique features of this new separation technique. Third, separations obtained through the application of a small constant voltage as well as a

voltage step made during the elution of the mixture are used to illustrate the sensitivity and capability of EMLC to fine-tune the separations of these compounds.

## EXPERIMENTAL

### Chromatographic Column Construction.

The general design of the EMLC column and the chromatographic instrumentation has been discussed elsewhere [33]. For the studies described herein, however, a column with dimensions of 9 cm long and 0.38 cm inner diameter was used. This column was constructed by milling a porous stainless steel tube (Mott Metallurgical Corp.) of 9 cm long and 0.32 cm inner diameter. This column diameter is somewhat larger than that used in our previous studies [33,35], and was employed as a means for decreasing the high operational backpressures observed with the present mobile phase/stationary phase combination. The conductive stationary phase consisted of uncoated porous graphitic carbon spheres (PGC, Shandon Chromatography). These spheres had an average diameter of  $\sim 7 \mu\text{m}$ , an average pore size of  $250 \text{ \AA}$ , and a mean surface area of  $\sim 200 \text{ m}^2/\text{g}$ . The spheres were dispersed in a slurry consisting of 10 parts dibromomethane and 7 parts methanol, and packed at 5000 psi into the empty EMLC column. This slurry solvent mixture was found to provide adequate dispersion of the PGC spheres, and its high density prevented sedimentation of the carbon particles even after several hours of standing without agitation. The packing solvent was degassed methanol.

To verify that a portion of the cations injected were not irreversibly lost through interaction with the internal wall of the EMLC column, we compared the area of the elution band for the anilinium cation to that obtained in a flow injection analysis experiment in which the injector was connected directly to the detector. Such interactions are theoretically possible if the analytes come into contact with the Nafion tube surface (a cation-exchange membrane) that lines the inside of the porous stainless steel column in our current EMLC design. The similarity of these peak areas confirmed that essentially none of the injected cations are irreversibly lost due to interaction with the Nafion. In addition, the similarity of the elution band widths and shapes for co-eluting cations and anions injected individually onto the EMLC column also supports the lack of any reversible secondary retention mechanisms at the Nafion tube wall for the cationic species.

#### **Mode of Operation.**

After packing, the EMLC column was equilibrated with degassed mobile phase (93% aqueous 0.10 M LiClO<sub>4</sub>, 0.1% v/v trifluoroacetic acid (TFA), pH 2.0 and 7% 0.10 M LiClO<sub>4</sub> in acetonitrile) at 0.90 mL/min until a stable detector baseline was obtained (~2-3 hr). A mobile phase pH of 2.0 was used to allow for complete dissociation of the aromatic sulfonates and complete protonation of the aromatic amines [36]. Operational backpressures were ~1400 psi. Analyte detection was accomplished at 207 nm. The dead volume of the column (0.63 mL) was determined by injection of water. Analyte solutions were 500 ppm in each compound, and were prepared in mobile phase solution that was adjusted to pH~2 with TFA.

**Reagents and Chemicals.**

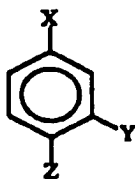
Benzenesulfonic acid, sodium salt, 4-ethylbenzenesulfonic acid, p-toluenesulfonic acid, sodium salt, p-hydroxybenzenesulfonic acid, sodium salt, aniline, 4-aminophenylacetic acid, 3-aminophenol, pyridine-3-acetic acid, pyridine-4-acetic acid, 4-hydroxypyridine, TFA, and lithium perchlorate were from Aldrich. Sulfanilic acid and acetonitrile (HPLC grade) were from Fisher. Naphthalene-1,5-disulfonic acid, disodium salt and N-methylaniline were from Eastman Kodak. 4-chlorobenzenesulfonic acid, sodium salt was from TCI America. Pyridine was from J.T. Baker. Table I lists the chemical structures and numerical designators for each analyte at pH 2.0. All chemicals were used as received. Water was obtained by passing in house triple-distilled water through a Millipore Milli-Q purification system.

**RESULTS AND DISCUSSION****Separation of the Mixture of Anions and Cations at Open Circuit.**

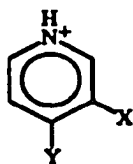
To assess the utility of EMLC for manipulating the separation of a mixture containing organic anions and cations, we examined first the separation of a fifteen component mixture of anions and cations obtained at open circuit ( $\sim 0.15$  V vs Ag/AgCl/sat'd NaCl). This separation elucidates the major interactions responsible for retention of these species at the PGC surface. In the next section, we present separations obtained at several constant  $E_{app}$ 's which both illustrate the ability of EMLC to manipulate electrochemically the separations of these compounds and also provide valuable insights into the electrochemical retention mechanism, particularly as it pertains to the cationic species.



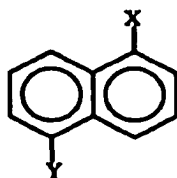
Table I. Chemical Structures of the Organic Anions and Cations.



ANALYTE NO.	X	Y	Z
1	$\text{NH}_3^+$	H	$\text{SO}_3^-$
2	H	H	$\text{SO}_3^-$
3	OH	H	$\text{SO}_3^-$
4	$\text{NH}_3^+$	H	H
5	$\text{CH}_3$	H	$\text{SO}_3^-$
7	$\text{NH}_3^+$	OH	H
9	$\text{CH}_2\text{CH}_3$	H	$\text{SO}_3^-$
10	$\text{NH}_3^+$	H	$\text{CH}_2\text{CO}_2\text{H}$
11	Cl	H	$\text{SO}_3^-$
12	$\text{NH}_2^+\text{CH}_3$	H	H



ANALYTE NO.	X	Y
6	H	H
13	$\text{CH}_2\text{CO}_2\text{H}$	H
14	H	$\text{CH}_2\text{CO}_2\text{H}$
15	H	OH

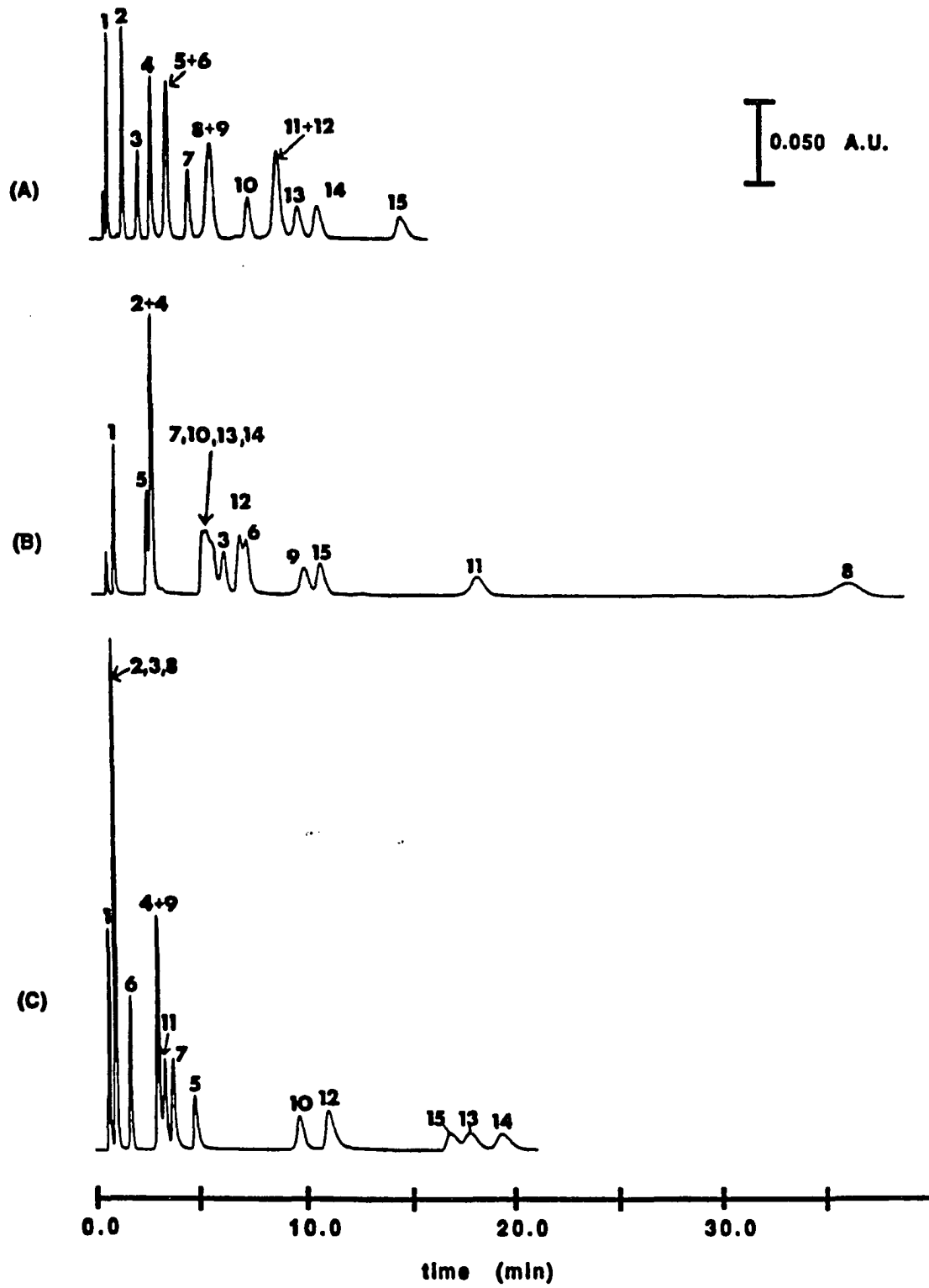


ANALYTE NO.	X	Y
8	$\text{SO}_3^-$	$\text{SO}_3^-$

Figure 1a shows a separation of the fifteen component mixture of anions and cations obtained at the EMLC column at open circuit. Importantly, at the pH of the mobile phase (pH=2.0), all of the analytes existed as either singly-charged (analytes 2,3,5,9,11) or doubly-charged anions (analyte 8), singly-charged cations (analytes 4,6,7,10,12,13,14,15), or uncharged (analyte 1) molecules. Relatively narrow and symmetrical elution bands are obtained for each analyte, with the complete elution of the mixture occurring in ~15 min. The first elution band (unlabelled) corresponds to that of TFA, which was used to adjust the pH of the analyte solution. Six of the analytes, however, are ineffectively separated under these conditions, as is evident by the overlap of the elution bands for analytes 5 and 6, 8 and 9, and 11 and 12.

As discussed previously [35], the relative elution order seen in Figure 1a results largely from a combination of the dispersion and donor-acceptor interactions of the analytes with the carbon surface, with a smaller but significant contribution from solvophobic interactions. Solvophobic interactions occur as a result of the increased hydrophobicity of the carbonaceous stationary phase relative to the predominately aqueous mobile phase, and give rise to an enhanced retention of hydrophobic molecules relative to hydrophilic molecules. Such interactions are used as the primary basis for separations in hydrophobic interaction chromatography [37] and conventional bonded phase reverse phase chromatography [38]. We additionally include the effects of the electrical double layer at the carbon surface, and its compaction on the retention of the analytes, into the solvophobic term. Dispersion and donor-acceptor interactions arise via interactions of the analytes with the polarizable and delocalized

**Figure 1. Separations of the 15 component mixture of anions and cations obtained at (a) open circuit, (b) +0.50 V, and (c) -1.00 V. The mobile phase consisted of 93% aqueous 0.10 M LiClO<sub>4</sub> + 0.1% v/v TFA, pH 2.0 and 7% 0.10 M LiClO<sub>4</sub> in acetonitrile. The flow rate was 0.90 mL/min.**



electronic band structure of carbon [39-41], and provide an additional dimension and selectivity to the separations obtained at carbonaceous stationary phases that is unavailable at alkyl bonded phases. The importance of each of these interactions on the retention of aromatic sulfonate derivatives (ASFs) at the carbon surface has been discussed elsewhere [33,35]. It was shown therein that although solvophobic and dispersion interactions affect retention at carbonaceous stationary phases, donor-acceptor interactions are dominant, and their presence alters significantly the elution order expected based solely on hydrophobic considerations.

The relative effects of solvophobic, donor-acceptor, and dispersion interactions on retention are evident, for example, from a comparison of the relative elution order of the cationic species with their relative hydrophobicities as predicted from hydrophobicity parameters ( $\log P$ ) [42]. These  $\log P$  values, as given in Table II, are defined such that a more positive value indicates a more hydrophobic molecule. For these species, the more hydrophilic cations (analytes 10,13-15) with  $\log P$ 's of -3.08, -2.76, -2.76, and -2.75, respectively, are more strongly retained at the carbon surface than the more hydrophobic cations (analytes 4 and 6) with  $\log P$ 's of -2.28 and -2.09, respectively. We attribute this reversal in the elution order to interactions of the hydrophilic and electron-rich carboxylic acid and hydroxyl groups of the former analytes with the carbon surface. Although solvophobic interactions appear to be insignificant for these species, their effects are somewhat more apparent in the weak retention of analyte 1 ( $\log P=-7.16$ ) as well as in the relative elution order of the ASFs, as discussed previously [35]. Although dispersion interactions

Table II. Observed slopes positive and negative of the pzc, substituent electronic parameters ( $\sigma$ )<sup>a</sup>, substituent steric parameters ( $E_s$ )<sup>b</sup>, and hydrophobicity parameters ( $\log P$ )<sup>c</sup> for each of the anions and cations.

Analyte No.	slope (logk'/volt)		$\sigma$	$E_s$	$\log P$
	$E > \text{pzc}^d$	$E < \text{pzc}^e$			
1	0.67	0.053	----	----	-7.16
2	0.94	0.094	0.00	0.00	-2.63
3	1.41	0.094	-0.37	0.32	-3.30
4	-0.010	-0.031	0.00	0.00	-2.28
5	0.95	0.11	-0.17	0.52	-1.97
6	-0.32	-0.055	0.00	0.00	-2.09
7	0.22	0.0093	-0.37	0.32	-2.95
8	2.31	0.36	----	----	-5.77
9	0.74	0.075	-0.15	0.56	-1.31
10	-0.29	-0.046	0.45 <sup>f</sup>	1.45 <sup>g</sup>	-3.08
11	0.96	0.14	0.23	0.55	-1.92
12	-0.21	-0.050	0.00	0.00	-2.64
13	-0.61	-0.090	0.45 <sup>f</sup>	1.45 <sup>g</sup>	-2.76
14	-0.61	-0.098	0.45 <sup>f</sup>	1.45 <sup>g</sup>	-2.76
15	-0.20	-0.029	-0.37	0.32	-2.75

<sup>a</sup>Hammett electronic parameters for the non-ionic substituents [42].

<sup>b</sup>Charton steric parameters for the non-ionic substituents [42].

<sup>c</sup>Hydrophobicity parameters were calculated using the fragment method of Rekker [42].

<sup>d</sup>Includes  $k'$  values between +0.50 V and -0.10 V for the anions, and between +0.30 V and -0.10 V for the cations.

<sup>e</sup>Includes  $k'$  values between -0.30 V and -1.0 V for the anions and cations.

<sup>f</sup>Electronic parameter for the carboxylic acid group.

<sup>g</sup>Steric parameter for the carboxylic acid group.

undoubtedly play a role in the retention of these species at open circuit [39-41], their overall influence appears to be small in comparison with donor-acceptor interactions. This conclusion is supported through a comparison of the molar volume (MV) of the strongly retained 4-hydroxypyridine (analyte 15,  $MV \sim 160 \text{ \AA}^3$ ) to those of the other analytes, all of which, except for pyridine, have larger MV's. Since molar volumes have been used as a measure of the maximal dispersive energy of a molecule [43,44], we expect analyte 15 to be retained more weakly if dispersion interactions were an important contributing factor to its retention. Clearly, analyte 15 exhibits the strongest retention of the components in the mixture despite its low MV. Together, these discussions illustrate that although solvophobic and dispersion interactions are likely involved to some extent in retention, the donor-acceptor interaction of the analytes with the carbon surface is the primary mechanism responsible for their retention.

#### **Separation of the Mixture of Anions and Cations at Various Constant Applied Voltages.**

**Overview of the electrochemical retention mechanism.** An important objective of this work, in addition to exploring the simultaneous separation of anions and cations, is to test further our mechanistic model of analyte retention via EMLC. As noted, the basis for this model stems primarily from the ability of EMLC to modify selectively the strength of the donor-acceptor and solvophobic interactions of analytes with the carbon surface through alterations in  $E_{app}$ . In our model, the observed capacity factor,  $k'$ , is treated as a reflection of the sum of the  $k'$  values due to each of these interactions (e.g.,  $k'_{da}$  and  $k'_{sol}$ , respectively) at each value of  $E_{app}$ . Dispersion interactions are treated as having a magnitude that is

independent of  $E_{app}$ , as discussed [35]. The donor-acceptor component, which was shown to be dominant for the ASFs [35], consists largely of a combination of four terms: (1) the electrostatic attraction or repulsion of the charged group to or from the carbon surface, (2) the dipolar coupling of the polar aromatic substituents with the charged carbon surface, (3) the interaction of the highest or lowest occupied molecular orbitals (HOMO and LUMO, respectively) of the aromatic ring  $\pi$ -electrons with those of the carbon surface, and (4) the interaction of the aromatic substituents with the carbon surface via  $\pi$ - $\pi$ ,  $n$ - $\pi$ , proton donor- $\pi$  interactions. The solvophobic component is considered to consist of two terms: (1) the increase in the effective hydrophilicity of the carbon surface as a result of the electrostatic attraction of electrolyte ions, and (2) the steric shielding of the carbon surface by electrolyte ions resulting from extensive compaction of the electrical double layer [45,46].

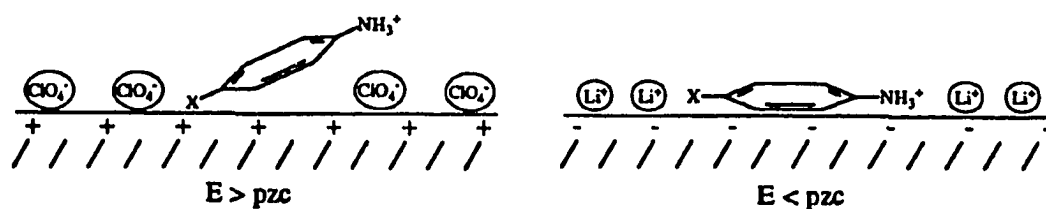
The voltage-dependent magnitude of each of these interactions was discussed in terms of its relation to the excess charge at the carbon surface relative to the potential of zero charge ( $pzc$ ,  $\sim -0.15$  V vs Ag/AgCl/sat'd NaCl). At  $E_{app} > pzc$ , the carbon surface has a net excess of positive charge, which increases its electron-accepting strength [47,48]. In contrast, at  $E_{app} < pzc$ , the carbon surface acquires a net negative charge, which increases its electron-donating strength. Importantly, the magnitude of the surface excess charge as well as the electron accepting/donating properties of the carbon surface are directly related to  $E_{app}$ , with increased excursions of  $E_{app}$  from the  $pzc$  resulting in larger surface excess charges and enhanced electron accepting/donating properties. According to our previous studies [35], we expect that the interactions of the electron-donating anions with the carbon surface will



increase at  $E_{app} > pzc$  as a result of their increased electrostatic attraction, HOMO-LUMO,  $n-\pi$ ,  $\pi-\pi$ , and proton donor- $\pi$  interactions, and dipole-dipole coupling, thereby leading to an increase in their  $k'$  values. At  $E_{app} < pzc$ , the anions will show decreased HOMO-LUMO interactions, as well as an electrostatic and dipolar repulsion, resulting in a decrease in their  $k'$  values. Based on earlier studies of the adsorption of aromatic anions at electrode surfaces [46-49], we postulated [35] that the anions interacted with the carbon surface in a parallel orientation at  $E_{app} > pzc$  to maximize their donor-acceptor interaction. Interactions at  $E_{app} < pzc$ , however, were thought to occur in a perpendicular orientation to minimize the electrostatic repulsion of the sulfonate group. A direct consequence of the parallel orientation of the anions at  $E_{app} > pzc$  is that the aromatic substituents can sterically reduce the magnitude of the voltage-dependent donor-acceptor interaction between the ring and the carbon surface. As will be discussed below, this steric effect plays an important role in determining the sensitivity of various analytes to changes in  $E_{app}$ .

These discussions can be used as a basis for predicting the behavior of the cationic species in both regions. At  $E_{app} > pzc$ , we expect that the tendency for the  $\pi$ -donating aromatic ring to engage in HOMO-LUMO interactions with the carbon surface will compete with the electrostatic and dipolar repulsion of the cationic group from the surface. The combination of these effects may lead to the interaction of the cations with the carbon surface in an orientation that is somewhat canted, as illustrated in Scheme I. The increased distance of the aromatic ring  $\pi$ -electrons from the surface should decrease dramatically their voltage-dependent HOMO-LUMO interaction [50,51], which, combined with their electrostatic and

Scheme I



dipolar repulsion, will result in a decrease in  $k'$  for the cations with increasing  $E_{\text{app}}$ . The HOMO-LUMO interaction can be either enhanced or decreased further depending on the electron accepting/donating properties of the aromatic substituent, X. At  $E_{\text{app}} < \text{pzc}$ , the cations will likely lie flat on the carbon surface, depending on the substituent X, to maximize  $\pi$ - $\pi$  and  $n$ - $\pi$  interactions of their electron-withdrawing substituents and the electrostatic attraction of the cationic group to the surface. The HOMO-LUMO interaction of the aromatic ring with the carbon surface should decrease in this voltage region, however, since both the ring and the carbon surface have electron-donating properties. Therefore, we expect the  $k'$  values for the cations to increase with the application of increasingly more negative values of  $E_{\text{app}}$ .

These changes in  $k'$  produced through alteration in the donor-acceptor properties and excess charge at the carbon surface are mediated by the changes in solvophobic interactions. As discussed above, solvophobic interactions resulting from double layer compaction will decrease the retention of both the anions and the cations at  $E_{\text{app}} > \text{pzc}$  and  $E_{\text{app}} < \text{pzc}$ . This will lead, for example, to a diminished ability to increase the  $k'$  values of anions but an enhanced ability to decrease the  $k'$  values of cations at  $E_{\text{app}} > \text{pzc}$ . Together, these discussions serve as a

model for predicting the electrochemically-controlled retention of both anions and cations using EMLC. The validity of this model will be tested below through its application to the experimental retention data obtained at several constant  $E_{app}$ 's.

**Variation in retention with applied voltage.** Figures 1b and 1c show separations of the fifteen component mixture obtained at constant  $E_{app}$ 's of +0.50 V and -1.00 V, respectively. Comparison of these separations to that obtained at open circuit yields trends in retention that agree with the predictions of our model. For example, at +0.50 V, a voltage which is positive of the pzc, the retention times for each of the anions increases by at least a factor of 1.8 as compared to those obtained at open circuit. These increases in retention time translate to increases in the  $k'$  values for benzenesulfonate (analyte 2) and 4-hydroxybenzenesulfonate (analyte 3), for example, from 1.45 to 2.50 at open circuit to 3.28 and 8.18 at +0.50 V, respectively. Impressively, the  $k'$  for the doubly-charged naphthalenedisulfonate compound (analyte 8) increases by a factor of 7 (i.e., from 7.41 to 51.29) due to the increased donor ability of a second sulfonate group and aromatic ring. In contrast, the  $k'$  values for the cationic species generally decrease. In general, only small changes were found. The  $k'$  for aniline (analyte 4) decreases by only a factor of 1.03 (i.e., from 3.37 to 3.28), whereas the  $k'$  for pyridine-4-acetic acid (analyte 14) decreases by a factor of  $\sim 2$  (i.e., from 14.68 to 7.38). Interestingly, 3-aminophenol (analyte 7), although cationic, shows an increase in its  $k'$  at +0.50 V by a factor of 1.2 (i.e., from 5.95 to 6.78), a behavior which resembles that of an anionic species. Similar but enhanced behavior is seen for the uncharged sulfanilic acid (analyte 1), which shows an increase in its  $k'$  by a factor of 1.8 (i.e., from 0.37 to 0.68).

Application of  $-1.00$  V, a voltage which is negative of the pzc, results in the opposite effect. That is, the  $k'$  values for the anions decrease and the  $k'$  values for the cations increase. The magnitudes of the decreases in  $k'$  for the anions ranges from a factor of 2.1 for 4-ethylbenzenesulfonate (analyte 9) to 11.8 for naphthalenedisulfonate (analyte 8), whereas the magnitudes of the increases in  $k'$  for the cations ranges from a factor of 1.06 for aniline (analyte 5) to 1.9 for pyridine-4-acetic acid. These data demonstrate that the retention of both anions and cations can be modulated electrochemically using EMLC, although each species displays a different sensitivity to changes in  $E_{app}$ .

These  $k'$  data are summarized in Figures 2 and 3, which give the logarithm of the  $k'$  values at several  $E_{app}$ 's for the anionic species (Figure 2) and for the cationic species (Figure 3). As observed previously [35], the curves for the anionic species largely show two linear regions of different slope, with the voltage corresponding to the slope change being near the pzc of  $\sim -0.15$  V. Larger slopes are observed positive of the pzc than negative of the pzc. Most of the cations whose curves are shown in Figure 3 display a similar behavior but of opposite polarity, as expected from the above discussions. For the cationic species, larger slopes are also observed at voltages above the pzc. Table II lists the slope for each of the anions and cations at  $E_{app} > pzc$  and  $E_{app} < pzc$ . In addition, a third region of increased slope (dashed lines) is seen for each of the cations in Figure 3 between  $+0.30$  V and  $+0.50$  V that is not observed for the anions in Figure 2.



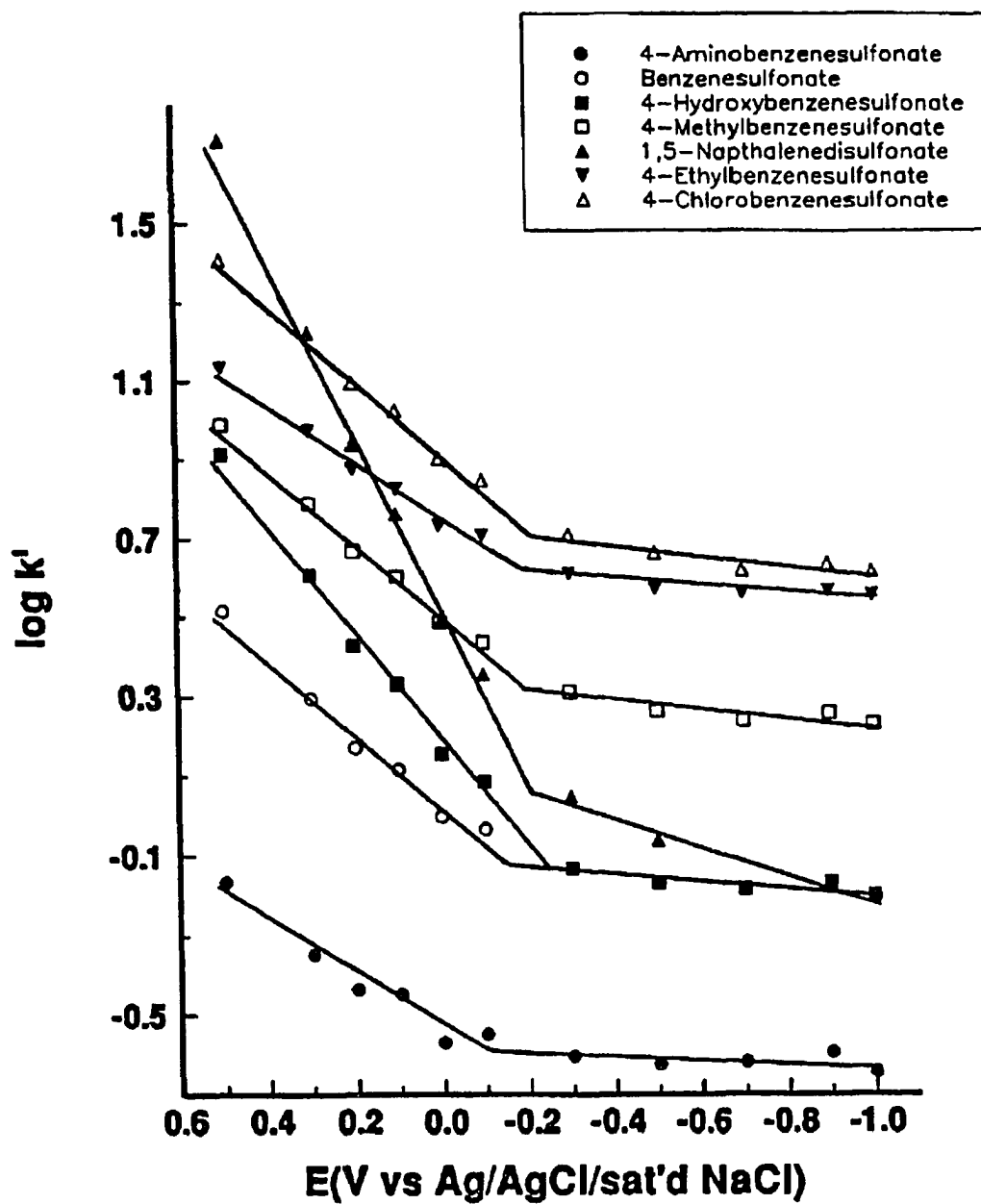
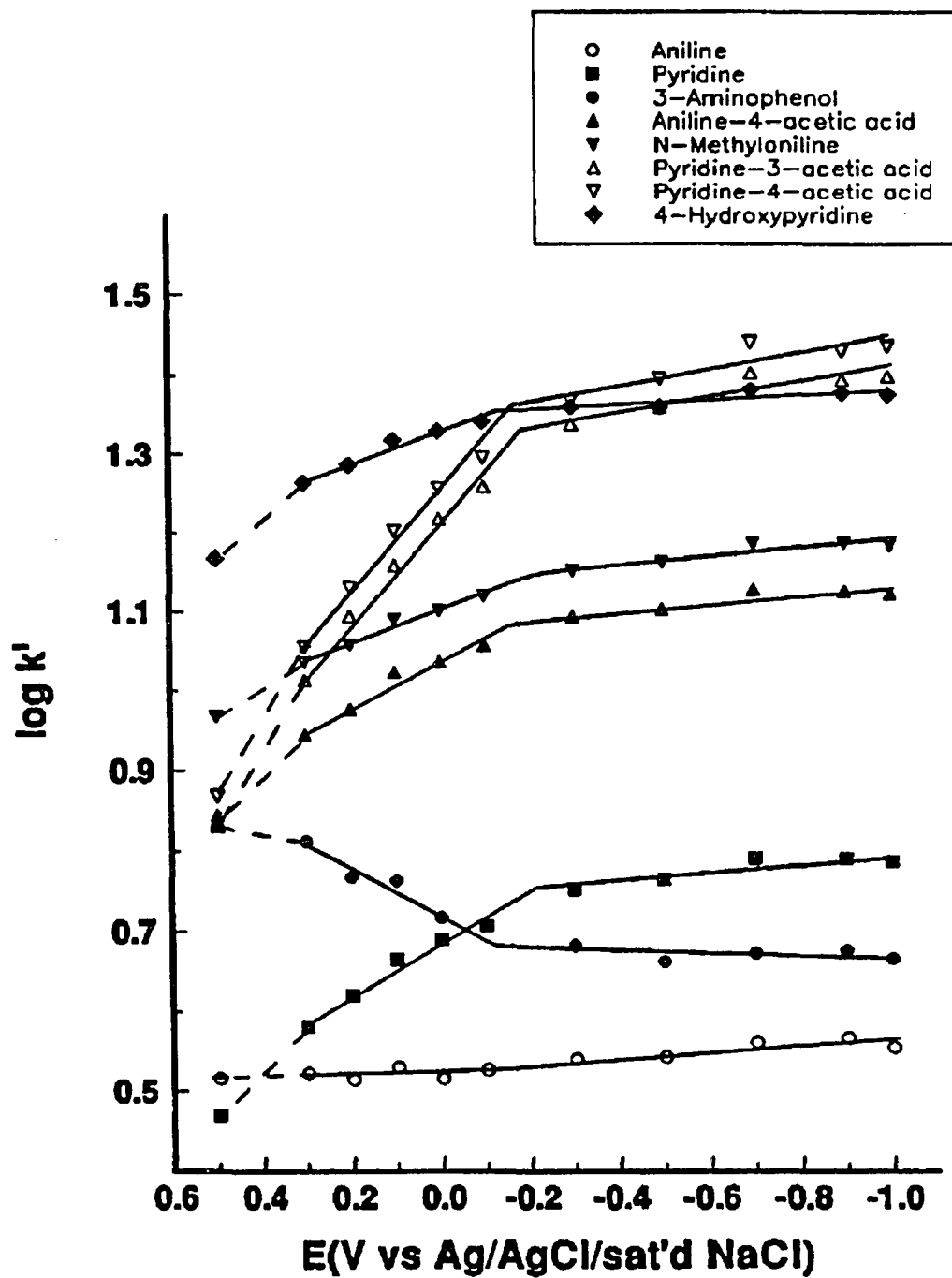


**Figure 3. Plot of the logarithm of  $k'$  versus  $E_{app}$  for the cationic species. The mobile phase consisted of 93% aqueous 0.10 M  $\text{LiClO}_4$  + 0.1% v/v TFA, pH 2.0 and 7% 0.10 M  $\text{LiClO}_4$  in acetonitrile. The flow rate was 0.90 mL/min.**





### Discussion of the electrochemical retention mechanism for anions and cations.

The relative slopes for the anions and cations tabulated in Table II can be understood, to a large extent, through a comparison of their abilities to interact with the carbon surface through donor-acceptor and solvophobic pathways in each voltage region. Table II lists the substituent electronic parameters ( $\sigma$ ) and substituent steric parameters ( $E_s$ ) for each analyte. The  $\sigma$  parameters are used as a qualitative measure of the ability of the substituents of each analyte to undergo donor-acceptor interactions with the carbon surface. As defined by Hammett [52], a positive value indicates an electron-withdrawing substituent, whereas a negative value indicates an electron-donating substituent. The  $E_s$  parameters are used to predict the relative extent of steric hindrance of the HOMO-LUMO interaction of the analyte aromatic ring with the carbon surface by its substituents [42]. In general, bulky substituents have larger values than smaller substituents.

As outlined in a previous work [35], the relative slopes for the ASFs at  $E_{app} > pzc$  (i.e.,  $8 > 3 > 11 \sim 2 \sim 5 > 9$ ) are predominately determined by their ability to undergo donor-acceptor interactions with the carbon surface. Using the  $\sigma$  values in Table II as a guide, it is apparent that naphthalenedisulfonate (analyte 8) should have the largest slope (2.31) due both to the strong electron-donating ability of its second aromatic ring and sulfonate group, and to its increased electrostatic attraction to the positively charged carbon surface. Of the singly-charged ASFs, hydroxybenzenesulfonate (analyte 3), which has the strongest electron-donating substituent, i.e., the hydroxyl group ( $\sigma = -0.37$ ), should have the largest slope (1.41). The small size of this substituent ( $E_s = 0.32$ ) also serves to minimize its disruption of the

HOMO-LUMO interaction between the aromatic ring and the carbon surface. The similarity of the slopes for 4-chlorobenzenesulfonate (analyte 11, slope=0.96), 4-methylbenzenesulfonate (analyte 5, slope=0.95), and benzenesulfonate (analyte 2, slope=0.94) can also be qualitatively explained as resulting from a compromise between the additional attractive interactions of the chloro and methyl ( $\sigma=-0.17$ ) substituents via dipole and HOMO-LUMO interactions relative to benzenesulfonate, respectively, and the steric hindrance provided by these groups. The importance of this steric effect is also somewhat apparent in the significantly smaller slope of ethylbenzenesulfonate (analyte 9, slope=0.74,  $E_s=0.57$ ) relative to the other ASFs. These trends are in qualitative agreement with those observed previously [35].

The relative slopes for the ASFs at  $E_{app} < pzc$  show an order of  $8 > 11 > 5 > 2 \sim 3 > 9$ . As discussed [35], this order differs from that at  $E_{app} > pzc$  due largely to the electrostatic repulsion of the sulfonate group from the negatively charged carbon surface, which causes a change in the orientation by which the ASFs interact with the carbon surface. This orientational change causes the substituents meta or para to the sulfonate group to interact most significantly with the carbon surface. Therefore, these interactions will primarily determine the retention of the analyte at the carbon surface. Such an argument can be used to explain the increase in the slope for chlorobenzenesulfonate (analyte 11) relative to the other singly-charged ASFs, since its chloro group should be repelled from the surface at  $E_{app} < pzc$  via dipole-dipole repulsion.

As discussed [35], the slopes for each of the ASFs is larger at  $E_{app} > pzc$  than at  $E_{app} < pzc$  due to the decreased interaction of the ASFs with the carbon surface in the latter voltage range. The reasons for the absolute differences in the slopes for the ASFs observed at the PGC stationary phase used in these studies and the nonporous glassy carbon (GC) phase used in our previous studies [35] are, however, unclear. The slopes are somewhat larger for a few of the ASFs (i.e., analytes 3 and 8) at the PGC phase at  $E_{app} > pzc$  and are smaller for all of the ASFs at  $E_{app} < pzc$ . Such differences may result from variations in the structure of the two carbon surfaces (e.g., edge to basal plane ratio), or from solvophobic effects resulting from differences in the mobile phases used for the two studies. These differences may also help to explain the lack of a decrease in the slopes for the ASFs above +0.30 V, as observed previously [35]. This slope decrease was attributed to the saturation of the carbon surface with charge, which decreases the effects of additional increases in surface charge on the  $k'$  values of the ASFs. Experiments are currently being devised to explore each of these possibilities.

Comparison of the relative slopes for the cationic species at  $E_{app} > pzc$  and  $E_{app} < pzc$  yields additional insights into the electrochemically-controlled retention mechanism. As an example, the pyridine derivatives exhibit a trend in their relative slopes at  $E_{app} > pzc$  which can be predicted based solely on the electron withdrawing/donating properties of their aromatic substituents. As is evident from Table II, pyridinium cations possessing strong electron-withdrawing substituents generally show the largest slopes. For example, analytes 13 and 14, which have strong electron-withdrawing carboxylic acid substituents ( $\sigma=0.45$ ) show slopes

(-0.61) that are larger than that for pyridine (-0.32). In contrast, substitution of the pyridine ring with an electron-donating hydroxyl group ( $\sigma=-0.37$ , analyte 15) has the effect of decreasing the slope (-0.20 vs -0.61 for analyte 14) due to a stronger attraction of the aromatic ring and the hydroxyl group to the carbon surface via HOMO-LUMO interactions. At  $E_{app} < pzc$ , the order of the slopes is similar, except that the slope of analyte 14 is increased somewhat over that of analyte 13. This effect may arise from the partial shielding of the pyridinium nitrogen by the acetic acid group in the meta position. Such shielding could potentially reduce the electrostatic attraction of the cationic nitrogen with the carbon surface, thereby decreasing the slope.

Examination of the relative order of the slopes for the aniline derivative at  $E_{app} > pzc$ , however, reveals some anomalous behavior. This behavior is typified by that for the parent compound aniline, which shows a slope that is ~30 times smaller than that for pyridine. Further, 3-aminophenol, a cationic species, shows a positive slope (i.e., an increase in  $k'$ ) in this voltage region, a behavior which is typical of an anionic species. Apparently, the electron-accepting ability of the ammonium group is nearly comparable to the electron-donating ability of the benzene ring. This causes the decrease in  $k'$  produced by the electrostatic repulsion of the ammonium group to be offset by the increase in  $k'$  produced through the HOMO-LUMO interaction of the benzene ring  $\pi$ -electrons with the carbon surface, resulting in a dramatically decreased sensitivity of its  $k'$  to changes in  $E_{app}$ . This biphasic behavior is circumvented for the pyridinium cation, however, in which the cationic nitrogen is part of the aromatic ring  $\pi$  system. In this molecule, the positive charge can be

readily delocalized throughout the aromatic ring, thereby decreasing significantly the electron-donating ability of the ring [53]. These data suggest that the donor-acceptor properties of the aromatic ring and its nonionic substituents can affect significantly the retention of charged species in EMLC in cases where the donor-acceptor properties of the charged groups are weak.

Using these arguments as a guide, the anomalous behavior seen for 3-aminophenol (analyte 7) seems reasonable since addition of an electron-donating hydroxyl group ( $\sigma=-0.37$ ) to the benzene ring should have the effect of increasing the electron-donating strength of the aromatic ring relative to that in the anilinium cation. This results in a dominance of electron-donating character for the molecule, and therefore a positive slope. A similar but enhanced anionic behavior is seen upon addition of a more highly electron-donating sulfonate group to the aromatic ring as in sulfanilic acid (analyte 1). This molecule, although containing both a cationic ammonium group and an anionic sulfonate group, displays strong anionic-type retention behavior, resulting from the combined electron-donating abilities of the sulfonate group and the aromatic ring.

In contrast, addition of an electron-accepting acetic acid functionality ( $\sigma=0.45$ ) to the aromatic ring increases the electron-accepting properties of the molecule considerably. Aniline-4-acetic acid, for example, shows a slope that is ~20 times larger than that for aniline. Methyl substitution of the ammonium group (i.e., N-methylaniline, analyte 12) also increases significantly the slope (-0.21) relative to that of aniline (-0.010). At present, we do not understand the reasons for such a large increase in slope for this compound relative to aniline.

Since the acid dissociation constants of secondary ammonium ions are generally larger than those of primary ammonium ions [36], it seems reasonable to propose that the ammonium group of analyte 12 has enhanced electron-accepting abilities over those of analyte 4. However, further studies with other N-substituted anilines are needed to unravel this interesting effect.

At  $E_{app} < pzc$ , the slopes for the cationic compounds are smaller than those at  $E_{app} > pzc$ , a behavior similar to that obtained for the anionic compounds. The relative order of increasing slope is qualitatively similar to that at  $E_{app} > pzc$ . Interestingly, however, the slope for aniline appears to increase relative to the other cations in this voltage region. More importantly, its slope appears to be larger when compared to that at  $E_{app} > pzc$ . Indeed, the slope for aniline (-0.031) is similar to that of 4-hydroxypyridine (-0.029). This increase in slope is consistent with the discussions posed above. At  $E_{app} < pzc$ , HOMO-LUMO interactions of the aromatic ring (an electron-donor) with the negatively charged carbon surface (an electron-donor) should decrease and become negligible, whereas the electrostatic attraction of the ammonium group to the carbon surface should increase. Therefore, the competition between the donor properties of the aromatic ring and the acceptor properties of the ammonium group should decrease at  $E_{app} < pzc$ , thereby allowing for the accepting properties of the ammonium group to become dominant. A similar argument can be used to explain the somewhat increased slope of pyridine relative to the other cations as well. Similar to the anions, the decreased slopes for the cations at  $E_{app} < pzc$  relative to those at  $E_{app} > pzc$  likely result from a decreased interaction of the cations with the carbon surface. In this

voltage range, mainly electrostatic and dipole coupling interactions are operative, whereas HOMO-LUMO interactions of the aromatic ring are negligible.

Figure 3 also shows that the cations appear to display an enhanced sensitivity to changes in  $E_{app}$  above +0.30 V (i.e., dashed lines). This enhanced sensitivity results in an increased slope between +0.30 V and +0.50 V. At present, we attribute this effect to the compaction of the electrical double layer at the carbon surface with electrolyte anions. Since these electrolyte anions compete with the analytes for surface sites, an increase in their interfacial concentration produced through double layer compaction will decrease the interaction of the cations with the carbon surface in this voltage range, as discussed above, thereby leading to an increased slope. This decrease is further facilitated by the very weak interaction of the cations with the carbon surface at  $E_{app} > pzc$ . Interestingly, the ASFs do not appear to be affected significantly by this compaction at the PGC stationary phase. This disparity may result from the much stronger interaction of the ASFs with PGC, as is evident from their larger, positive slopes at  $E_{app} > pzc$ . Together, these discussions illustrate the ability of the EMLC column to act as a transducer that converts differences in electron-accepting or electron-donating ability into differences in electrochemically-manipulated retention. These differences can then be used to modify selectively the separations, as discussed in the next section.

### **Improvement of the Separation Through Application of Fixed and Variable Voltages.**

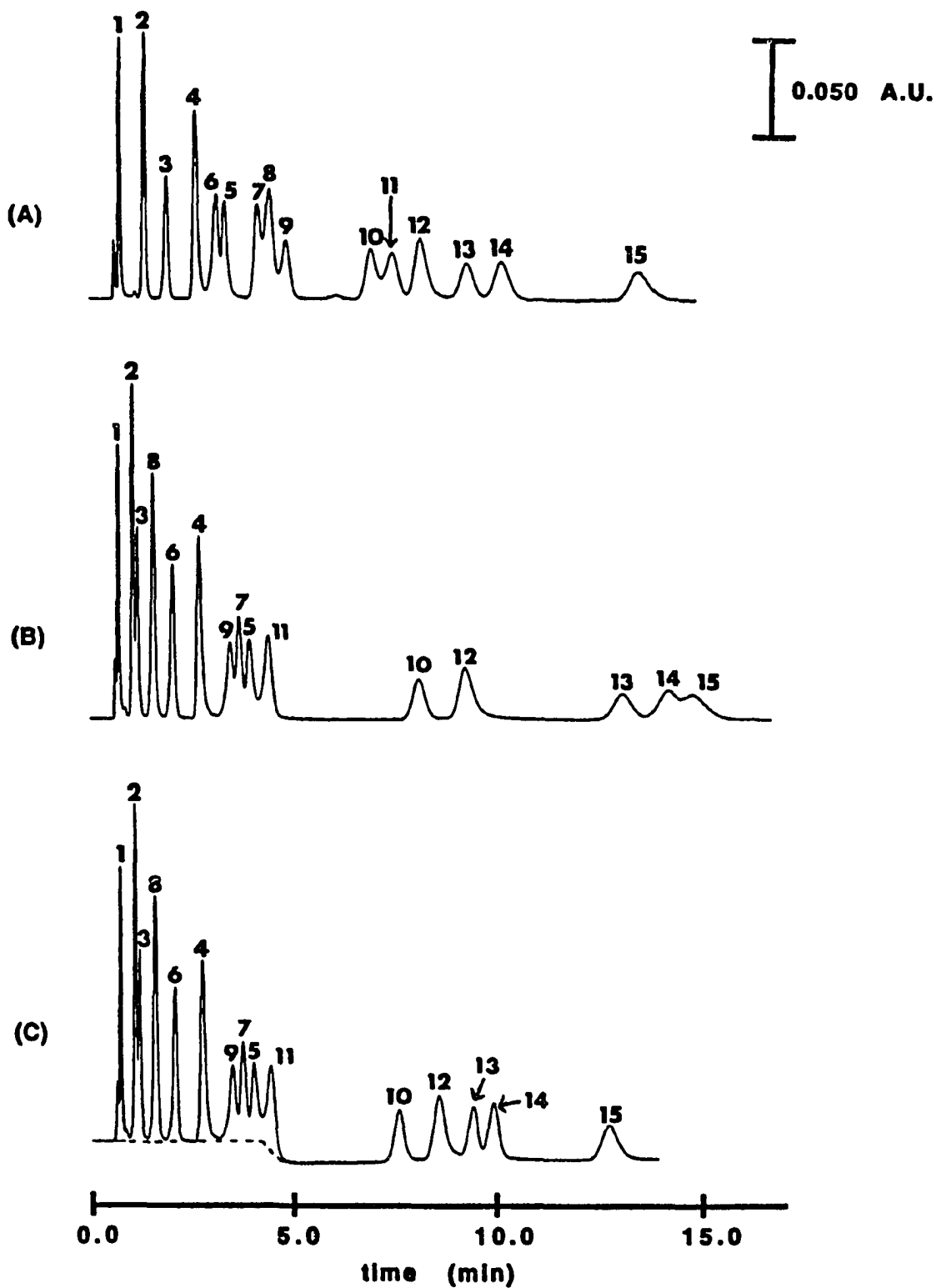
In this section, we investigate the ability of EMLC for fine-tuning the separation of the mixture through the application of fixed and variable voltages to the column. These results

demonstrate how the differences in electron-donating or accepting properties of the molecules outlined in the previous section can be exploited for improving the separations. Figure 4a shows a separation of the mixture obtained at a constant  $E_{app}$  of +0.125 V. Importantly, this voltage is only  $\sim 0.025$  V negative of the open circuit voltage ( $\sim +0.15$  V). As is evident, elution bands for all fifteen analytes are observable. This is in contrast to the separation obtained at open circuit, in which six of the analytes were completely unresolved. The improvement in this separation occurs as a result of the differing polarities and magnitudes of the slopes for the anionic and cationic species, as summarized in Table II. Clearly, a very small change in  $E_{app}$  can produce dramatic improvements in the separation, thereby illustrating the sensitivity of the EMLC technique for manipulating the separations of these compounds.

As demonstrated previously [30,33,35], changes in  $E_{app}$  made during elution can also be used to improve the efficiency of a separation. As examples, Figures 4b and 4c show separations of the sample obtained at a constant  $E_{app}$  of -0.20 V and upon application of a voltage step from -0.20 V to +0.50 V made 4.1 min after sample injection, respectively. At -0.20 V, although elution bands for all fifteen analytes are observable, the resolution of analytes 14 and 15 is poor and the total analysis time is relatively long ( $\sim 15$  min). This separation can be readily improved through application of a step in  $E_{app}$  from -0.20 V to +0.50 V after the elution of analyte 11. Such a voltage step method seems viable since the  $k'$  values of analytes 10 and 12-15, all of which are cations, should decrease through application of a positive step in  $E_{app}$ . Further, analytes 13 and 14 have much larger slopes than analyte 15 at  $E_{app} > pzc$ , and therefore should show larger decreases in their retention times, resulting in an improved



**Figure 4. Separations of the fifteen component mixture of anions and cations obtained at (a) +0.125 V and (b) -0.20 V. The separation in (c) was obtained through application of a step in  $E_{app}$  from -0.20 V to +0.50 V 4.1 min after injection. The dashed line shows the profile of the background obtained under identical conditions but without analyte injection. The mobile phase consisted of 93% aqueous 0.10 M LiClO<sub>4</sub> + 0.1% v/v TFA, pH 2.0 and 7% 0.10 M LiClO<sub>4</sub> in acetonitrile. The flow rate was 0.90 mL/min.**



resolution between these two groups of cations. Figure 4c shows the result. The dashed line shows the profile of the baseline obtained under identical conditions but without injection of the mixture. The decrease in the baseline observed upon application of the voltage step results from an uptake of the perchlorate mobile phase anions into the electrical double layer at the carbon surface [35]. The baseline gradually increases back to its initial value after ~20 min. As is apparent from Figure 4c, the voltage step results in a dramatic improvement in the resolution of analytes 14 and 15 as well as a significant decrease in the elution band widths for all five analytes. For example, the half-widths of the elution bands for analytes 13 and 14 decrease by factors of ~2 as compared to those obtained at -0.20 V. The total analysis time is also decreased somewhat from 15 min to ~13 min in the voltage step. These two examples illustrate clearly the ability of EMLC to manipulate and fine-tune the separations of anionic and cationic compounds.

## CONCLUSIONS

This paper has demonstrated the utility of the EMLC technique for manipulating and fine-tuning the separations of mixtures containing organic anions and cations. Through tests of the retention of these species at several constant  $E_{app}$ 's, a preliminary mechanism for the electrochemical modulation of the retention of cationic species was proposed that is based on the mechanism postulated previously for anionic species [35]. This mechanism is founded on the ability of changes in  $E_{app}$  to alter the capability of the carbon surface to interact with the analytes via donor-acceptor and solvophobic forces. For the cations, the EMLC technique

was found to have the greatest sensitivity and selectivity for strong electron-accepting species, and reduced sensitivity for weak electron acceptors. This behavior is opposite to that for anionic species, for which the strongest electron donors showed the greatest sensitivity. The sensitivity of EMLC for fine-tuning the separation of these compounds was further illustrated through examination of separations obtained after application of a small ( $\sim 0.025$  V) constant  $E_{app}$  relative to the open circuit voltage and also through alteration of  $E_{app}$  dynamically during elution by means of a voltage step. Both examples clearly illustrate the utility of EMLC for manipulating and improving the separations. Future studies will be aimed primarily at further investigation of the electrochemically-controlled retention mechanism and its applications.

#### ACKNOWLEDGMENTS

R.S.D. gratefully acknowledges the support of an ACS Analytical Division Summer Fellowship sponsored by Dow Chemical U.S.A. This work was supported by the National Science Foundation (Grant CHE-9003308) and by Iowa State Universities' Microanalytical Instrumentation Center. The Ames Laboratory is operated for the U.S. Department of Energy by Iowa State University under contract No. W-7405-Eng-82.

## REFERENCES

1. H. Miyagi, J. Miura, Y. Takata, S. Kamitake, S. Ganno, and Y. Yamagata, *J. Chromatogr.*, 239 (1982) 733.
2. E. Coca, B. Ribas, G. Trigueros, J. Mtnez-Sarmiento, M. Borque, D. Ortega, A. Sobrino, A. Mallen, I. DePablos, and J.A. Fdez-Represa, *J. Liq. Chromatogr.*, 17 (1994) 1349.
3. V.T. Turkelson and M. Richards, *Anal. Chem.*, 5 (1978) 1420.
4. W. Rich, E. Johnson, L. Lois, P. Kabra, B. Stafford, and L. Morton, *Clin. Chem.*, 26 (1980) 1492.
5. R.F. Pfeifer and D.W. Hill, *Adv. Chromatogr.*, 22 (1984) 37.
6. R.A. Sherwood, A.C. Titheradge, and D.A. Richards, *J. Chromatogr. Biomed. Appl.*, 528 (1990) 293.
7. J.F. Davey and R.S. Ersser, *J. Chromatogr.*, 528 (1990) 9.
9. P. Edwards, *Food Technol.*, June (1983) 53.
10. M. Calull, R.M. Marce, and F. Borrull, *J. Chromatogr.*, 590 (1992) 215.
11. L.W. Doner and K.B. Hicks, *Anal. Biochem.*, 115 (1981) 225.
12. R. Benlloch, R. Farre, and A. Frigloa, *J. Liq. Chromatogr.*, 16 (1993) 3113.
13. G. Achilli, G.P. Cellerino, and G.M. d'Eril, *J. Chromatogr. A*, 661 (1994) 201.
14. J. Hsu, *Anal. Chem.*, 64 (1992) 434.
15. I.S. Kim, F.I. Sasinos, D.K. Rishi, R.D. Stephens, and M.A. Brown, *J. Chromatogr.*, 589 (1991) 177.
16. M.J.M. Wells, D.D. Riemer, and M.C. Wells-Knecht, *J. Chromatogr. A*, 659 (1994) 337.

17. O.A. Shpigun and Y.A. Zolotov, *Ion Chromatography in Water Analysis*, Ellis Horwood Limited, Chichester, England, 1988.
18. E. Sawicki, J.D. Mulik, and E. Wittgenstein, *Ion Chromatographic Analysis of Environmental Pollutants*, Ann Arbor Science, Ann Arbor, Mich., 1977.
19. C. Prandi and T. Venturini, *J. Chrom. Sci.*, 19 (1981) 308.
20. R.H.A. Sorel and A. Hulshoff, *Adv. Chromatogr.*, 21 (1983) 87.
21. M.T. Hearn, *Adv. Chromatogr.*, 18 (1980) 59.
22. T.O. Crowley and R.A. Larson, *J. Chrom. Sci.*, 32 (1994) 57.
23. R.E. Smith, *Ion Chromatography Applications*, CRC Press, Boca Raton, Fl., 1988.
24. G.A. Harlow and D.H. Morman, *Anal. Chem.*, 36 (1964) 2438.
25. L.W. Yu and R.A. Hartwick, *J. Chrom. Sci.*, 27 (1989) 176.
26. R.F. Antrim, R.A. Scherrer, and A.M. Yacynych, *Anal. Chim. Acta*, 164 (1984) 283.
27. A.R. Ghatak-Roy and C.R. Martin, *Anal. Chem.*, 58 (1986) 1574.
28. H. Ge and G.G. Wallace, *J. Liq. Chromatogr.*, 13 (1990) 3245.
29. H. Ge, P.R. Teasdale, and G.G. Wallace, *J. Chromatogr.*, 544 (1991) 305.
30. R.S. Deinhammer, K. Shimazu, and M.D. Porter, *Anal. Chem.*, 63 (1991) 1889.
31. T. Nagaoka, M. Fujimoto, Y. Uchida, and K. Ogura, *J. Electroanal. Chem.*, 336 (1992) 45.
32. T. Nagaoka, M. Fujimoto, H. Nakao, K. Kukuno, J. Yano, and K. Ogura, *J. Electroanal. Chem.*, 350 (1993) 337.
33. R.S. Deinhammer, E. Ting, and M.D. Porter, *J. Electroanal. Chem.*, 362 (1993) 295.

34. T.Nagaoka, M. Fujimoto, H. Nakao, K. Kukuno, J. Yano, and K. Ogura, *J. Electroanal. Chem.*, 364 (1994) 179.
35. R.S. Deinhammer, E.Ting, and M.D. Porter, in preparation for submission to *Analytical Chemistry*.
36. R.M. Smith and A.E. Martell, *Critical Stability Constants*, vols. 1-6, Plenum Press, New York, 1975.
37. J. Gehas and D.B. Wetlaufer, *J. Chromatogr.* 511 (1990) 123.
38. C. Horvath, W. Melander, and I. Molnar, *J. Chromatogr.*, 125 (1976) 129.
39. B.J. Bassler and R.A. Hartwick, *J. Chrom. Sci.*, 27 (1989) 162.
40. N. Tanaka, T. Tanigawa, K. Kimata, K. Hosoya, and T. Araki, *J. Chromatogr.*, 549 (1991) 29.
41. C.K. Lim, *Advan. Chromatogr.*, 32 (1992) 1.
42. C. Hansch and A. Leo, *Substituent Constants for Correlation Analysis in Chemistry and Biology*, Wiley, New York, 1979.
43. W.J. Moore, *Physical Chemistry*, 4th ed., Prentice Hall, Englewood Cliffs, NJ, 1972.
44. T.M. Engel, S.V. Olesik, M.R. Callstrom, and M. Diener, *Anal. Chem.*, 65 (1993) 3691.
45. S. Sarangapani and V.K. Venkatesan, *Proc. Indian Nat. Sci. Acad.*, 49 (1983) 124.
46. E. Dutkiewicz and J. Stuczynska, *Electrochim. Acta*, 33 (1988) 19.
47. E.A. Nechaev, *Elektrokhimiya*, 19 (1984) 972.
48. D. Rolle and J.W. Schultze, *Electrochim. Acta*, 31 (1986) 991.
49. J.M. Parry and R. Parsons, *J. Electrochem. Soc.*, 113 (1966) 992.

50. B.B. Damaskin, S.L. Dyatkina, and V.M. Gerovich, *Elektrokhimiya*, 21 (1985) 716.
51. K. Morokuma, *Acc. Chem. Res.*, 10 (1977) 294.
52. L.P. Hammett, *Chem. Rev.*, 17 (1935) 125.
53. J. McMurry, *Organic Chemistry*, Cole Publishing Co., Monterey, CA, 1984.



## CHAPTER 6. THE FINE-TUNING OF PHENOL SEPARATIONS USING ELECTROCHEMICALLY- MODULATED LIQUID CHROMATOGRAPHY (EMLC)

A paper to be submitted to the Journal of Chromatography

Randall S. Deinhammer, EnYi Ting, and Marc D. Porter<sup>1</sup>

### ABSTRACT

The utility of the new analytical separation technique, termed electrochemically-modulated liquid chromatography (EMLC), for fine-tuning and optimizing the separation of fifteen phenols is demonstrated. Eleven of these phenols have been listed as priority pollutants by the environmental protection agency (EPA). The stationary phase consisted of 7  $\mu\text{m}$  porous graphitic carbon spheres that were connected as the working electrode in a novel three-electrode electrochemical cell design. Tests of the retention of the phenols at several constant applied voltages ( $E_{\text{app}}$ ) revealed that their capacity factors ( $k'$  values) could be altered by up to a factor of four through modification of  $E_{\text{app}}$  between +0.50 V and -1.00 V. At both of these voltages, the separation of the mixture was improved as compared to that obtained at open circuit. In general, the  $k'$  values of the phenols increased at  $E_{\text{app}}$ 's positive of the potential of zero charge (pzc) at the carbon surface ( $\sim -0.15$  V) and decreased at  $E_{\text{app}}$ 's negative of the pzc. These effects resulted from the electrochemical alteration of the ability of

---

<sup>1</sup>Author to whom correspondence should be addressed.

the carbon surface to participate in donor-acceptor and solvophobic interactions with the phenols. Differences in the sensitivity of each phenol to changes in  $E_{app}$  were attributed likewise to differences in their abilities to participate in these interactions with the carbon surface. Qualitative correlations of these sensitivities with the ionization potential, the highest occupied molecular orbital (HOMO) energy, and the substituent electronic and steric parameters of each phenol were used to substantiate these claims.

Further improvement in the separation is demonstrated through application of a voltage step to the column during the elution process, which resulted in the near baseline resolution of the mixture. Simultaneous combinations of both voltage and mobile phase changes made during elution are also shown to be effective methods for increasing resolution and decreasing the total analysis time. These tests further revealed that this combined elution method can yield separations that are improved over those obtained using conventional solvent gradient elution techniques. Finally, tests of the retention of these phenols on the column in their deprotonated, anionic forms at negative  $E_{app}$ 's indicated that their sensitivities to changes in  $E_{app}$  were increased by ~ten fold after deprotonation. This large increase in sensitivity was attributed largely to an increased electrostatic repulsion of the anionic phenols from the negatively charged carbon surface.

## INTRODUCTION

The determination of phenolic compounds in water and biological samples has gained considerable interest in recent years due to the results of several studies that have elucidated

their toxic and mutagenic properties [1-3]. These compounds are found in the environment and in the human body as a result of the degradation of pesticides and fungicides [4-6], and as by products of water chlorination [4,7]. Chromatographic methods used for separation and determination of these compounds include gas chromatography [5,8,9] and high performance liquid chromatography [10-14]. Although such methods provide adequate separations of mixtures of such compounds, they often suffer from excessively long analysis times and incomplete resolution when separations of complex mixtures is desired.

Recently, we [15-19] and others [20-27] have proposed a versatile new separation technique termed electrochemically-modulated liquid chromatography, or EMLC. This technique is based on the ability to manipulate selectively the capacity factors ( $k'$  values) of analytes through modification of the composition of a conductive stationary phase both prior to [15-19,20-27] and during [15-19] elution. Such changes are produced electrochemically through the application of various fixed or variable voltages [15-17,19] and charges [18] to a stationary phase that is packed into a novel chromatographic system. Importantly, EMLC allows for changes in analyte  $k'$  values to be produced **without** modification in the composition of a mobile phase, thereby providing an alternate method for performing gradient elution and for fine-tuning analytical separations. Recent studies in our laboratory have focused on the separation of both anionic [15-18] and cationic [19] species, and on the development of a mechanism which can be used as a basis for explaining the electrochemically-modulated retention of these species using EMLC.

In this paper, we investigate the utility of EMLC for modifying and fine-tuning the separations of neutral compounds at a porous graphitic carbon (PGC) stationary phase. A mixture consisting of fifteen structurally similar phenols, eleven of which have been deemed as priority pollutants by the environmental protection agency (EPA), is used as a test sample. A primary goal of this work is to probe the ability of EMLC to utilize changes in the applied voltage ( $E_{app}$ ) for modifying and improving the separation of the phenols over that obtained at open circuit without manipulation in the composition of the mobile phase. These separations are also investigated in terms of the utility of simultaneous combinations of both voltage and mobile phase changes made during analyte elution for further fine-tuning and optimizing the separation. An additional important goal is to characterize the voltage-dependent retention of the phenols in terms of the insights that can be gained into the electrochemical retention mechanism proposed previously for ionic species [18,19]. Finally, a comparison of these separations to those obtained for the analogous phenolate anions is used to illustrate the differences in the ability of EMLC for modifying the separations of neutral and anionic compounds.

## EXPERIMENTAL

### Chromatographic Column Construction.

The general design of the EMLC column and the chromatographic instrumentation has been discussed elsewhere [16].

**Mode of Operation.**

After packing, the column was equilibrated with degassed mobile phase at 0.90 mL/min (50% aqueous 0.10 M LiClO<sub>4</sub> containing 0.1% v/v trifluoroacetic acid (TFA), pH 2, and 50% 0.10 M LiClO<sub>4</sub> in acetonitrile) until a stable detector baseline was reached (~2-3 hr). A mobile phase pH of 2.0 was used to prevent dissociation of the phenols. The detection wavelength was 218 nm. The dead volume of the column (0.59 mL) was determined by injection of water. Operational back pressures were ~1900 psi. Analyte solutions were ~500 ppm in each phenol, and were prepared in acetonitrile. To verify that electrochemically-induced changes in the pH of the mobile phase were not produced during the experiments, the pH of the mobile phase was monitored using a flow-through pH electrode (Fisher Scientific) that had an internal volume of ~50  $\mu$ L.

**Molecular Orbital Calculations.**

Calculation of the highest occupied molecular orbital (HOMO) energies of the phenols was accomplished using the complete neglect of differential overlap (CNDO) method of Pople [28]. This method has been previously reviewed by others [29]. For the calculations, the chloro groups were treated as part of the  $\pi$ -system.

**Reagents and Chemicals.**

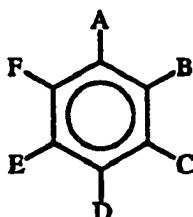
Hydroquinonesulfonic acid, potassium salt, resorcinol, 4-fluorophenol, *o*-cresol, *m*-cresol, 2-chlorophenol, 4-chlorophenol, 2-nitrophenol, 3-nitrophenol, 4-nitrophenol,

4-chloro-3-methylphenol, 2,4-dichlorophenol, 3,5-dichlorophenol, 2,6-dichlorophenol, lithium perchlorate, lithium hydroxide, and TFA were from Aldrich. Catechol, chlorobenzene, phenol, and acetonitrile (HPLC grade) were from Fisher. Table I lists the chemical structures of these phenols. All chemicals were used as received. At the pH of the mobile phases (pH=2.0 or pH=12.2), all phenols existed in either their protonated or fully deprotonated forms, respectively. Water was obtained from a Millipore Milli-Q purification system.

## RESULTS AND DISCUSSION

The work presented in this paper focused on demonstration of the utility of EMLC for modifying and fine-tuning the separations of uncharged phenolic compounds. A primary goal is an in-depth investigation of the mechanism through which the capacity factors ( $k'$  values) of the phenols could be modified electrochemically to alter the separations. This section is divided into four parts. First, a separation of a mixture containing fifteen phenolic compounds obtained at open circuit is analyzed to identify the specific interactions that affect their retention and relative elution order at the carbonaceous stationary phase. Second, separations of the mixture obtained at several values of  $E_{app}$  are presented and discussed in terms of the ability of EMLC to modify the separations and also in terms of the insights which they offer concerning the electrochemical retention mechanism. Third, a separation of the mixture obtained under conditions of a step in  $E_{app}$  made during analyte elution is presented to illustrate the ability of EMLC to improve the separation over that obtained at open circuit. This separation is also compared to those obtained using conventional solvent gradient elution

Table I. Chemical Structures of the Phenolic Compounds.



<u>ANALYTE NO.</u>	A	B	C	D	E	F
1	OH	H	SO <sub>3</sub> <sup>-</sup>	OH	H	H
2	OH	H	OH	H	H	H
3	OH	OH	H	H	H	H
4	OH	H	H	F	H	H
5	OH	H	CH <sub>3</sub>	H	H	H
6	OH	CH <sub>3</sub>	H	H	H	H
7	OH	Cl	H	H	H	H
8	Cl	H	H	H	H	H
9	OH	H	H	Cl	H	H
10	OH	H	H	Br	H	H
11	OH	H	NO <sub>2</sub>	H	H	H
12	OH	NO <sub>2</sub>	H	H	H	H
13	OH	H	CH <sub>3</sub>	Cl	H	H
14	OH	Cl	H	Cl	H	H
15	OH	H	Cl	H	Cl	H
16	OH	Cl	H	H	H	Cl
17	OH	H	H	H	H	H

methods both with and without simultaneous changes in  $E_{app}$  to assess the utility of these methods for further improving the separation. Finally, separations of eleven phenolate anions are obtained at several constant  $E_{app}$ 's to illustrate the differences in the ability of EMLC to manipulate the retention of charged and uncharged species.

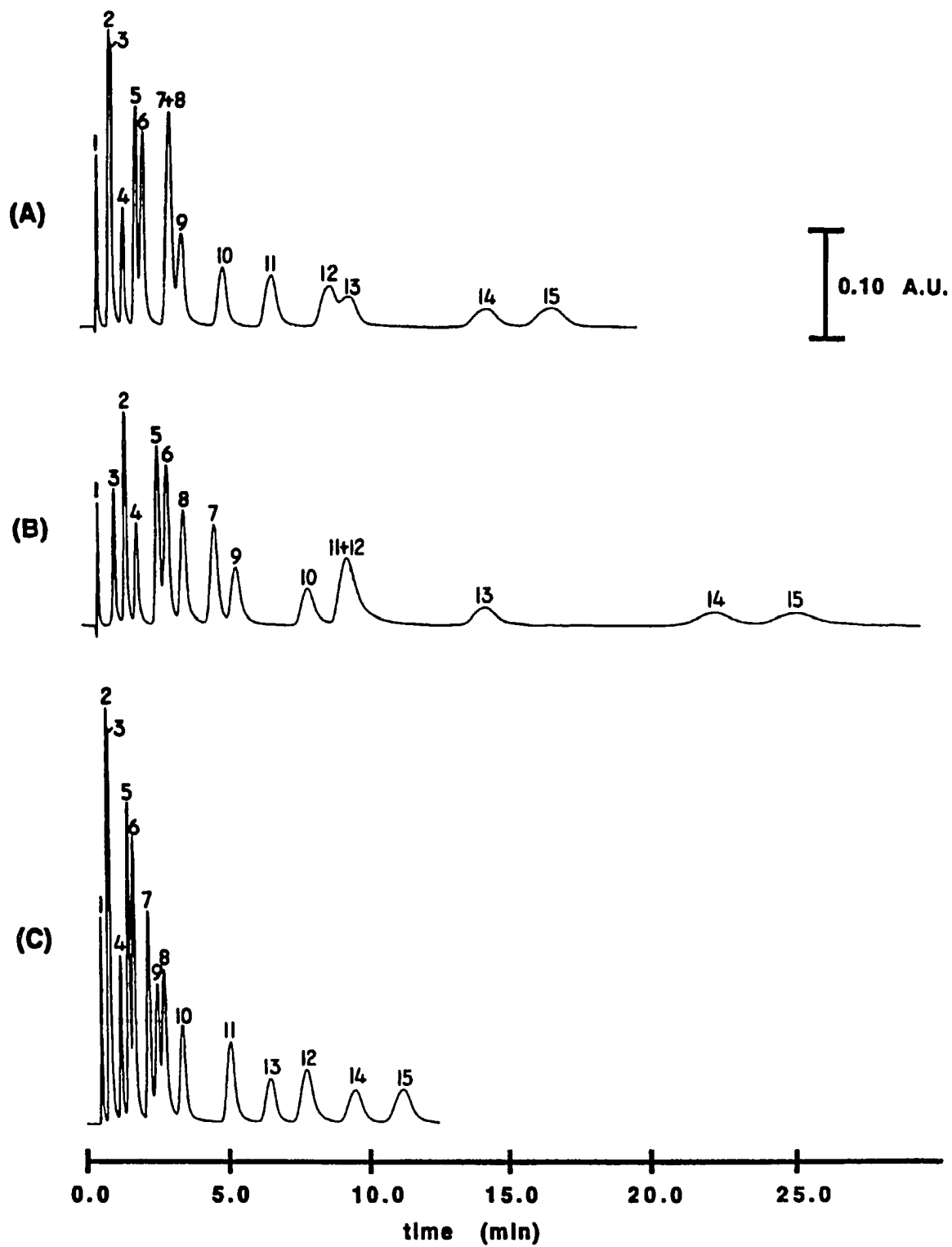
### **Separation of the Mixture of Phenols at Open Circuit.**

Figure 1a shows a separation of the fifteen component mixture of phenols obtained at open circuit, each at a concentration of ~500 ppm. Relatively narrow and symmetrical elution bands are seen for each of the phenols, leading to the complete elution of the mixture in ~17 min. Under these conditions, however, analytes 2 and 3 (*o*- and *m*-dihydroxybenzene), analytes 7-9 (2-chlorophenol, chlorobenzene, and 4-chlorophenol), and analytes 12 and 13 (2-nitrophenol and 4-chloro-3-methylphenol) are poorly resolved.

The retention of compounds at carbonaceous stationary phases has been attributed to a complicated mixing of their donor-acceptor, dispersion, and solvophobic interactions with the carbon surface [30-33]. Briefly, donor-acceptor interactions can occur largely as a result of the interaction of the molecular orbitals of the analytes with the delocalized electronic band structure of carbon [31,32]. The magnitude of these interactions is dependent on the relative donor and acceptor strengths of the analytes and the carbon surface. Dispersion interactions are also facilitated by interaction of the analytes with the polarizable band of electrons at the carbon surface via Van der Waals forces. These interactions generally increase as the molar volume of the analyte increases [34,35] due to a more extensive contact with the carbon surface. Solvophobic interactions can occur as a result of the increased hydrophobicity of the



**Figure 1. Separations of the fifteen component mixture of phenols obtained at (a) open circuit, (b) +0.50 V, and (c) -1.00 V. The mobile phase consisted of 50% aqueous 0.10 M LiClO<sub>4</sub> + 0.1% v/v TFA, pH 2.0 and 50% 0.10 M LiClO<sub>4</sub> in acetonitrile. The flow rate was 0.90 mL/min.**



carbon surface relative to the mobile phase, and generally increase the retention of hydrophobic analytes relative to hydrophilic analytes. These latter interactions have been identified as a primary mode of retention at alkyl bonded phases in conventional reverse phase chromatography [36]. Importantly, donor-acceptor and dispersion interactions, which have been shown to be the predominate modes of retention at carbonaceous stationary phases, can provide additional selectivity to analyte separations when compared to separations obtained at conventional bonded phases. The effects of these interactions on the separations of organic anions [18] and cations [19] using EMLC has been discussed elsewhere.

An extension of these discussions can be qualitatively made to predict the relative elution order of the phenols. For example, comparison of the relative hydrophobicities of the phenols, as given by their log P values in Table II [37], with their relative elution order suggests that, to some extent, increases in hydrophobicity (i.e., more positive log P) translate to increases in retention. That is, the most hydrophilic compounds hydroquinone sulfonate (analyte 1, log P=-3.74) and the dihydroxybenzene isomers (analytes 2 and 3, log P~0.80) show weak retention at the carbon surface, whereas the most hydrophobic dichlorophenol compounds (log P>+3.00, analytes 14 and 15) show the strongest retention, and elute last.

However, some inconsistencies are apparent, such as the weak retention of the hydrophobic chlorobenzene (log P=2.84), and the strong retention of the more hydrophilic nitrophenol compounds (log P~2, analytes 11 and 12). These inconsistencies result from the effects of dispersion and donor-acceptor interactions of these molecules with the carbon surface. For chlorobenzene, the tendency for an increased retention due to its hydrophobicity

Table II. Observed slopes positive and negative of the pzc, ionization potentials (IP), calculated HOMO energies ( $E_{\text{HOMO}}$ )<sup>a</sup>, substituent electronic parameters ( $\sigma$ )<sup>b</sup>, substituent steric parameters ( $E_s$ )<sup>c</sup>, and hydrophobicity parameters ( $\log P$ )<sup>d</sup> for the phenolic compounds.

No.	slope (logk'/volt)	$IP_{\text{exp}}$ (eV)	$IP_{\text{sub}}$ (eV) <sup>c</sup>	$E_{\text{HOMO}}$ (eV)	$\sigma$	$E_s$	$\log P$
	$E > \text{pzc}$ <sup>f</sup>	$E < \text{pzc}$ <sup>g</sup>					
1	---- <sup>h</sup>	----	----	----	----	----	- 3.74
2	1.02	0.059	8.06	8.51	-8.83	-0.37	0.78
3	0.84	0.061	8.32	8.51	-9.02	-0.37	0.84
4	0.57	0.035	----	9.20	-9.25	0.06	1.77
5	0.61	0.042	8.29	8.82	----	-0.17	1.96
6	0.59	0.038	8.32	8.82	----	-0.17	1.97
7	0.69	0.044	9.28	9.07	-9.48	0.23	2.15
8	0.25	0.019	9.07	----	----	----	2.84
9	0.70	0.051	9.07	9.07	-9.57	0.23	2.44
10	0.72	0.048	9.04	8.98	----	0.23	2.65
11	0.49	0.034	----	9.92	-9.75	0.78	2.00
12	0.17	0.015	----	9.92	-9.74	0.78	1.73
13	0.62	0.045	----	8.83	----	0.23	3.10
						-0.17	0.55
14	0.63	0.046	----	9.12	-9.66	0.23	3.06
						0.23	0.55
15	0.59	0.044	----	9.12	-9.49	0.23	3.23
						0.23	0.55
16	----	----	----	9.12	-9.58	0.23	3.08
						0.23	0.55
17	----	----	8.51	----	-9.40	----	1.51

<sup>a</sup>HOMO energies were calculated using the CNDO method of Pople [28].

<sup>b</sup>Hammett electronic parameters for the non-phenolic substituents [37].

<sup>c</sup>Charton steric parameters for the non-phenolic substituents [37].

<sup>d</sup>Hydrophobicity parameters were calculated using the method of Hansch [37].

<sup>e</sup>The ionization potential of a singly-substituted benzene compound containing the non-phenolic functional group.

<sup>f</sup>Includes k' values between +0.30 V and -0.10 V.

<sup>g</sup>Includes k' values between -0.20 V and -1.00 V.

<sup>h</sup>Unretained component.

is offset by its low molar volume ( $\sim 180 \text{ \AA}^3$ ), which reduces its ability to participate in dispersion interactions, for example, relative to the larger 3,5-dichlorophenol (analyte 15, molar volume  $\sim 250 \text{ \AA}^3$ ). For the nitrophenol compounds, the additional  $\pi$ -electrons present in their nitro groups can participate in donor-acceptor interactions with the carbon surface, thereby increasing their retention relative to the other phenols. Similar arguments can be used to explain the relative elution order of the other phenols. Among isomeric compounds, the ortho isomer is usually retained more strongly than the meta or para isomer. This effect, termed the *ortho effect*, arises from the adsorptive nature of the interaction between the aromatic ring of the phenols and the planar carbon surface [33,38,39]. Although this behavior is seen for the dihydroxybenzene (analytes 2 and 3), cresol (analytes 5 and 6), and nitrophenol (analytes 11 and 12) isomers, it appears to be reversed for the chlorophenol isomers (analytes 7 and 9), for which the para isomer elutes after the ortho isomer. At present, we do not understand the anomalous behavior of these two isomers. Nevertheless, the majority of the isomeric compounds tested display the *ortho effect*, as expected. Together, these discussions illustrate that the ability of each phenol to participate in donor-acceptor, dispersion, and solvophobic interactions with the carbon surface will affect their retention and their elution order.

#### **Modification of the Separation Through Alteration in Applied Voltage Prior to Elution.**

As a means for investigating the ability of EMLC to alter electrochemically the separation of the phenols in Figure 1a, we obtained separations of the mixture at several constant  $E_{app}$ 's. The analysis of these separations also provided additional insights into the

electrochemical retention mechanism, as discussed below. Figures 1b and 1c show examples of separations that were obtained at  $E_{app}$ 's of +0.50 V and -1.00 V, respectively. At +0.50 V, the  $k'$  values for the phenols are increased as compared to those obtained at open circuit. The magnitude of this increase in  $k'$  ranges from a factor of 2.5 for resorcinol (analyte 2), which shows an increase in its  $k'$  from 0.62 to 1.57, to a factor of 1.1 for 2-nitrophenol (analyte 12), which shows a  $k'$  increase from 12.82 to 13.75. The total analysis time is also increased from 17 min to 26 min under these conditions. More importantly, these increases in  $k'$  result in dramatic improvements in the resolution of the first nine phenols. At +0.50 V, analytes 2 and 3 as well as analytes 7, 8, and 9, all of which were poorly resolved at open circuit, are nearly baseline resolved. The resolution of analytes 12 and 13 is also considerably improved. Interestingly, the elution order of the first nine phenols is also altered at +0.50 V, with analyte 3 eluting before analyte 2 and analyte 8 eluting before analyte 7. Further, the elution bands of analytes 11 and 12, which were well resolved at open circuit, are completely overlapped.

The change in the elution order of analytes 2 and 3 deserves more discussion at this point. Such a change can be attributed not only to differences in the sensitivities of these analyte to alterations in  $E_{app}$ , but also to the reversible oxidation of the catechol species. This oxidation, which converts the catechol to its corresponding *o*-quinone form, reduces its electron-donating ability, resulting in a decrease in its  $k'$  at +0.50 V. This decrease in  $k'$  results in a dramatic improvement in the resolution of analytes 2 and 3. Support for this oxidation comes from a comparison of the UV spectra of catechol taken at several  $E_{app}$ 's, which begin to show changes indicative of *o*-quinone formation at  $E_{app} > +0.30$  V. Cyclic

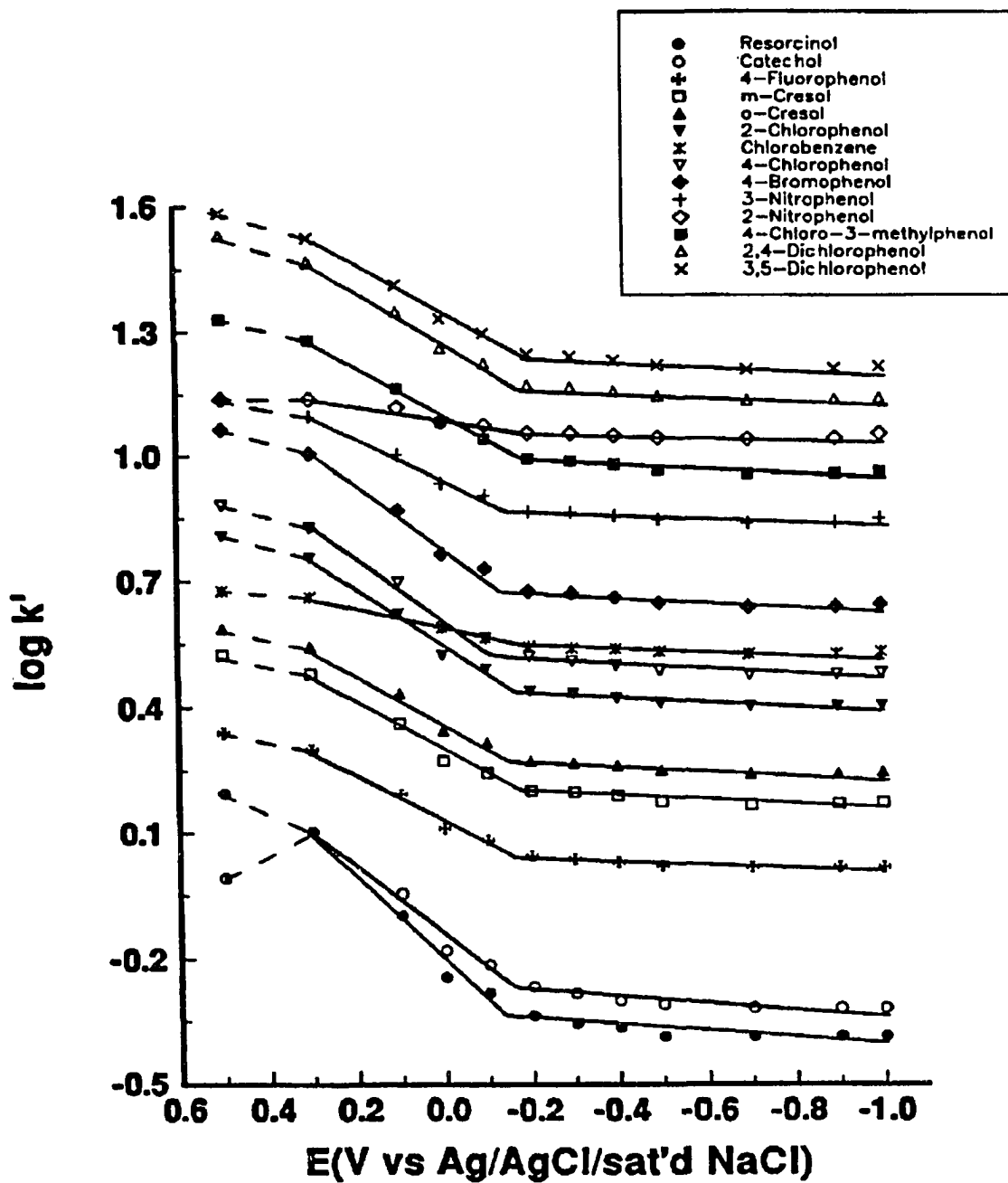
voltammetric studies of the oxidation of catechol in the mobile phase solution further support this conclusion. Although these spectral changes were also observed for the hydroquinone sulfonate compound (analyte 1), they were not observed for any of the other analytes. This oxidation appears to be complete at +0.50 V, since no further changes in the UV spectra are observable at more positive  $E_{app}$ 's. Importantly, the reversibility of this oxidation allows for catechol to be easily recovered post-column through its reduction. Therefore, an additional feature of EMLC, which is unknown with conventional liquid chromatographic columns, is its ability to manipulate the oxidation state of reversible redox species as an additional variable for manipulating retention and improving resolution.

At -1.00 V, the  $k'$  values for the phenols are decreased when compared to those at open circuit. The magnitude of this decrease ranges from a factor of 1.9 for catechol, which shows a decrease in its  $k'$  from 0.74 to 0.40, to a factor of 1.2 for 2-nitrophenol, which shows a decrease from 12.82 to 11.11. Although the overall resolution in the separation at -1.00 V is also improved when compared to that at open circuit, the resolution of the first nine phenols is decreased when compared to that at +0.50 V. However, analytes 11-15 show better resolution at -1.00 V than at +0.50 V. Analogous to the separation at +0.50 V, the elution order at -1.00 V is also different than that at open circuit, with analyte 9 eluting before analyte 8 and analyte 13 eluting before analyte 12.

The voltage-dependent  $k'$  data are summarized in Figure 2, which shows a plot of the logarithm of the  $k'$  values for each phenol as a function of  $E_{app}$ . The data for analyte 1 is not shown since it was unretained at the carbon surface at each value of  $E_{app}$  tested. As is evident,

**Figure 2. Plot of the logarithm of  $k'$  versus  $E_{app}$  for the phenolic compounds. The mobile phase consisted of 50% aqueous 0.10 M LiClO<sub>4</sub> + 0.1% v/v TFA, pH 2.0 and 50% 0.10 M LiClO<sub>4</sub> in acetonitrile. The flow rate was 0.90 mL/min.**





the  $k'$  values for all fourteen phenols generally increase at positive  $E_{app}$ 's and decrease at negative  $E_{app}$ 's. Further, three linear regions of different slope are observed for each analyte, with the changes in slope occurring at  $\sim -0.20$  V and at  $+0.30$  V. The former voltage is close to the experimentally determined potential of zero charge (pzc) at the carbon surface of  $-0.15$  V. Interestingly, the magnitudes of these three slopes also appears to vary greatly among the phenols. Such behaviors are in general agreement with those observed previously for aromatic sulfonates (ASFs) [18] and for organic cations [19].

The model invoked previously [18,19] to explain these behaviors is founded on description of the measured  $k'$  as the sum of the  $k'$  values for each analyte due to their donor-acceptor ( $k'_{da}$ ), dispersion ( $k'_{dis}$ ), and solvophobic ( $k'_{sol}$ ) interactions with the carbon surface at each value of  $E_{app}$ . Alterations in  $E_{app}$  were assumed to modify the ability of the carbon surface to participate in, to a large extent, donor-acceptor and solvophobic interactions with the analytes. Electrochemically-induced changes in the dispersion component,  $k'_{dis}$ , were found to be insignificant when compared to the changes in  $k'_{da}$  and  $k'_{sol}$ . Therefore, this term is treated as being important for retention of the phenols at the carbon surface as discussed above, but with a magnitude that is independent of  $E_{app}$ . For the electron-donating ASFs used previously [18],  $k'_{da}$  was found to be dominant and to determine, to a large extent, the slope observed in the  $\log k'$  versus  $E_{app}$  plot. These interactions were assumed to result primarily from a combination of four terms: (1) the electrostatic attraction or repulsion of the charged sulfonate group to or from the charged carbon surface, (2) the dipolar coupling of polar aromatic substituents with the carbon surface, (3) the interaction of the highest/lowest

occupied or unoccupied molecular orbitals (HOMO and LUMO, respectively) of the aromatic ring with the carbon surface, and (4) the interaction of the aromatic substituents via  $\pi$ - $\pi$ ,  $n$ - $\pi$ , proton donor- $\pi$  interactions with the carbon surface. Since the carbon surface has a net positive excess charge and is an electron acceptor at  $E_{app} > pzc$  [40], each of these interactions should be attractive in nature at  $E_{app} > pzc$  and increase with increasing  $E_{app}$ . At  $E_{app} < pzc$ , the electrostatic and dipolar terms become repulsive in nature due to the negative excess charge at the carbon surface. Further, the HOMO-LUMO,  $n$ - $\pi$ ,  $\pi$ - $\pi$ , and proton donor- $\pi$  terms decrease to zero in magnitude as the carbon surface increases its electron-donating strength. At extreme deviations from the pzc, however, the effects of further increases in  $E_{app}$  on the strength of donor-acceptor interactions should decrease, due to a saturation of the GC surface with charge. This effect was previously shown to cause a decrease in the slopes for several ASFs above +0.30 V [18]. Although the electrostatic term will be negligible for the uncharged phenols, we expect the other terms to remain operative. The solvophobic interaction term was treated as having a maximum at the pzc where the carbon surface has no net charge, and to decrease at both  $E_{app} > pzc$  and  $E_{app} < pzc$ . This decrease in  $k'_{sol}$  was attributed to a compaction of the electrical double layer by electrolyte ions, which compete with the analytes for sites at the carbon surface. Such competition can decrease the retention of the analytes at the carbon surface when large interfacial concentrations of electrolyte ions are built up, i.e., at extremes in  $E_{app}$ .

The general similarity of the curves in Figure 2 to those obtained previously for the ASFs [18,19] is not surprising, since the phenols are also expected to be good electron-

donors. The somewhat smaller magnitudes of these slopes as compared to those of the ASFs is also expected based on the inability of the phenols to interact electrostatically with the charged carbon surface. It was shown previously [18,19] that the relative slopes among the ASFs could be predicted, as a starting point, from examination of their ability to undergo donor-acceptor interactions with the carbon surface. The potential of each phenol to participate in these interactions can be estimated from evaluation of their ionization potentials (IP) [40,41] as well as the electron accepting/donating and steric properties ( $\sigma$  and  $E_s$ , respectively) of their non-phenolic substituents [18,19]. Table II lists these parameters for each of the phenols. In general, phenols with smaller IP's are better electron donors than those with higher IP's. Since the ionization potentials of several of the phenols were unavailable in the literature, we additionally list the IP's for benzene that is substituted with the non-phenolic functional groups (i.e., chlorobenzene, toluene, nitrobenzene, etc.) for comparison. These values are denoted as  $IP_{sub}$  in Table II. The  $\sigma$  and  $E_s$  parameters given for each phenol can be used as a qualitative measure of the tendency of these aromatic substituents to donate or withdraw electrons to or from the carbon surface (i.e.,  $\sigma$ ) and also their tendency to sterically disrupt the HOMO-LUMO interaction of the aromatic ring and the phenol group with the carbon surface (i.e.,  $E_s$ ). The  $\sigma$  parameters are defined such that a negative value indicates electron donation, and a positive values suggests electron withdrawal by the substituent. The  $E_s$  parameters are defined such that larger values correspond to substituents that display increased steric effects. As an additional predictive tool, we have calculated the HOMO energies for several of the phenols using the CNDO method of Pople

[28,29]. For these parameters, a more positive value suggests an increased electron-donating capability.

Comparison of the magnitudes of these parameters in Table II to the relative slopes of the phenols at  $E_{app} > pzc$  suggests that phenols possessing the lowest IP's and  $E_{homo}$ 's generally have the largest slopes. For example, both catechol and resorcinol have the lowest IP's (8.32 and 8.06, respectively) and the lowest  $E_{homo}$ 's (-9.02 and -8.83 eV, respectively) as well as the highest slopes (0.84 and 1.02, respectively). The relative order of the slopes for these two isomers also correlates well with their relative donor ability, with the better donor (i.e., resorcinol) having the largest slope. In contrast, 2-nitrophenol has the highest IP ( $IP_{sub}=9.92$  eV) and the highest  $E_{homo}$  (-9.74 eV) as well as the smallest slope (0.17). This trend is also revealed upon comparison of the IP's for the para isomers of fluorophenol ( $IP_{sub}=9.20$  eV, slope =0.57), chlorophenol ( $IP_{sub}=9.07$  eV, slope=0.70), and bromophenol ( $IP_{sub}=8.98$  eV, slope =0.72).

However, these simple arguments do not explain the larger than expected slope of the two chlorophenol isomers (slope  $\sim$ 0.70,  $IP_{sub}\sim$ 9.07 eV) relative to the cresol isomers (slope $\sim$ 0.60,  $IP_{sub}\sim$ 8.82 eV), or the four-fold larger slope of 3-nitrophenol (slope=0.49) relative to 2-nitrophenol (slope=0.17). Arguments based on consideration of their relative hydrophobicities also do not clearly explain these results, since, for example, the chlorophenol isomers are somewhat more hydrophobic than the cresol isomers. The larger slopes of the chlorophenol isomers relative to the cresol isomers may result, as discussed previously [18], from an increased attraction of the former species to the positively charged carbon surface via

dipole-dipole interactions. The similarity of the slopes for the dichlorophenol isomers (i.e., analytes 14 and 15) to those of the cresol isomers, however, do not entirely fit with this argument. The increased dipole-dipole interaction of the additional chloro group should result in larger slopes for the dichloro compounds relative to both the monochlorophenols and the cresol isomers. We postulate, therefore, that the second chloro group can sterically hinder the aromatic ring from interacting with the carbon surface [42,43], thereby resulting in a decreased overall donor-acceptor interaction. The presence of this steric effect also serves to explain the smaller relative slope of the 4-chloro-3-methylphenol (analyte 13, slope=0.62) relative to 4-chlorophenol (analyte 9, slope=0.70).

In addition to hindering sterically the HOMO-LUMO interactions of the aromatic ring, bulky substituents can also sterically shield the hydroxyl group from interacting via proton donor- $\pi$  interactions with the surface. The importance of the electron-donating ability of this hydroxyl group as a factor which contributes to a large slope is clearly seen in the small slope of chlorobenzene (analyte 8, slope=0.25), which lacks this group in its chemical structure. In such a case, substituents ortho to the hydroxyl group should provide the greatest steric effects and cause the largest decrease in slope, whereas para substituents will affect the hydroxyl group the least. The presence of these steric effects is suggested from the predominance of lower slopes for the ortho isomers of several of the phenols relative to their meta or para isomers. For example, the slopes of the ortho isomers of dihydroxybenzene (analyte 3, slope=0.84), cresol (analyte 6, slope=0.59), chlorophenol (analyte 7, slope=0.69), and nitrophenol (analyte 11, slope=0.17) are smaller than their corresponding meta or para

isomers (slopes of 1.02, 0.61, 0.70, and 0.49, respectively). Of these groups, the ortho and meta isomers of dihydroxybenzene and nitrophenol show the largest differences. The increased positional sensitivity of these isomers may be due to intramolecular hydrogen bonding interactions between the hydroxyl groups or between the hydroxyl group and the nitro group, which will decrease the electron-donating ability of the hydroxyl group. The large steric size of the nitro group ( $E_s=1.39$ ) may also cause an increased steric effect for the nitrophenols.

At  $E_{app}>+0.30$  V (dashed lines), the slopes for all of the phenols decrease relative to those between +0.30 V and -0.10 V. As discussed previously [18,19], we attribute this decrease to a saturation of the carbon surface with charge, such that further increases in surface charge have little effect on the  $k'$  values for the phenols. In a similar manner to the ASFs studied previously [18], the phenols which interact most weakly with the carbon surface at  $E_{app}>pzc$  (i.e., analytes 8 and 12) show the most significant decreases in their slopes. Although not as apparent, a similar effect is seen in the data at  $E_{app}<-0.90$  V.

At  $E_{app}<pzc$ , the relative order of increasing slope for the phenols is qualitatively similar to that at  $E_{app}>pzc$ , but appears to be more affected by dipolar repulsion effects. This dipolar repulsion is evident in the enhanced slopes of the chlorophenol and dichlorophenol isomers relative to those of the dihydroxybenzene isomers. Although the electron-withdrawing chloro groups ( $\sigma=0.23$ ) could potentially interact with the carbon surface through HOMO-LUMO interactions, resulting in a decreased slope, this effect appears to be small in comparison with their dipolar repulsion. As observed previously for anions [18] and for cations [19], the magnitude and range of slopes at  $E_{app}<pzc$  is also considerably smaller

than at  $E_{app} > pzc$ . For example, Table II indicates that the slopes for each of the phenols are decreased by a factor of ~ten at  $E_{app} < pzc$ . Further, the slopes vary by only a factor of ~four at  $E_{app} < pzc$ , whereas the variance was a factor of ~six at  $E_{app} > pzc$ . These observations are consistent with our model, since the retention of the phenols via donor-acceptor interactions should decrease at  $E_{app} < pzc$ . This decreased retention leads to a decrease in the ability of the carbon surface to affect the retention of the phenols and to discriminate effectively between their various electron-donating abilities. Thus, separations using EMLC are most effective at  $E_{app} > pzc$  where the interactions of the analytes with the carbon surface are strong.

In total, the phenolic compounds appear to behave similarly at both  $E_{app} > pzc$  and  $E_{app} < pzc$  to the ASFs studied previously [18] in terms of their electron-donating ability and the types of interactions that affect their ability to respond to changes in  $E_{app}$ . The relative slopes for the phenols appear to be ~two times smaller in both voltage regions, however. This effect is likely due to the absence of an electrostatic donor-acceptor term for the uncharged phenols, which has been shown to have a significant effect on the slopes in both voltage regions for anionic species [18]. The absence of electrostatic effects may additionally decrease the slope at  $E_{app} < pzc$  by decreasing the tendency of the phenols to reorient at the carbon surface-mobile phase interface, as previously proposed for ionic species [18,19]. This reorientation (i.e., from parallel to perpendicular) was proposed to occur for charged analytes as a means for minimizing the electrostatic repulsion of their negatively charged group from the negatively charged carbon surface. Such reorientation serves to decrease the interaction of the analyte with the carbon surface via dispersion and, to some extent, donor-



acceptor interactions, thereby leading to an increased slope. The accuracy of these assertions will be investigated in detail during the final section of this paper.

### **Modification of the Separation Through Dynamic Changes in Applied Voltage and Mobile Phase Composition.**

As elucidated previously [15-19], an attractive feature of EMLC is the ability to modulate the  $k'$  values of analytes during the elution process. Such dynamic modulation can be used to fine-tune a separation and to improve its overall quality. As an example, Figure 3 shows a separation of the fifteen component mixture that was obtained through application of a step in  $E_{app}$  from +0.50 V to -1.00 V immediately after sample injection. Use of this voltage step method allows for a combination of the improved resolution of analytes 1-9 obtained at +0.50 V with the improved resolution of analytes 11-15 obtained at -1.00 V. Notice that the overall resolution of the phenols obtained with this strategy is improved *dramatically* over that found at either open circuit, +0.50 V, or -1.00 V.

Although the quality of this separation is improved dramatically when compared to that at open circuit, the total analysis time is not decreased in the voltage step, as might be expected based on the much shorter time required to complete the separation at -1.00 V. Clearly, the column does not respond instantaneously to changes in  $E_{app}$ . This effect is a result of the electrical resistance observed upon passage of large currents within the electrochemical cell, which slows the equilibration of the column at the new value of  $E_{app}$ . Although further improvements in the design of the EMLC column are necessary to minimize this effect, the present design functions well enough to allow for large improvements in the

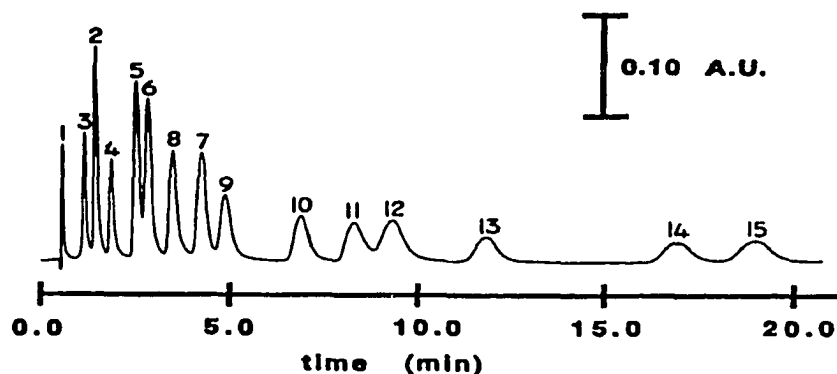
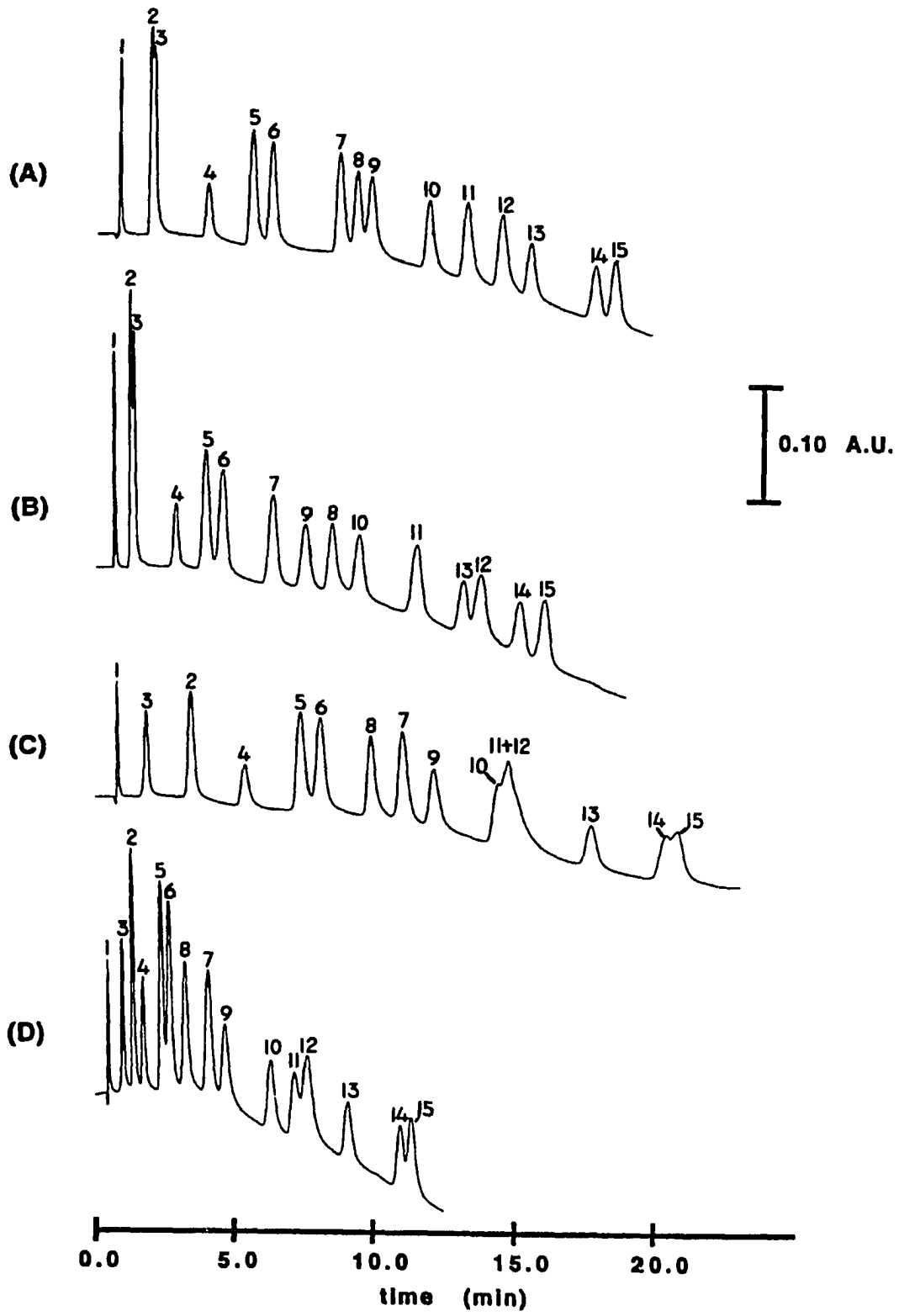


Figure 3. Separation of the fifteen component mixture of phenols obtained by application of a voltage step from +0.50 V to -1.00 V immediately after injection. The mobile phase consisted of 50% aqueous 0.10 M LiClO<sub>4</sub> + 0.1% v/v TFA, pH 2.0 and 50% 0.10 M LiClO<sub>4</sub> in acetonitrile. The flow rate was 0.90 mL/min.

separation to be obtained, as shown in Figure 3.

An important issue that needs to be addressed is an assessment of the ability of the EMLC technique to provide separations that are comparable to or improved over those obtained using conventional solvent gradient elution techniques. To address this issue, we investigated the separation of the mixture on the EMLC column at open circuit using solvent gradient elution. Figure 4a shows the optimum separation obtained using an aqueous/ acetonitrile mobile phase combination. This separation was obtained by application of a linear

**Figure 4.** Separations of the fifteen component mixture of phenols obtained at (a) open circuit, (b) -1.00 V, and (c) +0.50 V by application of a linear solvent ramp to the column from an initial composition of 70% aqueous 0.10 M LiClO<sub>4</sub> +0.1% v/v TFA, pH 2.0 and 30% 0.10 M LiClO<sub>4</sub> in acetonitrile to a final composition of 100% 0.10 M LiClO<sub>4</sub> in acetonitrile. The solvent ramp was applied 4 min after injection and spanned a period of 25 min. The separation in (d) was obtained by the simultaneous application of a step in  $E_{app}$  from +0.50 V to -1.00 V immediately after injection and a linear solvent ramp from 50% aqueous 0.10 M LiClO<sub>4</sub> +0.1% v/v TFA, pH 2.0 and 50% 0.10 M LiClO<sub>4</sub> in acetonitrile to 100% 0.10 M LiClO<sub>4</sub> in acetonitrile to the column over a period of 25 min.



solvent ramp to the column from 70% aqueous 0.10 M LiClO<sub>4</sub> + 0.1% v/v TFA, pH 2.0 and 30% 0.10 M LiClO<sub>4</sub> in acetonitrile to 100% 0.10 M LiClO<sub>4</sub> in acetonitrile over a period of 25 min. The solvent ramp was applied to the column 4 min after sample injection. As expected, the resolution of the mixture obtained using this procedure is improved significantly as compared to that obtained under isocratic conditions (Figure 1a). This improvement is reflected in the increased resolution of analytes 7-9 as well as of analytes 12 and 13. However, analytes 2 and 3 remain poorly resolved, and analytes 7-9 are not baseline resolved. Comparison of this separation to that in Figure 3 shows that the elution band widths for analytes 10-15 are also decreased by at least a factor of 3 when compared to those obtained with the voltage step. Nevertheless, use of the highly aqueous mobile phase for the initial starting point of the solvent ramp results in broadening of the elution bands for the first nine phenols, as a result of an increased solvophobic interaction [44,45]. Overall, the quality of the separation in Figure 4a in terms of the resolution between the phenols, their band widths, and the total analysis time (both separations have run times of ~19 min) is similar to that obtained with the voltage step.

The experiments discussed above suggest the possibility of combining changes in  $E_{app}$  with changes in mobile phase composition to improve further the separation. In such an experiment, changes in  $E_{app}$  could be used to fine-tune the resolution between the phenols whereas changes in mobile phase composition could be used to sharpen the elution bands and decrease the total analysis time. Figures 4b and 4c show examples which illustrate the use of this strategy. Figure 4b shows a separation obtained using the same mobile phase gradient as

that used in Figure 4a, except that  $E_{app}$  was held constant at -1.00 V throughout the separation. As expected from the constant voltage separation obtained at -1.00 V under isocratic conditions (Figure 1c), the resolution of analytes 2 and 3 as well as analytes 7-9 is improved. Under these conditions, analytes 7-9 are fully baseline resolved, in contrast to the partial resolution obtained at open circuit in Figure 4a. Additionally, the total analysis time is decreased from 19 min to 17 min when compared to that obtained in Figure 4a. Clearly, the overall quality of this separation is improved over that obtained using solvent gradient elution alone.

Figure 4c shows a separation of the mixture obtained through combination of solvent gradient elution with a constant  $E_{app}$  of +0.50 V. Again as expected from the separation obtained at +0.50 V under isocratic conditions (Figure 1b), the resolution of the first nine phenols is dramatically improved when compared to that obtained at open circuit or at -1.00 V. This improvement in resolution is clearly seen in the complete baseline resolution of analytes 2 and 3 as well as analytes 7-9. However, analytes 10-12 and analytes 14 and 15 are poorly resolved under these conditions. The total analysis time is also increased from 19 min at open circuit to 21 min at +0.50 V.

Based on these results, an ideal separation scheme would appear to be one in which a step in  $E_{app}$  is made from +0.50 V to -1.00 V during the solvent ramp. This strategy would allow for a combination of the improved resolution of analytes 2 and 3 at +0.50 V with the improved resolution of analytes 10-12 and 14,15 at -1.00 V. Unfortunately, all our attempts at implementing this strategy yielded separations which were more poorly resolved than that in

Figure 4b. This poor resolution occurred primarily between analytes 7-9, since analytes 7 and 9 both elute after analyte 8 at +0.50 V and before analyte 8 at -1.00 V. The relatively long retention of these analytes on the column at +0.50 V with the solvent ramp (~12 min) causes their retention to be affected significantly by the voltage step, resulting in their overlap with the elution band of analyte 8. Such an effect was not observed in the voltage step performed under isocratic conditions (Figure 3) since analytes 7 and 9 elute from the column in less than 5 min and are therefore less affected by the voltage step.

In light of this finding, we attempted to improve the separation by another route which involved application of the solvent ramp from the original 50% aqueous/50% acetonitrile mobile phase composition to 100 % 0.10 M LiClO<sub>4</sub> in acetonitrile in combination with a voltage step from +0.50 V to -1.00 V. Figure 4d shows the result. As expected, the half-widths of the elution bands for at least the first nine phenols are decreased significantly under these conditions when compared to the separations shown in Figures 4a-c due to decreased solvophobic interactions in the more highly organic mobile phase. The overall resolution is improved when compared to that in Figure 4c, but decreased when compared to that in Figure 4b. However, the total analysis time is decreased from 19 min at open circuit to ~12.5 min with the voltage step. Together, these discussions illustrate the unique ability of EMLC for fine-tuning the separations as well as the versatility and flexibility that can be added to conventional liquid chromatographic elution methods through the electrochemical alteration in the composition of the stationary phase.

### Separation of Phenolates.

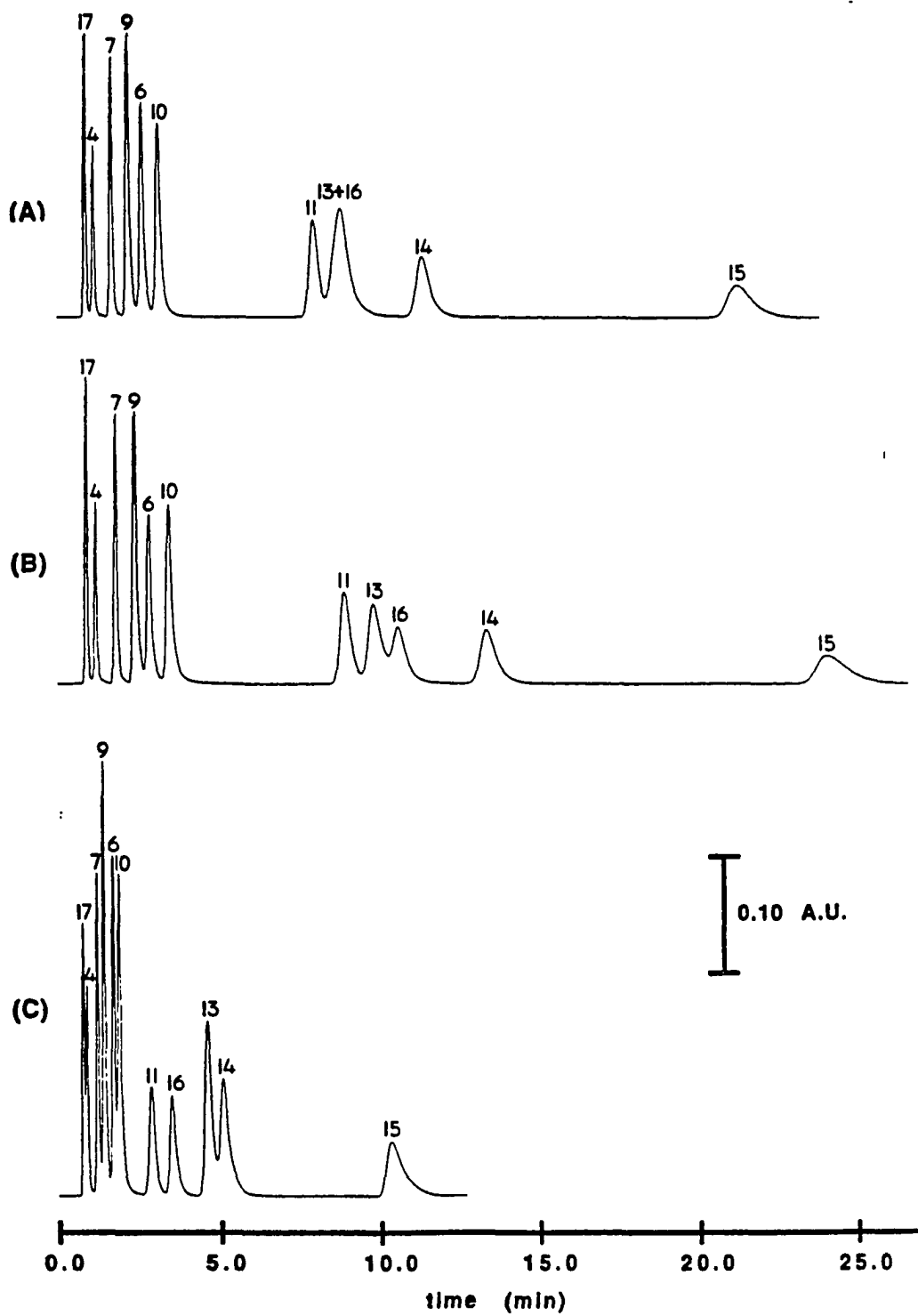
As a means for a more direct comparison of the ability of EMLC to modify the separations of uncharged versus charged species, we investigated the separation of several phenolic compounds at pH 12.2. At this pH, all of the phenols used in these studies existed in their fully deprotonated, i.e., anionic, forms [46]. Deprotonation of each phenol was confirmed through examination of their UV spectrum and by comparison of this spectrum to that for the analogous protonated phenolate. Differences in the sensitivity of the EMLC technique for these two species should be reflected as differences in their relative slopes obtained from the  $\log k'$  versus  $E_{app}$  plot.

Figures 5a-c show separations of eleven phenolates obtained at the EMLC column at open circuit (a), 0.00 V (b), and -1.00 V (c). The mobile phase used for these studies consisted of 97% aqueous 0.10 M LiClO<sub>4</sub> + 0.02 M LiOH, pH 12.2 and 3% 0.10 M LiClO<sub>4</sub> in acetonitrile. Due to the facile electrochemical oxidation of the phenolate anions [47], the positive voltage for these experiments was restricted to 0.00 V. However, comparisons of the relative slopes at  $E_{app} < pzc$  to those for the phenols are still instructive. The relative elution order obtained at open circuit (Figure 5a) is nearly identical to that obtained for the phenols, except that *o*-cresolate elutes after 2-chlorophenolate and 4-chlorophenolate. Although not fully clear, this elution order reversal may be due to a solvophobic effect resulting from differences in the mobile phase used for the two studies.

In contrast to the phenols, the phenolates appear to be much more sensitive to changes in  $E_{app}$ . This increased sensitivity can be readily seen through comparisons of the relative



**Figure 5. Separations of an eleven component mixture of phenolates obtained at (a) open circuit, (b) 0.00 V, and (c) -1.00 V. The mobile phase consisted of 97% 0.10 M LiClO<sub>4</sub> +0.02 M LiOH, pH 12.2 and 3% 0.10 M LiClO<sub>4</sub> in acetonitrile. The flow rate was 0.90 mL/min.**



slopes for the two species found from construction of their  $\log k'$  versus  $E_{app}$  plots.

Figure 6 shows such a plot for the phenolates, and Table III lists the slopes for each analyte.

For the slope calculation, the data points for 3-nitrophenolate at -0.70 V, -0.90 V, and -1.00 V are intentionally left out since we suspect its electrochemical reduction is occurring at

Table III. Calculated slopes negative of the pzc for the deprotonated phenols<sup>a</sup>.

Analyte No.	slope ( $\log k'/\text{volt}$ ) <sup>b</sup>
4	0.37
6	0.31
7	0.31
9	0.35
10	0.34
11	0.31 <sup>c</sup>
13	0.36
14	0.45
15	0.37
16	0.54
17	0.31

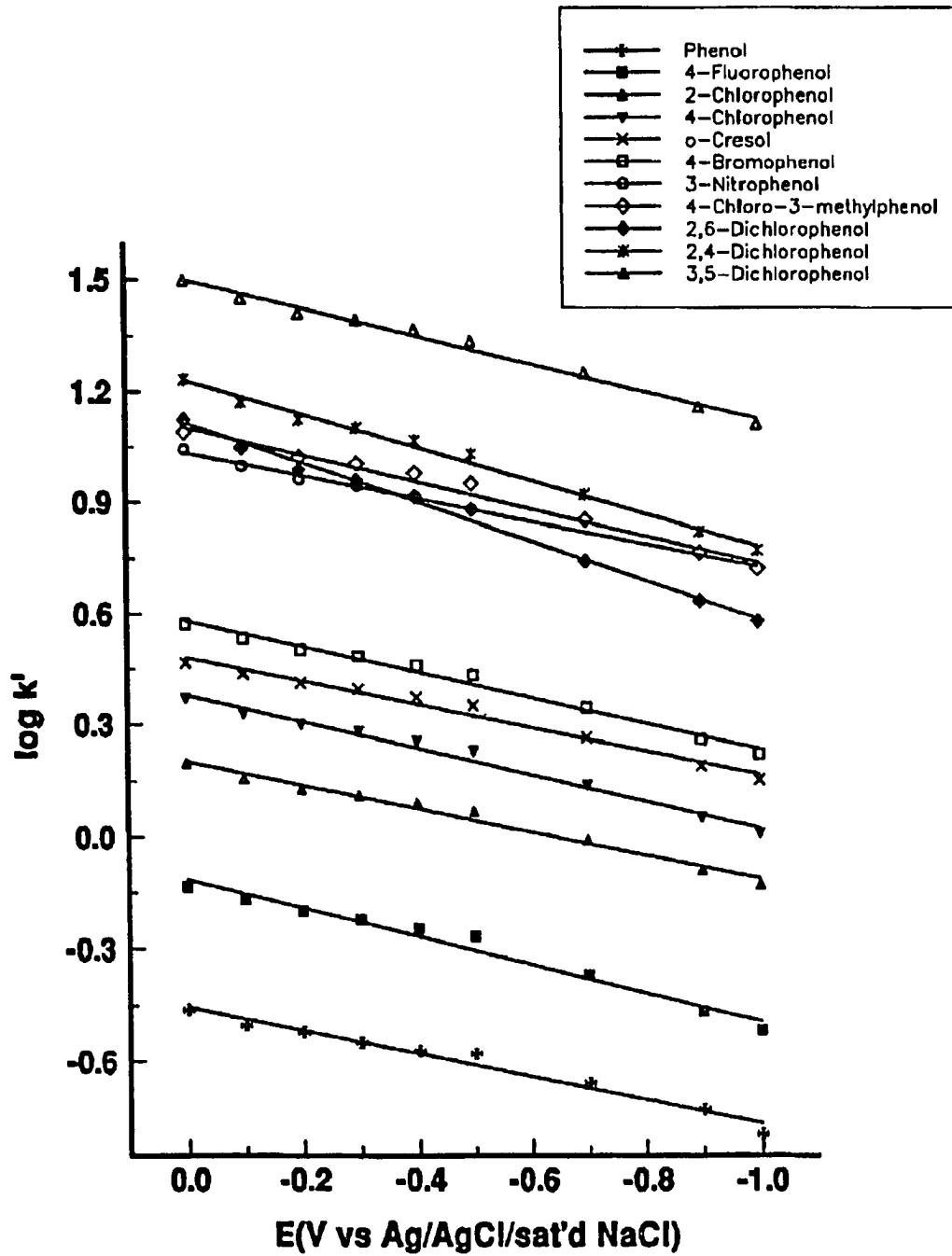
<sup>a</sup>The mobile phase pH was ~12.2.

<sup>b</sup>Includes  $k'$  values between 0.00 V and -1.00 V.

<sup>c</sup>Includes  $k'$  values between 0.00 V and -0.50 V.

these voltages. Such a conclusion is supported by the differences in the UV spectra obtained for this compound at 0.00 V and -0.70 V. Careful examination of the spectra for the other phenolates at each  $E_{app}$  revealed no such changes, however. Table III shows that the slopes for the phenolates are about ten times larger than those for the phenols. This large increase in slope is likely a result of the increased electrostatic repulsion of the phenols from the

**Figure 6. Plot of the logarithm of  $k'$  versus  $E_{app}$  for the phenolates. The mobile phase consisted of 97% 0.10 M LiClO<sub>4</sub> +0.02 M LiOH, pH 12.2 and 3% 0.10 M LiClO<sub>4</sub> in acetonitrile. The flow rate was 0.90 mL/min.**



negatively charged carbon surface as a result of their deprotonation. As postulated for the anionic ASFs, this electrostatic repulsion likely causes the phenolates to interact with the GC surface in a perpendicular orientation to minimize this repulsion. This increased electrostatic repulsion and orientational change helps to overcome the attraction of the analytes to the carbon surface via dispersion interactions. As discussed previously, this electrostatic term appears to be an important interaction that affects the sensitivity of analytes to changes in  $E_{app}$  [18]. For the phenolates, the electrostatic repulsion is further enhanced through direct  $\pi$ -conjugation of the phenolate oxygen with the aromatic ring, which allows for the negative charge to be distributed throughout the entire aromatic ring via resonance.

The relative order of the slopes seen in Table III is also in qualitative agreement with the order observed in Table II for the phenols. In general, the highly chlorinated phenolates (analytes 14,15,16) show larger slopes than the other phenolates due to a stronger dipole-dipole repulsion. However, a few of the phenolates show unexpectedly large slopes (i.e., analyte 4) or unexpectedly small slopes (analytes 7 and 9). These differences cannot be readily explained using the data in Table II. Despite these differences, the data presented in this section clearly illustrate the enhanced sensitivity of the EMLC technique for charged compounds, and provide further support for our mechanism of the electrochemical modulation of analyte retention.

## CONCLUSIONS

This paper has demonstrated the utility of EMLC for manipulating and fine-tuning of the separations of phenolic compounds. Through tests of the retention of the phenols at several  $E_{app}$ 's, the range over which their  $k'$  values could be altered to manipulate their separation was identified. These tests also provided further support for our electrochemical retention mechanism through analysis of the relative slopes obtained in plots of  $\log k'$  versus  $E_{app}$  for each phenol. The ability of each phenol to interact with the surface through donor-acceptor and solvophobic interactions were found to be important factors which determine the sensitivity of each phenol to changes in  $E_{app}$ . In general, the phenols displaying the strongest electron-donating properties had the largest slopes.

Separations obtained under conditions in which voltage changes and mobile phase changes were applied to the column both separately and simultaneously during elution demonstrated the unique ability of EMLC to fine-tune and improve the separation over that obtained using conventional elution techniques. Finally, tests of the separation of the phenols as phenolate anions illustrated clearly the increased sensitivity of the EMLC technique for charged species over neutral species. Future studies will be directed toward further elucidation of the electrochemically-controlled retention mechanism and also toward identification of additional applications for the fine-tuning ability of EMLC.

### ACKNOWLEDGMENTS

R.S.D. gratefully acknowledges the support of an ACS Analytical Division Summer Fellowship sponsored by Dow Chemical USA. Several fruitful discussions concerning the molecular orbital calculations with C.J. Zhong are greatly appreciated. This work was supported by the National Science Foundation (Grant CHE-9003308) and by Iowa State Universities' Microanalytical Instrumentation Center. The Ames Laboratory is operated for the U.S. Department of Energy under contract No. W-7405-Eng-82.

### REFERENCES

1. D.R. Buhler, E.M. Rasmusson, and H.S. Nakaue, *Environ. Sci. Technol.*, 7 (1973) 929.
2. H. Savolainen and K. Pekari, *Res. Comm. Chem. Path. Pharmacol.*, 23 (1979) 97.
3. H.W. Klemer, L. Wong, M.M. Sato, E.L. Reichert, R.J. Korsak, and M.N. Rashad, *Environ. Cotam. Toxicol.*, 9 (1980) 715.
4. K. Uglund, E. Lundanes, T. Greibrokk, and A. Bjorseth, *J. Chromatogr.*, 213 (1981) 83.
5. E.M. Lores, T.R. Edgerton, and R.F. Moseman, *J. Chrom. Sci.*, 19 (1981) 466.
6. F.P. Bigley and R.L. Grob, *J. Chromatogr.*, 350 (1985) 407.
7. A. Bjorseth, G.E. Carlberg, and M. Moller, *Sci. Total. Environ.*, 11 (1979) 197.
8. J.M. Schulz and K. Herrmann, *J. Chromatogr.*, 195 (1980) 95.
9. R.D. Hartley, *J. Chromatogr.*, 54 (1971) 335.
10. H.C. Smit, T.T. Lub, and W.J. Bloom, *Anal. Chim. Acta*, 122 (1980) 267.
11. E. Buirtscher, H. Binder, R. Concin, and O. Bobleter, *J. Chromatogr.*, 252 (1982) 167.



12. F. Dondi, A. Betti, and C. Bigli, *J. Chromatogr.* 257 (1983) 69.
13. N.G. Buckman, J.O. Hill, R.J. Magee, and M.J. McCormick, *J. Chromatogr.*, 284 (1984) 441.
14. C.P. Ong, H.K. Lee, S.F.Y. Li, *J. Chromatogr.*, 464 (1989) 405.
15. R.S. Deinhammer, K. Shimazu, and M.D. Porter, *Anal. Chem.*, 63 (1991) 1889.
16. R.S. Deinhammer, E. Ting, and M.D. Porter, *J. Electroanal. Chem.*, 362 (1993) 295.
17. R.S. Deinhammer, K. Shimazu, and M.D. Porter, to be submitted to the Journal of Electroanalytical Chemistry.
18. R.S. Deinhammer, E. Ting, and M.D. Porter, in preparation for submission to the Journal of Electroanalytical Chemistry.
19. R.S. Deinhammer, E. Ting, and M.D. Porter, in preparation for submission to the Journal of Chromatography.
20. R.F. Antrim, R.A. Scherrer, and A.M. Yacynych, *Anal. Chim. Acta*, 164 (1984) 283.
21. R.F. Antrim and A.M. Yacynych, *Anal. Lett.*, 21 (1988) 1085.
22. A.R. Ghatak-Roy and C.R. Martin, *Anal. Chem.*, 58 (1986) 1574.
23. H. Ge and G.G. Wallace, *J. Liq. Chromatogr.*, 13 (1990) 3245.
24. H. Ge, P.R. Teasdale, and G.G. Wallace, *J. Chromatogr.*, 544 (1991) 305.
25. T. Nagaoka, M. Fujimoto, Y. Uchida, and K. Ogura, *J. Electroanal. Chem.*, 336 (1992) 45.
26. T. Nagaoka, M. Fujimoto, H. Nakao, K. Kakuno, and J. Yano, *J. Electroanal. Chem.*, 350 (1993) 357.

27. T. Nagaoka, M. Fujimoto, H. Nakao, K. Kakuno, and J. Yano, *J. Electroanal. Chem.*, 364 (1994) 179.
28. J.A. Pople, *Trans. Faraday Soc.*, 49 (1953), 1375.
29. J. Griffiths, *Chem. Brit.*, (1986) 997.
30. J.H. Knox, K.K. Unger, and H. Mueller, *J. Liq. Chromatogr.*, 6 (1983) 1.
31. B.J. Bassler and R.A. Hartwick, *J. Chrom. Sci.*, 27 (1989) 162.
32. N. Tanaka, T. Tanigawa, K. Kimata, K. Hosoya, and T. Araki, *J. Chromatogr.*, 549 (1991) 29.
33. J. Kriz, E. Adamcova, J.H. Knox, and J. Hora, *J. Chromatogr. A*, 663 (1994) 151.
34. T.M. Engel, S.V. Olesik, M.R. Callstrom, and M. Diener, *Anal. Chem.*, 65 (1993) 3691.
35. W.J. Moore, *Physical Chemistry*, 4th ed., Prentice Hall, Engelwood Cliffs, NJ, 1972.
36. C. Horvath, W. Melander, and I. Molnar, *J. Chromatogr.*, 125 (1976) 29.
37. C. Hansch and A. Leo, *Substituent Constants for Correlation Analysis in Chemistry and Biology*, Wiley, New York, 1979.
38. J. Kriz, L. Vodicka, J. Puncocharova, and M. Kuras, *J. Chromatogr.*, 219 (1981) 53.
39. J. Kriz, J. Puncocharova, L. Vodicka, and J. Vareka, *J. Chromatogr.*, 437 (1988) 178.
40. D. Rolle and J.W. Schultze, *Electrochim. Acta*, 31 (1986) 991.
41. W. Holstein and H. Hemetsberger, *Chromatographia*, 15 (1986) 186.
42. B.B. Damaskin, S.L. Dyatkina, and V.M. Gerovich, *Elektrokhimiya*, 21 (1985) 716.
43. R.I. Kaganovich, V.M. Gerovich, and O.Y. Gusakova, *Elektrokhimiya*, 3 (1967) 946.

44. C.F. Poole and S.A. Schuette, *Contemporary Practice of Chromatography*, Elsevier, Amsterdam, 1984.
45. H. Itoh, T. Kinoshita, and N. Nimura, *J. Liq. Chromatogr.*, 10 (1987) 2721.
46. R.M. Smith and A.E. Martell, *Critical Stability Constants*, vols.1-6, Plenum Press, New York, 1975.
47. J. Stradins and B. Hasanli, *J. Electroanal. Chem.*, 335 (1993) 57.

## CHAPTER 7. ELECTROCHEMICAL OXIDATION OF AMINE-CONTAINING COMPOUNDS: A ROUTE TO THE SURFACE MODIFICATION OF GLASSY CARBON ELECTRODES

A paper published in *Langmuir*<sup>1</sup>

Randall S. Deinhammer, Mankit Ho, James T. Andereg, and Marc D. Porter<sup>2</sup>

### ABSTRACT

A method for the modification of glassy carbon electrodes (GCEs) with amine-containing compounds for electrocatalytic and biosensor purposes is investigated. The method utilizes the electrooxidation of amines to their analogous cation radicals to form a chemically stable covalent linkage between the nitrogen atom of the amine and edge plane sites at the GCE surface. Using x-ray photoelectron spectroscopy (XPS) for coverage assessment, the capability of this route is demonstrated by the immobilization of a simple primary amine at the GCE surface. An investigation of the influence of substituents on the nitrogen atom (e.g., primary, secondary, tertiary amines) revealed that the surface coverage of primary amines was ~3 times higher than that of secondary amines, whereas tertiary amines were not immobilized at a detectable level. This behavior is attributed to a strong steric effect whereby bulky substituents on the nitrogen atom hinder accessibility of the reactive amine cation radical to surface binding sites. Amine salts and amides also showed no detectable

---

<sup>1</sup>Reprinted with permission from *Langmuir* 1994, 10, 1306-13. Copyright © 1994 the American Chemical Society.

<sup>2</sup>Author to whom correspondence should be addressed.

coverage by XPS. The utility of the method for creation of a GCE with electrocatalytic activity is demonstrated by the immobilization of dopamine (DA) at the GCE surface. The DA-modified GCE is used to facilitate oxidation of  $\beta$ -NADH via a surface EC mechanism. These examples illustrate the facility of this route for simplifying and shortening dramatically the processing required for immobilization using other synthetic methods. A mechanism for the immobilization process is also briefly discussed.

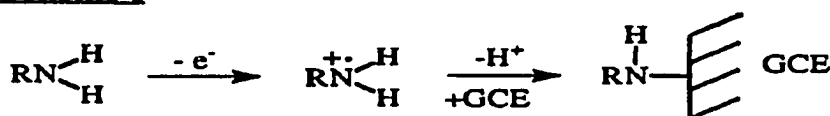
## INTRODUCTION

Over the past several years, there has been a continued interest in the use of carbon-based materials for electrochemical purposes [1-3]. The impetus for this interest is the potential of such materials as replacements for precious metal electrodes. Often, however, these materials require some form of surface pretreatment [4-9] or bulk material processing (e.g., doping of carbon with noble metals [10]) to overcome sluggish electron-transfer kinetics or to enhance selectivity for electroanalysis. Such processing in the former case can involve a lengthy sequence of steps, including oxidative [4-6] and coupling agent [4,7-9] pretreatments that are followed by the immobilization of a target moiety through linkage with the coupling agent. Therefore, in view of the importance of these types of materials to electrosynthesis [7,8], electrocatalysis [11-14], and biosensor [15-19] technologies, it is of fundamental importance to develop new, less complex routes for the modification of carbon surfaces.

Recently, a novel route has been devised for modifying carbon fibers as components in composite materials [20]. This route is based on the electrooxidation of amine-containing

compounds, and is generalized in Scheme I. As proposed, the process proceeds initially via the one-electron oxidation of an amine functionality to its corresponding cation radical, which subsequently forms a carbon-nitrogen linkage at the carbon surface. In the composite materials application,  $\omega$ -diamines are used to enhance the mechanical toughness of the composite whereby one of the amine groups of the diamine is linked to the surface of the carbon fiber and the other to reactive groups in an epoxy resin.

**Scheme I**



Based on our interests in the surface modification of carbon-based materials as stationary phases for new forms of chemical separations [21,22], we have explored the extension of Scheme I as a facile means for altering the interfacial architecture of glassy carbon electrodes (GCEs). In the following sections, we describe the results of an investigation of the range and scope of Scheme I as a route for the creation of chemically modified GCEs. Our investigation included an assessment of: (1) the extent of the immobilization of different types of amine-containing compounds (i.e., primary, secondary, and tertiary alkylamines); (2) the ability to create an electrocatalytic GCE via the immobilization of dopamine; and (3) the ability to create a biotinylated GCE surface capable of binding the protein avidin. The focus of the latter effort, which was demonstration of the utility of Scheme I for the fabrication of a platform for anchoring enzymes at carbonaceous



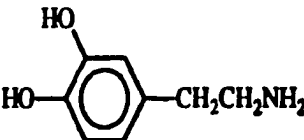
materials for biosensor purposes [17-19], is described elsewhere [23]. In each of our assessments, particular attention was given to defining the experimental conditions that resulted in a maximal modifier coverage. X-ray photoelectron spectroscopy (XPS) was used as the primary tool for coverage assessment. The coverage of the dopamine-modified GCE was also determined electrochemically. Finally, an extension of the immobilization mechanism is proposed that is based, in part, on our results from attempts to modify the basal plane of highly oriented pyrolytic graphite (HOPG) electrodes using Scheme I.

## EXPERIMENTAL

### Reagents and Chemicals.

N-acetylenediamine, N-propylacetamide, butylamine, N-methylbutylamine, N-ethylbutylamine, N,N-dimethylbutylamine, and 3-hydroxytyramine hydrochloride (dopamine hydrochloride) were from Aldrich. Triethylamine was from Eastman. Table I gives the chemical structures for each of these compounds. Catechol, disodium hydrogen phosphate, sodium chloride, and perchloric acid (70%) were from Fisher.  $\beta$ -nicotinamide adenine dinucleotide ( $\beta$ -NADH) was from Sigma, and was stored at 0°C. Sodium dihydrogen phosphate was from Mallinckrodt. Lithium perchlorate (anhydrous) was from G. Frederick Smith. Alpha-alumina (1.0  $\mu\text{m}$ ) was from Buehler. Absolute ethanol (punctilious grade) was from Quantum Chemical Co. The liquid amine-containing compounds were purified by distillation before use. All other chemicals were used as received. House distilled water was

Table I. Chemical structures, anodic peak current voltages ( $E_p$ ), and N/C values for various nitrogen-containing compounds.

Chemical Name	Chemical Structure	Conditions	$E_p$ (V)	100 (N/C)
N-acetylenediamine		1 voltage cycle 2 voltage cycles	+1.30 V	6.4 6.5
N-propylacetamide		1 voltage cycle	—	trace
Butylamine	$\text{CH}_3(\text{CH}_2)_3\text{NH}_2$	1 voltage cycle 1 voltage cycle (HOPG)	+1.25 V +1.35 V	3.7 trace
N-methylbutylamine	$\text{CH}_3(\text{CH}_2)_3\text{NHCH}_3$	1 voltage cycle 2 voltage cycles	+1.03 V	1.4 1.4
N-ethylbutylamine	$\text{CH}_3(\text{CH}_2)_3\text{NHCH}_2\text{CH}_3$	1 voltage cycle	+1.02 V	0.9
N,N-dimethylbutylamine	$\text{CH}_3(\text{CH}_2)_3\text{N}(\text{CH}_3)_2$	1 voltage cycle 2 voltage cycles	+0.88 V, +1.02 V	trace trace
Triethylamine	$(\text{CH}_3\text{CH}_2)_3\text{N}$	1 voltage cycle	+0.86 V	trace
Dopamine		1 voltage cycle injection method	+1.25 V	1.3 3.5



further processed using a Millipore Milli-Q water purification system, and was used in all solution and electrode preparations. The phosphate buffer solution (pH ~7) consisted of 0.1 M NaCl, 10 mM Na<sub>2</sub>HPO<sub>4</sub>, and 10 mM NaH<sub>2</sub>PO<sub>4</sub>. The amino group of dopamine hydrochloride was deprotonated by addition of triethylamine.

#### **Carbon Substrate Preparation.**

The GCEs (Tokai Carbon, grade GC-20) were prepared by polishing first with silicon carbide powder (600 grit) followed by 1.0 μm alumina on a polishing pad (Buehler). The GCEs were sonicated in water for 15 min after each polishing step. After the initial polishing, the GCEs were resurfaced using 1.0 μm alumina only. All GCEs were sonicated for 15 min in water, rinsed with water and ethanol, and dried with a stream of high purity nitrogen immediately before use. After electrochemical treatment in the amine-containing electrolytic solutions, the GCEs were rinsed with ethanol and water and sonicated for 15 min in pH 7 phosphate buffer. This process was used to remove any physisorbed, unreacted materials from the electrode surface. Samples were then characterized using XPS or electrochemical techniques. The HOPG electrodes (Union Carbide, grade ZYB) were prepared by removal of a thin top-layer of the material with adhesive tape to expose a fresh surface.

#### **Electrochemistry.**

Electrochemical experiments were performed using a CV-27 potentiostat (Bioanalytical Systems) and a Houston Instruments Omnigraphic 2000 XY recorder. Voltage steps were generated using a PAR 175 Universal Programmer that was connected to the

potentiostat. A conventional three-electrode cell was used with the geometric area of the electrode defined by the circular opening in an inert elastomer gasket ( $0.40 \text{ cm}^2$ ). A Pt coil auxiliary electrode and a Ag/AgCl/sat'd  $\text{LiClO}_4$  reference electrode ( $-34 \text{ mV vs SCE}$ ) were used; all voltages are given with respect to this reference. All electrolysis solutions were  $0.1 \text{ M LiClO}_4$  in absolute ethanol.

### **X-Ray Photoelectron Spectroscopy.**

The XPS data were acquired with a Physical Electronics Industries Model 5500 multi-technique surface analysis system equipped with a hemispherical analyzer, a monochromator, and a multichannel detector. Monochromatic Al  $K\alpha$ -radiation ( $1486.6 \text{ eV}$ ) at  $300 \text{ W}$  was used for excitation. The photoelectrons were collected at  $10^\circ$  from the surface parallel to maximize surface detection sensitivity [24]. Binding energies were referenced to the C(1s) emission band at  $284.3 \text{ eV}$ . Acquisition times for the survey spectra were typically  $2 \text{ min}$ , and those for the high resolution spectra were between  $2\text{-}7 \text{ min}$  for the N(1s) region. The base pressure of the ion-pumped UHV chamber was less than  $1 \times 10^{-9} \text{ torr}$  during analysis. The elemental nitrogen-to-carbon ratio, (N/C), was used as the major parameter for assessing the extent of modifier coverage. Values for N/C were calculated by dividing the total number of counts under the N(1s) band by that under the C(1s) band and multiplying the result by 100, after accounting for differences in sensitivity factors [25]. The N/C values are reported as averages of  $2\text{-}6$  samples, and varied by  $\sim 10\text{-}15 \%$  between similarly prepared samples.

## RESULTS AND DISCUSSION

### Feasibility of Immobilizing Amine-Containing Molecules at GCEs via Scheme I.

To assess the range and scope of Scheme I as a route for the modification of carbon surfaces, we began with an examination of the immobilization of several simple, structurally-related alkylamines at the GCE surface. These studies, presented in this and the next section, provide a general picture of the utility of this immobilization method, the stability of the modified surface, and insights into the types of nitrogen-containing functional groups that can be used for the modification.

Figure 1 shows a typical cyclic voltammetric (CV) curve obtained at a GCE in an ethanolic solution containing 1 mM N-acetylenediamine and 0.1 M LiClO<sub>4</sub> (solid line). The voltage scan was initiated at 0.00 V and reversed at an upper limit of +1.40 V. The scan rate was 10 mV/s. A broad, chemically irreversible oxidation wave is apparent, with a peak-current voltage ( $E_p$ ) of +1.30 V. A comparison with a scan at a GCE in only supporting electrolyte (dashed curve) suggests the onset of an oxidative process near +0.30 V. We attribute this wave to the one-electron oxidation of the amine group to its corresponding cation radical. This interpretation is based both on the earlier literature for the oxidation of amines at carbon-based electrodes [20,26,27] and on the absence of the oxidative wave in scans at a GCE in an electrolytic solution containing N-propylacetamide. We have also found, in agreement with the literature, that basic aqueous solutions [26] ( $\text{pH} > \text{pK}_a$  of amine) as well as other nonaqueous solvent supporting electrolyte combinations (e.g., acetonitrile and

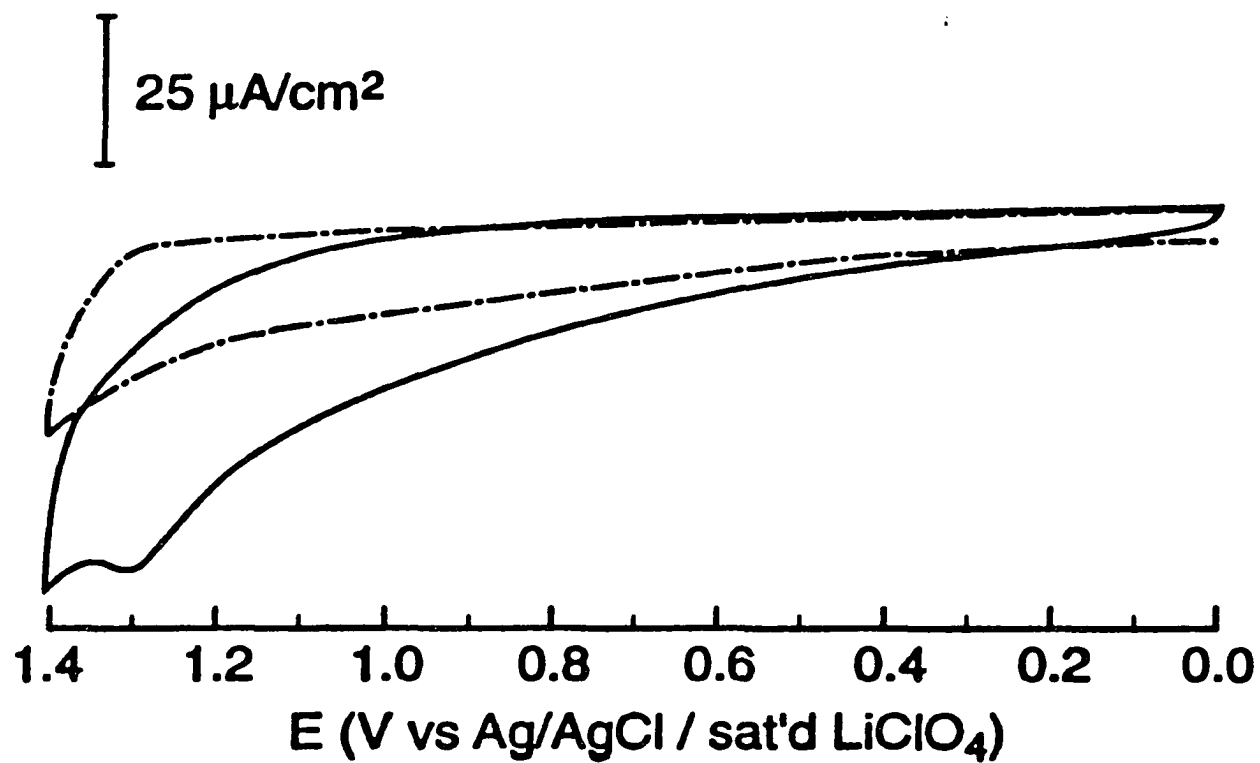


Figure 1. Cyclic voltammogram obtained at a freshly polished GCE in an ethanolic solution containing 1 mM N-acetythylenediamine (solid curve). The dashed curve was obtained in supporting electrolyte only. The sweep rate was 10 mV/s.

tetrabutylammonium salt) support this process [20]. We, however, utilized ethanol because of the higher solubility of the amine-containing biomolecules dopamine and biotin in this solvent.

To verify that the electrooxidation of the amine functionality is requisite for immobilization, XPS was used to follow the changes in the relative nitrogen content at the GCE surface as a function of the anodic voltage limit in a single sweep CV experiment. Figure 2 presents the findings of the XPS characterization in the N(1s) region using the above N-acetythylenediamine solution. N-acetythylenediamine instead of a simpler primary amine was used as a probe molecule for these experiments because the two nitrogens in its molecular structure provided increased detection sensitivity. Figure 2a is the result for a GCE immersed in solution with the applied voltage ( $E_{app}$ ) held at 0.00 V for 5 min. Figures 2b-d are data for GCEs cycled between 0.00 V and different upper voltage limits: +0.70 V (Figure 2b), +1.00 V (Figure 2c), and +1.40V (Figure 2d). These voltage limits were chosen to span the range of the anodic wave in Figure 1. Figure 2a therefore represents the result for a GCE treated prior to the onset of amine oxidation, and Figures 2b-d the results for increases in the extent of amine oxidation. Figure 2e shows the XPS spectrum in the N(1s) region for a freshly polished but untreated GCE for comparison. The XPS spectrum for a GCE immersed into solution at open circuit is effectively the same as in Figures 2a and 2e. At best, trace levels of nitrogen are detected at the GCEs in Figures 2a and 2e. In contrast, scanning to an upper limit of +0.70 V (Figure 2b) leads to the detection of a nitrogen-containing species at the GCE surface (N/C=1.6). Upon scanning to the two more positive voltage limits, the nitrogen content at the GCE surface increases further, reaching N/C values of 2.9 at +1.00 V

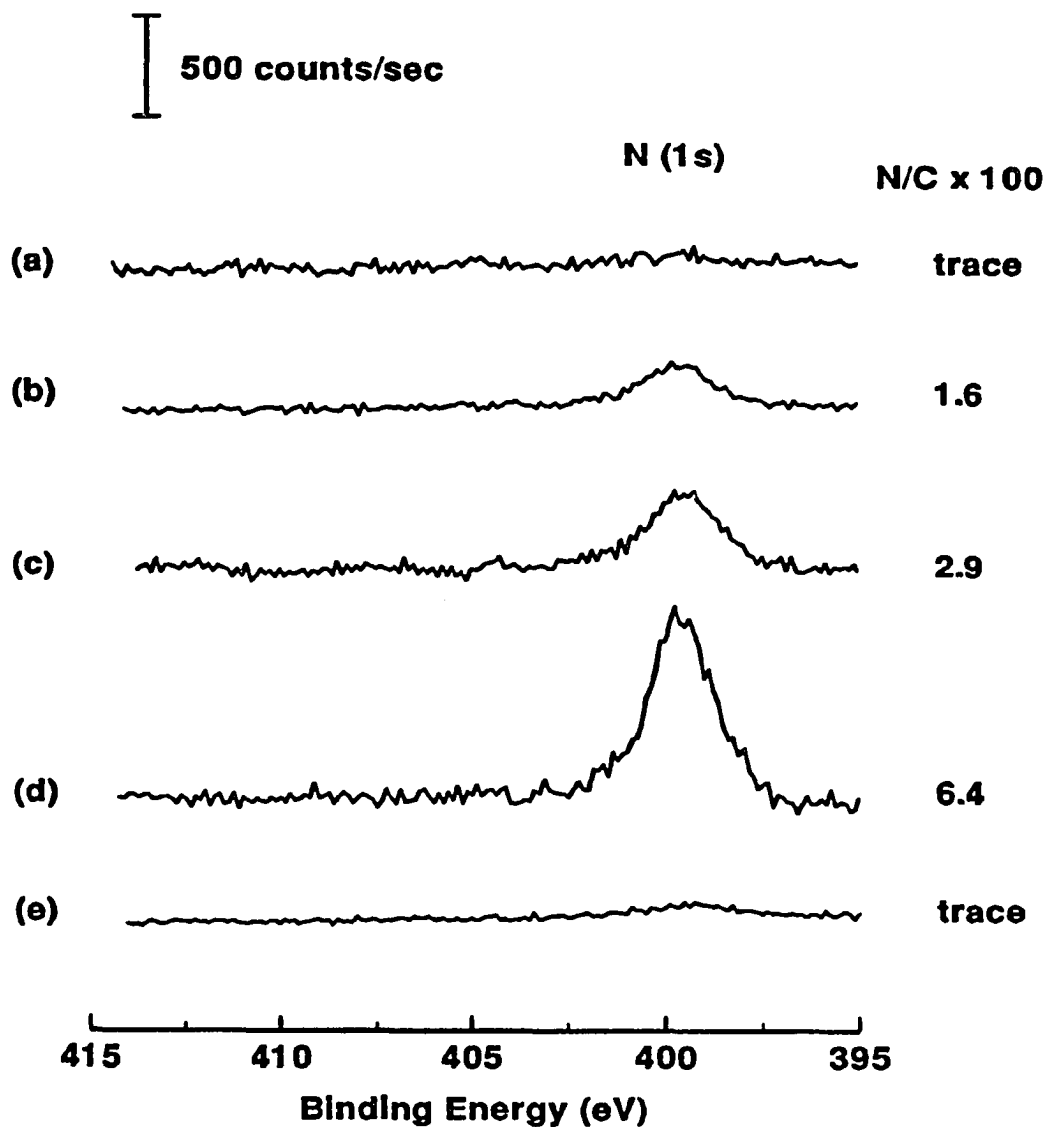


Figure 2. X-ray photoelectron spectra in the N(1s) region for freshly polished GCEs immersed in an ethanolic solution containing 1 mM N-acetylenehydrazine and held at 0.00 V for 5 min (a), or cycled once at 10 mV/s between 0.00 V and (b) +0.70 V, (c) +1.00 V, and (d) +1.40 V. The spectrum in (e) was obtained from an "as polished" GCE.

(Figure 2c) and 6.4 at +1.40 V (Figure 2d). These data show that oxidation of the amine functionality is requisite for immobilization at the GCE surface, as suggested in Scheme I [28].

Repetitive cycling between 0.00 V and +1.40 V or scanning to an  $E_{app}$  more positive than +1.40 V (e.g., +1.60 V) did not significantly increase the N/C value, indicating that the maximal coverage can be obtained with a single voltage cycle between 0.00 V and +1.40 V at this sweep rate. In addition, the N/C value did not significantly increase if 5 mM instead of 1 mM solutions of N-acetylenediamine were used. More detailed studies of the sweep rate and concentration dependence are planned.

Further support for the immobilization scheme derives from the XPS data and from tests of chemical stability. From the XPS data, the position of the peak maximum (399.3 eV) is consistent with the formation of a carbon-nitrogen bond between the amine cation radical and an aromatic moiety of the GC surface. Comparatively, the N(1s) binding energies for aliphatic primary amines are near  $\sim 398.0$  eV [29]. Although this conclusion is complicated by the presence of the amide group of the N-acetylenediamine, the position of the bands for simpler, immobilized amines such as N-butylamine (see next section) are similar.

Tests of the stability of immobilization also support the formation of a covalent linkage. For instance, N-acetylenediamine-coated GCEs that were prepared by scanning to +1.40 V were sonicated for  $\sim 15$  min (in addition to the 15 min sonication as part of the general preparation protocol; see Experimental Section) in a variety of solutions, including water, ethanol, and pH 7 phosphate buffer. In all cases, the XPS spectra in the N(1s) region

were not observably different from that in Figure 2d. Importantly, sonication was found to be very effective in removing physisorbed aromatic amines (see below) from the GCE surface. For example, the surface coverage of strongly physisorbed dopamine decreased by ~95% after a 15 min sonication in the pH 7.0 phosphate buffer.

As an additional test of stability, the butylamine-modified GCE was immersed in 0.1 M H<sub>2</sub>SO<sub>4</sub> for 24 hr. Examination by XPS showed no observable decrease in the surface coverage of this amine after soaking. This result, in addition to demonstrating the excellent stability of the amine-GCE linkage under harsh exposure conditions, supports the formation of a hydrolytically stable nitrogen-carbon bond. Other types of immobilized species such as amides or salts formed with acidic surface oxides would be highly unstable under these acidic conditions. These findings support the formation of an immobilized species that is covalently bonded to the GCE surface, and is consistent with the process detailed in Scheme I.

To test the stability of the amine-GCE linkage under conditions of potential cycling, a butylamine-modified GCE (see next section for preparation) was cycled between +0.20 V and +0.80 V in aqueous 0.1 M HClO<sub>4</sub>. Examination by XPS after 100 cycles indicated a ~10% decrease in the N/C ratio. A dopamine-modified GCE (see "Immobilization of Dopamine..." section for preparation) that was subjected to the same testing exhibited a much larger decrease in the N/C ratio (~23%). We suspect this decrease arises primarily from an increased destabilization of the surface linkage from the redox process.



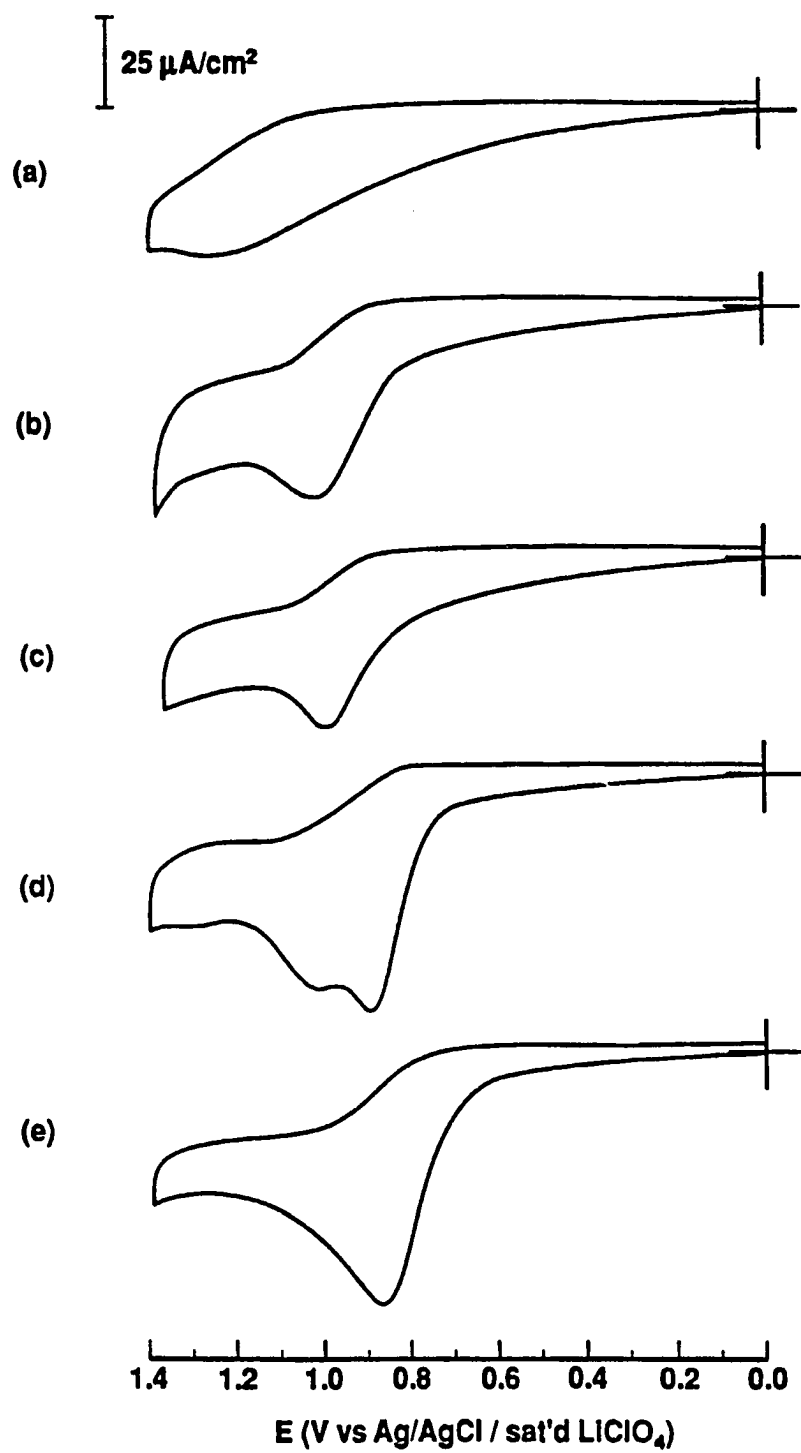
**Immobilization of Various N-Substituted Alkylamines at the GCE Surface.**

To examine the generality of Scheme I, we probed the feasibility of immobilizing primary, secondary, and tertiary amines at the GCE surface. Figures 3a-e show CV curves obtained at a GCE in ethanolic 0.1 M LiClO<sub>4</sub> solutions containing either 1 mM of butylamine (Figure 3a), N-methylbutylamine (Figure 3b), N-ethylbutylamine (Figure 3c), N,N-dimethylbutylamine (Figure 3d), or triethylamine (Figure 3e). Chemically irreversible oxidation waves are apparent for all five of the amine-containing compounds. The negative shift in the E<sub>p</sub> values (c.f. Table I) and sharpening of the oxidation peak observed as alkyl substituents are added to the amine group is consistent with the stabilization of the amine cation radical form by the alkyl groups [26,27]. Therefore, generation of the amine cation radical is most facile for tertiary amines, and least facile for primary amines.

Interestingly, a single oxidative wave was observed in the CV curves in all cases except for N,N-dimethylbutylamine. The curve for the latter species contains two clearly observable anodic waves. We do not at present understand the origin of the multiple wave character for this species. Initially, we had suspected the presence of an electroactive impurity. Both waves, however, persisted even after purifying the compound carefully via distillation. Nevertheless, this disparity in voltammetric behavior does not translate to an observable difference in the results from testing the ability of tertiary amines to bind at the GCE surface (see below).

Figures 4a-d show XPS spectra in the N(1s) region for GCEs cycled once between 0.00 V and +1.40 V in ethanolic 0.1 M LiClO<sub>4</sub> solutions containing 1 mM of either butylamine, N-methylbutylamine, N-ethylbutylamine, or N,N-dimethylbutylamine,

**Figure 3. Cyclic voltammograms obtained at freshly polished GCEs in ethanolic 0.1 M LiClO<sub>4</sub> solutions containing 1 mM of (a) butylamine, (b) N-methylbutylamine, (c) N-ethylbutylamine, (d) N,N-dimethylbutylamine, and (e) triethylamine. The sweep rate was 10 mV/s in each case.**



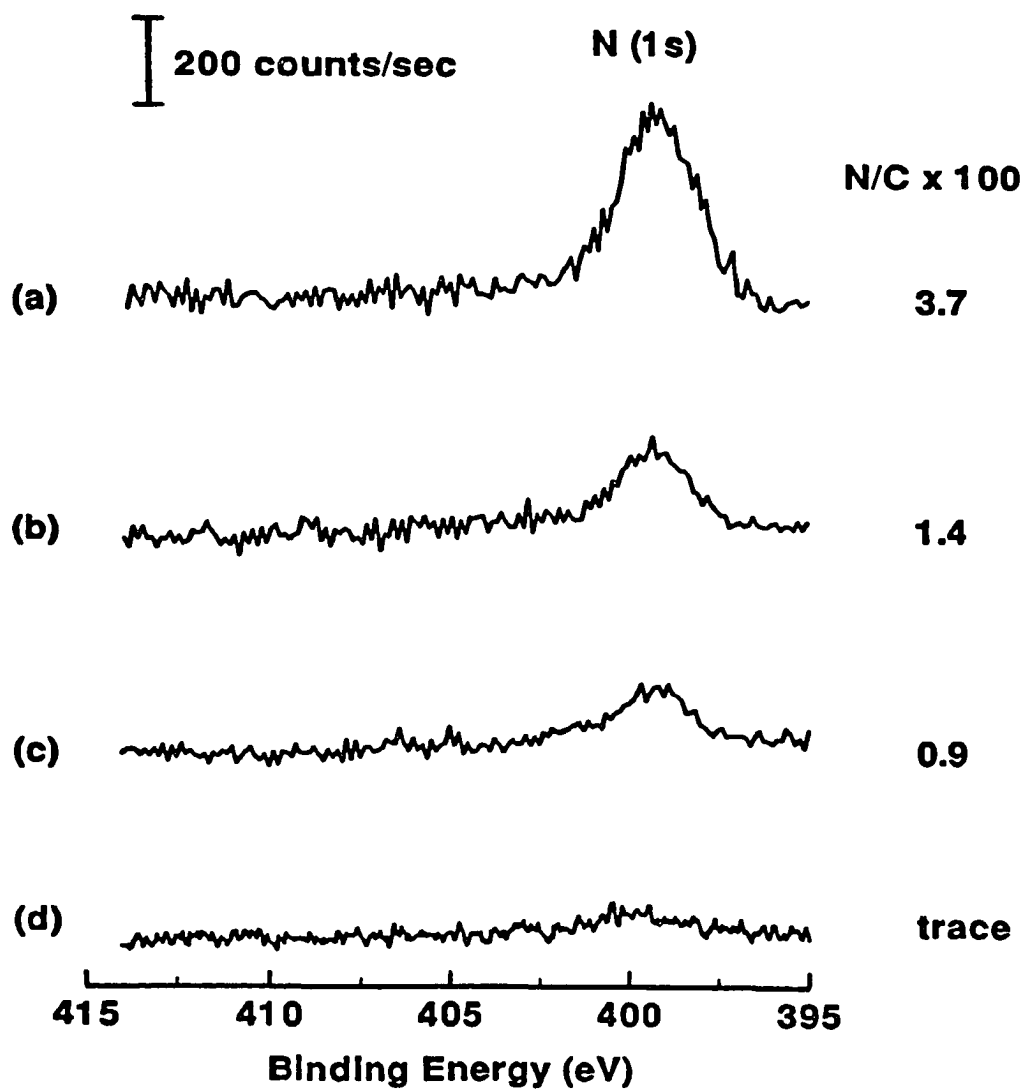


Figure 4. X-ray photoelectron spectra in the N(1s) region for freshly polished GCEs immersed in an ethanolic solution containing (a) 1 mM butylamine, (b) 1 mM N-methylbutylamine, (c) 1 mM N-ethylbutylamine, and (d) 1 mM N,N-dimethylbutylamine. The applied voltage was cycled once between 0.00 V and +1.40 V at 10 mV/s in each case.

respectively. The XPS spectrum for a scan in a 1 mM electrolytic solution of triethylamine is also represented by Figure 4d. As expected from the data for the primary amine N-acetylenediamine in Figure 2, Figure 4a indicates that butylamine is immobilized with an N/C value of 3.7, a value reasonably consistent with the differences in the number of nitrogens in the two compounds. Comparisons of Figure 4a to Figures 4b-d show, however, that the extent of immobilization is strongly influenced by the presence of substituents on the nitrogen atom. For example, the surface coverage of the methyl-substituted secondary amine (N/C=1.4) is less than half that of the primary amine (N/C=3.7). In contrast, both of the tertiary amines, N,N-dimethylbutylamine and triethylamine, are not immobilized at the GCE surface at a detectable level, exhibiting XPS spectra effectively the same as that in the control experiments (i.e., Figure 2e).

These results show that, in spite of the more facile and more extensive oxidation of secondary and tertiary amines, their corresponding cation radicals cannot bind effectively to the GCE surface. We attribute this difference to a steric effect whereby the presence of the additional substituents on the amine functionality hinders accessibility to active sites at the GCE surface. This conclusion is supported further by the lower surface coverage (N/C=0.9) obtained for the immobilization of N-ethylbutylamine (Figure 4c), a more sterically hindered secondary amine than N-methylbutylamine, at the GCE surface.

To ensure that the differences in the extent of immobilization were not a result of differences in the reactivity of the primary, secondary, and tertiary amine cation radicals toward the GCE surface, we attempted to increase the surface coverage of the secondary and

tertiary amines by cycling repetitively between 0.00 V and +1.40 V at 10 mV/s. For these experiments,  $E_{app}$  was cycled twice at a GCE in electrolytic ethanolic solutions containing 1 mM of either N-methylbutylamine or N,N-dimethylbutylamine. Although this procedure exposes the GCE surface to significantly larger amounts of secondary and tertiary amine cation radicals during the second voltage cycle, there were no observed differences in surface coverages (see Table I). These results support the existence of a strong steric effect in the immobilization step. We note that the inability to immobilize tertiary amines at the GCE surface may also reflect a dependence of the reaction mechanism on the loss of a proton from the amine cation radical (c.f. Scheme I) [20].

#### **Immobilization of Dopamine at the GCE Surface.**

The results presented in this section focused on demonstrating the utility of Scheme I for the creation a GCE surface with electrocatalytic capabilities. To this end, several recent reports have shown that GCEs modified with dopamine (DA) using more complex synthetic routes [12] catalyze via a surface EC mechanism [12,14] the oxidation of the cofactor  $\beta$ -NADH, the oxidation of which is kinetically slow at a freshly polished GCE. These data, coupled with the presence of the primary amine functionality that is linked through a short alkyl chain to its catechol moiety, make DA an attractive candidate for such a demonstration. However, as shown by the N(1s) XPS spectrum in Figure 5a, use of the single scan coating method that led to maximal immobilization of N-acetythylenediamine and butylamine resulted in a much lower coverage of DA at the GCE surface. This GCE was coated in an ethanolic solution containing 2 mM of DA hydrochloride (DAHCl), 2 mM of triethylamine

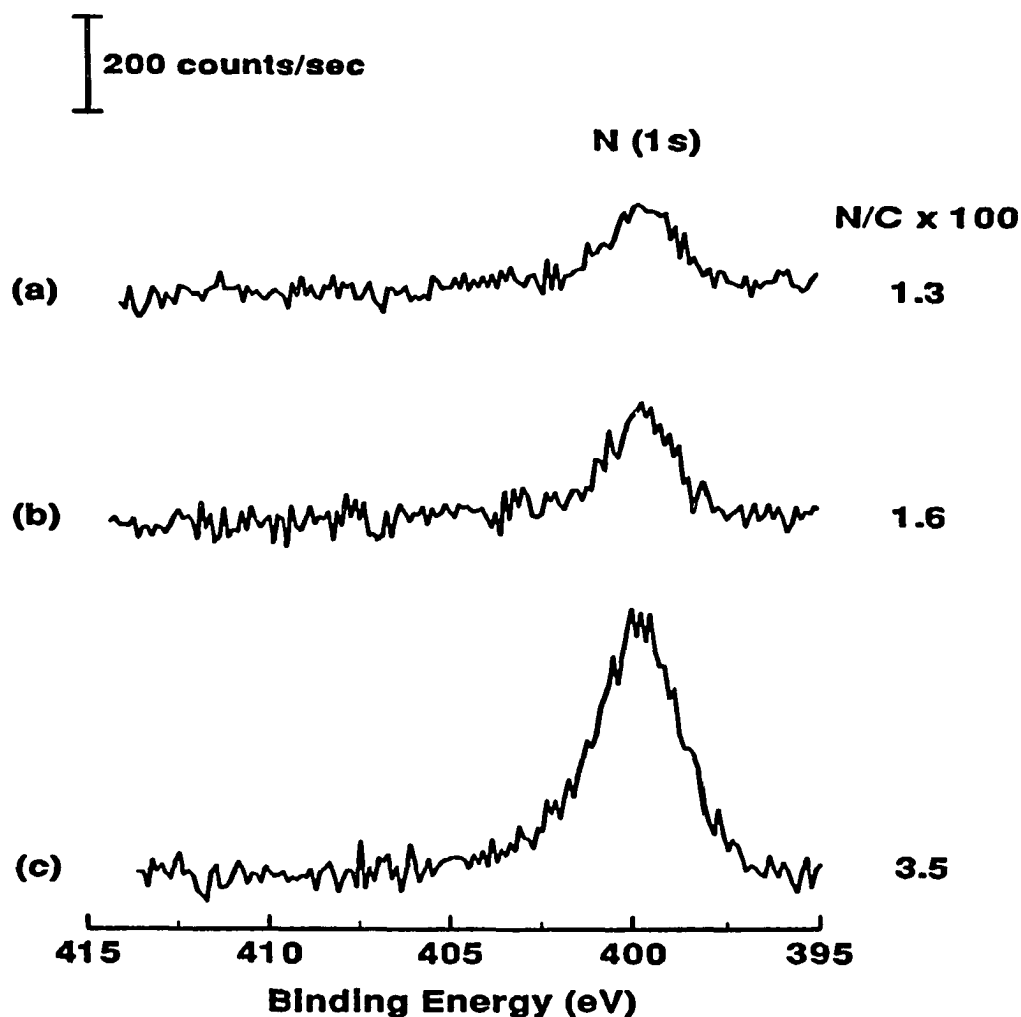


Figure 5. X-ray photoelectron spectra in the N(1s) region for freshly polished GCEs immersed in an ethanolic solution containing (a) 2 mM DAHCl, 2 mM Et<sub>3</sub>N, and (b) 1 mM N-acetylenehydramine, 1 mM catechol. The applied voltage was cycled once between 0.00 V and +1.40 V at 10 mV/s in each case. The spectrum in (c) was obtained by stepping first  $E_{app}$  from 0.00 V to +1.40 V in the supporting electrolyte only, and then injecting 1 mL of 10 mM DAHCl, 30 mM Et<sub>3</sub>N, in supporting electrolyte at +1.40 V. The applied voltage was held at +1.40 V for an additional 5 sec, and then stepped back to 0.00 V.

(Et<sub>3</sub>N), and 0.1 M LiClO<sub>4</sub>; the Et<sub>3</sub>N was used to deprotonate the amine group of DAHCl [30]. The N/C value of 1.3 for the DA-modified GCE is less than half that obtained for the immobilization of butylamine by the same method (i.e., N/C=3.7). Multiple CV scans did not notably increase the coverage.

Since many types of aromatic species adsorb strongly to the surface of GCEs through charge-transfer interactions [31-33], we suspected that the low surface coverage of DA relative to butylamine was a consequence of a blocking of active surface sites by the adsorption of DA through its catechol functionality. To test this possibility, we attempted a surface modification using our single scan method in an electrolytic solution 1 mM in N-acetylenediamine and 1 mM in catechol. If, as speculated, binding sites are blocked by the adsorption of catechol, the relative surface coverage of N-acetylenediamine would be less than that for the preparation in the absence of catechol (i.e., Figure 2d). Figure 5b shows the result of the XPS characterization in the N(1s) region. Importantly, the N/C value (N/C=1.6) for the modification in the presence of catechol is dramatically less than that in the electrolytic solution without catechol (N/C=6.4). This finding therefore argues that the lower coverage of the DA-modified electrode reflects a blocking of surface binding sites by the catechol moiety.

In light of the above findings, we altered the procedure for immobilization to minimize the adsorption of DA prior to amine electrolysis. To accomplish this, E<sub>app</sub> was first stepped from 0.00 V to +1.40 V in an ethanolic solution containing only supporting electrolyte. Immediately after the step, 1 mL of an ethanolic solution of 10 mM DAHCl,



30 mM Et<sub>3</sub>N, and 0.1 M LiClO<sub>4</sub> was injected into the electrolysis cell with a syringe with its tip placed ~0.5 cm above the GCE surface while holding E<sub>app</sub> at +1.40 V. The applied voltage was maintained at +1.40 V for an additional 5 s after injection, and then stepped back to 0.00 V to reduce the oxidized surface bound DA. Figure 5c shows the N(1s) XPS spectrum for a GCE treated in this manner. Importantly, the N/C value at this GCE (N/C=3.5) is similar to that obtained at GCEs coated with primary alkylamines (N/C=3.7), pointing to the effectiveness of the modified immobilization strategy. With this technique, use of oxidation times shorter than 5 s resulted in smaller N/C values, whereas times longer than ~5 s yielded no further increases in the surface coverage.

Figure 6 presents a CV curve for a GCE modified with DA at maximum coverage. The curve was recorded in aqueous 0.1 M HClO<sub>4</sub> at a scan rate of 100 mV/s. The anodic and cathodic waves located at +0.54 V correspond to the two-electron oxidation and reduction of the surface-bound DA. The shapes and peak separation of the response are diagnostic of a surface-bound redox species: the oxidation and reduction waves are symmetrical in shape and the separation of the anodic and cathodic peak current voltages is ~10 mV [34]. In addition, the peak currents scale linearly with the sweep rate over a tested range of 50-400 mV/s. These characteristics confirm the immobilization of an electroactive redox species. The surface coverage of DA, as estimated by integration of the area under either the anodic or cathodic waves [35], is  $(1.8 \pm 0.2) \times 10^{-10}$  mol/cm<sup>2</sup>. This coverage compares favorably with that found using our earlier CV coating method ( $\sim 7 \times 10^{-11}$  mol/cm<sup>2</sup>) as well as with that obtained previously ( $\sim 6 \times 10^{-11}$  mol/cm<sup>2</sup>) for GCEs modified with DA through an amidization

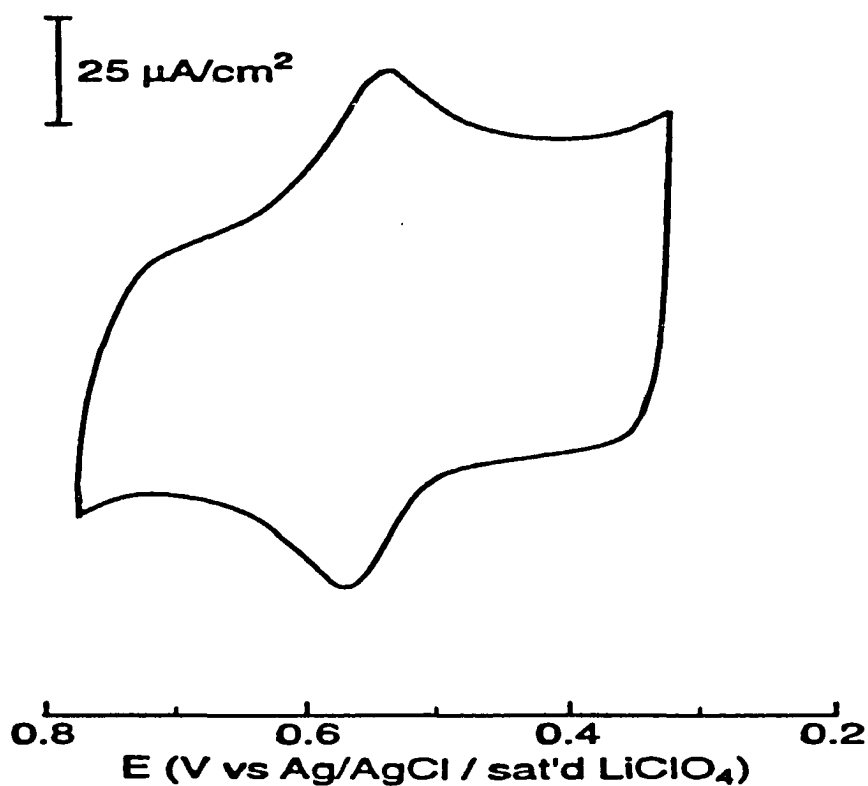


Figure 6. Cyclic voltammogram obtained at a DA-modified GCE in aqueous 0.1 M  $\text{HClO}_4$  solution. The sweep rate was 100 mV/s.

reaction [12]. The surface coverage of DA is, however, somewhat smaller than that predicted for a closest packed monolayer of DA molecules in which the catechol moieties are either perpendicular ( $\sim 5.0 \times 10^{-10} \text{ mol}/\text{cm}^2$ ) or parallel ( $\sim 2.4 \times 10^{-10} \text{ mol}/\text{cm}^2$ ) to the GCE surface [36]. This difference suggests the existence of specific sites for the bonding of the amine cation radical to the GCE surface, as will be discussed in the next section.

The DA-modified GCEs were also examined for their ability to catalyze the oxidation of  $\beta$ -NADH. Figure 7a illustrates the sluggish oxidation of  $\beta$ -NADH at a freshly polished GCE. The CV was recorded at 50 mV/s in a pH 7 phosphate buffer solution containing 0.5 mM  $\beta$ -NADH. A single broad oxidation wave is seen with an  $E_p$  of +0.45 V. For comparison, Figure 7b shows the oxidation of  $\beta$ -NADH at a DA-modified GCE, with Figure 7c showing the CV curve for a DA-modified GCE in supporting electrolyte only. Both the shift of the wave in curve b to a value negative of that in curve a and the increase in the peak current relative to curve c are diagnostic of a surface EC mechanism [13,14]. Together, these findings clearly demonstrate the utility of Scheme I for the facile fabrication of GCEs that display electrocatalytic properties.

#### **Proposed Mechanism of Bonding.**

In this section, we propose an extension of the mechanism outlined in Scheme I. This extension is based primarily on the combined weight of our experimental results and, to a lesser extent, on the literature concerning the solution phase reactions of amine cation radicals with substituted aromatic compounds [37,38]. Of particular importance is a comparison of the maximal surface coverage of the amine-containing compound DA ( $\sim 1.8 \times 10^{-10}$  mol/cm<sup>2</sup>) that can be obtained via Scheme I to that expected for a closest packed monolayer [36] in which the catechol moieties are either perpendicular ( $\sim 5.0 \times 10^{-10}$  mol/cm<sup>2</sup>) or parallel ( $\sim 2.4 \times 10^{-10}$  mol/cm<sup>2</sup>) to the GCE surface. Though only a semiquantitative comparison at best [35], the differences in coverage argue that the immobilized DA is oriented with its ring

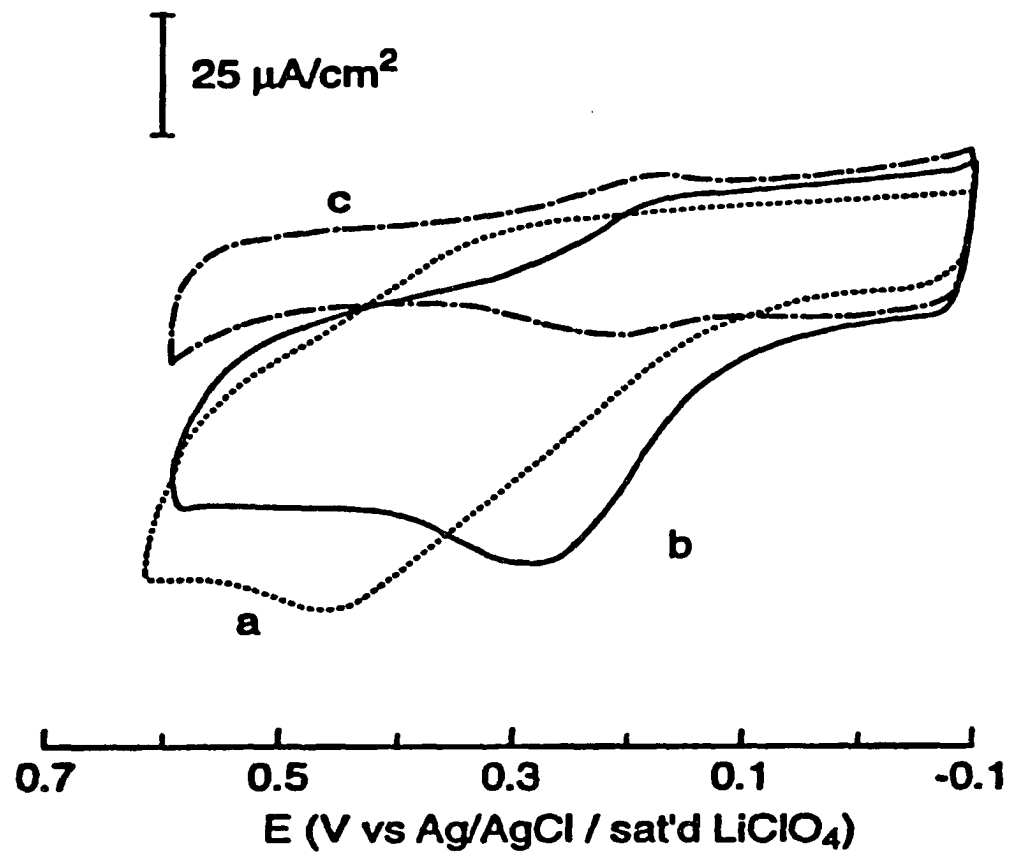


Figure 7. Cyclic voltammograms obtained in an aqueous solution containing 0.5 mM  $\beta$ -NADH and pH 7 phosphate buffer at (a) a freshly polished GCE and (b) a DA modified GCE. The CV curve in (c) was obtained at a DA modified GCE in supporting electrolyte only. The sweep rate was 50 mV/s.

parallel to the GCE surface. This conclusion, however, requires that the GCE reacts uniformly with the electrogenerated amine cation radicals. Thus, both the edge and basal planes of the GCE, which exist in roughly equal proportions [39,40], must exhibit comparable reactivity in the immobilization of DA.

As a test for verification, we attempted to immobilize butylamine at the basal plane of HOPG electrodes via Scheme I. The CV curve obtained at such an electrode in an ethanolic solution containing 1 mM of butylamine and 0.1 M LiClO<sub>4</sub> showed a small wave with an E<sub>p</sub> of +1.35 V indicative of amine oxidation. However, the total charge passed during this oxidation was significantly smaller than that passed for the analogous oxidation at a GCE (Figure 3a), suggesting that the kinetics of amine cation radical formation are much slower at HOPG electrodes. Importantly, the XPS spectrum in the N(1s) region for an HOPG electrode after attempting to immobilize butylamine was indistinguishable from that at a freshly polished GCE. To ensure that this inability to immobilize butylamine at HOPG was not simply due to insufficient amine cation radical generation, we tested the effects of multiple sweeps as well as of extending the positive limit of the sweep to +1.90 V. In each case, we found no evidence from an XPS characterization for immobilization. Therefore, although amine radicals are generated at an HOPG electrode, the basal plane of HOPG is not reactive towards the immobilization process of Scheme I. It then follows that immobilization via Scheme I takes place at the edge and not the basal plane of the GCE surface.

Since the edge planes of polished GCE surfaces are known to contain a significant amount of oxygen functional groups such as phenols, quinones, and carboxylic acids [5,41],

the literature suggests that the amine radical coupling reactions may be directed and their rates affected, in part, by the different types of oxygen-containing groups at the edge planes. Such a possibility reflects the large body of literature concerning electrophilic substitution reactions of substituted aromatic compounds with amine radicals [37,38] as well as earlier arguments for free radicals reacting rapidly with the oxygen-containing edge planes on carbon electrodes [42,43]. In the former, studies have shown that amine radical-arene coupling reactions are strongly activated for ortho and para attack by electron releasing substituents such as hydroxyl groups and ketones and strongly deactivated by electron withdrawing substituents such as carboxylic acids. By analogy, the phenol, quinone, and carboxylic acid functionalities at the edge plane of the GCE can either activate or deactivate the immobilization reaction. Experiments to test for contributions of this interesting possibility are presently being devised.

## CONCLUSIONS

This paper has demonstrated the ability to create chemically modified GCEs for electrocatalytic purposes via the electrooxidation of amine-containing compounds. The application of this method to the immobilization of biotin for biosensor purposes has been described elsewhere [23]. Importantly, this procedure dramatically simplifies the fabrication of modified electrodes, a process which often involves an extended series of pretreatment, activation, and functionalization steps. This procedure also provides a comparatively higher coverage of the immobilized species. In addition, we have found that the extent of immobilization is strongly dependent on the degree of substitution at the amine functionality,

whereby the electrooxidation of primary amines yields the largest relative surface coverage and tertiary amines show no detectable surface coverage. The differences in the coverages are attributed primarily to a strong steric effect which hinders the accessibility of the amine cation radicals to binding sites at the GCE surface. Results further indicate that immobilization occurs at the edge vs basal plane sites of a GCE surface. Together, these studies provide the basis for future work that will examine the immobilization of amines containing redox-active groups onto the surface of GC spheres to be used as "charge-controllable stationary phases" in a new form of chemical separations. Further application of this method for the fabrication of biotin-containing biosensors is also underway in our laboratory. Studies focused on unraveling further the bonding mechanism are planned.

#### ACKNOWLEDGMENTS

R.S.D. gratefully acknowledges the support of an ACS Analytical Division Summer Fellowship sponsored by the Dow Chemical Corporation. This work was supported by the National Science Foundation (Grant CHE-9003308). The Ames Laboratory is operated for the U.S. Department of Energy under contract W-7405-eng-82.

#### REFERENCES AND NOTES

1. Murray, R.W. *Electroanalytical Chemistry: A Series of Advances*, Bard, A.J., Ed., Marcel Dekker: New York, 1984; vol. 13, p. 191.
2. Van Der Linden, W.E.; Dieker, J.W. *Anal. Chim. Acta* **1980**, *119*,1.

3. Kinoshita, K. *Carbon: Electrochemical and Physicochemical Properties*, Wiley: New York, 1988.
4. Dautartas, M.F.; Evans, J.F.; Kuwana, T. *Anal. Chem.* **1979**, *51*, 104.
5. Kepley, L.J.; Bard, A.J. *Anal. Chem.* **1988**, *60*, 1459.
6. Engstrom, R.W.; Strasser, V.A. *Anal. Chem.* **1984**, *56*, 136.
7. Watkins, B.F.; Behling, J.R.; Kariv, E.; Miller, L.L. *J. Am. Chem. Soc.* **1975**, *97*, 3549.
8. Firth, B.E.; Miller, L.L.; Mitani, M.; Rogers, T.; Lennox, J.; Murray, R.W. *J. Am. Chem. Soc.* **1976**, *98*, 8271.
9. Lin, A.W.C.; Yeh, P.; Yacynych, A.M.; Kuwana, T. *J. Electroanal. Chem.* **1977**, *84*, 411.
10. Pocard, N.L.; Alsmeyer, D.C.; McCreery, R.L.; Neenan, T.X.; Callstrom, M.R. *J. Am. Chem. Soc.* **1992**, *114*, 769.
11. Lennox, J.C.; Murray, R.W. *J. Electroanal. Chem.* **1977**, *78*, 395.
12. Tse, D.C.S.; Kuwana, T. *Anal. Chem.* **1978**, *50*, 1315.
13. Ueda, C.; Tse, D.C.S.; Kuwana, T. *Anal. Chem.* **1982**, *54*, 850.
14. Zak, J.; Kuwana, T. *J. Electroanal. Chem.* **1983**, *150*, 645.
15. Bourdillon, C.; Bourgeois, J.; Thomas, D. *J. Am. Chem. Soc.* **1980**, *102*, 4231.
16. Wieck, H.J.; Heider, G.H.; Yacynych, A.M. *Anal. Chim. Acta* **1984**, *158*, 137.
17. Pantano, P.; Morton, T.H.; Kuhr, W.G. *J. Am. Chem. Soc.* **1991**, *113*, 1832.
18. Pantano, P.; Kuhr, W.G. *Anal. Chem.* **1991**, *63*, 1413.
19. Pantano, P.; Kuhr, W.G. *Anal. Chem.* **1993**, *65*, 623.
20. Barbier, B.; Pinson, J.; Desarmot, G.; Sanchez, M. *J. Electrochem. Soc.* **1990**, *137*, 1757.



21. Deinhammer, R.S.; Shimazu, K.; Porter, M.D. *Anal. Chem.* **1991**, *63*, 1889.
22. Deinhammer, R.S.; Ting, E.; Porter, M.D. *J. Electroanal. Chem.* **1993**, *362*, 295.
23. Deinhammer, R.S.; Ho, Mankit; Anderegg, J.W.; Porter, M.D. *Langmuir* **1994**, *10*, 1306.
24. Bussing, T.D.; Holloway, P.H. *J. Vac. Sci. Tech. A* **1985**, *3*, 1973.
25. Scofield, J.H. *J. Elec. Spec.* **1976**, *8*, 129.
26. Masui, M.; Sayo, H.; Tsuda, Y. *J. Chem. Soc. (B)* **1968**, 973.
27. Mann, C.K. *Anal. Chem.* **1964**, *36*, 2424.
28. In addition to the lack of an oxidative wave for the N-propylacetamide, a characterization using XPS failed to detect the presence of the immobilized form of this amide.
29. Nordberg, R.; Albridge, R.G.; Bergmark, T.; Ericson, U.; Hedman, J.; Nordling, C.; Siegbahn, K.; Lindberg, B.J. *Arkiv for Kemi* **1968**, *28*, 257.
30. A single voltage cycle in an electrolytic solution containing only DAHCl showed no detectable coverage of immobilized DA at the GCE surface by XPS.
31. Vasquez, R.E.; Imai, H. *J. Electroanal. Chem. Bioelectrochem. Bioeng.* **1985**, *14*, 389.
32. Zhang, J.; Anson, F.C. *J. Electroanal. Chem.* **1992**, *331*, 945.
33. McDermott, M.T.; Kneten, K.; McCreery, R.L. *J. Phys. Chem.* **1992**, *96*, 3124.
34. Bard, A.J.; Faulkner, L.R. *Electrochemical Methods*, Wiley: New York, 1980.
35. The estimated roughness factor of polished GCE's is  $\sim 1.9$  [44], which places the actual surface coverage of DA closer to  $\sim 9.5 \times 10^{-11}$  mol/cm<sup>2</sup>.
36. Soriaga, M.P.; Hubbard, A.T. *J. Am. Chem. Soc.* **1982**, *104*, 2735.
37. Minisci, F.; Galli, R.; Cecere, M. *Chim. Ind.* **1966**, *48*, 725.

38. Minisci, F. *Synthesis* 1973, 1.
39. Bowling, R.J.; Packard, R.T.; McCreery, R.L. *J. Am. Chem. Soc.* 1989, 111, 1217.
40. Rice, R.J.; Pontikos, N.M.; McCreery, R.L. *J. Am. Chem. Soc.* 1990, 112, 4617.
41. Takahagi, T.; Ishitani, A. *Carbon* 1984, 22, 43.
42. Besenhard, J.O.; Fritz, H.P. *Angew. Chem. Int. Ed. Engl.* 1983, 22, 950.
43. Oyama, N.; Brown, A.P.; Anson, F.C. *J. Electroanal. Chem.* 1978, 87, 435.
44. Pontikos, N.M., McCreery R.L. *J. Electroanal. Chem.* 1992, 324, 229.

## SUMMARY AND DISCUSSION

The feasibility of manipulating analytical separations through alterations in the voltage or charge applied to a charge-controllable stationary phase has been investigated and demonstrated. The wide range over which the capacity factors of analytes can be modified electrochemically without alteration in the composition of the mobile phase points to the effectiveness of this new method. Changes in the applied voltage and charge initiated both prior to and during elution were found to be versatile pathways for manipulating and fine-tuning the resolution between analytes. Comparison of these electrochemically-controlled separations to those obtained using conventional solvent gradient elution techniques showed that the overall quality of the separations obtained by these two methods was similar. However, simultaneous changes in the applied voltage and the mobile phase composition, in which the former was used to fine-tune analyte resolution and the latter was used to decrease elution band widths and analysis time, were found to provide separations that were superior to those obtained by either method alone.

Through a series of detailed examinations of the retention of a variety of hazardous waste components and biologically-active species as a function of the applied voltage, a mechanism that describes the ability of changes in the applied voltage to modify the retention of analytes was developed. For the charge-controllable stationary phases consisting of polypyrrole, this mechanism involved manipulation of the anion-exchange capacity, hydrophobicity, and porosity of the film through alterations in the applied voltage. For the uncoated carbonaceous phases, the mechanism entailed the selective manipulation of the

ability of the carbon surface to participate in, to a large extent, donor-acceptor and solvophobic interactions with the analytes. In general, hydrophobic, electron-donating anions were found to be the best candidates for separations using EMLC on the former phases, whereas hydrophilic molecules displaying strong electron-donating or electron-accepting characteristics were found to be the best candidates on the latter phases.

These mechanistic studies also revealed that this new technique, in addition to its viability as a separation method, can be potentially used to study a variety of fundamental phenomena. Such phenomena include the voltage-dependent properties of conductive polymers [58,110,111] or other adsorbates [112-120], the double layer structure at surfaces [121,122], reaction mechanisms [123-125], and the effects of the derivatization or functionalization of surfaces on their interaction with solution-based species [126,127]. Further, the column can also be potentially used to characterize groups of molecules based on intrinsic properties such as hydrophobicity, electron-donating ability, polarity, or molecular size. The ability to measure precisely the retention time of a species injected onto the column provides a convenient method for studying quantitatively these phenomena. These studies are further facilitated by the very large area to volume ratio in the EMLC column, which ensures that each injected molecule will interact with the surface independently [42].

Studies of this nature will also be facilitated by the results presented in Chapter 7, which propose a new method for derivatization of carbon surfaces that is based on the electrochemical oxidation of amine-containing compounds [128,129]. This new method simplifies dramatically the procedures required for functionalization of these electrodes, which

have previously involved an extended series of pretreatment, derivatization, and functionalization steps [130-132]. Use of this method for functionalization of carbonaceous charge-controllable stationary phases should also prove valuable as a convenient route for modifying the selectivity of such phases and increasing the versatility of the EMLC technique.

Although the work described in this dissertation has firmly laid the foundation for analytical separations based on EMLC, a considerable amount of developmental work remains. For example, studies designed to unravel further the electrochemically-controlled retention mechanism in terms of establishing a quantitative model that describes the relevant interactions need to be developed. Other work aimed at further investigation of the utility of alterations in the oxidation states of organic redox species (i.e., catecholamines) as a method for manipulation of their separations needs to be done. The advantages of such a method were touched upon in Chapter 6. Electrochemically-induced changes in the pH of the mobile phase may also prove fruitful as an elution method for analytes containing pH-sensitive functionalities (i.e.,  $\text{CO}_2\text{H}$ ,  $\text{NH}_2$ ). Along these lines, the indirect derivatization of the carbonaceous stationary phase with mobile phase species that can be adsorbed or desorbed through changes in applied voltage (i.e., ionic surfactants) should also be valuable as a simple and indirect means for altering selectively the interactions of analytes with the carbon surface. Further, the application of EMLC to the separation of species whose separations are not amenable to conventional solvent gradient elution needs to be investigated. As discussed briefly in Chapter 2, studies which probe further the usefulness of EMLC for concentrating dilute solutions of analytes prior to their analysis also need to be continued.

Re-design of the EMLC column will also be required eventually to improve further its temporal response to changes in the applied voltage. Such an improvement may allow for changes in the applied voltage to be made continuously throughout a particular isocratic or gradient elution separation for fine-tuning the resolution of analytes where it is needed. Column redesign may also aid in the development of a method for focussing electrochemically the elution bands of analytes. Such a scheme, which may be implemented through the application of a voltage gradient *down the length of the column*, might allow for the retention of the tailing edges of analyte elution bands to be decreased relative to the leading edges of the bands, leading to a focussing effect. This focussing effect has potential for sharpening significantly the elution bands of analytes, resulting in an improved resolution and ability to quantitate more accurately these species.

Finally, work directed toward utilization of electrochemical gradient elution as an elution method in microcolumn liquid chromatography would appear promising, since solvent gradient elution is often difficult to perform with these columns due to their excessively small internal volumes [133,134]. Some of this work is currently underway in our laboratory [135]. Together, the work described in this dissertation has provided the framework for a new and exciting analytical separation technique that is based on the electrochemical manipulation of analyte retention.

## REFERENCES

1. Smith, R.E. *Ion Chromatography Applications*; CRC Press: Boca Raton, Fl., 1988.
2. Calull, M.; Marce, R.M.; Borrull, F. *J. Chromatogr.* **1992**, *590*, 215.
3. Coco, F.L.; Valentini, C.; Novelli, V.; Ceccon, L. *J. Liq. Chromatogr.* **1994**, *17*, 603.
4. Ruiz, E.; Santillana, M.I.; DeAlba, M.; Nieto, M.T.; Garcia-Castellano, S. *J. Liq. Chromatogr.* **1994**, *17*, 447.
5. Neilen, M.W.F.; Brinkman, U.A.Th.; Frei, R.W. *Anal. Chem.* **1985**, *57*, 806.
6. Frei, R.W.; Nielen, M.W.F.; Brinkman, U.A.Th. *Intern. J. Environ. Anal. Chem.* **1986**, *25*, 3.
7. Kim, I.S.; Sasinos, F.I.; Rishi, D.K.; Stephens, R.D.; Brown, M.A. *J. Chromatogr.* **1991**, *589*, 177.
8. Koester, C.J.; Clement, R.E. *CRC Crit. Rev. Anal. Chem.* **1993**, *24*, 263.
9. Miyagi, H.; Miura, J.; Takata, Y.; Kamitake, S.; Ganno, S.; Yamagata, Y. *J. Chromatogr.* **1982**, *239*, 733.
10. Coca, E.; Ribas, B.; Trigueros, G.; Mtnez-Sarmiento, J.; Borque, M.; Ortega, D.; Sobrino, A.; Mallen, A.; DePablos, I.; Fdez-Represa, J.A. *J. Liq. Chromatogr.* **1994**, *17*, 1349.
11. Liebich, H.M.; Forst, C. *J. Chromatogr.* **1990**, *525*, 1.
12. Feste, A.S. *J. Chromatogr.* **1992**, *574*, 23.
13. Grunau, J.A.; Swiader, J.M. *J. Chromatogr.* **1992**, *594*, 165.

14. Medlicott, N.J.; Ferry, D.G.; Tucker, I.G.; Rathbone, M.J.; Holborow, D.W.; Jones, D.S. *J. Liq. Chromatogr.* 1994, 17, 1605.
15. Hearn, M.T.W. *Adv. Chromatogr.* 1982, 20, 1.
16. Pfeifer, R.F.; Hill, D.W. *Adv. Chromatogr.* 1983, 22, 37.
17. Boschetti, E. *J. Chromatogr. A* 1994, 658, 207.
18. Watson, I.D. *Adv. Chromatogr.* 1987, 26, 117.
19. Hubball, J. *Adv. Chromatogr.* 1992, 32, 131.
20. Rop, P.P.; Grimaldi, F.; Bresson, M.; Fornaris, M.; Viala, A. *J. Liq. Chromatogr.* 1993, 16, 2797.
21. Armstrong, D.W. *J. Liq. Chromatogr.* 1984, 7, 353.
22. Pirkle, W.H.; Pochapsky, T.C. *Adv. Chromatogr.* 1987, 27, 73.
23. Davankov, V.A. *J. Chromatogr. A* 1994, 666, 55.
24. Fujinaga, T.; Nagai, T.; Takagi, C.; Okazaki, S. *Nippon Kagaku Zasshi* 1963, 84, 941.
25. Blaedel, W.J.; Strohl, J.H. *Anal. Chem.* 1964, 36, 1245.
26. Roe, D.K. *Anal. Chem.* 1964, 36, 2371.
27. Eckfeldt, E.L. *Anal. Chem.* 1959, 31, 1453.
28. Voorhies, J.D.; Davis, S.M. *Anal. Chem.* 1960, 32, 1855.
29. Bard, A.J. *Anal. Chem.* 1963, 35, 1125.
30. Finlayson, M.B.; Mowat, J.A.S. *Electrochem. Technol.* 1965, 3, 148.
31. Johansson, G. *Talanta* 1965, 12, 163.
32. Blaedel, W.J.; Strohl, J.H. *Anal. Chem.* 1965, 37, 64.



33. Fujinaga, T. *Pure. Appl. Chem.* **1971**, *25*, 709.
34. Fujinaga, T. Kihara, S. *CRC Crit. Rev. Anal. Chem.* **1977**, 223.
35. Bamberger, R.L.; Strohl, J.H. *Anal. Chem.* **1969**, *41*, 1450.
36. Strohl, J.H.; Dunlap, K.L. *Anal. Chem.* **1972**, *44*, 2166.
37. Hern, J.L.; Strohl, J.H. *Anal. Chem.* **1978**, *50*, 1954.
38. Bamberger, R.L. Ph.D. Dissertation, West Virginia University, Morgantown, West Virginia, 1969.
39. Giles, C.; D'Silva, A.; Easton, I. *J. Coll. Interfac. Sci.* **1974**, *47*, 766.
40. Antrim, R.F.; Scherrer, R.A.; Yacynych, A.M. *Anal. Chim. Acta* **1984**, *164*, 283.
41. Antrim, R.F., Ph.D. Dissertation, Rutgers, The State University of New Jersey, 1984.
42. Poole, C.F.; Schuette, R.A. *Contemporary Practice of Chromatography*; Elsevier: Amsterdam, 1984.
43. Delahay, P. *Double Layer and Electrode Kinetics*; Interscience: New York, 1967.
44. Bard, A.J.; Faulkner, L.R. *Electrochemical Methods*; Wiley: New York, 1980.
45. Antrim, R.F.; Yacynych, A.M. *Anal. Lett.* **1988**, *21*, 1085.
46. Espenscheid, M.W.; Martin, C.R. *J. Electroanal. Chem.* **1985**, *188*, 73.
47. Ghatak-Roy, A.R.; Martin, C.R. *Anal. Chem.* **1986**, *58*, 1574.
48. Zumbrennen, H.R.; Anson, F.C. *J. Electroanal. Chem.* **1983**, *152*, 111.
49. Miller, L.L.; Lau, A.N.K.; Miller, E.K. *J. Am. Chem. Soc.* **1982**, *104*, 5242.
50. Ge. H.; Wallace, G.G. *Anal. Chem.* **1989**, *61*, 198.
51. Ge. H.; Wallace, G.G. *Anal. Chem.* **1989**, *61*, 2391.

52. Ge, H.; Wallace, G.G. *J. Liq. Chromatogr.* **1990**, *13*, 3245.
53. Wallace, G.G.; Maxwell, K.E.; Lewis, T.W.; Hodgson, A.J.; Spencer, M.J. *J. Liq. Chromatogr.* **1990**, *13*, 3091.
54. Ge, H.; Teasdale, P.R.; Wallace, G.G. *J. Chromatogr.* **1991**, *544*, 305.
55. Nagaoka, T.; Fujimoto, M.; Nakao, H.; Kukuno, K.; Yano, J.; Ogura, K. *J. Electroanal. Chem.* **1993**, *350*, 337.
56. Nagaoka, T.; Fujimoto, M.; Nakao, H.; Kukuno, K.; Yano, J.; Ogura, K. *J. Electroanal. Chem.* **1994**, *364*, 179.
57. Nagaoka, T.; Kakuno, K.; Fujimoto, M.; Nakao, H.; Yano, J.; Ogura, K. *J. Electroanal. Chem.* **1994**, *368*, 315.
58. Diaz, A.F.; Castillo, J.I.; Logan, J.A.; Lee, W.Y. *J. Electroanal. Chem.* **1981**, *129*, 115.
59. Shimidzu, T.; Ohtani, A.; Iyoda, T.; Honda, K. *J. Electroanal. Chem.* **1987**, *224*, 123.
60. Naoi, K.; Lien, M.M.; Smyrl, W.H. *J. Electroanal. Chem.* **1989**, *272*, 273.
61. Zhong, C.; Doblhofer, K. *Electrochim. Acta* **1990**, *35*, 1971.
62. Schmidt, V.M.; Heitraum, J. *Electrochim. Acta* **1993**, *38*, 349.
63. Ge, H.; Wallace, G.G. *J. Chromatogr.* **1991**, *588*, 25.
64. Ge, H.; Gilmore, K.J.; Ashraf, S.A.; Too, C.O.; Wallace, G.G. *J. Liq. Chromatogr.* **1993**, *16*, 1023.
65. Ge, H.; Gilmore, K.G.; Wallace, G.G. *J. Liq. Chromatogr.* **1994**, *17*, 1301.
66. Nagaoka, T.; Fujimoto, M.; Uchida, Y.; Ogura, K. *J. Electroanal. Chem.* **1992**, *336*, 45.
67. Porter, M.D.; Kuwana, T. *Anal. Chem.* **1984**, *56*, 529.

68. Ho, M.; Chung, C.; Schwabacher, A.; Porter, M.D., in preparation for submission to *Journal of the American Chemical Society*.
69. Porter, M.D.; Bright, T.B.; Allara, D.L.; Chidsey, C.E.D. *J. Am. Chem. Soc.* **1987**, *109*, 3559.
70. Bain, C.D.; Troughton, E.B.; Tao, Y.T.; Evall, J.; Whitesides, G.M.; Nuzzo, R.G. *J. Am. Chem. Soc.* **1989**, *111*, 321.
71. Dubois, L.H.; Nuzzo, R.G. *Annu. Rev. Phys. Chem.* **1992**, *43*, 437.
72. Bender, M.L.; Komiyama, M. *Cyclodextrin Chemistry*, Springer-Verlag: Berlin, 1978.
73. Fujimura, K.; Ueda, T.; Kitagaura, M.; Takayanagi, H.; Ando, T. *Anal. Chem.* **1986**, *58*, 2668.
74. Ahuja, S. *Chiral Separations by Liquid Chromatography*, ACS symposium Series, vol. 471, American Chemical Society: Washington D.C., 1991.
75. Deinhammer, R.S.; Shimazu, K.; Porter, M.D. *Anal. Chem.* **1991**, *63*, 1889.
76. Deinhammer, R.S.; Shimazu, K.; Porter, M.D., in preparation for submission to the *Journal of Electroanalytical Chemistry*.
77. Kirkland, J.J.; Glajch, J.L. *J. Chromatogr.* **1983**, *255*, 27.
78. Jandera, P.; Churacek, J. *Gradient Elution in Column Liquid Chromatography*, Elsevier: Amsterdam, 1985.
79. Deinhammer, R.S.; Ting, E.; Porter, M.D. *J. Electroanal. Chem.* **1993**, *362*, 295.
80. Deinhammer, R.S.; Ting, E.; Porter, M.D. in preparation for submission to *Analytical Chemistry*.

81. Kaur, B. *LC-GC* 1990, 3, 41.
82. DerLinden, W.E.; Dieker, J.W. *Anal. Chim. Acta* 1980, 119, 1.
83. Zittel, H.E.; Miller, F.J. *Anal. Chem.* 1965, 37, 200.
84. Monien, H.; Specker, H.; Zinke, K. *Anal. Chem.* 1967, 225, 342.
85. Alder, J.F.; Fleet, B.; Kane, P.O. *J. Electroanal. Chem.* 1971, 30, 427.
86. Pontikos, N.M.; McCreery, R.L. *J. Electroanal. Chem.* 1992, 324, 229.
87. Yamada, S.; Sato, H. *Nature* 1962, 193, 261.
88. Unger, K.K. *Anal. Chem.* 1983, 55, 361A.
89. Knox, J.H.; Kaur, B.; Millward, G.R. *J. Chromatogr.* 1986, 352, 3.
90. Street, G.B.; Clarke, T.C.; Kronubi, M.; Kanazawa, K.; Lee, V.; Pfluger, P., Scott, J.C.; Weiser, G. *Mol. Cryst. Liq. Cryst.* 1982, 83, 1253.
91. Erlandsson, R.; Inganas, O.; Lundstrom, I.; Salaneck, W.R. *Synth. Met.* 1985, 10, 303.
92. Kiselev, A.V.; Nikitin, Y.S.; Frolov, I.I.; Yashin, Y.I. *J. Chromatogr.* 1974, 91, 187.
93. Knox, J.H.; Unger, K.K.; Mueller, H. *J. Liq. Chrom.* 1983, 6, 1.
94. Knox, J.H.; Kaur, B.; Hartwick, R.A.; Brown, P.R. *High Performance Liquid Chromatography*; Wiley: New York, 1989, pp. 189-222.
95. Colin, H.; Eon, C.; Guiochon, G. *J. Chromatogr.* 1976, 119, 41.
96. Cicciooli, P.; Tappa, R.; DiCorcia, A.; Liberti, A. *J. Chromatogr.* 1981, 206, 35.
97. Werkhoven-Gowie, C.E.; Brinkman, U.A.Th.; Frei, R.W. *Anal. Chem.* 1981, 53, 2072.
98. Ghauri, F.Y.K.; Simpson, C.F. *Anal. Proc.* 1989, 26, 69.
99. Bassler, B.J.; Hartwick, R.A. *J. Chrom. Sci.* 1989, 27, 162.

100. Gu, G.; Lim, C.K. *J. Chromatogr.* 1990, 515, 183.
101. Tanaka, N.; Tanigawa, T.; Kimata, K.; Hosoya, K.; Araki, T. *J. Chromatogr.* 1991, 549, 29.
102. Forgacs, E.; Cserhati, T.; Valko, K. *J. Chromatogr.* 1992, 592, 75.
103. Coquart, V.; Hennion, M.C. *J. Chromatogr.* 1992, 600, 195.
104. Kriz, J.; Adamcova, E.; Knox, J.H.; Hora, J. *J. Chromatogr. A* 1994, 663, 151.
105. Engel, T.M.; Olesik, S.V.; Callstrom, M.R.; Diener, M. *Anal. Chem.* 1993, 65, 3691.
106. Davies, M.J.; Smith, K.D.; Carruthers, R.A.; Chai, W.; Lawson, A.M.; Hounsell, E.F. *J. Chromatogr.* 1993, 646, 317.
107. Deinhammer, R.S.; Ting, E.; Porter, M.D., to be submitted to *Journal of Chromatography*.
108. Deinhammer, R.S.; Ting, E.; Porter, M.D., to be submitted to *Journal of Chromatography*.
109. Itoh, H.; Kinoshita, T.; Nimura, N. *J. Liq. Chromatogr.* 1993, 16, 809.
110. Marque, P.; Roncali, J.; Garnier, F. *J. Electroanal. Chem.* 1987, 218, 107.
111. Orata, D.; Buttry, D.A. *J. Am. Chem. Soc.* 1987, 109, 3574.
112. Evans, J.F.; Kuwana, T.; Henne, M.T.; Royer, G.P. *J. Electroanal. Chem.* 1977, 80, 409.
113. Nowak, R.; Schultz, F.A.; Umana, M.; Abruna, H.; Murray, R.W. *J. Electroanal. Chem.* 1978, 94, 219.
114. Tse, D.C.S.; Kuwana, T.; Royer, G.P. *J. Electroanal. Chem.* 1979, 98, 345.

115. Murray, R.W. *Acc. Chem. Res.* **1980**, *13*, 135.
116. Bouwman, R.; Freriks, I.L.C.; Wife, R.L. *J. Catal.* **1981**, *67*, 282.
117. Daum, P.; Murray, R.W. *J. Phys. Chem.* **1981**, *85*, 389.
118. Ueda, C.; Tse, D.C.S.; Kuwana, T. *Anal. Chem.* **1982**, *54*, 850.
119. Espenscheid, M.W.; Martin, C.R. *J. Electroanal. Chem.* **1985**, *188*, 73.
120. Popenoe, D.D.; Deinhammer, R.S.; Porter, M.D. *Langmuir* **1992**, *8*, 2521.
121. Tobias, H.; Soffer, A. *J. Electroanal. Chem.* **1983**, *148*, 221.
122. Oren, Y.; Tobias, H.; Soffer, A. *J. Electroanal. Chem.* **1984**, *162*, 87.
123. Gruver, G.A.; Kuwana, T. *J. Electroanal. Chem.* **1972**, *36*, 85.
124. Firth, B.E.; Miller, L.L.; Mitani, M.; Rogers, T.; Lennox, J.; Murray, R.W. *J. Am. Chem. Soc.* **1976**, *98*, 8271.
125. Zak, J.; Kuwana, T. *J. Electroanal. Chem.* **1983**, *150*, 645.
126. Soffer, A.; Folman, M. *J. Electroanal. Chem.* **1972**, *38*, 25.
127. Miller, C.W.; Karaweik, D.H.; Kuwana, T. *Anal. Chem.* **1981**, *53*, 2319.
128. Barbier, B.; Pinson, J.; Desarmot, G.; Sanchez, M. *J. Electrochem. Soc.* **1990**, *137*, 1757.
129. Deinhammer, R.S.; Ho, M.; Anderegg, J.W.; Porter, M.D. *Langmuir* **1994**, *10*, 1306.
130. Watkins, B.F.; Behling, J.R.; Kariv, E.; Miller, L.L. *J. Am. Chem. Soc.* **1975**, *97*, 3549.
131. Lin, A.W.C.; Yeh, P.; Yacynych, A.M.; Kuwana, T. *J. Electroanal. Chem.* **1977**, *84*, 411.
132. Dautartas, M.F.; Evans, J.F.; Kuwana, T. *Anal. Chem.* **1979**, *51*, 104.

133. Jinno, K.; Sandra, P. *12th International Symposium on Capillary Chromatography*; Industrial Publications and Consulting: Tokyo, 1990, p.14.
134. Chervet, J.P.; Meijvogel, C.J.; Ursem, M.; Salzmann, J.P. *LC-GC*, 1992, 10, 140.
135. O'Toole, R.P.; Coldiron, S.J.; Deninger, W.D.; Deinhammer, R.S.; Burns, S.G.; Bastiaans, G.J.; Braymen, S.D.; Shanks, H.R.; Porter, M.D. *SAE Trans.* 1992, #SAE921179.